EFFECT OF pH ON PARTICLE AGGLOMERATION AND RADIATIVE TRANSFER IN NANOPARTICLE SUSPENSIONS

A Dissertation

by

Layth Wadhah Ismael Al-Gebory

Submitted to the

Graduate School of Sciences and Engineering
In Partial Fulfillment of the Requirements for
the Degree of

Doctor of Philosophy

in the
Department of Mechanical Engineering

Özyeğin University
August 2018

EFFECT OF pH ON PARTICLE AGGLOMERATION AND RADIATIVE TRANSFER IN NANOPARTICLE SUSPENSIONS

Approved by:

Prof. Dr. M. Pinar Mengüç,
Advisor,
Department of Mechanical Engineering
Özyeğin University

Prof. Dr. Ali Koşar,
Department of Mechatronics Engineering
Sabancı University

Prof. Dr. Kürşat Şendur,
Department of Mechatronics Engineering
Sabancı University

Assist. Prof. Dr. Özgür Ertunç,
Department of Mechanical Engineering
Özyeğin University

Date Approved: 02 August 2018

Assist. Prof. Dr. Altuğ Başol,
Department of Mechanical Engineering
Özyeğin University

To my family …

ABSTRACT

Nanoparticle suspensions (NPSs) are solid-fluid mixtures where small dielectric or metallic particles (with sizes <100 nm) used in a base fluid. NPSs have unique and tunable thermo-optical properties, and for that reason they can be used extensively to improve the thermal efficiency of different systems where they show remarkable enhancement in heat transfer compared with those of a base fluid. The effectiveness of solar thermal systems used for photo-thermal energy conversion is measured by their ability of absorb radiative energy by the working medium; for such applications NPSs are much better choice than traditional fluids. NPSs have also been used in coatings as they can be tuned to improve or alter the appearance of an object, as radiative and optical properties play significant roles. Although NPSs are considered very promising for these applications, there is some concern about their stability and their long-term use. Particle agglomeration in NPSs remains one of the most important challenges faced in terms of their usage. In all of these applications, the pH value and its effects on the particle agglomeration may have significant impact on the nanoparticles stability behavior, and consequently on the radiative transfer of energy. Steric and electrostatic stabilization methods are among the two approaches used for particulate suspensions to avoid such problems. In thermal applications, especially in high temperature ones, electrostatic stabilization method is usually preferred.

In this dissertation, both experimental and theoretical investigations were carried out to determine the stability and optical properties of individual (water/TiO_2 and water/Al_2O_3) and hybrid (water/TiO_2+Al_2O_3) nanoparticle suspensions. The

experimental studies include the preparation, characterization, and optical property measurements of the nanoparticle suspensions. The impact of the electrostatic stabilization (zeta potential and pH values) on the size and structure of particles due to agglomeration behavior are explored. The particle size distribution and the average (effective) particle agglomerate size for the nanoparticle suspensions in different conditions (the pH and particle volume fraction) were measured by using the dynamic light scattering (DLS) technique. The effects of the different particle agglomerates under different pH values on the dependent and independent scattering and their boundaries are investigated and demarcated for different conditions, where the relationship between the distance between particle to particle surface and the incident wavelength for different particle types are explored. The effects of particle agglomeration (similar and dissimilar particle agglomerations), particle size distribution and their contributions to the radiative properties of the nanoparticle suspensions are determined using the UV-Vis spectroscopy technique. The numerical part included the study of the optical and radiative properties and thermal radiation transfer based on the average (effective) particle agglomerate size obtained from the experimental studies. The optical and radiative properties of nanoparticle suspensions are calculated based on the Lorenz-Mie theory applying the single-scattering approximation technique. The influence of the particle size distribution on the scattering coefficient of nanoparticle suspensions is studied theoretically to account for the effect of compact particle agglomerates. The thermal radiation transfer in the nanoparticle suspensions is assessed by solving the radiative transfer equation using the discrete ordinates method, where the volumetric radiative heat flux and the thermal flux efficiency are calculated.

The results show the impact of pH value on the stability of individual and

hybrid nanoparticle suspensions. The different particle agglomerate types, sizes, and shapes yield different behavior of suspensions, including their stability or sedimentation rates, which help formation of optically thicker media. Light scattering in such media is significantly different as a function of the proximity of particles to each other. If they are closer to each other roughly less than dominant wavelength of the radiation, then their behavior is defined as dependent scattering, which is explored in this study. It is shown that a significant enhancement in the radiative properties, specifically in the UV/Vis spectrum, can be observed , which has an important effect on the thermal radiation transfer of the incident solar radiation. The demarcation of dependent and independent scattering regimes is explained for the individual and hybrid nanoparticle suspensions based on their pH value. NPSs with different effective particle agglomerate sizes have a considerable effect on the volumetric radiative heat flux, where the losses in radiative energy were decrease in comparison to those of pure water. The results also show the effects of composite particle agglomerates in the hybrid nanoparticle suspensions on the radiative properties, which are produced from dissimilar suspended particles.

The results of this dissertation show that the pH value has a dominant effect on the radiative transfer involving nanoparticle suspensions, compared to other parameters. Adjusting the pH value based on the isoelectric point of the nanoparticle is an efficient method when specific radiative properties are required for specific applications. Such impact of pH value on optical and radiative properties of NPSs is studied for the first time in the literature.

ÖZETÇE

Nanopartikül süspansiyonlar (NPS) 100 nm den küçük nano-parçacıkların bir baz sıvı içersinde katı-sıvı olarak bulundukları karışımlardır. NPS termal ve optik özelliklerinden dolayı farklı termal sistemler de termal verimliliği artırmak için yaygınca kullanılır. Solar termal sistemler nonopartükel süspansiyonların en çok kullanıldığı sistemlerdir. Bu sistemlerinin verimliliği, güneş enerjisinin system sıvısı tarafından en çok emilmesi (absorb edilmesi) ile ölçülür. Foto-termal enerji çevrimine ilaveten, nanopartikül süspansiyonlar, kaplamalarda ve boyalarda da optik ve spektral özelliklerden dolayı, esas olarak nesnelerin görünümünü iyileştirimek amacıyla, önemli bir rol oynarlar. Öte yandan, nanopartikül süspansiyonların uzun süreli kullanımı ve stabilitesiyle ile ilgili sorunları vardır. Nanopartikül topaklaşması, kullanımı esnasında en çok görülen problemlerden birisidir. NPS kullanım aşamasında, pH değerlerindeki değişiklikler partikül topaklaşması, nanopartikül stabilitesi ve optik özelliklerini etkiler. Bu nedenlerle, NPS sistemlerinde pH değerini değiştirerek ışınımla ısı transferini etkilemek mümkündür.. NPS stabiletesi için kullanılan metodlar arasında elektrostatik ve sterik stabilizasyon metodlari vardır. Termal uygulamalarda ve bilhassa yüksek ısı uygulamalarında elektrostatik stabilizasyon daha çok tercih edilir.

Bu tez süresince, aynı tür (su/TiO_2 ve su/ Al_2O_3) ve hibrid (su/TiO_2+Al_2O_3) nanopartikül süspansiyonların stabilitelerini ve optik özelliklerini hem deneysel hem de sayısal olarak çalışılmıştır. Deneysel bölüm, nanopartiküllerin hazırlanışı, karakteristikleri ve optik özelliklerinin ölçümünü içerir. Bu amaçla, topaklaşmadan

kaynaklanan partikül büyümesinin elektrostatik stabilizasyonu (pH ve zeta potansiyel değerleri) araştırılmıştır. Dinamik ışık saçılması tekniğiyle (DLS) partikül boyut dağılımı ve ortalama (efektif) partikül boyutu farklı şartlarda (pH ve partikül hacim fraksiyonu) ölçülmüştür. Farklı partikül topaklaşmasının etkileri, farklı ph değerlerine bağlı olarak irdelenmiştir. Ayrıca, partikül-partikül arası mesafe bağlantısı ile farklı partikül tiplerinin dalga boylarına oranlarının optik özelliklerine etkisi de incelenmiştir. Partikül topaklaşma efektleri (benzer ve benzemeyen partikül topaklaşmaları), partikül boyut dağılımı ve bu nanopartikül süspansiyonların dağılım katsayı faktörlerinin katkısı UV-Vis spektroskopy tekniği kullanılarak bulunmuştur. Sayısal çalışmada ise, ışınımla ısı transferi hesaplamaları için optik ve ışınımsal özelliklerin değerlendirilmesini ve termal radyasyon transferlerini deneysel kısımdan elde edilen ortalama verilere göre değerlendirilmiştir. Emilme, soğrulma, ve saçınlanma özellikleri Lorenz-Mie teorisinin "single scattering approximation" tekniğine göre değerlendirilmiştir. Nanopartikül süspansiyonlarındaki termal ışınımsal ısı transferi "discrete ordinate" metoduyla çözülmüştür; burada volumetrik ışınımla ısı transferi akısı hesaplanmıştır.

Sonuçlar, nanopartiküllerin pH değerleri değiştirilerek aynı tür ve hibrid süspansiyonlarda topaklanmanın önlenebileceğini ve stabil olabileceklerini göstermiştir. Burada özellikle UV-Vis spektrumunda ve solar spektrumdan kaynaklanan ışınımla ısı transferi olgusunun belirgin bir etkisi olduğu gözlemlenmiştir. Aynı tür ve hibrid nanopartikül süspansiyonların pH değerlerine göre bağımlı ve bağımsız saçılmalarının (dependent/independent scattering) farklı sınırları da ayrıca çalışılmıştır. Bu sınırlar iki durum içinde irdelenmiş, ve partikül topaklaşmalı ile topaklaşmamış halleri açıklanmıştır. Partiküllerin topaklaşma büyüklüklerine göre ışınımla ısı transferine büyük bir etkisi olduğu saptanmıştır.

Bu sonuçlara göre, pH değerinin değiştirerek nanopartikül süspansiyonlarının stabiletelerini ve topaklaşmalarını etkileyebilecek çalışmalar mümkündür. Spesifik uygulamalarda, NPS optik özellikleri, nanopartiküllerin isoelektrik noktasının pH değerinin ayarlanması ile değiştirilebilmektedir. Bu gözlemler, tasarımsal olarak yeni NPS oluşturulmasına ve etkin kullanımlarına yardım edecek çok önemli bulgulardır.

ACKNOWLEDGMENTS

I would like to express my deepest gratitude to my advisor, Prof. Dr. M. Pinar Mengüç, for his inspiration, guidance and encouragement. He always supports me in all times with his invaluable contributions and guidance to my life.

I would also like to acknowledge the other members of my dissertation committee, Prof. Dr. Ali Koşar, Asst. Prof. Dr. Özgür Ertunç, and Asst. Prof. Dr. Altuğ Başol, for their valuable effort and contributions to this dissertation. I would like to extend a special gratitude to Prof. Dr. Kürşat Şendur, for his advice and contribution.

I would like to special thanks to the Center for Energy, Environment and Economy (CEEE) at Özyeğin University, Istanbul, for the support that I received during my studies. I am very proud to be a member of CEEE family.

I am grateful to my colleagues who have contributed to my Ph.D. lifespan by their wonderful friendship. Thank you for all of the meetings, chats and coffees over the years.

Thank you,

Layth

TABLE OF CONTENTS

LIST OF TABLES

LIST OF FIGURES

NOMENCLATURE

A	surface at which the electromagnetic energy crosses, m^2
C	cross section, m^2
D	diffusion coefficient
d_{agg}	particle agglomerate diameter, m
$d_{eff,agg}$	Average (effective) particle agglomerate diameter, m
d_A	diameter of a non-spherical particle equivalent to the diameter of a sphere that would have the same area, m
d_f	fractal dimension
d_H	hydrodynamic diameter of the particles, m
d_L	diameter of a non-spherical particle equivalent to the diameter of a sphere that would have the longest dimension, m
d_p	particle diameter, m
d_{per}	diameter of a non-spherical particle equivalent to the diameter of a sphere that would be the same perimeter, m
d_V	diameter of a non-spherical particle equivalent to the diameter of a sphere that would have the same volume, m
E_i, E_m, E_p, E_s	incident electric field, electric field in the medium, electric field inside a particle, and scattered electric field, respectivly
f	correction factor
g	gravitational acceleration, m/s^2
H	collector height, m
H_i, H_m, H_p, H_s	incident magnetic field, magnetic field in the medium, magnetic field inside a particle, and scattered megnetic field, respectivly
$h_{sur,p}$	surface to surface particle distance, m
I_λ	radiative intensity at wavelength, W/(m^2 sr m^{-1})
$I_{b,\lambda}$, $I_{pb,\lambda}$	black body intensity at wavelength and particle black body intensity at wavelength and current particle temperature, respectively
$\bar{k}$	index of absorption
k_B	Boltzmann constant, 1.38×10^{-23} J/K
k_{medium}	complex component of the refractive index for the medium
$\bar{k}_{ap,\Delta\lambda}$,	equivalent particle absorption coefficient
m	complex refractive index
m_{agg}	mass of particle agglomerate, kg
m_p	mass of particle, kg
N	number of particles per unit volume, m^{-3}
N_{int}	number of particles in an agglomerate
$\boldsymbol{n}$	unit surface vector directed outwards from the boundary
n	number of ordinates, number of dipoles
$\bar{n}$	index of refraction
P	moments of a dipole

Q_{scat},Q_{abs}, Q_{scat}	scattering, absorption, and extinction efficiency factors, respectively
q	radiative heat flux, W/m^2
q_{inc}	incident radiation, W/m^2
$q_{r,\lambda}$	volumetric heat flux, W/m^3
$q_{r,source}$	volumetric radiative source, W/m^3
R_{agg}	particle agglomerate radius, m
r_p	radius of the nanoparticle, m
S	Pointing vector, W/m^2
s	distance in the solid angle direction
$\acute{s}$	unit vector along the distance coordinate leaving the boundary
s^s	unit vector from the incoming ray considered for the specular reflection
T	temperature, K
T_λ	spectral transmittance
t	particle suspension time, s
t_p	particle agglomeration time constant, s
V_A	attractive force, N
V_R	repulsive force, N
V_T	tatal force, N
W	stability ratio
w_j	quadrature weights which depend on the ordinates
x	size parameter

Greek symbols

$\beta_{ep,\lambda}$, $\beta_{et,\lambda}$	extinction coefficients of the particle and the nanosuspension at wavelength, respectively, m^{-1}
$\beta(h_{sur,p})$	hydrodynamic interaction factor
ε	emisivity
$\varepsilon_{w,\lambda}$	diffuse emissivity
η_{ther}	thermal flux efficiency
θ	polar angle, rad
$\kappa_{ap,\lambda}$, $\kappa_{am,\lambda}$	absorption coefficients of the particle and the medium at wavelength, respectively, m^{-1}
κ_{abs}	absorption coefficient, m^{-1}
λ	wavelength, m
μ	fluid viscosity, kg/m.s
υ_p	sedimentation velocity of particles, m/s
π_{eff}	half moment for the ordinate set
ρ	reflectivity
ρ_p, ρ_f	density of the particle and the fluid, respectively, kg/m^3
$\rho_{w,\lambda}^d$, $\rho_{w,\lambda}^s$	diffuse and specular reflectivity, respectively
σ_{scat}	scattering coefficient, m^{-1}

$\sigma_{sp,\,\lambda}$	scattering coefficient of the particle at wavelength, m^{-1}
$\bar{\sigma}_{sp,\Delta\,\lambda}$	equivalent particle scattering coefficient
$\tau_{w,\lambda}$	interface boundary transmissivity
$\emptyset$	particle volume fraction
Ω	solid angle, sr
ω_{λ}	single scattering albedo

Abbreviations

DASC	direct absorption solar collectors
DDA	discrete dipole approximation
DISRs	dependent and independent scattering regimes
DL	double layer
DLCA	diffusion-limited cluster agglomeration
DLS	dynamic light scattering
DLVO	the Derjaguin–Landau–Verwey–Overbeek theory
DOM	discrete ordinate method
EPLS	elliptically polarized light scattering
FT-IR	Fourier transform infrared spectroscopy
HPA	homogeneous phase approach
LMT	the Lorenz-Mie theory
MPA	multiphase approach
NP	nanoparticle
NPS	nanoparticle suspension
PSD	particle size distribution
QCA	quasi-crystalline approximation
RLCA	reaction-limited cluster agglomeration
RTE	radiative transfer equation
SEM	scanning electron microscopy
TEM	transmission electron microscopy
TGA	thermogravimetric analysis
XRD	X-ray diffraction analysis

CHAPTER I

NANOPARTICLES AND NANOPARTICLE SUSPENSIONS: AN OVERVIEW

1.1 Introduction

Nanoscience is the science that deals with materials, technologies, and systems in nanometer dimensions. Nano is about the small size as it appears in the world of material science, chemistry, and engineering. Nano is a word indicating the minus 9^{th} power of ten; namely one billionth, which is applied to the size. One nanometer is very small in length, identical to one thousandth of a micrometer, one millionth of a millimeter, and one billionth of meter (Nogi et al., 2012). Therefore, the science of nanostructures is often defined as the science that deals with objects on a size scale of 1–100 nm. The nanometer scale is the smallest one when the hydrogen atom is of a diameter of approximately one-tenth of a nanometer. It can then be used for constructing machines, and these are the bases of the principles from conventional mechanics. Nanoscience is a field of modern science which has arisen over recent decades. Nowadays, it includes many different fields and research areas, and plays an important role in key technology in a wide range of engineering and industrial applications (Rodgers, 2010; Wee, 2009).

A new direction has emerged in different research fields, broadly known as "nanoscale science and technology". These new trends involve the capability of the synthesis, characterization, and the manipulation of structures whose features and properties are controlled at the nano-size level, which are adopted in different fields of research as diverse as physics, material science, and engineering. Research and

applications in this direction have been triggered by the availability of revolutionary instruments and theoretical models that allow both investigation and development. Nanoscience is strongly included in the pioneering fields of research which have revealed new properties such as physical, thermal, optical, and chemicals, etc. of matter at a level intermediate between the bulk and atomic/molecular levels (Lane, 2001).

1.2 A historical perspective on nanoscience: nanoparticles and nanoparticle suspensions

The term nano, which means dwarf, was derived from the Greek word nano which designates a fraction of a unit, e.g., of a meter (Roco, 1999). Man-made nanostructure materials in this form of nanocomposites have been known for more than 2500 years. The Sumerians used gold nanoparticles in pigment production, where a red pigment was used in the decorations of their pottery. These gold nanoparticles were stabilized with tin oxide and embedded in a glass matrix. Clearly, the fundamentals of nanostructure materials were available much earlier. In fact, 4.5 billion years ago, nanostructure materials already existed in the solar nebula or in the presolar dust as extracted from the nanosized C_{60} molecules in the Allende meteorite (Becker et al., 1999). Albert Einstein estimated in his doctoral research from the experimental data of the diffusion of sugar in water that a single sugar molecule has a size of about 1 nm [Stix, 2001]. During his lecture on the optical properties of gold in 1857, Michael Faraday remarked that ". . . a mere variation in the size of the (nano) particles gave rise to a variety of resultant colors" (Faraday, 1857). Indeed, more than 50 years earlier, R. Feynman emphasized that ". . . there is plenty of room at the bottom . . . in the science of ultra-small structures" (Feynman, 1959).

Since its early appearance, the field of nanoscience has developed more and more and obtained great importance in the worldwide scientific research. For the characterization of the nanoscience research field, the notations “Nanotechnology” or “Nanostructured” sciences were coined by Drexler K. E. (Drexler et al., 1991). The investigation and development of nanoscience and nanostructure materials began when the scanning tunneling microscope (STM) technique was discovered around 1980, and where the concept of nanostructured solids was proposed (Binnig et al., 1982; Gleiter, 1981).

Since the nineteenth century, the suspension of nanoparticle in the base medium has been well-known in the area of chemistry science; however, at that time this science was called as colloid chemistry. Nanoparticle suspensions are formed by suspending nanoparticles in base fluids such as water, ethylene glycol, and oil, etc. The term nanoparticle suspensions was coined by Choi et al. in 1995 and describes the class of new nanotechnology-based fluids that exhibit different properties superior to those of their base fluids and conventional suspended particles (Choi and Eastman, 1995). When a very small amount of nanoparticles are suspended stably and dispersed uniformly in the base fluids, this can supply significant improvements in the thermophesical properties of base fluids in addition to other properties (chemical, physical, and radiative, etc.) of suspensions. Since the novel concept of nanoparticle suspensions was conceived by Choi, the studies on nanoparticle suspensions by engineers and thermal scientists have been rapidly growing. And nanoparticle suspensions research groups have made scientific breakthroughs in discovering different concepts of nanoparticle suspensions. As a result, the research field of nanoparticle suspensions has been receiving increased attention throughout the world (Das et al., 2007).

1.3 Nanoparticles

1.3.1 Building blocks for nanoscience

Nanoparticles (NPs) are ultrafine particles in the nanometer size, and have been very interesting materials in the nanophysics and modern materials science over the past decades due to their high technological importance. Nanoparticles are neither unnatural nor new materials. In nature, for example, mammals and some birds apply magnetic nanoparticles, which is a sense called magnetoception for navigation (Roco, 1999).

Firstly, it is important to find some general conceptions regarding the nanosized materials. Nano-objects are physical objects where differ in terms of their properties from the corresponding bulk materials by having a minimum of a nanometer dimension of not more than 100 nm. The meaning of nanoparticles varies dependent upon the areas, materials, and applications. In a narrower sense, nanoparticles are considered as particles which are a size smaller than 10-20 nm, and the properties of materials would totally change in this size range. However, the particles that are in a range of a nanometer to a micrometer size could be referred as nanoparticles, but here these particles would be regarded as smaller than those that are known conventionally as "submicron particles", and less than the wavelength of visible light (its lower limit is approximately 400 nm) as a measurement. Therefore, it is necessary to treat nanoparticles differently to the submicron particles (Nogi et al., 2012).

The massive diversity of nanoparticles arises from their shapes, morphologies, chemical nature, the state of dispersion of the particles, and the medium in which the particles are present. Figure 1.1 shows the different parameters (Chemical composition, particle shape, dispersion medium, and dispersion state) which affect the

diversity of the engineered nanoparticles. Further, and importantly, because of the possible surface modifications to which the nanoparticles can be exposed; this is an essential active field of science (Nagarajan and Hatton, 2008).

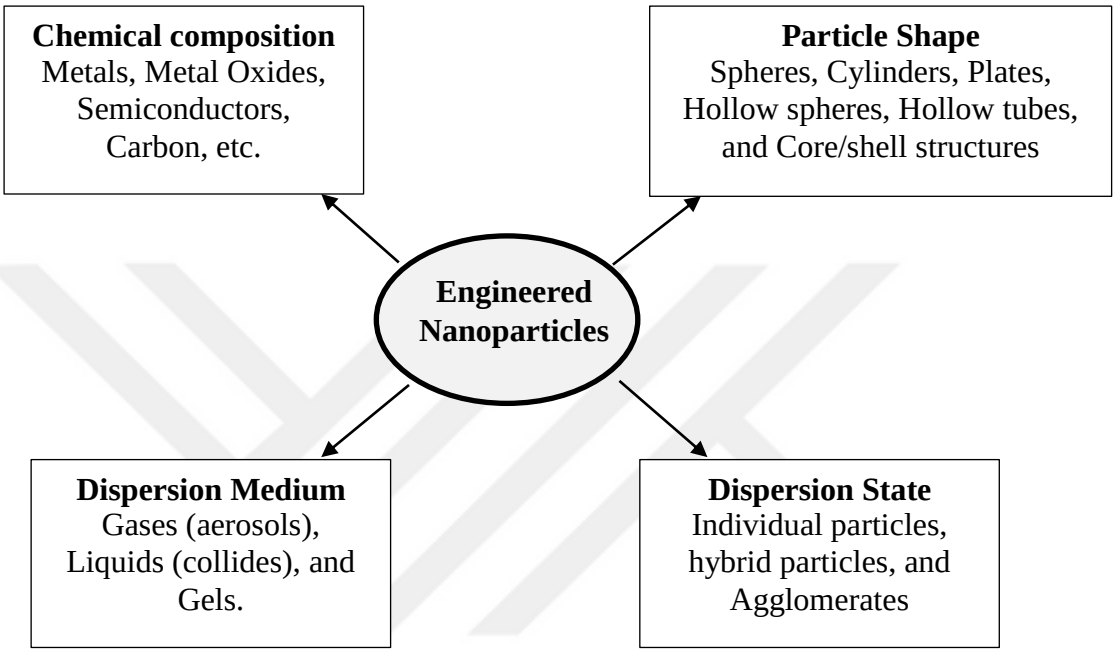

Figure 1.1 Different parameters affecting the diversity of engineered nanoparticles.

1.3.2 Synthesis of nanoparticles

Ongoing advances in nanotechnology research have established a variety of methods to synthesize NPs from a diverse range of materials, including metals, semiconductors, ceramics, and metal oxides, etc. NPs possess unique physicochemical, structural and morphological characteristics depending upon their origin and synthesis methods which are significant in a wide variety of applications concomitant to electronic, optoelectronic, optical, electrochemical, engineering, and environment fields, etc. Dependent on the required application, the nanomaterials can

be synthesized into varying shapes and dimensions. For the preparation of NPs, there are two basic approaches commonly applied; 1) The top-down approach, where synthesis is initialized with the bulk counterpart that leaches out systematically bit-after-bit leading to the generation of fine NPs. 2) The bottom-up approach, which involves the coalescence or assembling of atoms and molecules to generate diverse range of NPs. In general, NPs synthesis methods can be divided into two groups; 1) physical methods, 2) chemical methods (Dhand et al., 2015; Schmid, 2005).

By using a variety of methods, the gas, liquid or solid phase processes can be used to synthesize NPs. These include gas phase processes, in which physical and chemical vapor deposition synthesis; colloidal or liquid phase methods, in which chemical reactions in the solvents cause the formation of colloids; and mechanical processes of size reduction, which include grinding, milling and alloying (Vollath, 2013).

As shown in Figure 1.2, gas phase synthesis approaches are founded on the homogeneous nucleation of a supersaturated vapor and subsequent particle growth by condensation, coagulation and capture. The methods vary in the way that the starting molecules are generated by vaporization or by chemical reaction/precipitation. The nuclei may be amorphous or crystalline and lead to amorphous or crystalline nanoparticles. Because of their intrinsic instability, the nanoparticles may form agglomerates that can be easily re-dispersed or form non-dispersible aggregate clusters (Nagarajan and Hatton, 2008; Schmid, 2005). Depending on the chemical nature of the material, the supersaturated vapor can be generated in many ways; however, it is usually carried out by heating a solid and evaporating it into a carrier gas phase. The supersaturation is obtained by cooling or by a chemical reaction or by a combination of these. The supersaturated vapor can be nucleated homogeneously in the gas phase

and also heterogeneously through contact with the surfaces. The nuclei grow by collision and condensation to give rise to a distribution of particle sizes and morphologies. A wide range of gas phase methods such as flame pyrolysis (fumed silica, TiO_2), laser induced vaporization and pyrolysis (silica and iron), thermal and microwave plasmas (metals and metal oxides), sputtering (metals) depending on the heating and cooling process used, and a laser ablation was applied (Nagarajan and Hatton, 2008). Vapor deposition methods are based on forming a vapor by pyrolysis, followed by reduction, oxidation and by allowing the deposition of the vapor on a surface. Starting from the initial nuclei existing as islands on a surface, the growth is controlled by various ways to produce nanoparticles (TiO_2, ZnO, SiC). An important example of this approach is the production of carbon nanotubes (Dhand et al., 2015).

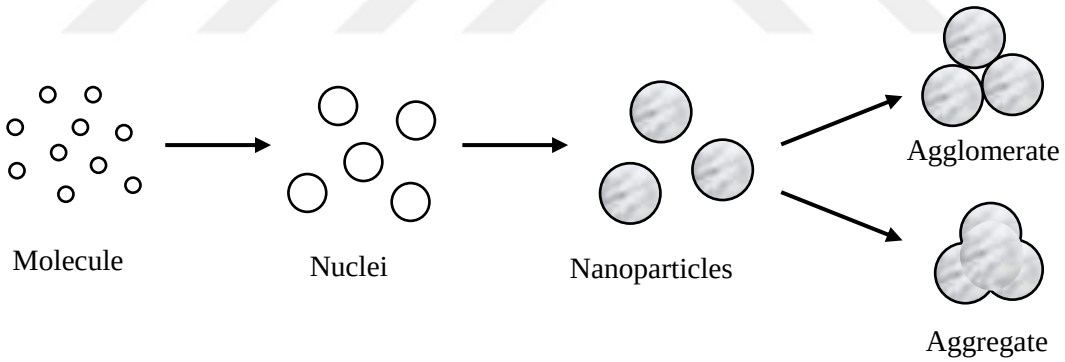

Figure 1.2 Mechanism of nanoparticle production using vapor phase or liquid phase/colloidal methods (Nagarajan and Hatton, 2008).

Colloidal methods are based on the precipitation processes in solutions. For example, solutions of different ions can be mixed under the controlled conditions of temperature and pressure to form insoluble precipitates. By controlling the nucleation

and growth kinetics, particles of various sizes and morphologies can be produced. The method has been implemented in bulk solutions and also in confined systems such as reverse micelles. To control the process of nucleation, ultrasonic or sonochemical effects have also been employed. A wide range of metal, metal oxide and organic nanoparticles have been produced by the colloidal wet chemical approach (Vollath, 2013). The molecular self-assembly method is a spontaneous process by which nanoparticles are created starting from molecules. This is a particularly effective method for the production of polymeric nanoparticles starting from amphiphilic block copolymer molecules. An added advantage of this approach is the ability to produce thermodynamically stable nanoparticles whose sizes and shapes can be controlled by the choice of the block copolymer (type, block composition, and molecular weight) and the choice of the solvent and self-assembly conditions. As well as the nanoparticle synthesis approaches in the gas or liquid phases, there is also the possibility of using solid substrates as heterogeneous nucleating sites to build up the nanoparticles at the solid-liquid interfaces. Undeniably, by using patterned surfaces, it may be possible for the nucleation and growth processes to be controlled, thereby affecting the nature of the nanoparticles that are produced (Vollath, 2013).

All of the above synthesis approaches start at the molecular level to build up or create the nanoparticles. In the opposite direction, mechanical size reduction methods such as grinding and milling have also been used to generate nanoparticles. These types of methods are the traditional approaches used to produce fine particles, and to generate nanoparticles from minerals such as clay, coal and metals has been possible in these ways. To prevent particle agglomeration in the course of the size reduction process, the grinding and milling operations are frequently done with colloidal stabilizers (Schmid, 2005).

1.3.3 Basic properties of nanoparticles

All the solid particles consist of atoms or molecules. As they are in a micron size, the behavior of atoms or the molecules affect the behavior of their corresponding particles and these particles show different properties from those of the same bulk same materials. It is attributable to the change of the bonding of the atoms or the molecules which construct the particles. For the micron size solid particles, the surface area is increased in terms of the particle size. In this case, when the particle of 1cm decreases in size to 1μm and 10 nm, the surface area becomes ten thousand and a million times, respectively. As the increase in the specific surface area directly influences such properties such as the solution and reaction rates of the particles, it is one of the major reasons for the unique properties of the nanoparticles differing from the bulk material together with the change in the surface properties of the particles (Das et al., 2007; Lane, 2001).

As mentioned above, with the decreasing particle size, the solid particles generally tend to show different properties from the bulk material and even the physical properties such as the dielectric constant and the melting point, which are considered as the specific properties of the particles may change when the particles become of nanometer size. This change in the fundamental properties of the particle size is called the "particle size effect" in a narrower sense (Das et al., 2007). In a broader sense, it could also include the change in the different behaviors and characteristics of the particles with the particle size. The nanoparticles have different unique features in the various properties, including mechanical, electromagnetic, optical, and thermal, as described in the following:

1.3.3.1 Mechanical properties

It is known that the hardness of the crystalline materials generally increases

with the decreasing crystalline size, and that the mechanical strength of the materials significantly increases by decreasing the size of the metal and ceramic material or composing them in the nano range (Koichi, 1991). Moreover, because the ceramic material has a crystalline size less than several hundred nanometers, the unique superplastic phenomenon shows that it extends several to several thousand times from the original size at the higher temperature of over 50% in the melting point, which may make it possible of form and process ceramics such as metallic materials (Das et al., 2007).

1.3.3.2 Electromagnetic properties

Nanoparticles are used in a wide range of electronic devices. Particle size and the electrical properties of these nanoparticles have a significant role in terms of the improvement of product performance (Matsui, 2005). As an example, there is a strong demand for materials with a high dielectric constant to develop small and thin electronic devices.

Concerning the magnetic property; ferromagnetic fine particles possess one single magnetic domain structure as they become very small as in the order of less than approximately 1 μm and show a super-paramagnetic property when they get even further. In this respect, although the individual particles are ferromagnetic with one single magnetic domain structure, the particles collectively act as a paramagnetic. It is magnetized as a whole in the same direction as the external magnetic field; however, the magnetization vanishes because the thermal fluctuation when the external magnetic field is taken away. The time that the magnetization disappears depends upon the particle size, meaning that the magnetization of the material responds quickly to the external magnetic field as a paramagnetic when the particles are small enough, but gradually decreases as the particle size becomes larger. As a result of such a

change in the electromagnetic properties of the nanoparticles, it is known, for example that gold, being a stable substance, as a bulk, demonstrates unique catalytic characteristics as nanoparticles (Kestell and DeLorey, 2009).

1.3.3.3 Optical properties

Nanoparticles possess interesting optical properties; absorption, scattering, and emission. They exhibit enhanced optical properties regards to the small size of the particles. As the size of the particles reaches the several nanometers range, they absorb the light with a specific wavelength as the plasmon absorption is caused by the plasma oscillation of the electrons and the transmitted light with different color depending upon the kind of material and particle size obtained. Characterization and measurement of the optical properties of nanoparticles with different anisotropic shapes have drawn significant attention, which have the potential applications in different systems including photo-thermal devices (Kumbhakar et al., 2014; Matsui, 2005).

The optical properties are closely related to the electromagnetic properties of the material. But as we shall see other factors also come into the picture when dealing with optical properties. When one is talking about optical properties of nanoparticles, one is usually referring to the interaction of electromagnetic radiation with these particles. The simple picture one can start with is by considering a ray of an electromagnetic wave entering a medium from vacuum. This ray could be reflected, transmitted (refracted) or absorbed. From a more fundamental perspective, there are only two possibilities (of interaction of a medium with electromagnetic radiation): scattering and absorption. If one considers a wider spectrum of frequencies, then some part of the spectrum could be absorbed while the other frequencies could be scattered (Hoffman and Driggers, 2016; Hulst and van de Hulst, 1957).

1.3.3.4 Thermal properties

When the atoms and molecules based on the particle surface become effective in the nanometer order, the melting point of the material decreases from the bulk material because they have a tendency to move easier at the lower temperature. The decline in the melting point of the ultrafine particles is thought to be one of the unique features of the nanoparticles in terms of the agglomeration and grain growth of the nanoparticles or the improvement of the sintering performance in the ceramic materials. The nanoparticles usually illustrate collective functions, so the dispersing state and the surrounding conditions as well as the physical properties of the particles themselves are indeed significant. In many situations, the nanoparticles are there as the agglomerates of the primary particles because of the adhesion and bonding throughout the process of production because of their strong adhesiveness (Das et al., 2006).

The existing state of the nanoparticles is greatly influenced by the surrounding conditions if they are in gas, liquid, solid or in a vacuum, and because of the type of interaction they have with the surrounding materials. The nanoparticles are rarely used by themselves, but are dispersed in other materials or combined with them. The dispersing process of the nanoparticles is a key for the nanoparticle technology as well as their preparation methods since the performance of the final products are affected by their dispersing conditions (Drexler et al., 1991). In this way, it is expected to be able to develop various new materials and applications by the nanoparticle technology producing and processing the nanoparticles, which have different properties from the bulk materials as mentioned above.

1.4 Nanoparticle suspensions

Nanoparticle suspensions (NPSs), suspensions of nanoparticles in base fluids in

the form of the solid-fluid mixture are widely involved in different engineering and industrial applications. NPSs can be prepared by dispersing single type NPs in a base fluid (individual NPSs) or by dispersing more than one type of NPs in a base fluid (hybrid NPSs). Since the first synthesis of NPSs, many researchers have found different and innovative applications for this type of suspension under the term nanotechnology. They have shown remarkable enhancement in thermophysical and radiative properties compared with those of base fluids. This enhancement contributes to improving the behavior and efficiency of different systems including solar thermal power plant and solar chemical processes. Several research studies have shown that an innovative method for the improvement in the thermal behavior of the base fluids involves suspending small solid particles in a nano-size range within it (Keblinski et al., 2005; Wang et al., 2003). The particle size distribution both before and after dispersion should be investigated extensively in order to verify the possibility of these nanoparticles being dispersed into base fluids. In NPSs, particle concentration and system heterogeneity have important influences on the heat and mass transfer, where the thermal transport in NPSs depends on different parameters such as particle size and size distribution, shape, and particle concentration. Therefore, it is quite important to include the effects of all these parameters in the investigations in order to explore their impacts on the mechanisms of heat and mass transfer in different types of NPSs (Choi et al., 2004; Xie et al., 2005).

An aerosol is one example of NPSs, it is a colloidal of liquid droplets or solid fine particles in air or any other kinds of gases. Aerosols can be classified as both artificial and natural. Some examples of artificial aerosols are: dust, particulate air, haze, smoke, and pollutants; and fogs, geyser steam, and forest exudates are some examples of natural aerosols. They may also result from the break-up of agglomerates

or the resuspension of powdered material. Nanofluids represent other types of NPSs, where particles in the nano-size with different types and structures are dispersed into the base fluids such as water and others. The distinct properties of nanofluids make them attractive and are implemented in various applications (Seinfeld and Pandis, 2016; Sheldon, 2000).

The composition of a homogeneous mixture is two or more substances that may not be noticeable in the mixture, even when using a microscope. Homogeneous mixtures are mainly composed of gases and miscible liquids, e.g., air or a mixture of water and alcohol. The constituents of a homogeneous mixture are not easily separated by using mechanical means such as precipitation or centrifugation. On the other hand, a heterogeneous mixture is composed of parts which can be distinguished with the naked eye or by using a microscope. Colloidal suspensions, emulsions, and NPSs are composed of distinguishable parts and are heterogeneous mixtures (Gibbs, 1879). Often, times colloids and NPSs are characterized as homogeneous suspensions. This term implies that the solid particles are uniformly distributed in the fluid, not that the suspension has the characteristics of a homogeneous mixture. Basically, everything except the vacuum is heterogeneous. Even in media which are considered to be homogeneous (e.g., pure gases and liquids), it is possible to distinguish the individual heterogeneities (molecules and atoms) with specific methods.

1.5 Characterization of nanoparticles and nanoparticle suspensions

The size of a spherical particle is equal to its diameter. The “size” of a non-spherical particle is subject to interpretation and must be well defined. However, the “size” of most of the irregularly shaped nanoparticles that are used with NPSs is not a well-defined variable. Following the practice of spherical particles, for which most of

the analytical and experimental work has been performed; an equivalent diameter may be defined for non-spherical particles. There have been several equivalent diameters proposed for non-spherical particles including the diameter of a sphere that would have the same area as ($d_A = \sqrt{4A/\pi}$); the diameter of a sphere that would be the same volume as ($d_V = \sqrt[3]{6V/\pi}$); and the diameter of a sphere that would be the same perimeter as ($d_P = P/\pi$) projected in the direction of the motion of the non-spherical particle as can be seen in Figure 1.3. For a sphere the three equivalent diameters are the same and equal to the actual diameter. Figure 1.3 demonstrates schematically the three diameters or "sizes" for a particle showing as an elongated parallelepiped. The three equivalent diameters, which are also depicted, which vary significantly in magnitude, can be seen in this figure. A precise definition or measurement of the "size" of particles must include how this "size" has been defined or measured because of this significant variation. A fourth equivalent diameter used with irregular particles and agglomerates, is the diameter of the minimum sphere, in which the irregular particle will fit. Typically this is the longest dimension of the particle, d_L (Michaelides, 2013; Michaelides, 2013).

The corresponding radii of the four diameters will be denoted as r_V, r_A, r_P, and r_L. While d_P depends on the direction for the motion of the particle and its magnitude may vary in an arbitrary way for all the shapes the inequality $d_V \leq d_A \leq d_L$ holds, with the equal sign applying to the spheres only (Michaelides, 2013).

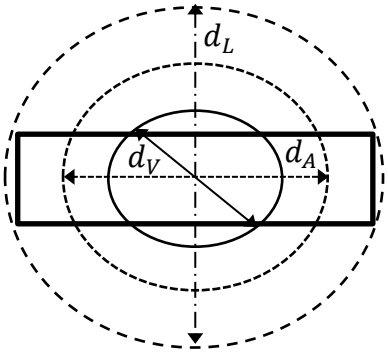

Figure 1.3 A schematic diagram of the three equivalent diameters for a particle with a parallelepiped shape (Michaelides, 2013).

The fractal dimension of particle agglomerates has been defined and used in many recent studies. To calculate the fractal dimension requires many measurements and calculations. However, it is not apparent how to make use of established results for spherical particles, e.g., for drag or heat transfer coefficients, with the fractal dimension of the irregularly shaped particles, and of this reason, this measure of size has not been widely used in engineering practices with particulate applications including NPSs (Bushell et al., 2002; s Vicsek, 1992). Another extensively used definition of an equivalent diameter with the sediments and sedimentary suspensions of the particles is the "sieve diameter," which is obtained from a sieve mesh analysis. This is the maximum standard sieve mesh size (or the minimum sieve aperture) through which the particles may pass through. However, the standard sieves do not extend to the nanometer size and this method does not extend to the nano-size range and is not used with NPs and NPSs (Schwarzkopf et al., 2011).

Unlike the spheres that only have only one significant length scale, nanoparticles have irregular shapes and several characteristic dimensions. For this reason, the size and surface characteristics of nanoparticles are typically inferred from several methods. The NPSs are characterized by the following techniques: scanning

electron microscopy (SEM), transmission electron microscopy (TEM), X-ray diffraction analysis (XRD), Fourier transform infrared spectroscopy (FT-IR), dynamic light scattering (DLS), thermogravimetric analysis (TGA), zeta potential analysis, static light scattering, and Elliptically polarized light scattering (EPLS). SEM analysis is carried out in order to study the micro structure and morphology of either nanoparticles or nanostructured materials, and TEM is like SEM, but a much higher resolution than SEM. XRD images are taken to identify and study the crystal structure of nanoparticles. FT-IR spectroscopy is carried out in order to study the surface chemistry of solid particles. DLS analysis is done to estimate the particle size distribution and the average disperse size of nanoparticles in the base liquid media. TGA is conducted to study the effect of heating and melting on the thermal stabilities of the nanoparticles. Related to the stability of nanoparticle dispersion in base fluid is the zeta potential. The static light scattering technique samples huge numbers of agglomerates at the same time, and gives a statistical average of the mixture for the agglomerate. EPLS techniques are also based on static light scattering and give even more details about the size, size distribution, shape and structure of the particles or their agglomerates (Aslan et al., 2006; Govindan et al., 1995; Mengüç and Manickavasagam, 1998; Mengüç, 2003).

Studies on the characterization reveal that important information such as the nanoparticle size, shape, chemical bonds, distribution and stability are discovered from characterization techniques. However, different set of techniques have been used by researchers and thus, there are no recommended standard tests which could confirm the heterogeneous and stable NPSs. To confirm the long term stability of dispersed nanoparticles in base fluid, standard accelerated tests should be carried out (Devendiran and Amirtham, 2016).

1.6 Nanoparticles/nanoparticle suspensions and radiative transfer

In many systems relevant to modern energy technologies, thermal radiation is a dominant mode of energy transfer. The majority of systems within this category are either porous in nature or contain particulates that actively participate in radiative transfer processes. Various examples of the particulate systems are fluidized and packed beds, surface combustors, catalytic reactors, microsphere and fibrous insulations, ceramic foam insulations, ceramic and metallic screens, porous and sintered materials, particulate solar collectors, and liquid-droplet radiators, which are used in different applications. Other examples where radiation from particles plays a significant role are: a nuclear winter scenario, large scale fires, and radiation transfer in the core debris of a melted reactor or in a containment building and numerous others (Gupta et al., 2012; Mishchenko, 2014; Rao et al., 2014).

Radiative transfers as well as combined heat transfer by conduction and radiation through participating, dispersed media capable of absorbing, emitting, and scattering radiation are significant problems in terms of engineering. All media scatter light and when photons so called electromagnetic waves interact with a medium including small particles, the radiative intensity may be changed due to scattering and/or absorption. How much and into which direction a particle scatters an electromagnetic wave depends on important parameters, which include the shape and the type of the particle, the clearance between particles, its relative size, medium properties, and incident wavelength (Bohren and Huffman, 2008; Minkowycz et al., 2016).

Radiative transfer has a crucial role in various engineering applications that comprise of continuous solid or fluid media embedding dispersed particles, which are generally referred to as “dispersed media”. Examples of these applications are the

photo-thermal energy conversion systems, the solar-thermochemical energy conversion, material processing, microstructure diagnostic via light scattering, fire suppression by water sprays, thermal insulations, and thermal barrier coating, etc. If a substance (solid, liquid, or gas) is so finely insolubly distributed in a homogeneous or heterogeneous medium that it is in a considerably higher state of energy, by virtue of a large surface area, then in its compact phase, the system will be considered as the dispersed phase. In this definition there are materials which contain holes dispersed in a solid matrix, where the scattering of radiation with bubbles instead of particles is to be considered. There are numerous high porosity materials, such as fibers, powders, foams, refractory materials, porous solids, composite materials, fluidized and packed beds which are widely used in many industrial applications. In such media, the relative importance of different modes of heat transfer depends on the physical properties of the material, as well as on the operating conditions. From a radiative transfer perspective, these materials act as participating media. For an accurate prediction of the coupled heat transfer, a simultaneous solution of the energy conservation equation and of the radiative transfer equation (RTE) is required. Of course, also needed are the radiative properties of the medium (Hoffman and Driggers, 2016; Howell et al., 2015; Modest, 2013). One obvious reason for this is the rapid increasing progress in modeling radiative heat transfer in two and three-dimensional, radioactively participating dispersed media. There are however, many more problems related to radiative transfer that have yet to be analyzed. In particular, radiative heat transfer in heterogeneous ones or multidimensional dispersed media are not well understood. Considering the importance of such systems to practical and industrial applications, the need for more research in this area has been recognized (Viskanta and Menguc, 1989). Because an exact solution for the radiative transfer issue in these particular

systems cannot be achieved, at least in the near future, coarse approximations are required. Treating the dispersed medium as continuous and homogeneous, and using the standard RTE with "effective radiative properties", which is different from the radiative properties of dilute media, is the most common assumption. This approximate method is known as "homogeneous phase approach, HPA". Another less-frequented technique is called the "multiphase approach, MPA" consisting of assigning to both continuous and dispersed phases, their own transport equation, but coupled with each other and their own effective radiative properties. Therefore, through the MPA, each phase is able to have its own temperature field (Randrianalisoa and Baillis, 2010). As far as we are aware, the capability of the MPA to model the radiative transfer in dispersed materials has yet to be sufficiently studied.

1.7 Scope and organization of the dissertation

This research is concerned with the interaction of electromagnetic radiation with particles and particle agglomerates in suspensions, which have important implications in a wide range of applications including solar energy utilization and coatings. Through the analysis of the major solar energy utilization technology, it is clear that photo-thermal conversions are important not only for the solar thermal utilization, but also for electricity generation and solar chemical technology. Solar thermal systems collectors are the most important part in those systems. Therefore, in this research, thermal systems collectors/pipes radiative efficiency is investigated in order to obtain an enhancement in their operation. Nanoparticles are used to increase the efficiency and reduce the size of the thermal systems (i.e. Energy efficient solar collectors), by using light induced energy conversion in the suspended nanoparticles, which refers to the direct absorption of solar radiation (Volumetric photo-thermal

energy conversion). There are different application fields based on light scattering and absorption by small particles, but in this research the focus is on the thermal scope. The thermal field includes solar water heating system collectors, green buildings applications in terms of optical and radiative properties.

The aim of this research is to investigate the effect of electrostatic stabilization on the radiation transfer mechanisms in TiO_2 and Al_2O_3 NPSs, both experimentally and numerically. The experimental part covers the preparation and characterization of the NPSs, where the effects of electrostatic stabilization (pH and zeta potential values) on the increasing effective particle size because of the particle agglomeration behavior, are explored. The numerical section includes the estimation of radiative properties and thermal radiation transfer based on the average (effective) particle agglomerate size that was obtained from the particle size distributions in the experimental part. The thermal radiation transfer is attained through solving the radiative transfer equation by the discrete ordinate method.

This dissertation is divided into six chapters: Chapter One demonstrates an overview of the nanoparticles and nanoparticle suspensions. A historical perspective on nanoparticles and nanoparticle suspensions is shown. Nanoparticles synthesis and their basic properties are explained. Nanoparticle suspensions concepts and characterization are explained. The radiative transfer in the nanoparticles and nanoparticle suspensions is also explained in this chapter.

Chapter Two shows a literature review on the nanoparticles and nanoparticle suspensions, which covers the following topics: Preparation and characterization of nanoparticle suspensions, pH value and nanoparticle suspensions, thermal radiation in nanoparticle suspensions, light scattering by nanoparticle suspensions, and applications of nanoparticles and nanoparticle suspensions (general applications,

radiative transfer applications, and renewable energy applications).

Chapter Three includes the interaction of light with particles and agglomerates, where the optical and radiative properties of nanoparticle suspensions are explained. The methods for optical and radiative properties and explanations includes; the Lorenz-Mie theory, the discrete dipole approximation method, and the Quasi-crystalline approximation method. The experimental techniques for the optical and radiative properties of the nanoparticle suspensions are shown, where the UV-Vis spectroscopy technique is explained for this purpose.

Chapter Four shows the research methodology which is divided into two sections; experimental and theoretical sections. In the experimental set-up section, the materials and devices which are used in the research are explained. Also, the experimental procedure is shown. In the theoretical section, the effect of the pH value on particle agglomeration, optical and radiative properties of nanoparticle suspensions, and the radiative transfer in nanoparticle suspensions are explained.

Chapter Five demonstrates the preparation, stability, and characterization of nanoparticles suspensions. The general issues and concerns and the preparation methods of nanoparticle suspensions are explained. The stability of the nanoparticle suspensions is shown, which includes the stability methods and electrostatic stabilization and pH effect. Nanoparticle agglomeration mechanisms and the pH value and particle agglomeration; particle granulometry and morphology are explained. The characterization of the nanoparticle suspensions; particle size and size distribution are explained. The related results and discussion are also included in this chapter.

Chapter Six includes the radiative transfer in the nanoparticle suspensions, the effects of the particle size and size distribution on the radiative properties are explained. Both dependent and independent scattering in nanoparticle suspensions is

shown; including the boundaries of the dependent and independent scattering and the effects of the pH and particle agglomeration on the dependent and independent scattering. The thermal radiation in the nanoparticle suspensions is explained, where the radiative heat flux and the numerical solution (the discrete ordinate method) are explained. The related results and discussion are also included in this chapter.

Chapter Seven shows the concluding comments and future studies, and the summary and future studies are explained.

1.8 Research objectives

1.8.1 Motivation

Due to the increasing concerns regarding global climate change, the use of renewable energy sources for power generation is becoming a necessity. New and different renewable energy modalities, mean that solar energy is the most attractive method in most regions of the world. In addition to the vast use of solar-PV (photovoltaic) systems, solar-thermal applications are also becoming widely available. In time, their prices will unavoidably drop and their reliability will increase. Unsustainable energy resources are unstable and expensive, and create a new trend for the reliance of modern technologies and engineering applications of renewable energy resources particularly solar thermal collectors. They are used for solar energy concentration, which is the most important part in solar thermal systems. Due to the low solar absorption of conventional working fluids, the efficiency of these collectors is usually low. Referring to the progress in nanotechnology over the past few years or so, applications of suspended nanoparticle in solar thermal collectors can be proposed. Nanoparticles are found to be an effective electromagnetic wave absorber within the UV–Visible wavelength range, where short wavelength radiations include high energy

photons. It is worth mentioning that 85% of solar energy is dissolved within the UV–Visible range; while, conventional base fluids absorb about 15% of it within the infrared region as shown in Figure 1.4 (Otanicar et al., 2009; Phelan et al., 2013; Tyagi et al., 2009).

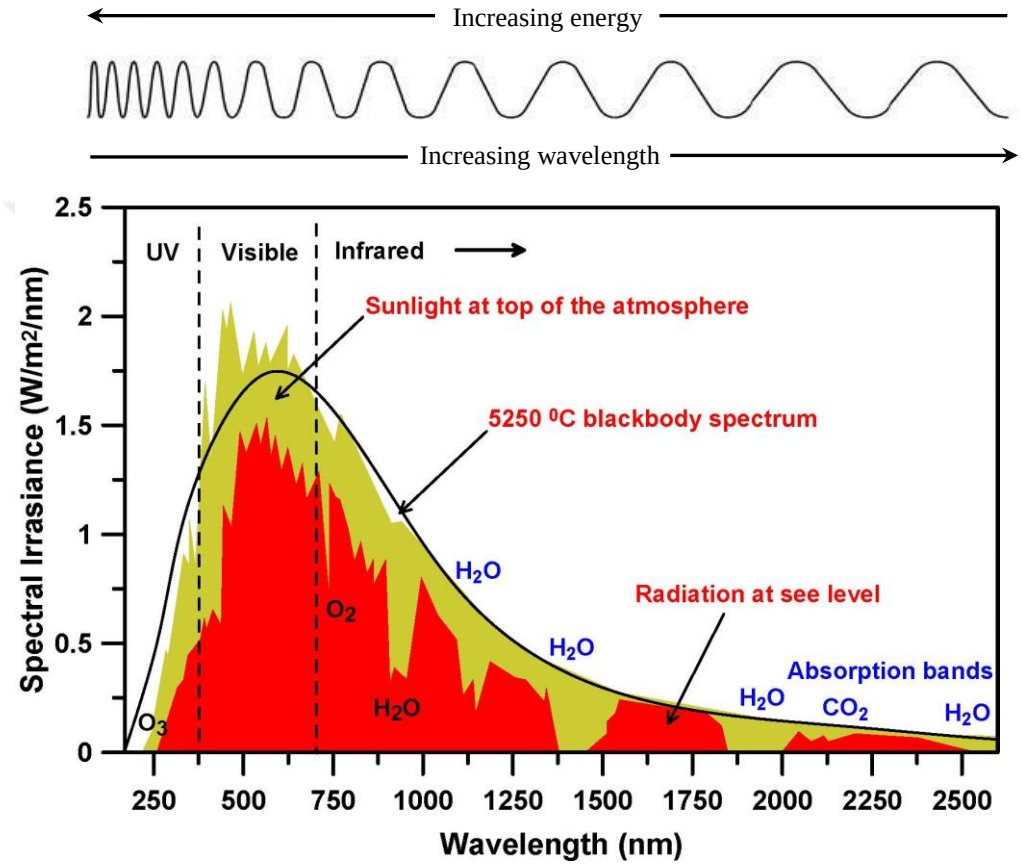

Figure 1.4 The wavelength ranges of the solar spectrum radiation (Du and Tang, 2015).

Applications of the flow, heat, and mass transfer of the particles, bubbles, and drops exist both in everyday life and in engineering practices. Many natural systems and engineering systems, ranging from nuclear reactors to internal combustion engines, and thermal systems are examples of this. Nanoparticle suspensions have

following benefits when compared to conventional fluids and other colloidal suspensions (Bianco et al., 2015; Gupta et al., 2012; Rao et al., 2014):

1. Because of the very small particle size, the suspended nanoparticles increase the surface area and the heat capacity of the medium.
2. The suspended nanoparticles enhance the thermal conductivity which results in an improvement in effectiveness of the heat transfer systems.
3. Heating within the fluid volume, transfers heat to a small area of fluid and allows the peak temperature to be based away from surfaces which lose heat to the environment.
4. The mixing fluctuation and turbulence of the fluid are intensified.
5. To make it suitable for different applications, the properties of the fluid can be changed by varying the concentration of nanoparticles.
6. Higher stability of the NPSs compared to other colloidal suspensions.
7. Lower pumping power needed in order to achieve the equivalent heat transfer.
7. Decreased particle clogging when compared to conventional colloids.
9. Unique thermal and radiative properties.
10. Absorption of solar energy will be maximized with the change in the size, shape, material, and volume fraction of the nanoparticles.
11. Higher level of control of the thermodynamics and transport properties through the variation of the particle material, concentration, size, and shape.

From the previous points, understanding particle agglomeration, particle size distribution and their effect on the radiative properties of NPSs is very important in different applications such as:

1. Photo-thermal energy conversion including solar energy harvesting and conversion (working media in solar thermal collectors).

2. Manipulation with radiative and thermal properties of material particles to obtain required properties for a specific application.
3. Surface coating with desired thermo-optical properties of particles and their agglomerates.

Indeed, promising applications can be achieved by the manipulation with radiative properties of NPSs by a trade-off between other properties (chemical and physical) of the medium and suspended particles. Adjusting the radiative properties of NPSs and particle agglomerate opens the door for different applications, where these agglomerates are in a suspension case or in other cases like particle surface deposition and coating (Bianco et al., 2015).

1.8.2 Specific objectives

The ultimate objective of this research is to investigate the effect of the electrostatic stabilization of NPSs on the particle agglomeration behavior, and to investigate these effects on the radiative transfer in NPSs. Figure 1.5 shows the graphical structure of this research. This figure shows the effect of the different topics related to particle stability and gglomeration on the radiative transfer problems considering pH value.

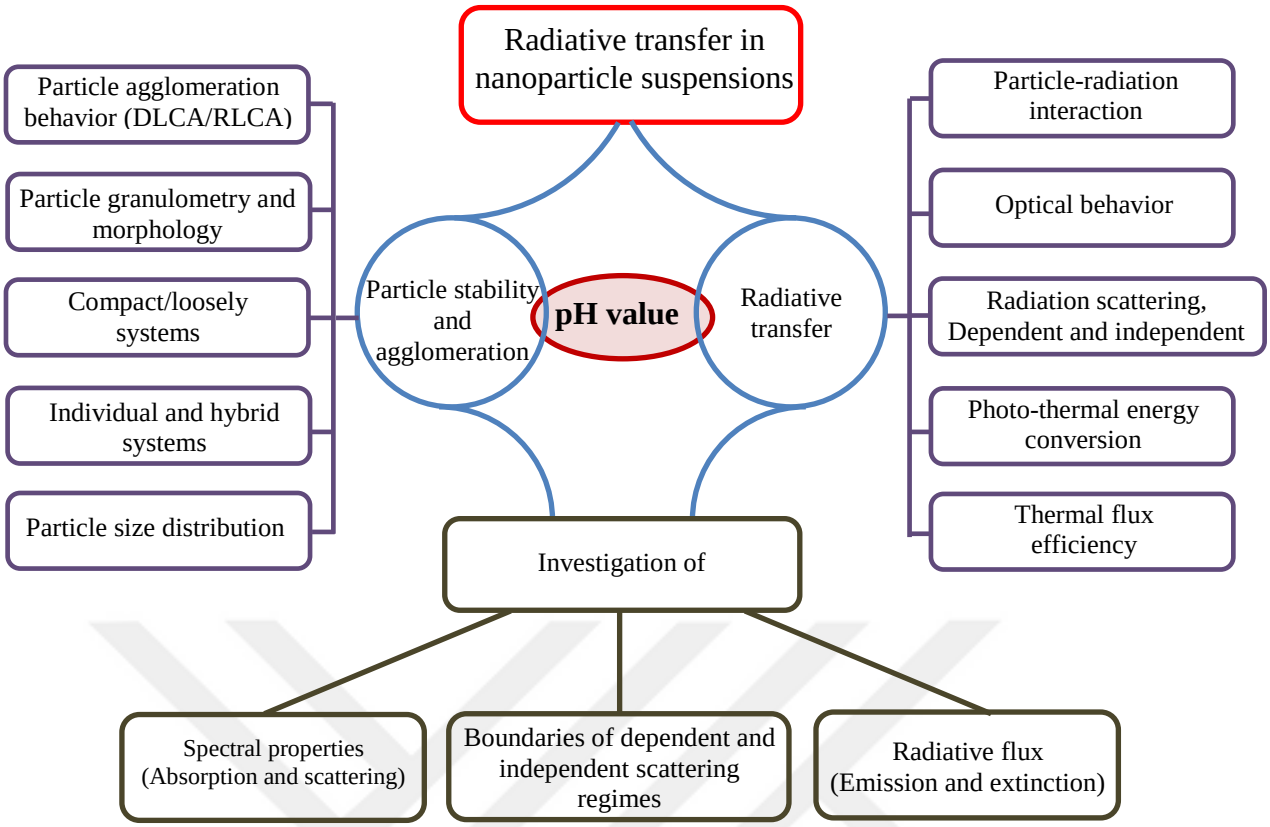

Figure 1.5 Graphical structure of the research.

The main objectives are explained as follows:

1. The effect of electrostatic stabilization (pH value) on nanoparticle agglomeration behavior of NPSs at different particle volume fractions.
2. Investigation of the effects of the particle agglomeration on the particle agglomerates' size and size distribution of NPSs under different conditions.
3. The investigation on particle agglomeration is carried out for Individual and Hybrid NPSs using TiO_2, Al_2O_3, and TiO_2+Al_2O_3 NPs.
4. Investigation of the effects of particle size and size distribution on the radiative properties of the NPSs.
5. Demarcation of the boundaries of the dependent and independent scattering regimes (DISRs) of particle agglomerates as a function to pH value.

6. Radiative properties of NPSs are determined using the average particle agglomerates based on the single scattering approximation (SSA) using the Lorenz-Mie theory.
7. Investigation the effect of the particle size distribution on the radiative properties in a particular NPS.
8. Studying the volumetric solar absorption (Volumetric heat generation). Explain the effects of NPSs on the volumetric radiative heat flux and the radiative energy losses.
9. An important part of particle agglomeration and their effects on the radiative properties to be explored experimentally, which are difficult to detect in the theoretical studies.

CHAPER II

LITERATURE REVIEW

2.1 Introduction

With the growing demands of modern technology for miniaturization of devices, there is a need to develop new types of working media that are more effective in terms of efficiency, and performance of different systems including energy conversion systems. It is expected that the heat base fluids can be enhanced by suspending solid particles into them. However, some drawbacks occur in the suspensions with millimeter or micrometer particles, such as poor dispersibility, and sedimentation as well as adhering to the inner surface of the system, which could easily lead to the degradation of the heat transfer performance, the increase in the pumping power, and more seriously pipe block (Raja et al., 2016; Wen et al., 2009). It has been proved that the dispersion of small amounts of nano-sized solid particles in base fluids improve thermal, radiative and other properties in addition to improving the thermal performance of heat transfer systems. Nanoparticle suspensions are essentially characterized by the fact that any settling motion due to gravity is overcome by the Brownian motion. Thus, as long as the particles remain small enough, a stable NPs is theoretically possible (Daungthongsuk and Wongwises, 2007; Pang et al., 2015; Yu and Xie, 2012).

One of the biggest challenges NPSs face is the preparation and long term stability, which are the principal prerequisites for achieving good thermophysical and radiative properties and further engineering applications. Accordingly, the research on

NPSs can generally be categorized into the following directions: preparation and stability (Lv et al., 2016; Zhang et al., 2016), thermophysical properties (Dehkordi et al., 2017; Soltanimehr and Afrand, 2016; Toghraie et al., 2016; Xiao et al., 2013), optical and radiative properties (Choi et al., 2008; Duffie and Beckman, 2013; Green, 1982; Karami et al., 2016), heat transfer research (Abedini et al., 2017; Goodarzi et al., 2016), engineering applications (Esfe et al., 2015; Eshgarf and Afrand, 2016; Mahian et al., 2017; Sepyani et al., 2017), energy applications (Kandasamy et al., 2014; Shan et al., 2014; Xia and Xia, 2010), and theoretical analysis, or model development (Shamshirband et al., 2015; Yang et al., 2016).

Over the last twenty years, the research concerning NPSs has been rapidly increasing due to their unique properties, and many researchers have carried out experimental or theoretical studies on different aspects of NPSs (Afrand et al., 2017; Esfe et al., 2016; Xiao et al., 2017). As an illustration, the trend in the growth in the number of publications that include NPSs in general (for different issues) and radiative transfer in NPSs in the title retrieved from “web of science” can be found in Figure 2.1. The title of the NPSs in this figure covers the words: nanoparticle suspensions, nanofluids, and nanosuspensions. While the title of the radiative transfer includes the subjects: radiative transfer, radiative properties, electromagnetic radiation, scattering, absorption, emission, and optical properties. This figure shows clearly that research regarding of NPSs is growing so speedily that a publication in 2017 was 30% of the whole total over the past twenty years. If the retrieval scope was relaxed to a full text and containing more search databases, the results could increase several times. Consequently, it is becoming increasingly challenging to provide a comprehensive review of all the types of NPSs because of the vast amounts of related literature. Moreover, in the last two years, a few reviews have focused on one aspect of property

or a certain kind of NPSs to provide more comprehensive reviews (Afrand et al., 2017; Yang and Du, 2017).

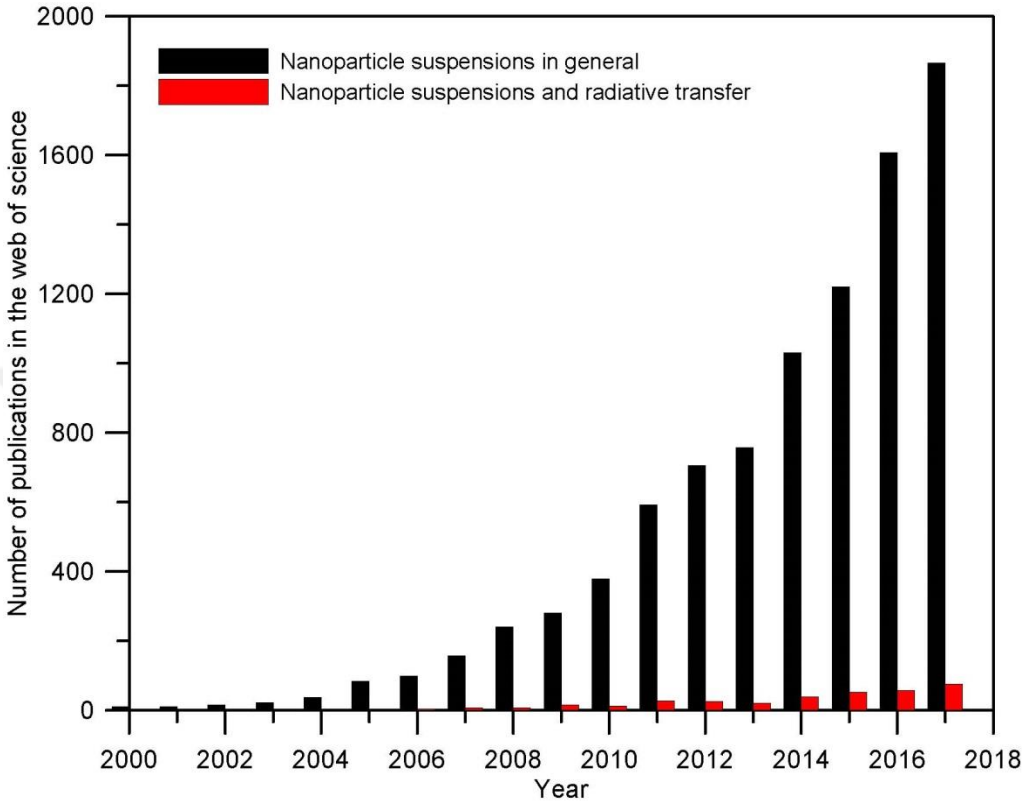

Figure 2.1 Number of publications containing "nanoparticle suspensions" in the title retrieved from the web of science.

2.2 Preparation of nanoparticle suspensions

2.2.1 Individual nanoparticle suspensions

A considerable number of investigations have been carried out on NPSs over the last few decades, including their preparation and characterization for different applications. An individual (single) nanoparticle has been suspended in the medium to obtain an individual NPS (Sarkar, 2011; Trisaksri and Wongwises, 2007; Wang and Mujumdar, 2007; Wong and De Leon, 2010). Many approaches have been considered for the preparation of NPSs, which can be classified as either a one-step or two-step

method (Hwang et al., 2008). Over the years, a significant amount of studies have addressed the problem of the solid-fluid interaction phenomenon (Choi, 2009; Kawanami and Sakurai, 2007; Yu et al., 2008). However, the impacts of different factors such as the particle shape and size, particle agglomeration and size distribution, and particle stabilization on the properties and performance of NPSs have yet to be extensively investigated. The probability of particle agglomeration increases with the decreasing particle size especially at the nanosize. A stabile NPS means that the suspended particles size does not increase in a large rate under the effect of agglomeration (Almohammed and Breuer, 2016; Du and Tang, 2015). In the field of particle suspension, the long term stability of suspended nanoparticles is the key for any application which includes such types of suspensions (Luo et al., 2014). There are many researchers interested in the NPSs, suspended particle in the base fluids who have studied the use of different methods for stability enhancement in order to introduce a clear idea about the mechanisms of those particles (Boisvert et al., 2001; Gu et al., 2014; van Dyk and Heyns, 1998). To justify the possibility of these nanoparticles being dispersed in base fluids, it is necessary to investigate the particle size distribution extensively before and after dispersion. In NPSs, the particle concentration and system heterogeneity have significant effects on the heat and mass transfer where the thermal transport in the NPSs depends on different parameters such as particle size and size distribution, shape, and particle concentration. Therefore, it is quite important to include the effects of all these parameters in investigations in order to explore their impacts on the mechanisms of heat and mass transfer in different types of NPSs (Keblinski et al., 2005; Wang et al., 2003; Xie et al., 2005).

A long-term colloidally stable superparamagnetic iron oxide nanoparticles (SPIONs) was conducted. The hydrodynamic size of the nanoparticles was measured

by the dynamic light scattering technique on the day of the nanofluids synthesis and also nine months later. The results indicated no significant change in the size of the nanoparticles, where no complex particle agglomerates were generated (Şeşen et al., 2012). An experimental investigation was introduced, including a magnetic actuation scheme both to enhance the nanofluids stability and to avoid particle deposition on the surfaces. In the designed system, the observed enhancement of the average two-phase heat transfer was 17%, while with the magnetic actuation, the enhancement of the average single phase was found to be 29%. The magnetically actuated nanoparticles were free from any kinds of precipitate and clusters after the experiments (Şeşen et al., 2013). The suspension of the nanoparticle in the base fluids has been investigated using different methods to produce long term stable nanosuspensions and to display a clear idea about suspended particle mechanisms (Gu et al., 2014; Widegren and Bergström, 2002).

The dispersion of Al_2O_3 and TiO_2 nanoparticles in the base fluids have received a wide interest in recent years (Bae et al., 2003; Fazio et al., 2008; Safaei-Naeini et al., 2012). There have been studies in regard to the suspensions of TiO_2 and Al_2O_3 nanoparticles in different aqueous or non-aqueous media using different mechanisms of dispersions, and there have also been studies on the stability of the prepared suspensions using different methods of stability enhancement (Saltiel et al., 2004; van Dyk and Heyns, 1998). Aqueous TiO_2/water NPSs in differing particle sizes and concentrations displayed stable behavior for months after the preparation without any dispersants (He et al., 2007; Muthusamy et al., 2016). The investigations on the Al_2O_3/water NPSs with the particle size of 13 nm and with particle concentration of 0.05-0.1% vol. without additives showed that a good stability behavior was achieved (Said et al., 2013). Additionally, the stability of different NPSs (Al_2O_3, ZnO, and

Fe_2O_3/water) with the particle sizes (45, 60, and 30 nm, resp.) were investigated without using any additives, which showed that the Al_2O_3/water NPSs had a better stability than the others (Colangelo et al., 2013). A cavitating flow through micro orifices was proposed to enhance the stability of water/γAl_2O_3 NPSs to prevent particles agglomeration and sedimentation. In this method, the particle agglomerates interact with the emerging bubbles and lead to a decrease in the agglomerates size through the generated shock waves by the bubbles collapsing. No surfactants or surface modifiers were used in the preparation of the nanofluids (Karimzadehkhouei et al., 2016). An experimental investigation was performed on the nucleate pool boiling heat transfer of water-TiO_2 and CuO nanoparticles-based nanofluids. The results demonstrated that the performance of the heat transfer was enhanced when the nanoparticles were placed in water. The enhancement was extremely dependent on the concentration of the particles. For the water-TiO_2 nanofluid, the largest enhancement was approximately 15% for the particle mass fraction 0.001%. However, for the water-CuO nanofluid, the enhancement was more than 35% for the particle mass fraction 0.2% (Karimzadehkhouei et al., 2017).

Generally, surfactants are required in the preparation of carbon nanotube (CNTs) solutions to obtain stable NPSs (Hordy et al., 2014; Kozan and Mengüç, 2008; Saltiel et al., 2005; Zhu et al., 2007). Additionally, the investigation showed that the stability of graphite/water NPSs could be achieved by using polyvinylpyrrolidone (PVP) surfactant (Lee et al., 2007). The investigation on the Multi-walled carbon nanotubes (MWCNTs) with the particle size of 10-30 nm and concentration of 0.2 wt.% in water showed unstable NPSs samples without surfactants (Yousefi et al., 2012). Due to the agglomeration of the single-walled carbon nanotubes (SWCNT) in the distilled water, a considerable increase in the transmittance was observed after

some minutes of preparation because of their sedimentation. SWCNT have diameter=1.2-1.5 nm and length 2-5 μm, and the CNT concentration was 5-100 mg/l (Gorji et al., 2015).

2.2.2 Hybrid nanoparticle suspensions

Nanoparticle suspensions with one type of nanoparticle do not necessary include all the required characteristics for thermal, optical, and rheological applications, etc. Then, NPSs can be prepared using different types of nanoparticles to tune the required properties for a specific application in hand. Hybrid nanosuspensions have combined chemical and physical properties of different types of nanoparticles. However, the behavior of hybrid NPSs in a working environment has yet to be studied extensively. Some hybrid NPSs are expected to yield better thermophysical and radiative properties when compared with individual NPSs, and they offer a potential for thermal applications; including solar thermal systems or other applications that require desired and tunable radiative properties (Keblinski and Cahill, 2005; Wang et al., 2003). The hybrid NPSs are new types of NPSs, and can be prepared by suspending two or more nanoparticles in the base fluid, that is to say hybrid (composite) nanoparticles in the base fluid. A hybrid nanoparticle is a substance combined with the physical and chemical properties of the constituent materials simultaneously and gives these properties in a homogeneous phase. In addition, when compared to individual NPSs due to the synergistic effect, the hybrid NPSs is expected to yield better thermal behavior (Sarkar et al., 2015; Sinz et al., 2016).

The main aim of hybrid NPSs research is to assure its application in any equipment connected to heat transfer. Broad experiments on the physiochemical properties of hybrid nanostructures for biotechnology application were conducted by Turco et al. (Turcu et al., 2007). In a study similar to the aforementioned, a hybrid

Nano-polymer was prepared for the applications in the solar cells and in the nanofluid for an application in evacuated tube solar collector (Jamil et al., 2016; Muhammad et al., 2016). Moreover, the use of Al_2O_3-Cu/water hybrid nanofluid in heat sink for an application in cooling electronics has demonstrated an increase in convective heat transfer compared to water (Takabi and Shokouhmand, 2015). Alumina-silver nanocomposite hybrid nanofluid in a helical heat exchanger to examine the thermal performance and pressure drop was used in another study. In this study, the hybrid nanofluid showed a higher percentage of heat transfer (31.58%) in comparison to the conventional heat transfer fluid (water) (Allahyar et al., 2016). Contrary to this, a different experimental result of Cu/TiO_2 hybrid nanocomposite/ water applied in a tubular heat exchanger showed an increase in the overall heat transfer of 30.4% at a volume concentration of 0.7% (Madhesh and Kalaiselvam, 2014).

2.3 Characterization of nanoparticle suspensions

The agglomeration of the nanoparticles in the NPSs is characterized by many micro-scale behaviors. The investigation of particle agglomeration can be divided into two methods: direct detection (Chen et al., 2017; Li et al., 2007; Song et al., 2016) and indirect feedback (Anushree and Philip, 2016; Fedele et al., 2011; Li et al., 2008). The meaning of direct detection is that the evolution of PSD in time is directly determined by Dynamic Light Scattering, electrical microscope (SEM and TEM), or other method types. In this way, one can obtain instant information about the nanoparticle agglomeration in NPSs. Usually, the difficulty in its operation is the disadvantage of the direct detection. First, much sample quantity is required. Some DLS instruments need dozens of samples of milliliters and several measurements are necessary. However, if the one-step method is used to prepare the sample, the sample quantity

will be extremely limited. Second, for some concentrated suspensions, the process of agglomeration is very quick. While many minutes are often required for each measurement, the direct detection method cannot really capture this dynamic process (Chen et al., 2017; Li et al., 2007; Song et al., 2016). Indirect feedback is to acquire the agglomeration process by testing the changing of the thermophysical properties, the optical property or stability (concentration distribution) of the suspension. The advantage of this method is its ease of operation, while the disadvantage is that it cannot obtain quantitative PSD, but only the qualitative dispersed state of nanoparticles in the nanofluid. In the practical application, direct detection and indirect feedback are usually combined due to their complementary properties (Anushree and Philip, 2016; Fedele et al., 2011; Li et al., 2008).

A comparative study of several measurement techniques used for the characterization of dispersions was conducted by Mahl et al. (Mahl et al., 2011). They investigated dispersions with almost monodisperse spherical silver nanoparticles (∼70 nm), and gold nanoparticles (∼15 nm) and these dispersions were characterized using differing techniques: scanning electron microscopy, transmission electron microscopy, dynamic light scattering, analytical disc centrifugation. This is also denoted as differential centrifugal sedimentation, and nanoparticle tracking analysis. The limits of the measurement techniques were examined. To find out whether the different techniques generate comparable results with respect to particle size was the main task. In addition, how the size distribution data for the mixture when compared to those of the individual particles was investigated (Mahl et al., 2011). Different methods of nanomaterial characterization and proposed dynamic light scattering (DLS) as a useful technique to evaluate particle size, size distribution, and the zeta potential of nanomaterials in solution was reviewed by Powers et al. (Powers et al., 2006). DLS

was used in both recent and past studies as early as 1975 as a base method for analyzing the suspension stability and measurement of the particle size in solution (Berne and Pecora, 2000; Simakov and Tsur, 2007; Williams et al., 2006; Wu et al., 2005). There was a detailed experimental/theoretical study conducted in order to explore the core nature of individual cotton fibers via light-scattering experiments. A new precision nephelometer was built and calibrated with quartz fiber for this purpose. The key parameters for the precision measurements determined were the opening (viewing angle), and scanning range and rate. A comparison of the experimental results was made regarding the theoretical predictions based on the finite element model. It was determined that the scattered intensity profiles as a function of the scattering angle may be connected to the quality (fineness) of the cotton (Aslan et al., 2003). An introduced was a hybrid methodology based on elliptically polarized light scattering (EPLS) so as to characterize the metal oxide colloidal suspension. The size and structure of the colloidal metal oxide (MgBaFeO) particles were determined by using an Elliptically Polarized Light Scattering (EPLS) technique. This approach was based on a hybrid experimental/theoretical study where the experimental data were compared to predictions attained using a T-Matrix model, which accounts for the irregularities of the particle shape. A power-law distribution function with two parameters was employed to account for the size of the particle distribution (Aslan et al., 2006).

2.4 pH value and nanoparticle suspensions

For good stability, the pH value of the NPSs need to be adjusted to a value far from the pH_{iso} of the nanoparticles, where a large value of the zeta potential is obtained. The structure and size of the agglomerates is dependant on the different

parameters, related to both the particles' composition and the boundary conditions. Nanoparticles in base fluids usually agglomerate, and one of the most significant challenges in the NPSs research field is to produce well dispersed and long-term stable (low particle agglomeration ratio) NPSs. The stability of the NPSs is impacted upon by different parameters such as the pH level of the suspension, particle size and shape, surfactant concentration, and sonication time (Konakanchi et al., 2015; Wamkam et al., 2011).

To prevent the re-agglomeration in the TiO_2 nanosuspensions, the pH value can be adjusted to 11 to achieve a higher zeta potential (40 mV) (He et al., 2007). $Al_2O_3-H_2O$ nanofluids were synthesized; their dispersion behaviors and thermal conductivity in water were examined under various pH values and sodium dodecylbenzenesulfonate (SDBS) concentrations. The results showed the stability and thermal conductivity enhancements of $Al_2O_3-H_2O$ nanofluids are extremely dependent on the pH values and differing SDBS dispersant concentrations of nano-suspensions (Zhu et al., 2009). In order to aim at the dispersion stability of nanofluids, Xian-Ju et al. scrutinized the absorbency and the zeta potential of TiO_2 and Al_2O_3 nanofluids under various pH values and dispersant concentrations. The results determined that in the mass fraction 0.05% alumina and 0.01% titanium dioxide nanosuspensions, the absolute value of the zeta potential and the absorbency of the two nanofluids with sodium dodecyl sulfate (SDS) dispersant are their highest at an optimal pH ($Al_2O_3 \approx 6.0$, $TiO_2 \approx 9.5$). In addition, it was found that there was a good correlation between the absorbency and zeta potential: the higher the absolute value of the zeta potential was, the greater the absorbency was, and the better the stability of the system was (Xian-Ju et al., 2011). The suspension of the 0.1% wt. of the TiO_2 nanoparticles into water was performed with the dispersion methods including adding

Sodium Dodecyl Sulfate (SDS), and by adjusting the pH value to 5 by using the ultrasonic vibration technique, it was found that the nanoparticles can remain stable for over one year (Ghadimi and Metselaar, 2013). Viscosity, heat transfer and pressure loss measurements were performed for 27 nm TiO_2 nanofluids with a concentration of up to 3% vol. at pH=10, and single-phase correlations were found to be successfully extended to such nanosuspensions (Vakili et al., 2013). The investigation demonstrated that the stability of the TiO_2/water nanosuspensions with the particle size of 25 nm and with the particle concentration of 20-50% wt. at pH=11 without any dispersant was stable for more than one month after the preparation. The ultrasonic vibration path was also used in the preparation (Sen et al., 2015). The stable TiO_2 nanosuspensions were obtained successfully from the surface modified nanoparticles in the same medium, where the particle concentration was up to 50% wt., and with low viscosity, the highest particle concentration (20% wt.) was achieved for the TiO_2 nanoparticles with an average particle size of 25 nm in aqueous solutions at pH=11, where these suspensions were limited by particle agglomeration and high viscosity (Sen et al., 2015). This method enhances the stability of the nanoparticles by achieving a higher zeta potential to avoid the adhesion of the nanoparticles by the higher electrostatic repulsion barriers (Devendiran and Amirtham, 2016). To achieve good dispersion for the NPSs, the adjustment of the pH value has been adopted by several researchers (Yang and Hu, 2017).

2.5 Radiative transfer in nanoparticle suspensions

The radiative properties of NPs and NPSs have been investigated extensively in recent years, and the effects of different nanoparticle types in addition to their physical and chemical characteristics on the radiative properties and radiative transfer have

been observed (Said et al., 2013; Viskanta and Menguc, 1989; Wei et al., 2012).

The study by Lorenz predates that of Mie, and proposed the general theory that describes radiative scattering by absorbing the spherical particle; the theory is known as the "Mie theory". Recently, in recognition of the contributions of Lorenz, the "Lorenz–Mie theory" becomes one of the most popular and most reliable theories (Mie, 1908). Lord Rayleigh discussed radiation scattering and absorption by single spheres during the latter part of the nineteenth century (Rayleigh, 1870). The discrete dipole approximation technique is one of the reliable methods to describe the optical properties of different nanoparticle agglomerates (DeVoe, 1964).

Both experimental and analytical analyses are used to calculate the radiative properties of the NPSs. A comparison was done on cases including both fluid base absorbing and non-absorbing matrix, and also for metal and non-metal particles (Wei et al., 2012). Optical and thermal properties (dielectric constant, refractive index, and thermal conductivity, etc.) change with the growth of the nanoparticle size, and some of them affect the individual particles and some affect the clusters. In the field of radiative transfer in NPSs, radiative properties scattering and absorption are for both the base fluid and the nanoparticles. Because of the different size and structure of the nanoparticles in the working medium, it is not just a simple summation of their absorption capacity for the nansuspensions. Scattering, on the other hand, is also a loss of intensity of incident light caused by the obstacle particles in the medium, which forces the incident light to be deviated from its straight trajectory (Hossain et al., 2015; Ortega et al., 2008). The characteristics of the particles dramatically affect the radiative properties of the NPSs; these characteristics include the particle size and shape, the number of particles, the particle size distribution, and the refractive index. In addition, the relationship between all these parameters with the incident

wavelength, has significant implications in the radiative properties of the nanoparticles (Doicu et al., 2006; Mishchenko et al., 2002). Spectral transmittance is one of the radiative properties parameters that describe the radiation phenomenon. This is used to explain the method by which the incident radiant leaves a surface or medium from a side other than the incident side, which is usually the opposite side. The spectral transmittance refers to the light attenuation and is related to the medium depth and extinction coefficient. Therefore, the calculation of the transmissivity of the NPSs is very important for the study of the effectiveness of the solar energy absorption with suspended particles. The spectral transmittance of several NPSs is very different, and these differences depend on different paramters related to the nature of the suspended particles and the medium. Also, the suspended particle size and size distribution play a significant role in the spectral transmittance (Mishchenko, 2014).

TiO_2 nanoparticles are used extensively because of their favourable radiative and thermophysical properties, and also because they are very suitable for energy production (solar thermal systems) and water treatment applications (Cheng et al., 2005). To obtain the extinction coefficient and refractive index of water based TiO_2 and Al_2O_3 nanofluids, classical theories such as Rayleigh, Maxwell–Garnett, and Lambert–Beer's approaches were used. The extinction coefficient and refractive index of TiO_2 nanofluids are found to be higher than Al_2O_3 nanofluids in the visible region of light for all the concentrations (Said et al., 2014).

2.6 Light scattering in nanoparticle suspensions

Light scattering by the NPs and their agglomerates play a significant role in a wide range of applications, including radiation transfer through the atmosphere, in measurement systems, in chemical processes, for new coatings, and many others. The

interaction of light with the particles is quite important, and understanding this interaction provides a clear idea of the radiative transfer of energy in complex systems. The different size and structure of the particle agglomerates exhibit different thermal, radiative, physical, rheological, and chemical properties. Light scattering is strongly affected by particle agglomeration, where different scattering behaviors can be obtained from the different size and structure of the particle agglomerates (Zhu et al., 2013).

The boundaries of the dependent and independent scattering regimes for particulate suspensions were first investigated by Tien et. al. They were presented the fundamentals of the scattering and absorption of thermal radiation in particulate systems. The common assumption is that each particle in the system scatters and absorbs radiation, which is not affected by the presence of others is the "independent" assumption. The departure of the net incidence on each particle because of the radiation scattered from the others, and the interference in the far field due to the phase addition of the scattered electric fields from the particles. The first causes an increase in the energy extinguished and scattered while the second leads to a decrease in the total scattered energy (Tien and Drolen, 1987). Several light scattering techniques have been used over the years to measure the optical and radiative properties of nanoparticles and agglomerates. Dependent and independent scattering regimes have been investigated by many researchers, where the effects of different parameters were explored (Aslan et al., 2006; Drolen and Tien, 1987). An earlier numerical study were carried out using the discrete dipole approximation method for closely packed systems containing up to 12 spherical particles so as to investigate the inception of agglomeration. The effects of dependent scattering in a medium consisting of two spheres at an arbitrary distance between them and the index of refraction typical for

that of soot particles were investigated (Ivezić and Mengüç, 1996). Dependent and independent scattering regimes were clarified for packed systems containing 10 spheres. A comparison study was carried out between the Foldy's effective field approximation (EFA) and the quasi-crystalline approximation (QCA) for the nanoparticle suspension in the Rayleigh scattering regime (Prasher and Phelan, 2005).

The scattering matrix element for agglomerates with different fractals was demonstrated. The influences of the different parameters such as the number and size of the monomers in agglomerates, the fractal dimension, as well as the wavelength of the incident light, were considered (Klusek et al., 2003). The small-angle light scattering technique was also used to determine the morphology of the different particle agglomerates by considering the fractal theory (Kozan and Mengüç, 2008). Discussed was procedure to find the agglomeration of soot particles in flames from multi-wavelength experiments. N-particle agglomerates are modeled by using a discrete dipole approximation. It was discovered that it is possible that the measurements of the differential scattering and absorption coefficients, and phase function, can be used for the determination of the number of agglomerated monomers, their size, and the structure of the formed agglomerate. The representative results were presented for a complex index of the refraction value typical for those soot particles that are produced during the combustion of hydrocarbon fuels (IveziĆ et al., 1997). By using the discrete dipole approximation (DDA), the light scattering from irregularly shaped particles with three different kinds of agglomerate morphologies was computed. It was discovered that even though there were noticeable differences in the particle morphology, their light-scattering responses were very similar, and the difference in light scattering often does not exceed the error bars that occur in the laboratory measurements of micron sized-particles. Contrarily, the effect of the

refractive index and size distribution on the light scattering seemed to be much stronger in comparison to the morphology of the complex, agglomerate particles. This discovery may simplify the interpretation of photo polarimetric observations of atmospheric aerosols, cosmic dust particles, etc., considerably because the exact specification of the target-particle shape is not required for the analysis (Zubko et al., 2015).

2.7 Applications of nanoparticles and nanoparticle suspensions

2.7.1 General applications

Nanoparticles and nanoparticle suspensions bring promising heat transfer applications, which are of significant importance to a variety of industrial sectors such as transportation, power generation, micro-manufacturing, electronics, engines, thermal therapy, heating, cooling, ventilation and air conditioning. Many of the studies have been shown an enhancement in thermal performance in NPSs (Keblinski et al., 2005; Raja et al., 2016). Figure 2.2 shows the major fields of the NPSs applications, where the NPSs play an important role.

TiO_2 nanoparticles are also used in coatings. It is well-known that there are two major reasons for applying a coating to substrates: beautification and protection (Dietz, 2003, 2004). The interaction of visible light with the coating film is needed for the basis of the opacity. The relationship between the particle size and the incident radiation is one of the most important parameters in establishing the desired opacity in the coatings (Diebold, 2014). TiO_2 NPSs are widely used in different applications because of their unique thermo-optical properties, including those of solar thermal utilization systems (Muhammad et al., 2016).

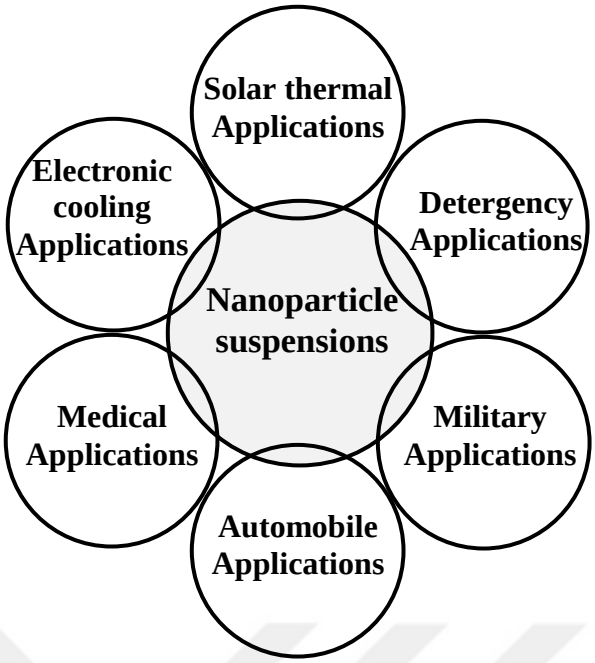

Figure 2.2 Major fields of applications for NPSs.

2.7.2 Energy applications

Solar energy utilization becomes an attractive area of research as solar radiation is a vast and renewable energy source. Solar thermal collectors are the most important part in solar thermal systems; however, the effectiveness of these collectors is generally low because of the low radiative properties of the working fluids. The notion of direct absorption solar energy within a volume of fluid, which is called the direct absorption solar collectors, was initially introduced by Minardi and Chuang (Minardi and Chuang, 1975). Nanoparticles are found to be effective radiation absorbers in low wavelength ranges, and thy have unique thermal and optical properties, which are the basis of thermal applications (Duffie and Beckman, 2013; Green, 1982). A few researchers have attempted to investigate nanofluids for their suitability in improving the performance of the solar thermal collectors. The theoretical model that was introduced by Tyagi et al. was the very first model to quantitatively assess the

effectiveness of a nanofluid-based direct absorption volumetric absorption solar collector (the working fluid describes a nanofluid- aluminum nanoparticles dispersed into water) (Tyagi et al., 2009). Referring to the progress in nanotechnology during the past years or so, the applications of nanoparticle suspensions in solar thermal collectors has been proposed because of their unique thermophysical and radiative properties (Green, 1982; Xuan and Li, 2000).

In the backdrop of the ever increasing energy demands and irreversible impact of burning fossil fuels to meet these demands, researchers around the globe are striving hard to improve existing solar thermal technologies (Hewakuruppu et al., 2015; Taylor et al., 2013; Veeraragavan et al., 2012). Subsequently, Otanicar et al. and Taylor et al. have further refined the model to simulate actual nanofluid-sunlight interaction in volumetric absorption solar collectors. Furthermore, these refined models have been very well validated through the proof of the concept experiments done by these researchers. The aforementioned numerical, as well as experimental studies, clearly point out that under certain controlled conditions (and for the optimum selection of the nanoparticle material, shape, size, and concentration) an enhancement on the order of 5-10% could be achieved in the nanofluid-based volumetric collectors relative to the conventional solar collectors (Otanicar et al., 2010; Taylor et al., 2011). In this direction, researchers have directed their attention to NPSs as potential volumetric absorbers as they promise better thermal efficiencies at high solar irradiance flux conditions. This may be attributed to the fact that as opposed to surface absorption-based receivers as here the sunlight directly interacts with the working fluid (nanofluid), which results in a more effective alteration of the solar irradiance to the thermal energy gain of the working fluid (Khullar, 2016; Khullar et al., 2014). It has been found that nanoparticle suspensions are effective electromagnetic wave

absorbers within UV-visible range. Consequently, the radiative properties of the suspended particles and the media containing those particles need to be investigated intensely. As there are many particles in a particulate medium, the scattered photon from a particle may interact with those from other particles. This means, incident beams can be scattered more than one time and they can be scattered again by the nearby particles (Mishchenko et al., 1999).

Various kinds of nanoparticles are being used in solar thermal collectors, and TiO_2 and Al_2O_3 nanoparticles are extensively utilized where an enhancement in the thermal performance has been observed based shown based on not only the thermophysical but also the radiative properties. The investigations show that nanofluids have unique radiative properties, which play a significant role in photo-thermal energy conversion. Solar thermal collectors are the most important part in the solar thermal systems. However, the efficiency of conventional collectors (surface absorber collectors) is usually low due to the heat loss at the surface and the low radiative properties of the working fluids. This motivates the concept of using the nanofluids in the volumetric (direct absorption) solar collectors to enhance the thermal efficiency (Gupta et al., 2015; Kim et al., 2016; Minkowycz et al., 2016). The investigations show that TiO_2 and Al_2O_3 nanofluids have unique radiative properties, which play a significant role in the thermal performance of the photo-thermal energy conversion systems. The thermal efficiency of the proposed nanofluids in the concentrated solar collectors shows an enhancement (more than 10%) compared to the conventional collectors under the same conditions (Jing and Song, 2017; Muhammad et al., 2016). The efficiency of the direct absorption solar collector is also examined, where the water-based aluminium nanoparticles are used as a working fluid, and it has been reported that an improvement in the collector efficiency by up to 10% was

proposed (Tyagi et al., 2009). Nanosuspensions performance in solar collectors has been studied by Luo et al., and an improvement in the collector efficiency was observed up to approximately 2–25% as a result of the effect of adding nanoparticles (Luo et al., 2014). TiO_2 nanoparticles have attracted attention not only because of their radiative and thermophysical properties, but also because they are very suitable for many applications and a wide range of applications such as energy production (solar thermal systems) (Cheng et al., 2005). Solar radiation is difficult to transmit through the ZrC and TiO_2 nanofluid. While a remarkable amount of visible light can pass through the SiO_2 nanofluid. A highest solar absorption is shown for the ZrC nanofluid among the studied nanofluids (Mu et al., 2009). A simulation model for a nanofluid solar collector based on the direct absorption collection concept for building utilization was developed by Luo et al. This model was developed through finding solutions to the radiative transfer equations of nanoparticulate media as well as by combining and convection heat transfer equations. The system efficiency/temperature distributions were examined by considering the nanoparticles absorption/scattering and the matrix absorption. The simulation results agreed well with the experimental data. The nanofluids improved the outlet temperature and efficiency by 30–100 K and 2–25%, respectively (than the base fluid) (Luo et al., 2014).

Introduced by Zhang et al. was a heat transfer system of a glass evacuated solar collector with an inserted heat pipe which was researched upon experimentally. There were two different types of heat collector devices with a heat pipe using magnetic nanofluids and water as the working fluid respectively researched from different aspects of tilt angles, climate conditions and total solar radiations. The experimental finding showed that the solar collector with an inserted heat pipe using magnetic nano-fluids as the working medium had the lowest heat loss coefficient, the highest average

daily efficiency, and instant efficiency. The results obtained produced a new idea for improvement of the heat transfer performance of solar collectors (Zhang et al., 2012). Various studies have shown that with the use of core shell nanoparticles the efficiency of the direct absorption solar collector could be improved at very low volume fractions of the nanoparticles (Lv et al., 2013; Otanicar et al., 2013; Xuan et al., 2014).

It is envisaged that solar energy will be sustainably utilized in the near future instead of other alternative energy forms owing to its unlimited availability and desirable environmental and safety aspects. Because of the tremendous scientific and technological advances made during the last century and ongoing research and development, it is predicted that by 2100, solar technologies will supply about 70% of world energy consumption (Council, 2013).

This research provides the following contributions to the previous studies:

- The effect of pH on the stability and particle agglomeration (particle size and structure) for individual and hybrid nanoparticle suspensions.
- The relationship between the particle agglomerates size, structure, and size distribution with EM-wave under pH effect at different wavelength range.
- The role of pH on dependent/independent scattering and their boundaries for different conditions.
- The effect of the particle size distribution on the scattering behavior of nanoparticle suspensions to account the effect of compact particle agglomerates.
- The individual and hybrid nanoparticle suspensions (similar and dissimilar particle agglomerations) and their effects on the optical and radiative properties.
- The effect of particle agglomeration on the volumetric radiative heat flux, which is an important parameter in the thermal radiation transfer applications.

CHAPTER III

INTERACTION OF LIGHT WITH PARTICLES AND AGGLOMERATES

3.1 Introduction

The intensity of the radiation that interacts with NPSs changes by absorption, emission and scattering. Subsequently, the incident radiation will be attenuated and/or augmented under the effect of the above phenomena. The scattering of electromagnetic radiation in a particulate medium is strongly affected by the heterogeneity of the particles (heterogeneity of the particles scale or on the scale of particle agglomeration). Regardless of the type of heterogeneity, the underlying physics of the scattering of radiations is the same for all systems. Matter is made up of discrete electric charges: electrons and protons. If an obstacle, which may be a single electron, an atom or molecule, a solid or liquid particle, is illuminated by an electromagnetic wave, electric charges in the obstacle are put into oscillatory action by the electric field of the incident wave. Radiate electromagnetic energy is accelerated electric charges in all directions, and it is the secondary radiation which is known as the radiation scattered by the obstacle. In addition to reradiating electromagnetic energy, the excited elementary charges may transform part of the incident electromagnetic energy into other forms (thermal energy, for example), a process called absorption. An electromagnetic wave or photon passing through the immediate vicinity of the particles will be absorbed or scattered. The scattering is due to three separate phenomena, namely, (i) diffraction (waves never coming into contact with the

particle, but their direction of propagation is altered by the presence of the particle), (ii) reflection by a particle (waves reflected from the surface of the particle), and (iii) a refraction in a particle (waves that are penetrated into the particle and, after partial absorption, emerge again traveling into a another direction) (Hoffman and Driggers, 2016; Hottel et al., 1971; Hulst and van de Hulst, 1957).

3.2 Optical and radiative properties of nanoparticle suspensions

The interaction of electromagnetic radiation with nanoparticles and their agglomerates in the NPSs can be represented by the optical and radiative properties. These properties depend on (i) the shape of the nanoparticle, (ii) the material of the nanoparticle (i.e., the complex index of refraction, $m = \bar{n} + i\bar{k}$), (iii) its relative size, and (iv) the clearance between nanoparticles. Figure 3.1 schematically depicts the incident electromagnetic radiation on a NPS including spherical particles, where the radiative phenomena are given. In this figure, (H_i, E_i), (H_p, E_p) and (H_s, E_s) are the incident electromagnetic fields, the electromagnetic field inside a particle, and the scattered electromagnetic field respectively. A and θ are the surface at which the electromagnetic energy crosses and the polar angle, respectively (Howell et al., 2015; Modest, 2013). The particles in a collection of cloud or suspensions are electromagnetically coupled, each particle is excited by the external field and the resultant field scattered by the other particles; the field scattered by a particle is dependent on the total field to which it is exposed. The electromagnetic field (H_m, E_m) that surrounds a particle in the medium, is the superposition of incident and scattered electromagnetic fields; this is defined as, $H_m = H_i + H_s$ and $E_m = E_i + E_s$.

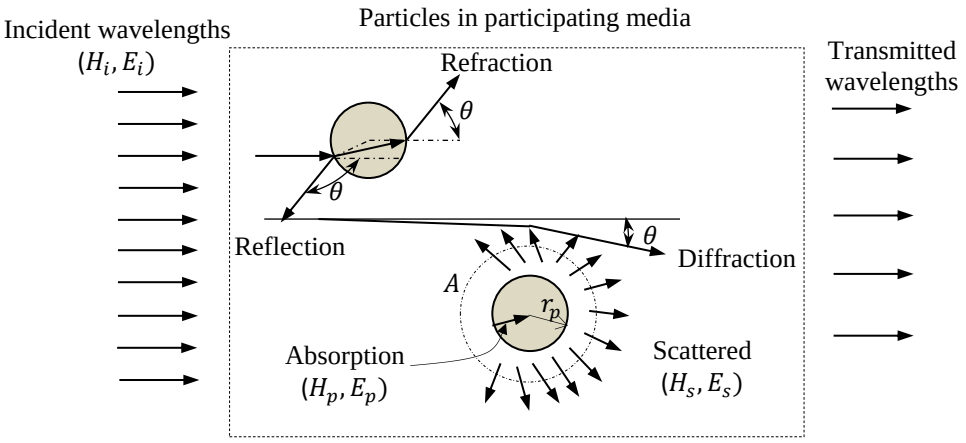

Figure 3.1 Interaction of electromagnetic radiation with a NPS.

In order to specify the electromagnetic field at any point in a NPS, a Poynting Vector (S) is applied to any point that it is surrounding a suspended particle. It is of fundamental importance in problems of propagation, absorption, and the scattering of electromagnetic radiation. From the definition of the electromagnetic field in a NPS, the time average Poynting Vector is defined by (Bohren and Huffman, 2008):

$$S = S_i + S_{sca} + S_{ext} \qquad (3.1)$$

where $S_i = 1/2Re\ (E_i \times H_i^*),\ S_{sca} = 1/2Re\ (E_s \times H_s^*),\ S_{ext} = 1/2Re\ (E_i \times H_s^* + E_s \times H_i^*)$.

For a NPS that includes two dissimilar nanoparticles (the hybrid particulate system). Then, the Poynting Vector is given by (Bohren and Huffman, 2008):

$$S = S_i + S_{sca,1} + S_{ext,1} + S_{sca,2} + S_{ext,2} \qquad (3.2)$$

where 1 and 2 are denoted as the two dissimilar particles (particle 1 and particle 2).

In Equation 3.2, the effect of the individual nanoparticles is considered, and the independent scattering between the nanoparticles is assumed. The different shapes and sizes of the particles and agglomerates have significant impacts on the optical and radiative properties of the particles and the media. The stability and particle

agglomeration parameters (pH, d_p, particle shape, $\emptyset$, and $h_{sur,p}$) have significant effects on the dependent/independent scattering (Howell et al., 2015; Modest, 2013). Therefore, all these parameters should be considered in order to explore their effects on the radiative transfer at different wavelength ranges.

3.3 Methods for optical and radiative properties

In the field of the radiative transfer in a particulate medium, the properties of different particles and fluids that constitute the medium needs to investigated. These properties may vary locally as they would depend on the particle volume fraction profiles, shape and size distributions, and material properties, etc. All these properties are wavelength dependent; therefore, they need to be predicted together with the solutions of the radiative transfer equation and the conservation of energy equation (Brewster and Tien, 1982). Different approaches (theoretical and experimental) have been used by researchers to obtain the radiative properties of a particulate medium, the goal is to find the best methods for describing the optical and radiative properties of any particulate medium. Experimental techniques; such as spectrophotometers, are also used in many studies to obtain the optical and radiative properties of the NPSs.

3.3.1 Theoretical models

3.3.1.1 An overview

Different theoretical methods are proposed for describing the optical and radiative transfer of the particles and particulate medium. The optical and radiative properties of NPSs can be modelled using the Rayleigh and Lorenz-Mie theories. The Rayleigh scattering is appropriate to tiny, dielectric (non-absorbing), spherical particles. For particles lot smaller than the incident wavelength, the Rayleigh theory is

suitable. For the Rayleigh scattering, $x \ll 1$ and $|m|x \ll 1$, where $x = \pi d_p/\lambda$ is the dimensionless size parameter. On the other hand, the Lorenz-Mie theory provides the general spherical scattering solution (absorbing or non-absorbing) without any particular bound on the particle size, if particle agglomerates are compact and can be defined as effective spheres (Hulst and van de Hulst, 1957; Mie, 1908; Rayleigh, 1870).

The T-matrix approach is used extensively to obtain the scattering profiles of symmetric particles. It is also known by other names which including the extended boundary condition method (EBCM) and the null-field method (NFM). It was Waterman who first published the T-matrix formulation (Waterman, 1965). In this approach, the matrix is built by matching the boundary conditions to obtain the solutions of the Maxwell equations. To model and formulate the three-dimensional structure and axisymmetric particle, Chebyshev polynomials were used. These are known as Chebyshev particles and the spherical coordinate system is used to give their shape function.

On the other hand, the discrete dipole approximation (DDA) technique is one of the most reliable methods to explain the optical properties of the various nanoparticle agglomerates. It is a numerical method, first proposed by DeVove (DeVoe, 1964), where the calculations were carried out for particles much smaller than the incident wavelength. Then, the formulations were later modified by Purcell and Pennypacker (Purcell and Pennypacker, 1973). There are several modifications and new versions of the DDA which were developed by many researchers (Manickavasagam and Mengüç, 1998; Singham and Bohren, 1988; Yurkin et al., 2007). In this approach, the arbitrary shapes of particles and their agglomerates can be modelled as included small dipoles. As expected, when increasing the number of

dipoles in a spherical particle of arbitrary size, the solution of the DDA approaches that of the Lorenz-Mie theory (Howell et al., 2015; Modest, 2013). The quasi-crystalline approximation (QCA), which was introduced by Lax, is a method to explain the multiple and dependent scattering in dense medium, where the radiative effects between closely packed particles takes place (Lax, 1952).

Figure 3.2 shows the different shapes of the particle agglomerates in the particulate media with the corresponding radiative method; the discrete dipole approximation (DDA) technique and the Lorenz-Mie theory. The particle shape plays an important role in the radiative properties and affects the radiation absorption and scattering by the particles. The different shape (linear, porous, and compact) of the particle agglomerates has a significant impact on the optical and radiative properties of the particles and the media (Hulst and van de Hulst, 1957; Mishchenko, 2014; Purcell and Pennypacker, 1973).

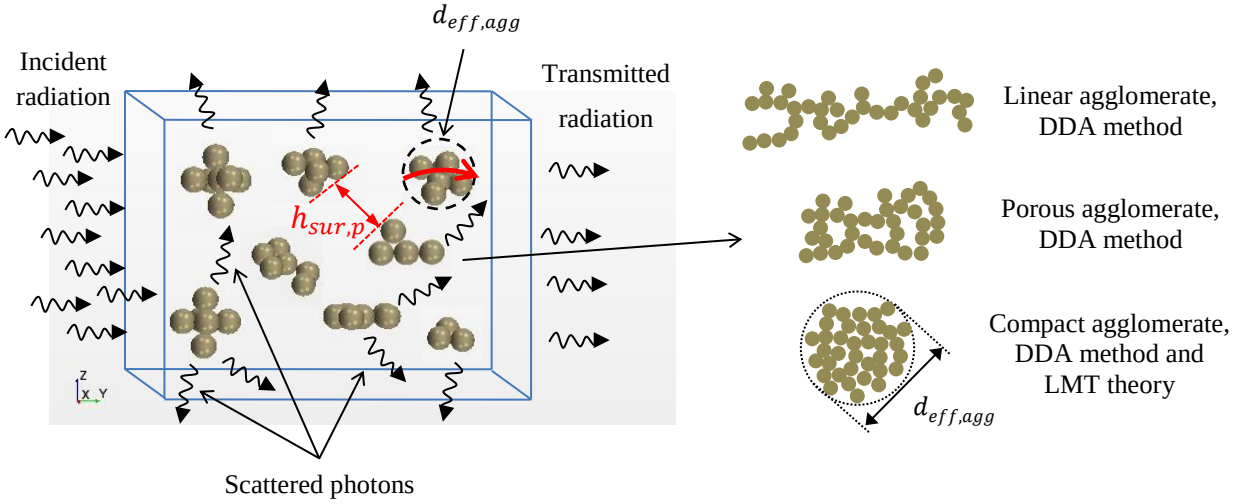

Figure 3.2 Incidence of radiative energy on a particulate media includes different particle agglomerates with the corresponding radiative method.

3.3.1.2 The Lorenz-Mie theory

To calculate the extinction, scattering and absorption coefficients, the Lorenz-Mie theory (LMT) is one of most celebrated theories which represent the interaction of incident wave with a homogenous spherical particle. For the interaction of radiation with a sphere, the efficiency factors (Q_i=C_i/ πr_p^2) are formulated by cross sections C_i normalized to the projected surface area (πr_p^2), where i refers to scattering ($i = scat$), absorption ($i = abs$) and extinction ($i = ext$). Then, the radiative efficiencies are defined as $Q_{ext} = C_{ext}/(\pi r_p^2)$, $Q_{abs} = C_{abs}/(\pi r_p^2)$ and $Q_{scat} = C_{scat}/(\pi r_p^2)$. In the above relationships, the particle radius and diameter (r_p and d_p) and particle number are replaced by the compact particle agglomerate radius and diameter (R_{agg} and d_{agg}) (Ivezić and Mengüç, 1996; Mie, 1908).

Based on the LMT, Mie coefficients can be obtained from the following (Howell et al., 2015):

$$a_n = \frac{\psi_n'(mx)\psi_n(x) - m\psi_n(mx)\psi'(x)}{\psi'(mx)\xi_n(x) - m\psi_n(mx)\xi'(x)}$$
$$b_n = \frac{m\psi_n'(mx)\psi_n(x) - \psi_n(mx)\psi_n'(x)}{m\psi_n'(mx)\xi_n(x) - \psi_n(mx)\xi_n'(x)} \quad (3.3)$$

where $\psi_n(z)$ and $\xi_n(z)$ are the Riccati-Bessel functions, and they are determined by the semi-integer order Bessel function and the Hankel function, and n is the order of the Bessel function.

After the Mie coefficients are determined, the scattering, absorption and extinction efficiencies are obtained as:

$$Q_{ext} = \frac{2}{x^2}\sum_{n=1}^{\infty}(2n+1)Re(a_n + b_n) \quad (3.4)$$

$$Q_{scat} = \frac{2}{x^2}\sum_{n=1}^{\infty}(2n+1)(|a_n|^2 + |b_n|^2) \quad (3.5)$$

$$Q_{ext} = Q_{scat} + Q_{abs} \quad (3.6)$$

3.3.1.3 The discrete dipole approximation method

The discrete dipole approximation (DDA) method is a numerical method, where the object of concern was given as a cubic lattice of polarizable points. There are no restrictions as to which of the cubic lattice sites are occupied. This means that DDA can show either an object or multiple objects of shapes and compositions that are arbitrary. In this method, two parameters are important: the inter-dipole spacing, and the wavelength of incident radiation (Howell et al., 2015; Modest, 2013).

The DDA approach is applied where there is an incident field on each dipole ($E_{inc,j}$) in addition to the contribution fields from other neighbouring dipoles. The total electric field at a point on a dipole located at r location is given as (Howell et al., 2015):

$$E_j = E_{inc,j} - \sum_{j \neq k} A_{jk} P_k \quad (3.7)$$

where A_{jk} is the tensor that show the interaction between a receiving dipole at r_j and the radiating dipole at r_k and P is the moments of a dipole. The incident field is given as:

$$E_{inc,j} = A_{jj} P_j + \sum_{j \neq k} A_{jk} P_k \quad (3.8)$$

The equation above can be made simpler by the combination of the two matrices since the non-zeros tensors do not overlap. Therefore:

$$\sum_{k=1}^{n} A_{jk} P_j = E_{inc,j} \quad (3.9)$$

where n is the number of dipoles.

Knowing P_j, different quantities such as the scattered field, dipole force, Poynting Vector, extinction, absorption and scattering cross sections, phase function, etc. may be calculated.

There are limitations to the LMT and DDA approaches. The LMT solutions converge very slowly for large values of particle size parameter; for example $x > 200$. The DDA solution is suitable for small values of x, and it is computationally expensive and cannot be used for large systems (real NPSs). Simpler methods are preferable to obtain the radiative properties of the particle with the agglomerates and irregular shape. If the particle agglomerates can be correlated to smooth and homogeneous spheres, then the LMT is the best method and could be used for this purpose (Ivezić and Mengüç, 1996). Furthermore, it is reasonable to proceed with a simpler methodology for the calculations for the radiative properties of the particle agglomerates using the LMT, where the properties of the agglomerates can be correlated to smooth, homogeneous spheres (a compact particle agglomerate).

The LMT and DDA approaches are the general approaches in the most radiative properties calculations for most particulate systems. However, there are important questions, 'Under what conditions can a particle agglomerate be represented as a homogeneous sphere?', 'How can the effects of the multiple shapes, sizes (the particle size distribution) of particle agglomerates with respect to incident radiation be concluded?', another question to be answered is 'How can the number of particles in each agglomerate by a number of independent particles be represented?'. The answers to all these questions will discover the boundaries between the dependent and independent scattering regimes for the different particle agglomerates.

3.3.1.4 The quasi-crystalline approximation method

To date, in the above relationships, a multiple and dependent scattering have not been considered. According to the nanoparticles concentration (the nanoparticles number), nanoparticle suspensions can be divided into two categories: diluted and concentrated. The effect of the number of particles should be considered, where increasing particle number leads to a decrease in the clearance of the particles; therefore, multiple and dependent scattering should be considered and examined (Lax, 1952). Moreover, in the Rayleigh regime where the particle size is small in comparison to the wavelength, multiple and dependent scattering should be considered also. For the calculation of the radiative properties in terms of the multiple and dependent scattering, related theories such as the quasi-crystalline approximation (QCA) ought to be applied (Prasher and Phelan, 2005).

The scattering cross-section (C_{scat}) and scattering coefficient (σ_{scat}) in the QCA are given as (Bohren and Huffman, 2008):

$$C_{scat} = 8\,\pi\, r_p^2\, x^4\, u^4/3 \qquad (3.10)$$

where $u = m^2 - 1/m^2 + 2$

For dependent scattering:

$$\sigma_{scat,dep} = \left(2u^2x^4/r_p\right)\phi(1-\phi)^4/(1+2\phi)^2 \qquad (3.11)$$

For multiple scattering:

$$\sigma_{scat,mult} = \left(2u^2x^4/r_p\right)\sqrt{1+3\phi u} \qquad (3.12)$$

In cases of multiple and dependent scattering approximations:

$\sigma_{scat,dep-mult}$

$$= \frac{\left(\frac{2u^2x^4}{r_p}\right)\phi\,(1-\phi)^4}{(1+2\phi)^2} \times\ (1-\phi u)\sqrt{1+(3\phi u/((1-\phi u))} \qquad (3.13)$$

According to the QCA formula, the significant effect of the size parameter and particles volume fraction on the scattering coefficient can be observed. Therefore, the QCA is more appropriate for calculating the scattering coefficient in the particulate suspensions in the Rayleigh regime and/or high particle volume fraction NPSs (Prasher et al., 2006; Sajid et al., 2014).

The nanoparticles in the suspension show a different particle size under the effect of agglomeration. One can clarify the condition of the scattering phenomena (dependent or independent), so that the radiative properties can be modelled accurately. In the case of independent scattering, the radiative properties of the nanoparticles or their agglomerates can be obtained by using the linear summation role (the radiative properties of a single particle multiplied by the number of particles). The scattering and absorption coefficients of the cloud nanoparticles can be calculated as $\sigma_{scat} = NQ_{scat}$ and $\kappa_{abs} = NQ_{abs}$, where N represents the number of particles per unit volume. This role is applicable for the independent scattering; it is applicable and valid for many applications considered in the field of radiative transfer (Howell et al., 2015).

The extinction (scattering and absorption) coefficient of the nanoparticles can be found as (Bohren and Huffman, 2008; Howell et al., 2015):

$$\beta_{ep,\lambda} = \sigma_{sp,\lambda} + \kappa_{ap,\lambda} \tag{3.14}$$

In the near-infrared and infrared spectrum, radiation is strongly absorbed by water. Therefore, any absorption by the medium must be incorporated into the analysis. Then, the absorption coefficient of the medium is obtained as (Taylor et al., 2011):

$$\kappa_{am,\lambda} = \frac{4\pi k_{medium}}{\lambda} \tag{3.15}$$

where k_{medium} is the complex component (absorption index) of the refractive index for the medium varying as a function of the wavelength.

The total extinction coefficient of NPSs, for the combination of the effects of the particle and medium, is given as:

$$\beta_{et,\lambda} = \beta_{ep,\lambda} + \kappa_{am,\lambda} \tag{3.16}$$

The effect of the scattering coefficient in the total extinction coefficient can be clarified using the single scattering albedo, It is the ratio of the scattering coefficient to the total extinction coefficient (Howell et al., 2015):

$$\omega_\lambda = \frac{\sigma_{sp,\lambda}}{(\beta_{ep,\lambda} + \kappa_{am,\lambda})} = \frac{\sigma_{sp,\lambda}}{\beta_{et,\lambda}} \tag{3.17}$$

where ω_λ is the single scattering albedo.

Single scattering albedo gives a clear idea about the particles scattering behavior and its importance, especially for non-absorbing (dielectric) particles.

3.3.2 Experimental techniques (Spectrophotometers)

A suspended particle in a media produces particle agglomerates with different size and structures in addition to the particle size distribution. Therefore, there is some difficulties in explaining all these aspects theoretically. The added effect is that the agglomeration of differing particle kinds is in the same medium when a hybrid particulate system is recommended. In which, a particle agglomerate shows the properties (the chemical, physical, and radiative, etc.) of the different materials that constructed such a particle agglomerate, where each particle type has its own properties. This becomes an additional effect besides the others from the different size and structure. For that, experimental investigations are required in order to realize these aspects and their effect on the radiative properties and transfer. The majority of experimental research regarding radiative properties are based on spectrophotometers,

or self-designed apparatus in accordance with the Lambert-Beer law. Spectrophotometers are used to obtain the optical and radiative properties of the NPSs including absorption, scattering and extinction properties (Duan and Xuan, 2014; Gorji et al., 2015; Lee and Jang, 2013).

Even though spectrophotometers have been applied; some extra treatments are still needed due to the following two reasons. Firstly, because NPSs samples need be dispersed in a glass or plastic container, the transmission and reflection of the container walls will be coupled with the optical properties of the NPSs. This is shown in Figure 3.3 (Taylor et al., 2011). Because a cuvette includes the liquid sample in the system, the resulting measurement is in fact a 'three-slab system'. This adds complexity since there can be multiple reflections at each interface which needs to be taken into account in the measurements. As is seen in the figure, some of the signals going through the three-slab system are lost in the reflections at the interfaces. Secondly, the NPSs are two-phase mixtures, i.e. inhomogeneous medium, and light transporting in an inhomogeneous (heterogeneous) medium may accompany the scattering, which leads to all the directions' diffusion other than the incident direction (Song et al., 2016). Thus, the acquired absorption coefficient always includes the contribution of some scattering light. Despite the spectrophotometer used, some other calculations are required in order to attain the extinction coefficients for the NPSs. Even though the two issues always exist in the measurement of the optical coefficients of NPSs, under particular conditions, either one or both of them may be negligible, which then means the experimental design can be made simpler.

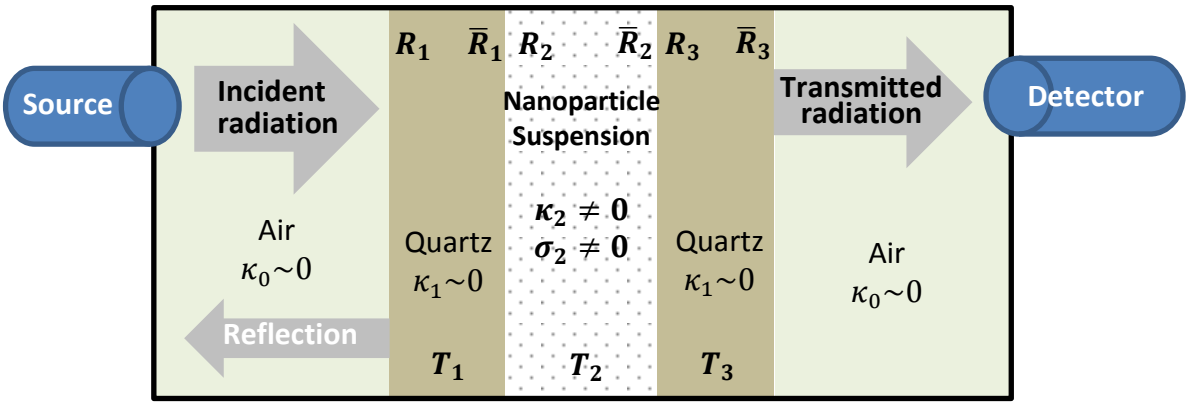

Figure 3.3 Diagram of three-slab system representation for a spectrometry measurement of a NPS- filled quartz cuvette (Taylor et al., 2011).

Spectral transmittance is the term used to describe the process by which incident radiant leaves a surface or medium from a side other than the incident side; usually the opposite side. The spectral transmittance is related to the medium depth and medium extinction coefficient. The spectral transmittance of a sample (T_λ) is defined as the fraction of photons that go through the sample over the incident number of the photons, which are based on the Beer-Lambert law, i.e., $T_\lambda = I/I_0$. Where, I is the transmitted wavelength intensity, I_0 is the incident wavelength intensity. The scattering contribution increases as the particles agglomerate to a greater extent (particle agglomerate size), the structure of the agglomerates also plays a significant role in the light attenuation and as a result it affects the spectral transmittance of the incident radiation (Kameya and Hanamura, 2011; Said et al., 2014; Song et al., 2016).

In conclusion, spectral scattering and absorption in a particulate media is a significant criterion for the radiative heat transfer, where a part of the incident intensity is converted into heat energy. Particles type, size, and shape play a significant role in the optical and radiative properties, where they affect the radiation absorption and scattering. Radiation is redirected by scattering, where deviated or redirected

radiation passes through multiple scattering in particulate media and can be absorbed by particles and/or the medium. These concepts represent the radiation augmentation and attenuation.The extinction coefficient (absorption and scattering) is one of the most important parameters in the photo-thermal energy conversion (Muhammad et al., 2016). The attenuation of the radiation within the NPSs, largely by the nanoparticles, leads to a temperature rise in the NPSs. The suspended nanoparticles themselves or their agglomerates act as heaters, which may then be exploited as thermal energy in thermal systems.

CHAPTER IV

RESEARCH METHODOLOGY

4.1 Introduction

This research represents the effect of the pH at different particle volume fractions on the nanoparticle agglomeration behavior and the radiative transfer in TiO_2 and Al_2O_3 NPSs. Two methods individual and hybrid using TiO_2 and Al_2O_3 NPs were prepared for the nanoparticle suspensions. For this purpose, the NPSs were first prepared in different conditions, and the corresponding particle agglomeration was characterized in order to obtain both the particle size distribution and the average (effective) particle agglomerate size. After that, the radiative properties of the prepared NPSs were determined based on the experiments using UV-Vis spectroscopy. The boundaries of the dependent and independent scattering regimes (DISRs) of the particle agglomerates as a function of the pH are demarcated, using the relationship between the wavelength and the clearance between the particles where the clearance between them are estimated by using Woodcock's equation.

To obtain the radiative properties for compact particle agglomerates theoretically based on the pH value, to compare the results with the experimental results, and to quantify the effect of the distribution on the particle size on the radiative properties of the NPSs, the Lorenz-Mie theory was used. The impact of the particle size distribution on the scattering behavior assuming a spherical shape of the agglomerates is calculated. This spherical shape (compact particle agglomerates) was used to understand the impact of the pH and particle size distribution of a NPS on the

scattering behavior in the NPSs in a general sense. The numerical part deals with the estimation of thermal radiation transfer based on the compact (average) particle agglomerate size, which was obtained from the distribution of the particle size in the experimental part, and the radiative properties of the NPSs from the Lorenz-Mie theory results are then used to estimate the volumetric photo-thermal energy conversion by solving the radiative transfer equation using the discrete ordinate method.

4.2 Experimental set-up

4.2.1 Materials and equipment

Two types of spherical shape titania and alumina (TiO_2 and Al_2O_3) nanoparticles were used. TiO_2 (anatase, 99.5%) and γAl_2O_3 (99%) nanoparticles had an average diameter of ($\sim 40\ nm$). The base fluid was distilled water (DI water). For the pH adjustment of the suspensions, Hydrochloric acid (HCl) and Potassium hydroxide (KOH) were used. The NPSs preparation was conducted without using any surfactant.

TiO_2 and Al_2O_3 NPs were selected because they showed good stability behavior under the electrostatic stabilization condition. Thus, the stability behavior of the two nanoparticles types was investigated under the same conditions (pH and $\emptyset$) and for the nanoparticles of equal size to observe their agglomeration behavior. Also, these two nanoparticles had differing optical properties (refractive index) which exhibited different spectral radiative properties. These have significant impacts on thermal radiation applications. Various kinds of nanoparticles are used in solar thermal collectors, and TiO_2 and Al_2O_3 nanoparticles are utilized widely where an enhancement in the thermal performance is observed based on the thermophysical and

radiative properties (Jing and Song, 2017; Muhammad et al., 2016; Said et al., 2014). The investigations showed that TiO_2 and Al_2O_3 NPSs have unique radiative properties, which play a significant role in the thermal performance of the photo-thermal energy conversion systems. The thermal efficiency of the proposed nanofluids in concentrating solar collectors shows an enhancement (more than 10%) compared to the conventional collectors under the same conditions (Gupta et al., 2015; Li et al., 2011; Yousefi et al., 2012). The most cost effective and widely used material in the family of engineering ceramics is alumina. Titanium dioxide has three types of crystal habits which are brookite, anatase and rutile. Brookite is one type of unstable crystal, with no industrial value, whereas the properties of anatase and rutile are stable, which are extremely significant in the applications (Haddad et al., 2014). Thus, it is important to attain a clear idea about the effects of NPs stability behavior and particle agglomeration on the radiation transfer for the TiO_2 and Al_2O_3 NPSs.

All the aqueous solutions (NPSs) were mechanically dispersed through sonication using an ultrasonic bath, and an Elmasonic S 100 (H) device was used for this purpose. The particle size distribution (PSD) and the average (effective) particle agglomerate size for each type of NPSs was measured based on the dynamic light scattering (DLS) technique, and the Malvern Zetasizer Nano ZS device was used for this purpose. The radiative properties of the NPSs were measured using the UV-Vis spectroscopy technique, and the Shimadzu UV-1280 spectrophotometer was used for this purpose (Prasher and Phelan, 2005).

4.2.2 Experimental procedure

The nanoparticles were uniformly dispersed in distilled water. The suspensions were prepared with volume fractions of 0.001, 0.006 and 0.01 v/v. All the aqueous solutions were set to a pH equal to $(2, 6, \text{and } 10)$ through the addition of acidic (HCl)

and basic (KOH). Acids have hydrogen ions (H^+) and are used for reducing pH values below ($pH = 7$), while bases have hydroxide ions (OH^-) and are used for increasing pH values higher than ($pH = 7$).

Using an ultrasonic bath for 30 minutes, the aqueous solutions (NPSs) were mechanically dispersed by sonication. The ultrasonic homogenizer is used to break large particle agglomerates that occur in the NPSs during the preparation processes. Ultrasonic energy is a form of mechanical vibratory energy, and its application over time leads to uniformly dispersed and stable NPSs. To be sure that the nanoparticles were well dispersed into the suspensions, all of the samples prepared were aged overnight at room temperature in a magnetic stirrer.

The dynamic light scattering technique is used for the zeta potential measurements as a function of the pH and to monitor the particle size distribution and the average (effective) size of particle agglomerates. In this technique, the scattered light from all the particles is correlated to the diffusion coefficient of the particles, and is based on the Stokes-Einstein equation, and the calculations for the diameter of spherical particles (hydrodynamic diameter) are calculated from the diffusion coefficient. The radiative properties of the particulate suspensions are sensitive to particle properties; including type, size, shape, concentration, and particle agglomeration, as well as the radiative properties of the medium. The spectral coefficients of the NPSs are investigated in ultraviolet and visible wavelength ranges using ultraviolet/visible spectroscopy, and the calculations are based on the Beer-Lambert law. The scattering behavior is different for the differing particle agglomerates' size and shape, where they play a significant role in the light attenuation and as a result, affect the spectral transmittance of the incident radiation.

4.3 Theoretical section

4.3.1 Optical properties of nanoparticle suspensions

In order to determine the radiative properties of the compact particle agglomerates, where compact particle agglomerates can be defined as effective spheres, the Lorenz-Mie theory was implemented. Then, the effect of the particle size distribution on the radiative properties of the NPSs was calculated assuming that the particle agglomerates have the compact spherical shape based on the pH value of the NPSs. Therefore, the effective (average) particle agglomerates, which were obtained from the experimental part (the dynamic light scattering technique), were used for this purpose. The obtained radiative properties from the Lorenz-Mie theory results were compared to the results from the experimental part obtained from the UV-Vis spectroscopy technique to quantify the behavior of the compact particle agglomerates in the thermal radiation transfer.

4.3.2 Dependent and independent scattering in nanoparticle suspensions

The dependent and independent scattering has significant effects on the radiative properties and transfer in the NPSs. The boundaries of the dependent and independent scattering regimes (DISRs) for the NPSs (individual and hybrid) under different conditions were observed. Used for this purpose are the different particle agglomerates for the varying NPSs types obtained from the dynamic light scattering in the experimental part. The relationship between the incident radiation and the distance (clearance) between the particle to particle surfaces should be quantified in order to specify the boundaries of the dependent and independent scattering.

The effects of the particle agglomeration with different parameters ($\mathrm{pH}, \phi,$ and d_p), as well as different particle agglomerate types (similar and dissimilar particle agglomerates), which are obtained from the individual and hybrid NPSs, are

demarcated on the boundaries of the dependent and independent scattering regimes.

4.3.3 Thermal radiation transfer in nanoparticle suspensions

In the NPSs, the thermal radiative transfer was acquired by solving the radiative transfer equation using the discrete ordinate method (DOM). The discrete ordinates method finds solution for the field equations for intensity of the radiation associated with a fixed direction, which is represented by a discrete solid angle. The discrete ordinates calculation requires the specification of the number of solid angles or "ordinates" into which the sphere surrounding any particular point is discretized. The volumetric radiative energy source and thermal flux efficiency were achieved through solving the radiative transfer equation using the DOM method. The compact particle agglomerates, which were obtained using the dynamic light scattering technique, and the radiative properties of the compact particle agglomerates using the Lorenz-Mie theory were used in order to solve the radiative transfer equation.

Figure 4.1 shows the structure of this research (experimental and theoretical sections) which is divided into three parts including NPSs preparation, characterization, and the investigation of the radiative transfer in the NPSs. The experimental sections cover the NPSs preparation, characterization, and radiative properties measurement. The theoretical part covers the calculation of the radiative properties of the compact particle agglomerates and the numerical solution of the RTE to obtain the radiative absorption and emission in the NPSs.

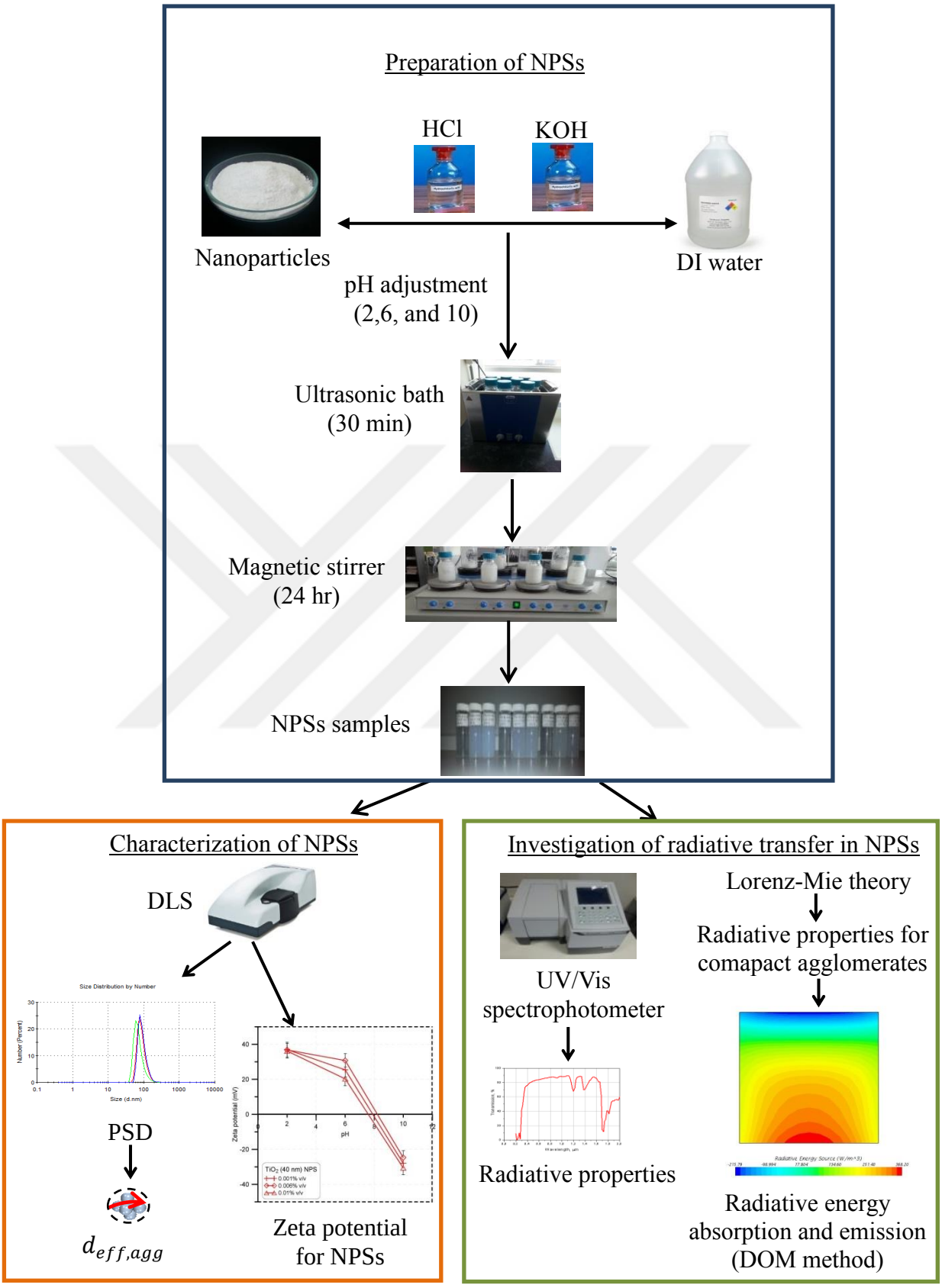

Figure 4.1 The structure of the research (experimental and theoretical sections).

CHAPTER V

PREPARATION AND STABILITY MEASUREMENT OF NANOPARTICLE SUSPENSIONS

5.1 Introduction

The stability of NPSs is one of the most important subjects for NPSs. The characteristics of the suspended particle and the base fluid, such as the particle morphology, the chemical structure of the particles, and the base fluid, strongly affect the stability of NPSs. Therefore, there are two phenomena that are critical to the stability of NPSs: agglomeration and sedimentation. Similar and dissimilar nanoparticles in the same medium have different stability behavior and show different properties. Therefore, it is important to investigate the stability behavior and its effects on the properties of NPSs such as the radiative properties for both the individual and hybrid NPSs (Behi and Mirmohammadi, 2012; Sarkar et al., 2015).

One of the main challenges of NPSs is particle agglomeration, and the agglomeration of particles is monitored by measuring the particle size variation and particle size distribution over time. The particles experience random thermal motion by the Brownian motion when the particle size in suspension is under tens of micrometer, and the speed of the particle movement differs according to the Stokes-Einstein equation depending on the size of the particle. The smaller particles move quicker, and the larger ones move more slowly. The another main challenge of the NPSs is the high cost of production. The commercialization of NPSs will be feasible and successful and there will be considerable developments in many applications by overcoming these challenges. The key to overcoming these difficulties is by

decreasing the rate of the particle agglomeration in order to avoid large size and complex shape particle agglomerates, which have a significant effect on the stability of the NPSs, which leads to the minimization of the particle sedimentation rate (Klusek et al., 2003).

5.2 Individual and hybrid nanoparticle suspensions

Nanoparticle suspensions are engineered colloids consisting of a base fluid and single (individual) type of nanoparticle. The definition of hybrid nanoparticle suspensions is nanoparticle suspensions, which are composed of two or more differing materials of nanometer size in the base fluids, and so hybrid NPSs are a very new type of NPSs. These days, this kind of NPSs is attracting the attention of researchers. The essential idea behind hybrid NPSs is to attain a favorable improvement in thermophysical, radiative, hydrodynamic and heat transfer properties when compared to mono NPSs. One single material does not possess all the favorable characteristics necessary for a particular purpose; it might have either good thermophysical and/or radiative properties or rheological properties for example. However, in practical applications, it is a requirement to have trade-off between several properties, which is where the use of hybrid NPSs comes in (Sarkar et al., 2015). A hybrid NPS is a suspension that is a combination of both the physical and chemical properties of various particles simultaneously, which provides these properties in a homogeneous phase. Synthetic hybrid NPSs exhibit remarkable physicochemical properties that do not exist in individual ones. The preparation, stability, thermophysical and radiative properties, and applications of hybrid NPSs are known but the use of these NPSs has not been studied as such. Work on hybrid NPSs is very limited and a lot of experimental studies are still required (Sundar et al., 2017).

Application areas of individual NPSs widely vary such as electronic cooling, engine cooling/vehicle thermal management, generator cooling, coolant in machining, welding, nuclear system cooling, lubrication, thermal storage, solar heating, cooling and heating in buildings, transformer cooling, biomedical, drug reduction, heat pipe, refrigeration, space, defense, and ships (Jyothirmayee Aravind and Ramaprabhu, 2012). The hybrid NPSs are still in the research and development phase as far as their applications in the industry are concerned. It is expected that hybrid NPSs will also be used for similar applications, but with better performance. However, the application-oriented research on hybrid NPSs is limited to very few applications (Sundar et al., 2017). Long term stability and particle agglomeration are the similar challenges that can be faced with hybrid NPSs also. The stability issue might be more for the hybrid NPSs of the two varying kinds of nanoparticles when compared to that of similar ones (Moghadassi et al., 2015). The suspension of the two different types (shape and size) of the nanoparticles may cause many problems such as a higher viscosity, and a high particle agglomeration rate, which leads to a higher sedimentation, etc. Hybrid NPSs have to be engineered properly by selecting suitable nanomaterials pairs in order to obtain good stability behavior and better properties. The production process for hybrid NPSs will be more complex, which leads to higher production costs, which is among the many reasons that may hinder the application of hybrid NPSs in industry. A thorough understanding of the synthesis, characterization, and thermophysical and radiative properties of hybrid NPSs is essential for the use of them in both domestic and industrial applications (Babu et al., 2017).

5.3 Preparation of nanoparticle suspensions

5.3.1 General issues and concerns

The stability of NPSs is the main issue for both scientific research and for practical applications. To maintain the stability of NPSs, the two stability methods; electrostatic stabilization and surfactants are used. In hybrid nanoparticles the stability of the suspended particles remains a major challenge because of the suspension of the two different types of nanoparticles. Almost all researchers have measured stability after the preparation of the selected NPSs, but they have not measured or reported the stability of their prepared NPSs after experiments under different conditions (Devendiran and Amirtham, 2016). Nanoparticles may exist in many configurations that range from a well-dispersed mode to a totally agglomerated state. The NPSs stability are classified into three category types: (i) Kinetic stability: The nanoparticles that are dispersed in the NPSs are under the Brownian motion, which overcomes their sedimentation caused by gravitational force; (ii) Dispersion stability: Because of the agglomeration of the nanoparticles, the nanoparticles' dispersion into the fluids may deteriorate over time; and (iii) Chemical stability: There are no chemical reactions between the suspended nanoparticles or between the base fluid and nanoparticles desired in the NPSs. Thus, it is a necessary requirement to carefully prepare the NPSs to ensure their long term stability (Das et al., 2007).

There are many issues and challenges regarding NPSs that need to be addressed and overcome before this field of study can be fully established. The main issues are: (i) the disagreements between most of the experimental data, as well as between the experimental findings and the theoretical model predictions (ii) the poor characterization of the NPSs, and (iii) the lack of understanding of the complex physical phenomena responsible for the anomalous behavior of NPSs. Preparing of

NPSs presents many challenges; both technical and financial. The main technical difficulty is in the production of a homogeneous suspension of the nanoparticles, mostly because the particles always tend to agglomerate due to the strong Vander Waals interactions (Wang and Mujumdar, 2008).

5.3.2 Preparation methods

The most important step in the preparation of a NPS is the mixing of the nanoparticles with the base fluid. A variety of methods have been discussed regarding the preparation of NPSs, which can be divided into two approaches (one-step and two-step approaches). In the one-step approaches, the NPSs are synthesized by dispersing the NPs directly in the base fluids. The vaporization of the base materials under vacuum conditions is included in this approach. One positive regarding this approach, is that the agglomeration of the nanoparticles is minimized. However, its negative is that the vapor pressure of the fluid is required to be very low. Because the NPSs are prepared in situ, only small quantities can be produced and this is mostly done in batches. This precludes the mass production of the NPSs in industrial processes that can be commercially available (Liu et al., 2005; Wang et al., 2003).

In the two-step approach, the nanoparticles are first synthesized into the desired shape and size, and then NPs are dispersed in the base fluids. The significant advantage of the two-step process is that NPs can be produced separately by an industrial method, which allows their huge and cheap production. The main disadvantage of this approach is that the NPs tend to agglomerate in the base fluids, and stabilizers are important for the stability enhancement. Producing a homogeneous suspension using the two-step method remains a challenge. However, this method is more preferable when the stability of the nanoparticles can be achieved (reducing the agglomeration rate) (Yang and Du, 2017).

The cost of the preparation and distribution of the NPSs will be an important factor in their commercial applications. The delicate preparation of a NPS is important because NPSs need special requirements such as an even suspension, stable suspension, low agglomeration of particles, and no chemical change in the fluid (Lee et al., 1999). Xuan and Li recommended methods used for the stabilization of the suspensions: (i) changing the pH value of suspension, (ii) using surface activators and/or dispersants, (iii) using ultrasonic vibration. These different methods can alter the surface properties of the suspended particles and may be used to suppress the formation of particle clusters in order to attain stable suspensions. Using these techniques is dependent on the necessary application of the NPSs. The choice of suitable activators and dispersants depends mainly upon the properties of both the solutions and particles. The stability of the dispersion of the nanoparticle in the base fluid is shown by the zeta potential value, and a high zeta potential value indicates good stability (Xuan and Li, 2000).

5.4 Stability of nanoparticle suspensions

5.4.1 Introduction to nanoparticle dispersion

The particles in the suspensions may adhere together as a result of their large surface area and attractive forces between them, where the different shape and size of the particle agglomerates are produced. The structure and size of agglomerates depend on different parameters connected to the particles composition and the boundary conditions (Kozan and Mengüç, 2008; Munday, 2000; Russel et al., 1989). Due to the weight of the agglomerates, the particles cannot remain in the suspension and the sedimentation takes place. Consequently, stability means that the suspended particles do not agglomerate at any significant rate. The agglomeration can be decreased by

stability enhancement via one of the stabilization methods. When the barrier between particles against agglomeration reinforces colloidal suspension becomes more stable. However, remaining as one of the key concerns for their reliable and repeatable applications is the nanoparticle suspensions stability. Their stability impacts the particle agglomeration and sedimentation, which have an important impact on thermophysical and radiative properties (Michaelides, 2014).

The process of particle agglomeration is a complex process that depends on several properties in the base fluid and the particles. A general theory has been developed in the past for agglomeration, which is referred to as the Derjaguin–Landau–Verwey–Overbeek theory, or the DLVO theory (Derjaguin, 1941; Verwey, 1947). Accordingly, the agglomeration process is modeled by the combination of the attractive and repulsive forces that act on a pair of particles in a single potential energy function. The Brownian motion of the nanoparticles results in a frequent collision with each other. The two basic interactions, attraction and repulsion, are involved in these collisions. The dispersion stability of the nanoparticles is thus determined by the interactions between the suspended nanoparticles. When the attraction dominates, a particle will adhere to the neighboring particles and forming particle agglomerates. If the attraction is overwhelmed by the repulsion, the nanoparticles can be stably dispersed. The complete possible energy of a particle is the sum of the attractive and repulsive energies as shown in Figure 5.1. It can be seen that the attractive energy increases rapidly as the particles approach each other, while the repulsive energy changes somewhat more slowly. As the particles approach each other, the total potential energy curve first reaches a maximum value point (maximum energy barrier), which implies that an energy barrier exists towards the adherence of the particles. Once the energy barrier is overcome, the particles will attract more strongly

and the potential energy falls rapidly to the primary minimum value of the curve (the minimum energy barrier). Therefore, the smaller the energy barrier is, the more possible the particles may agglomerate (Michaelides, 2013).

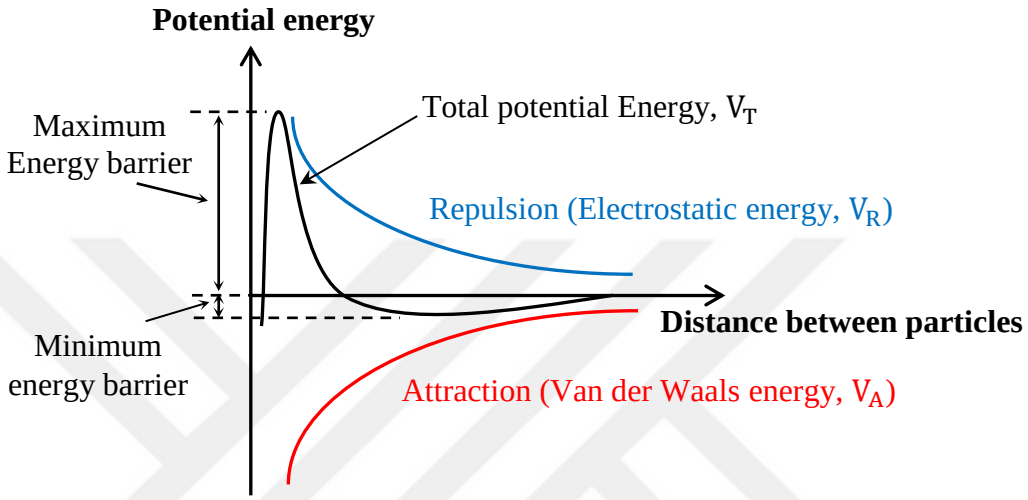

Figure 5.1 Potential energy versus the distance between suspended particles (Michaelides, 2013).

5.4.2 Steric stabilization

In the steric stabilization technique, surfactants (dispersants) are used in NPSs to enhance the stability of NPSs. An easy and economical way to enhance the stability of NPSs is by adding dispersants in the two-phase systems. Dispersants can have a significant impact on the surface characteristics of a system in small quantities. Dispersants include a hydrophobic tail portion, a long-chain hydrocarbon, and a hydrophilic polar head group. The reason that dispersants are employed is to increase the contact of the two materials, which is generally known as wettability. In a two-phase system, it is a dispersant that tends to locate at the interface of the two phases,

where it introduces a certain degree of continuity between both the nanoparticles and fluids. According to the composition of the head, the surfactants are separated into four groups: nonionic surfactants with no charge groups in its head (include polyethylene oxide, alcohols, and other polar groups), anionic surfactants with head groups negatively charged (anionic head groups include long-chain fatty acids, sulfosuccinates, alkyl sulfates, phosphates, and sulfonates), cationic surfactants with positively charged head groups (cationic surfactants may be protonated long-chain amines and long-chain quaternary ammonium compounds), and amphoteric surfactants with zwitterionic head groups (Hwang et al., 2008; Yu and Xie, 2012).

How to select suitable dispersants is a key issue. Generally, when the base fluid of the NPSs is polar solvent, water-soluble surfactants should be selected; if not, oil-soluble ones will be chosen. Polar solvents have big dipole moments (partial charges), and they include bonds between atoms with varying electro negativities such as oxygen and hydrogen; an example of a polar solvents is water. For nonionic surfactants, we can evaluate the solubility through the term the hydrophilic/lipophilic balance (HLB) value. The lower the HLB number is, the more oil-soluble the surfactants, and in turn, the higher the HLB number is, the more water-soluble the surfactants is (Yu and Xie, 2012). Even though surfactant addition is an effective way to improve the dispersibility of the nanoparticles, surfactants may cause several issues (Chen et al., 2008). For instance, the addition of surfactants could cause contamination in the heat transfer media. Surfactants may produce foams when heating, and heating and cooling are routine processes in heat exchange systems. Moreover, the surfactant molecules that attach themselves onto the surfaces of the nanoparticles could enlarge the thermal resistance between the nanoparticles and the base fluid, which may then limit the enhancement of the effective thermal conductivity. Thus, surfactants are

unsuitable for thermal applications, in particular at high temperatures (Michaelides, 2013; Munday, 2000; Wang et al., 2003).

5.4.3 Electrostatic stabilization and pH effects

The particle surfaces become charged in order to prevent their collisions in electrostatic stabilization. Electrostatic stabilization of NPSs can be achieved by the adjustment of the pH value of a NPS. The pH value has a significant impact on the particle agglomeration behavior of NPSs, which in turn affects the different properties such as absorption and scattering of the NPSs. Therefore, the particle agglomeration rate is strongly dependent on the pH value, and a low and/or high particle agglomeration rate can be observed under the effect of pH. In accordance with the DLVO theory, the suspensions' pH value could notably affect the nanoparticle agglomeration. The pH value effects are involved under the concept of the electrostatic stabilization of suspensions, which affects the potential barrier (electrostatic repulsive forces) between the suspended particles. The pH value of the suspensions influences the surface electrostatic potential of the suspended nanoparticles (Dhont, 1996; Rajagopalan and Hiemenz, 1997). This aspect of nanoparticle agglomeration as a function of the pH value has not been explained extensively, which is one of the objectives in this research. Moreover, particle agglomeration can be tuned to the desired effect by changing the pH value of both the individual and hybrid NPSs.

The pH value of particulate suspensions is one of the keys for particle stability, and it is a scale that refers to the hydrogen ions (positive and negative ions) in the colloidal suspensions. Ions concentrate around suspended particles and they form a layer. This layer is known as the double layer (DL), which includes the negative or positive ions attached to the particle surface based on the surface charge. The electrostatic stabilization is indicated by the zeta potential, which represents the

potential difference in the DL and the point in the medium under the effect of the ions consternation. That is to say that the zeta potential is the potential difference between the dispersion medium and the stationary layer of the fluid that is attached to the dispersed particle. The zeta potential value should be high enough in positive or negative values for good stability. In addition, there will be some regions surrounding the condition of zero zeta potential (i.e. the isoelectric point or pH_{iso}) at which the NPSs lose their stability. Within this unstable region, the particle agglomerations occur at a high rate and complex agglomerates are formed, thereby there is a significant increase in the particle size. An isoelectric point measurement indicates how the pH affects zeta potential and determines at which pH the zeta potential equals zero (Hunter, 2001; Russel et al., 1989).

To simplify all these concepts, Figure 5.2 shows the stability map of the NPSs and the two charged nanoparticles, where the electrical double layers are explained. The regions of the stability and instability as a function of the pH are explained by the stability map. In this figure, two suspended nanoparticles with negative charge surface in a base fluid are shown. Because of the negative charge on the surface of the particles, the positive ions are attached and surrounding the surface of the nanoparticles and they then form the DL. This layer also includes some negative ions which are attached to the positive ions that are close to the surface of the nanoparticle. Thus, the combination of the charges in the double layer and the negative charge of the particles produces an electrical potential that decreases with the distance from the particle surface.

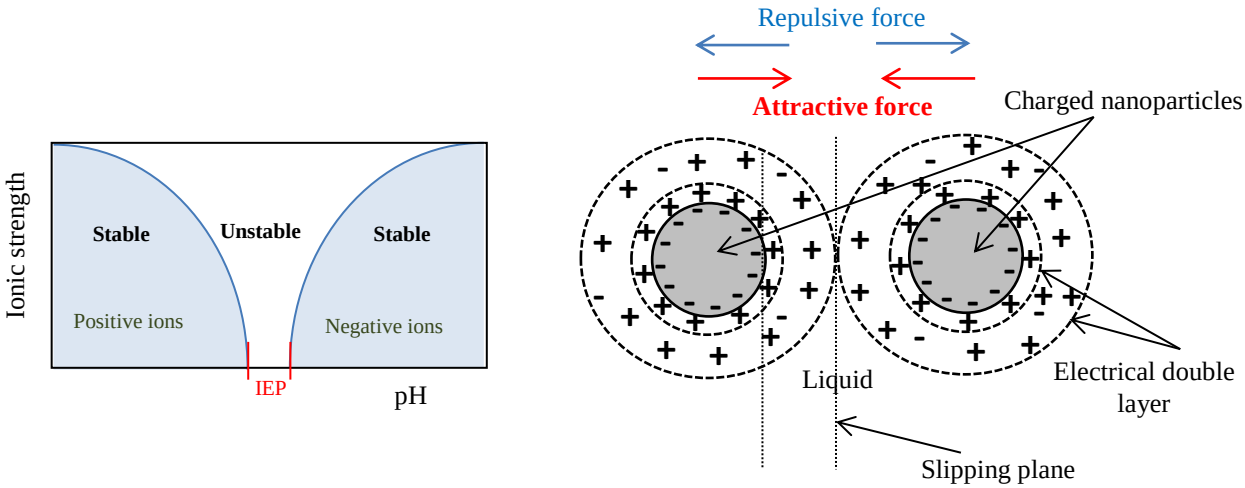

Figure 5.2 Electrostatic stabilization sketch of NPSs. (a) stability map and (b) electrical double layer.

The electrostatic stabilization of the NPSs depends on many parameters such as pH, temperature, zeta potential, and particle size, while the pH and zeta potential are the dominant parameters. It is usually preferred in thermal applications, specifically in the applications that include high temperatures. Thus, in thermal applications such as the solar thermal collectors where different temperature gradients occur, the stabilization of the nanoparticles can be achieved through the enhancement of the repulsive forces between the particles, which leads to a decrease in particle collisions; especially at high temperatures (Yu and Xie, 2012).

5.5 Nanoparticle agglomeration

5.5.1 Particle agglomeration and sedimentation

Most of the particles in nature are found in agglomerated forms, and understanding particle agglomeration concepts and mechanisms are important in a wide range of applications and processes. There are different factors that cause and

affect the interaction (attractive) force between particles which is one of the factors whereby the particles form bonds. Particle agglomeration behavior is controlled by surface forces; attractive and repulsive forces. With the decreasing particle size, particularly particles at the nano-size, the probability of particle agglomeration increases. That is because the distance between the particles decreases with the decreasing particle size making the attractive force more important, where the extremely large surface area of particles is in comparison with their volume (Mewis and Wagner, 2012; Tadros, 2012).

Yet, there is no clear and unambiguous model to describe a best fitted mathematical model to describe the particle agglomeration, where various morphological particle agglomerates are formed and real particle agglomerates show stochastic variations in the size and structure in addition to their properties. However, the scaling law is the most well-known and most commonly used method to describe the fractal structure of the agglomerates. Particle agglomeration can be described by fractal characterization; the fractal analysis provides information about the particles agglomeration, which is widely used for different agglomerated colloids (Manickavasagam and Mengüç, 1997). The number of particles in each agglomerate can be estimated as a function of different parameters (Witten Jr and Sander, 1981). In the scaling law, agglomerates are characterized by their radius of gyration and their relationship to the original particle size as follows (Nogi et al., 2012; Saltiel et al., 2004):

$$(R_{agg}/r_p)^{d_f} = (1 + t/t_p) \approx N_{int} \qquad (5.1)$$

where R_{agg} is the radius of particle agglomerate, r_p is the single particle radius, t is the particle suspension time, N_{int} represents the number of particles in each agglomerate, t_p is the agglomeration time constant, and d_f is the fractal dimension.

The fractal dimension value ranges from between 1.8 and 2.5, in the case of a high barrier between the particles ($d_f \approx 2.5$), whereas ($d_f \approx 1.8$) is for the weak repulsive barriers (Saltiel et al., 2004).

To obtain the mass of the particle agglomerates, the number of particles in the agglomerates has been considered, and from Equation 5.1 the total mass of the particles in a single agglomerate is given by (Prasher et al., 2006):

$$m_{agg} = m_p(1 + t/t_p) \tag{5.2}$$

where m_p and m_{agg} is the mass of the particle and its agglomerate, respectively.

The particle agglomeration rate can be represented by the particle agglomeration time constant (characteristic time for the doublet formulation), which is calculated from (Prasher et al., 2006):

$$t_p = \frac{\pi \mu r_p^3 W}{k_B T \emptyset} \tag{5.3}$$

where μ is the density of the fluid, W is the stability ratio, k_b is the Boltzmann constant, T is the temperature, and $\emptyset$ is the particle volume fraction.

Equation 5.3 shows that t_p decreases rapidly with the drop in the radius of the nanoparticle, which means that rapid particle agglomeration can take place for small nanoparticles. W represents the relationship between the attractive and repulsive forces between the nanoparticles when $W \ggg 1$, for the high repulsive force between the particles exists. In comparison to the effects of other parameters in Equation 5.3, t_p is strongly affected by the W and r_p.

To clarify the particle agglomeration process, Figure 5.3 shows a hypothetical shape of a homogeneous colloidal suspension. This figure explains the agglomeration process of the suspended particle with the approximate shapes of the particle agglomerates because there is no regular shape or structure of them inside a particulate

suspension. Also, this figure demonstrates the principle of the radius of gyration of particle agglomerate.

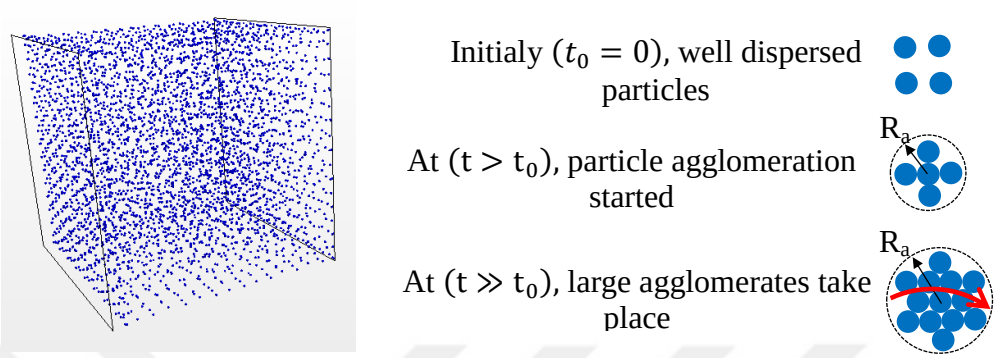

Figure 5.3 A hypothetical shape of a homogeneous a NPS explains the particle agglomeration process.

The stability ratio (W) of the NPs can be modeled using the DLVO theory, and it is defined as the ratio of the rate of the diffusion controlled particle collision to the rate of the interaction force controlled particle collision. In other words, the stability ratio is calculated by the repulsive (V_R) and attractive (V_A) forces between the nanoparticles as (Dhont, 1996; Russel et al., 1989):

$$W = 2r_p \int_0^{\infty} \beta(h_{sur,p})\ exp\left[\frac{V_R + V_A}{k_B T}\right] / \left(h_{\ sur,p} + 2r_p\right)^2 dh_{\ sur,p} \qquad (5.4)$$

where $\beta(h_{sur,p})$ is the hydrodynamic interaction factor and $h_{sur,p}$ is the surface to surface particle distance.

Equation 5.4 shows that the stability ratio is strongly affected by the particle size and repulsive and attractive forces, and the repulsive force is a function of the pH and the zeta potential. Therefore, the particle size, pH, and zeta potential have

significant impacts on the stability ratio of the NPSs. The particle agglomeration rate decreases rapidly by decreasing the stability ratio and particle size, and under this condition a large particle agglomerate is generated. Consequently, the stability implies that the suspended particles do not agglomerate at an important rate (Prasher et al., 2006).

The surface to surface particle distance, which is one of the most important parameters affecting the radiative properties of the NPSs is given as a function of the particle volume fraction, and the particle diameter, and it is estimated by using Woodcock's equation (Nogi et al., 2012; Woodcock, 1987):

$$h_{sur,p} = d_p[(1/(3\pi\emptyset) + 5/6)^{0.5}] \qquad (5.5)$$

One of the stability parameters of the NPSs is particle sedimentation, and the rise in the mass of particle agglomerates causes the acceleration of the sedimentation velocity, which is calculated as (Michaelides, 2014; Sajid et al., 2014):

$$v_p = \frac{2R_{agg}^2 g(\rho_p - \rho_f)}{9\mu} = \frac{m_{agg} g - 4/3\pi R_{agg}^3 \rho_f g}{6\pi\mu R_{agg}} \qquad (5.6)$$

where ρ_p and ρ_f are the densities of the particle and base fluid; respectively, and g is the gravitational acceleration.

In order to reduce the sedimentation velocity, the viscosity of the base fluid should be increased or the difference between the density of the nanoparticles and base fluid minimize, and the nanoparticle size reduced. Among the set of choices, the sedimentation velocity decreases remarkably with the reduction in the nanoparticle size. However, the agglomeration rate increases with smaller nanoparticles because the smaller nanoparticles have a higher surface energy. The nanoparticles in the suspension are under the Brownian motion, which can decrease the nanoparticles sedimentation caused by the gravitational force. Equation 4.6 demonstrates a balance

of buoyant, gravity, and frictional forces, which explain all the above notions that impact the stability of the suspended nanoparticles (Michaelides, 2013).

5.5.2 Diffusion and reaction limited particle agglomeration under the pH effect

As the particle agglomeration process continues, large clusters form. The growth in general takes place through encounters between the different clusters, and thus one refers to cluster-cluster agglomeration process. The resulting clusters are not regular, but are statistically self-similar. One refers to the diffusion limited cluster agglomeration (DLCA) or reaction limited cluster agglomeration (RLCA) depending on whether the agglomeration is fast or slow. The clusters have various features in each regime. DLCA clusters are loose and ramified ($d_f \approx 1.8$), but the RLCA clusters are more compact ($d_f \approx 2.5$). The distribution of the cluster size also varies in these two regimes. The pH value carries a significant impact on the stability behavior of the nanoparticles, which in turn carries the dominant impact on the particle agglomeration rate (Prasher et al., 2006). It is known that the increase and decrease of potential energy means that the forces between the particles are repulsive or attractive, respectively. In a suspension, the drastic and ceaseless Brownian motion may cause the nanoparticles to collide. These collisions reduce the distance between the nanoparticles; therefore, the Van der Waals attraction would hold them together without separating them again. This process of agglomeration is known as DLCA (Cosgrove, 2010; Lattuada et al., 2003). However, in the RLCA, only if the collision happens and the particles react with each other, will the agglomerates be formed. The difference between them is that in DLCA, the particles will form an agglomerate if collision occurs (Lattuada et al., 2003).

Differing sizes and structures (linear, porous, and compact) of particle agglomerates are produced dependant on the pH value of the particulate suspensions.

In the DLCA process, the repulsive (barrier) forces between the particles are weak as in the case of the pH value of the NPSs being equal or close to the pH_{iso}. The fast agglomeration is achieved in the DLCA process, where loose and more ramified (linear and/or porous) particle agglomerates are produced. In the RLCA process, the strong barrier (the repulsive forces) between the particles is achieved as in the case of the pH value being far from the pH_{iso}. Slow agglomeration occurs in the RLCA process, and more compact particle agglomerates are produced. The larger the cluster size, the quicker their settling velocity is, which in turn causes particles agglomerates sedimentation (Hunter, 2001; Russel et al., 1989). Table 5.1 shows a comparison between the characteristics of the two particle agglomeration processes (DLCA and RLCA).

Table 5.1 A comparison between the DLCA and the RLCA characteristics.

RLCA	DLCA
More compact	More ramified
Closely attached to the surfaces	Loosely attached to the surfaces
More efficient scattering	Less efficient scattering
Ideal particles spacing	Non-ideal particles spacing

Figure 5.4 shows the particle agglomeration curve for the TiO_2 particle, where different regions (stable and instable regions) are specified based on the pH_{iso} of TiO_2 particle. There is an intermediate region around the condition of the zero zeta potential at which the TiO_2 suspensions lose their stability (unstable region). In the unstable region, the particles agglomeration occurs at a higher rate, and complex agglomerates are formed (DLCA), thereby a significant increase in the particle size is observed. On

the other hand, the case of RLCA occurs in the stable region where the pH value is far from the pH_{iso} of the TiO_2 particle.

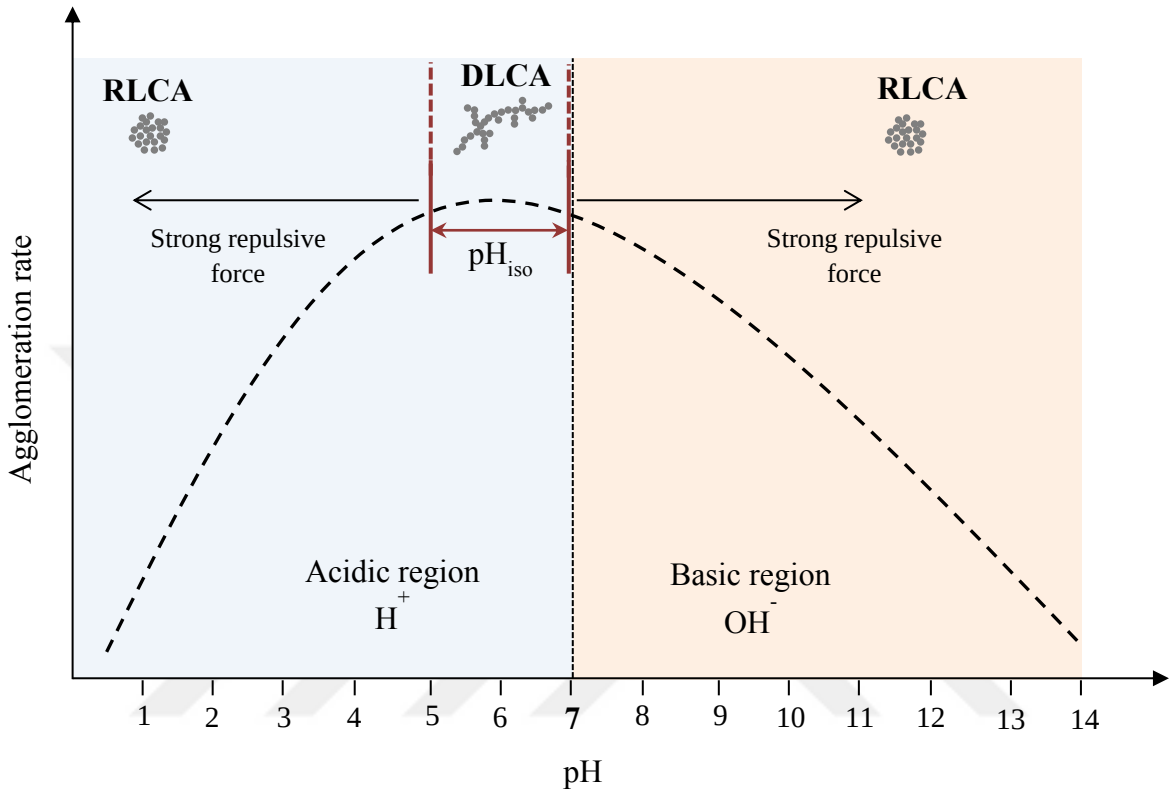

Figure 5.4 Particle agglomeration curve for the TiO_2 particle.

From the discussions above, challenges can be clearly found. Firstly, the agglomeration processes of the nanoparticles are complicated; thus, a more accurate model such as Brownian dynamic simulation may not be fast enough to simulate large systems such as those of the NPSs systems. Optimized arithmetic and high-powered hardware are needed. Second, basic optical models can only be applied based on some very strict conditions, which are difficult to apply in practice. Optical models considering particle agglomerates can explain complex scatters. However, before the application, the detailed structures of the particle agglomerates should be known. The

challenges mentioned above may be the important issues limiting the application of the NPSs. By overcoming these challenges, it is expected that the NPSs can be applied in a practical way to significantly enhance the different systems including solar-thermal conversion systems.

5.6 Nanoparticle characterization: the dynamic light scattering technique

Different theoretical methods and experimental techniques are used for the particle characterization of NPSs, including earlier studies (Aslan et al., 2003; Kozan et al., 2008). Theoretical methods may be too slow to solve a real NPSs system where a large number of particle agglomerates occur (the real particulate suspensions). Advanced measurement systems and optimization algorithms are needed to infer a meaningful interpretation of the results using the theoretical methods (Aslan et al., 2006; Jing and Song, 2017). Understanding the changes in the number of particles of a particular size is important to understand the agglomeration phenomenon in the NPSs. The characterization of the NPSs always reveals several important details such as the nanoparticle shape, size, distribution, and stability of the nanoparticles in the base fluid.

The DLS technique is an intensity based one, and the sample is in the solvated state. The particle diameter measured in the DLS is the hydrodynamic diameter. Among many experimental techniques, the dynamic light scattering (DLS) technique is extensively considered as the preferred technique for the determination of the particle size and particle size distribution characterization of the NPSs (Murdock et al., 2008; Powers et al., 2006). The DLS is a non-invasive technique, which is used for the size characterization of the dispersions in the sub-micrometer range. It is known as photon correlation spectroscopy or quasi-elastic light scattering also. The average

particle size (hydrodynamic diameter) is obtained from the particle size distribution (PSD) in the DLS technique. The intensity of the scattered light from the particles is correlated with the diffusion coefficient of the particles, and then the particle diameter is attained from the diffusion coefficient which is based on the Stokes-Einstein equation (Das et al., 2016; Taborda et al., 2016). Figure 5.5 shows a schematic diagram that describes the dynamic light scattering technique, which includes nanosuspension sample containing particle agglomerates with different sizes and structures. The benefits of the DLS technique are as follows; operators can acquire usable detailed data without having to have significant expertise, sample volumes are extremely small (down to just a few microliters), which makes this an attractive technique for early stage research where there are valuable materials involved, and this technique is fundamentally very good for the measuring of particle sizes across the range of ($\sim 0.3\ nm\ to\ \sim 10\ \mu m$). In addition, its ability to measure small particles is very valuable with most systems giving the correct reproducible data for particles. Thus, the size and particle concentration range with the high reproducibility of the technique allows for the DLS to be suitable for a wide variety of applications (Kaszuba et al., 2008; Murdock et al., 2008). In the DLS technique, the speed at which the particles diffuse due to Brownian motion is measured by recording the rate at which the intensity of the scattered light fluctuates. Smaller particles cause the intensity to fluctuate more rapidly than the large particles, as shown in Figure 5.6.

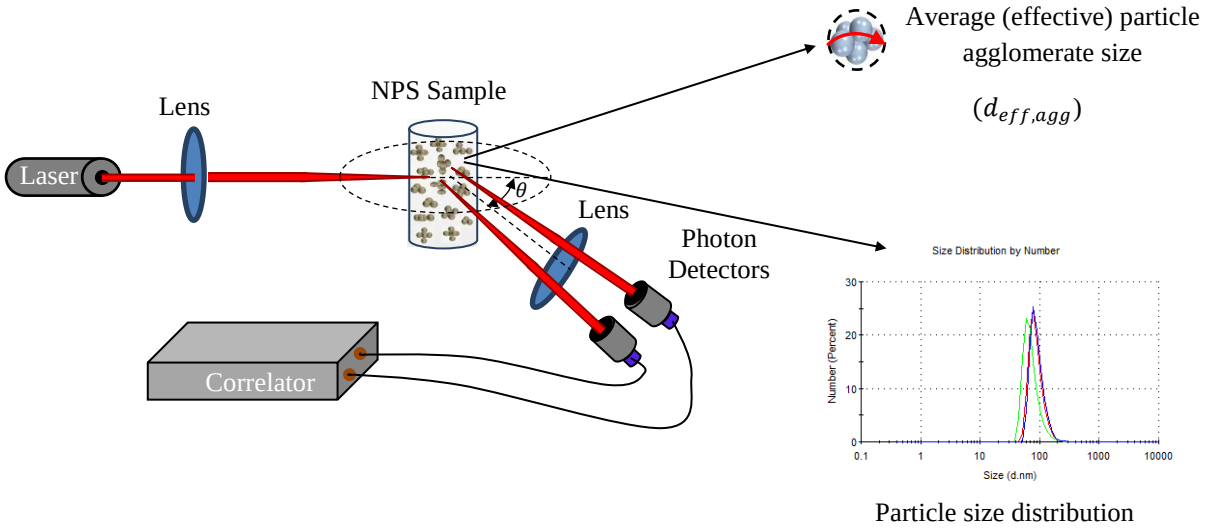

Figure 5.5 Schematic diagram of the dynamic light scattering technique.

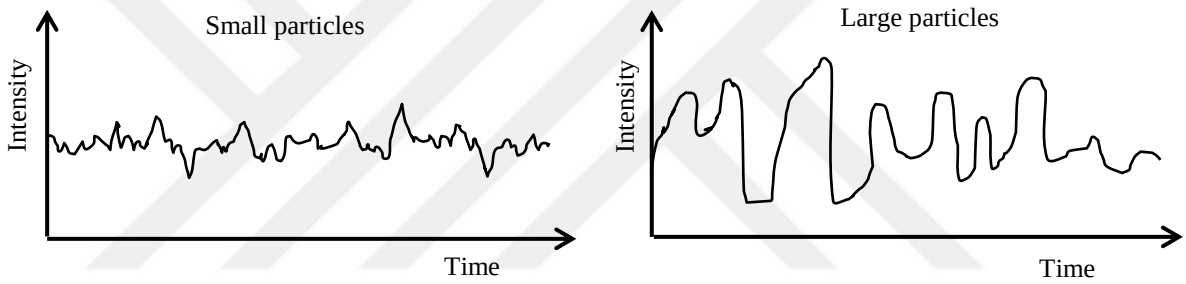

Figure 5.6 Typical intensity fluctuations for large and small particles.

The main principle of DLS is the scattering of light by the particles in a suspension. According to the Stoke-Einstein equation, the diffusion coefficient (D) is inversely proportional to the hydrodynamic diameter of the particles. This means that small particles show relatively large diffusion coefficient. From this, it follows that smaller particles move more rapidly than larger particles. It is possible to determine the hydrodynamic size, via an autocorrelation function by observing the motion and determining the diffusion coefficient of particles in liquid media, fluctuations of scattered light intensities over time (Hassellöv et al., 2008; Kaszuba et al., 2008; Xu, 2001).

$$D = \frac{k_B T}{3\pi\mu d_H} \qquad (5.7)$$

where d_H is the hydrodynamic diameter, and D is the diffusion coefficient.

DLS determines a scattering intensity weighted particle size distribution. Larger particles typically dominate the size results because the intensity of the scattered light generally increases with the particle size. The Rayleigh approximation postulates that the intensity is proportional to the size by the exponent of six for small particles below 100 nm. For instance, the scattered intensity of a 100 nm particle is one million times higher as the scattered light of a 10 nm particle of the same composition. This leads to a shadowing of the smaller particles. Therefore, small particles or any weak scatters are underestimated or even not detected in a polydisperse suspension using DLS. The quality of the measurement with a DLS instrument is also affected by many parameters, such as the oriented movements (sedimentation), the temperature (convective drift), and the concentration of the material. Due to this, the measured suspension should be stable for at least the measurement time in order to generate valid results. The velocity distribution of the particle movement by measuring the dynamic fluctuations of light scattering intensity yields an overall measurement of the particle perpendicular to the light source at that time. The measurement technique is carried out by using the Zetasizer Nano-ZS to measure the zeta potential of the particles in a solution. This technique uses a laser, which is passed through the sample, to measure the particle velocity in an applied electric field of a known value. This is known as electrophoretic mobility.

5.7 Results and discussion

In this chapter, the results of the preparation, stability, and characterization of NPSs; individual (TiO_2 and Al_2O_3) and hybrid ($TiO_2 + Al_2O_3$) NPs in the base fluid (DI water) are discusses in two sections. The first section is for the preparation and stability of the NPSs under different conditions (pH and $\emptyset$), where the zeta potential of the NPSs is investigated. Also, the effect of the nanoparticle type on the zeta potential and the stability of NPSs are discussed under different conditions. The second section is for the characterization of the NPSs, where the particle size and size distribution under the effect of particle agglomeration are investigated. The effects of the similar and dissimilar nanoparticles in the same medium on the particle agglomeration are explored. The effect of the different type, size, and structure of the particle agglomeration on the surface to surface particle distance is explored. The sedimentation rate of the particle agglomerates is calculated, which has a significant effect on the NPSs properties including radiative and thermophysical properties and the performance and the efficiency of the systems. Table 4.2 provides the thermophysical properties of the base fluid (water) and the nanoparticles.

Table 5.2 Thermophysical properties of base fluids and nanoparticles (Bianco et al., 2015).

Thermophysical Properties	Density (kg/m^3)	Heat Capacity [J/ (kg·K)]	Thermal Conductivity [W/(m·K)]	Dynamic Viscosity [kg/(m·s)]
Water	999	4182	0.597	9.93×10^{-4}
Alumina	3880	773	36	-
Titania	4175	692	8.4	-

5.7.1 Preparation and stability of NPSs

The photographs of the prepared NPSs (individual and hybrid) inside clear glass containers are shown in Figure 5.7. The effects of the different parameters (particle type, $pH, and\ \emptyset$) on the stability behavior of the three types of NPSs are explored, while the pH has significant effects in terms of the electrostatic stabilization of suspensions. Prepared were three different types of NPSs (water based TiO_2, Al_2O_3, and $TiO_2 + Al_2O_3$ NPs) under the same conditions so as to display their stability behavior and their effects on the radiative transfer in the NPSs.

A high stability suspension means that the repulsive forces between the suspended particles are intensified and become stronger than the attractive forces between them, and the particles repel each other and remain in the suspension state for a long period of time. Thus, the pH value of the suspension should not be equal or close to the isoelectric point (pH_{iso}) of the nanoparticle, at which the particle carries no electrical charge to enhance the repulsive forces between the suspended particles. It can be observed from water based TiO_2 NPSs in Figure 5.7-a that at pH=6, the suspensions have poor stability behavior, and a high level of particle agglomeration almost occurred after a few hours of preparation, because the isoelectric point is $pH_{iso} = 5 - 7$ for the TiO_2 nanoparticle (Nogi et al., 2012). For water based Al_2O_3 NPSs which is shown in Figure 5.7-b, the NPSs also show poor stability behavior at pH=6 and 10, because the isoelectric point is $pH_{iso} = 7 - 8.5$ for the Al_2O_3 nanoparticle (Shih et al., 2012). From Figure 5.7-c, it can be observed that the water based hybrid ($TiO_2 + Al_2O_3$) NPSs display an enhancement in stability in comparison with the individual NPSs in the same conditions; specifically at pH=6, which can be observed clearly in the section of the particle characterization. Note that, different particles have their own chemical and physical properties, and they display different

behavior in the hybrid case than in their individual existence at different pH values.

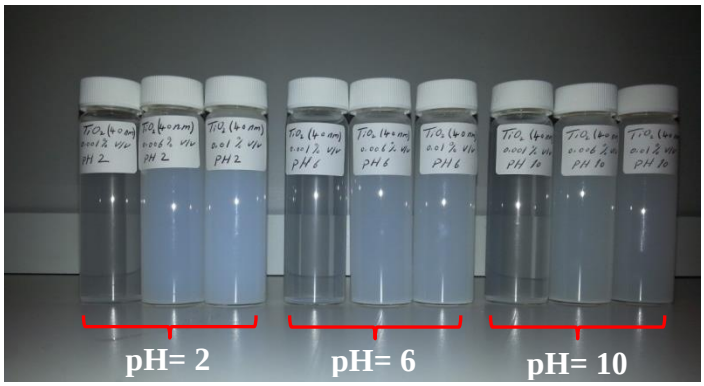

(a) Water based TiO_2 NP

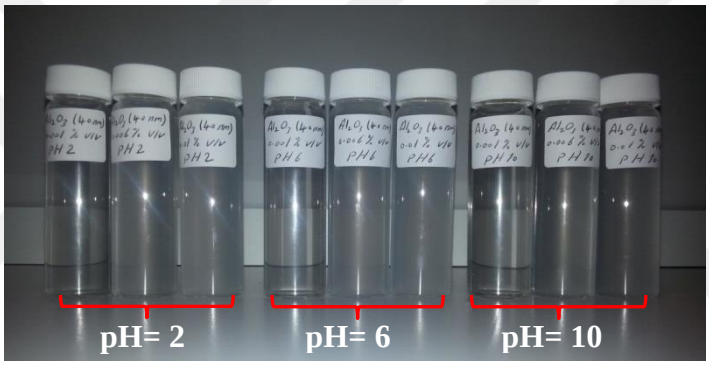

(b) Water based Al_2O_3 NP

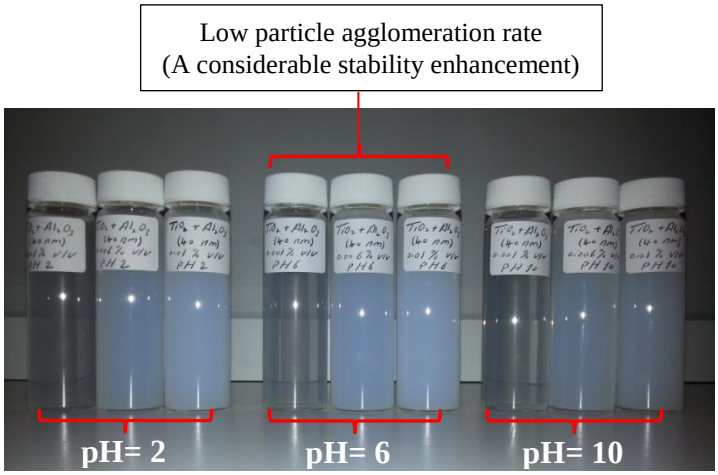

(c) Water based $TiO_2 + Al_2O_3$ NPs

Figure 5.7 Photographs of nanoparticle suspensions (individual and hybrid NPSs) at different conditions (Ø and pH).

Figure 5.8 shows the zeta potential curve of the NPSs as a function of the pH, where the zeta potential measurement provides a clear indication about the NPSs stability. The zeta potential represents the potential difference between the charged particle and the medium layer attached to the particle surface. In other words, the system of the electrical charge is modelled by the potential difference between the two considered spheres; the first one represents the charged particle and the second one represents the layer which includes the concentrated ions attached to the particle surface. According to the general chemistry principles of the particulate suspensions, the dispersion systems show poor stability when the magnitude of the zeta potential has low values; either negative or positive (i.e. absolute value). In addition, in the region of the zero zeta potential, the NPSs systems are not particularly stable. Within this unstable region, a large rate of particle agglomeration and particle sedimentation can be achieved (Munday, 2000; Russel et al., 1989).

From the results in Figure 5.8, the zeta potential values of the hybrid NPSs have positive values in all the pH values as shown in Figure 5.8-c, which is different behavior to those of the individual NPSs as shown in Figures 5.8-a and 5.8-b where the nanoparticle surface charge and the surrounding electrostatic layer are different in different situations. Therefore, the hybrid NPSs show a significant enhancement in the stability in comparison to the other two types; specifically at pH=6. The results in Figure 5.8 demonstrate the effect of the different parameters on the zeta potential, while the zeta potential value is affected primarily by the pH.

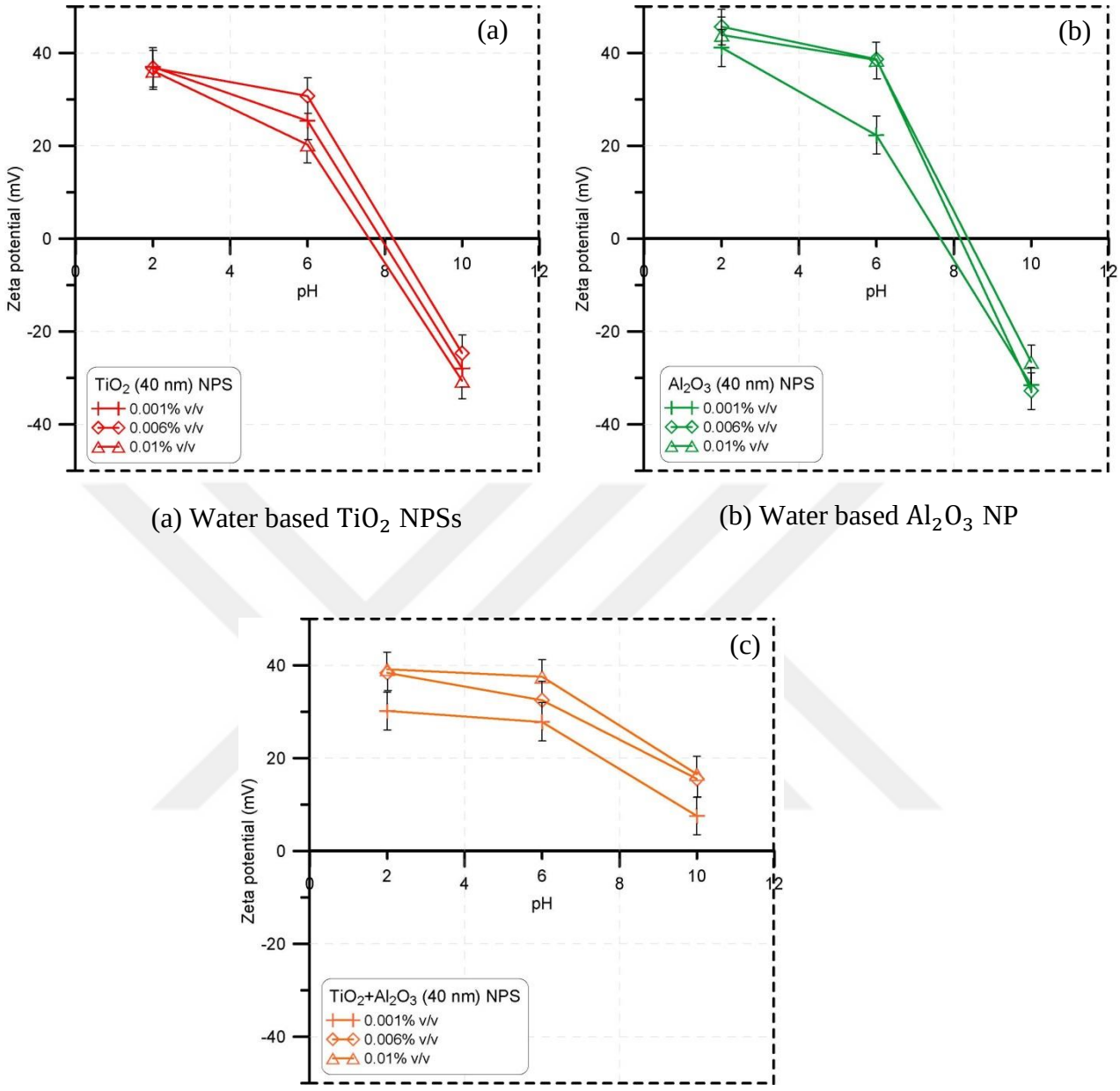

(a) Water based TiO_2 NPSs

(b) Water based Al_2O_3 NP

(c) Water based $TiO_2 + Al_2O_3$ NPs

Figure 5.8 Zeta Potential curves for the individual (water based TiO_2 and Al_2O_3) NPSs and hybrid (water based $TiO_2 + Al_2O_3$) NPSs.

5.7.2 Characterization of NPSs

The particle size distribution (PSD) and the average (effective) particle size of the individual and hybrid NPSs are investigated based on the DLS technique, and three readings were taken for each type of the NPSs. Figures 5.9, 5.10, and 5.11 show three samples of the particle size distribution for the three NPSs types with the same particle volume fractions (NPSs with $\emptyset = 0.001\%\ v/v$) and at different pH values (pH=2, 6, and 10), the particle size distribution for the other NPSs samples are demonstrated in Appendix A. The distribution of the particle size is displayed by a number of particles in these figures. The particle size increase from its original size is because of the particle agglomeration. The impact of the differing parameters on the particle size distribution can also be noted. Furthermore, the average (effective) particle agglomerate size under the effect of agglomeration for each kind of NPSs can be achieved by using this technique. All of the results are at a stable temperature equal to 25^0C.

Figure 4.9 shows the effect of the pH=2 on the three NPSs types, Figure 5.10 shows the effect of the pH=6 on the three NPSs types, and Figure 5.11 shows the effect of the pH=10 on the three NPSs types. When compared the three figures, it is shown that the hybrid NPSs have a low average size of particle distribution, while the other two individual types show a high average size of particle size distribution; specifically for the NPSs at pH=6. The average (effective) particle size ($d_{eff,agg}$) is displayed for each type of NPSs in these figures. Therefore, the hybrid NPSs display a low average particle agglomeration rate in comparison with the other two individual types at a specific pH value, which can be seen clearly from the average particle agglomerate size.

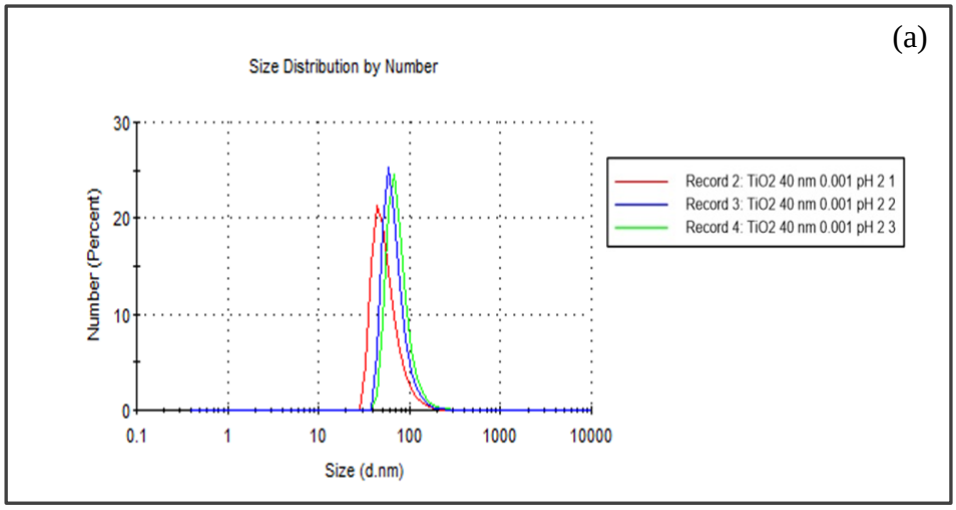

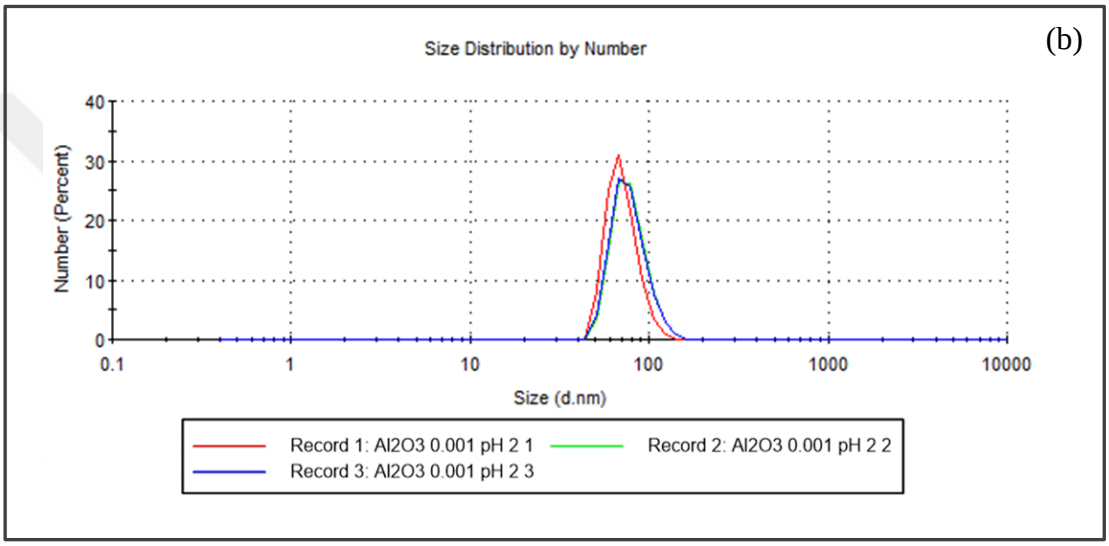

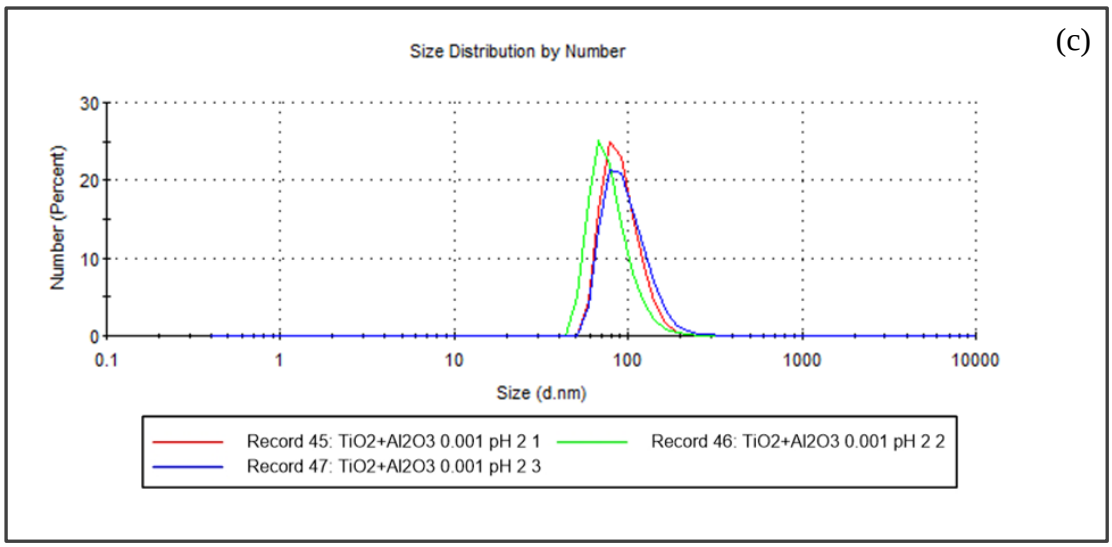

Figure 5.9 Particle size distribution by particle number for NPSs with ($\emptyset = 0.001\%\ v/v$) and at pH=2. (a) TiO_2 NPS with $d_{eff,agg} = 198\ nm$, (b) Al_2O_3 NPS with $d_{eff,agg} = 209\ nm$, and (c) $TiO_2 + Al_2O_3$ NPS with $d_{eff,agg} = 226\ nm$.

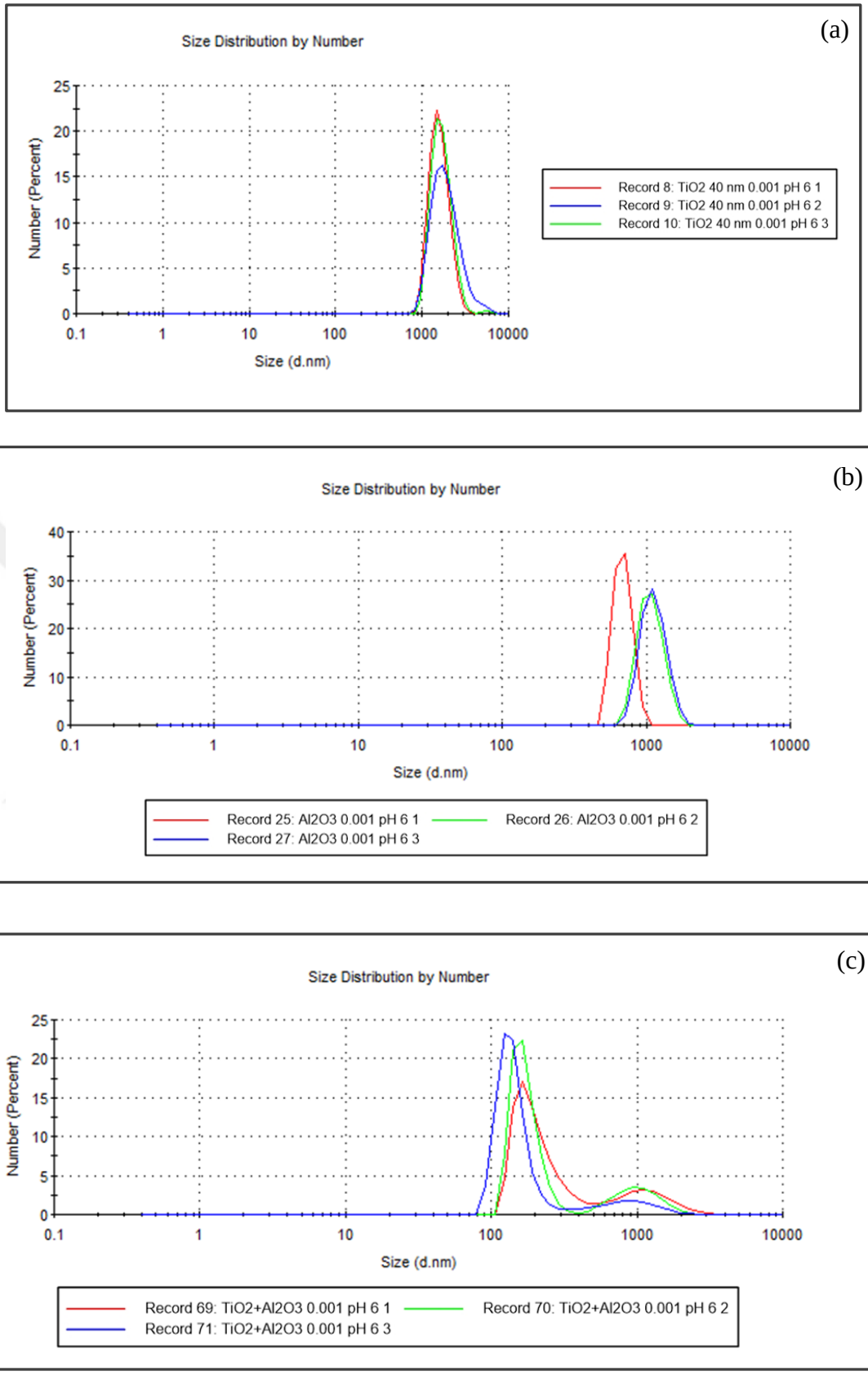

Figure 5.10 Particle size distribution by particle number for NPSs with ($\emptyset = 0.001\%\ v/v$) and at pH=6. (a) TiO_2 NPS with $d_{eff,agg} = 2354\ nm$, (b) Al_2O_3 NPS with $d_{eff,agg} = 1889\ nm$, and (c) $TiO_2 + Al_2O_3$ NPS with $d_{eff,agg} = 631\ nm$.

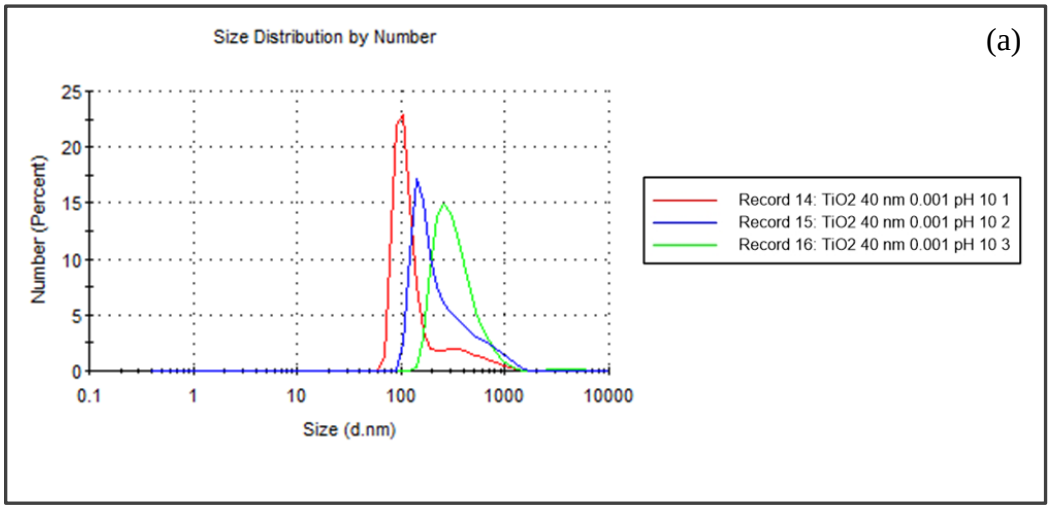

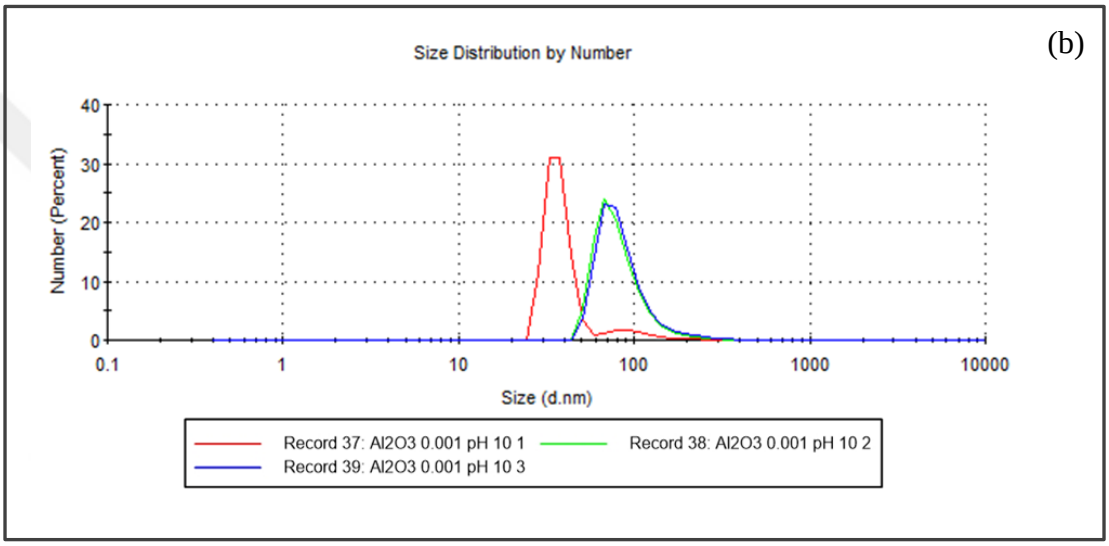

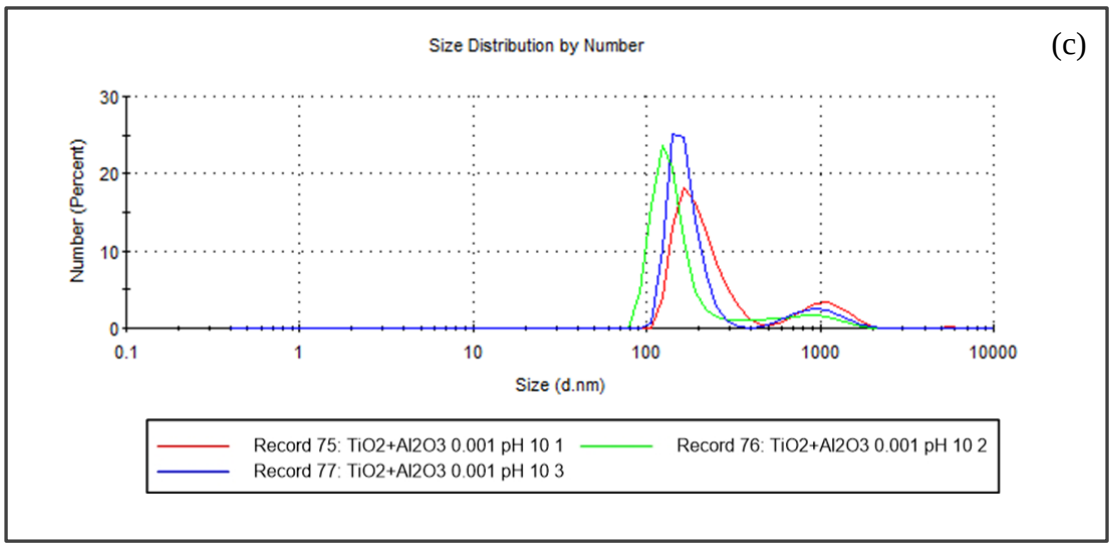

Figure 5.11 Particle size distribution by particle number for NPSs with ($\emptyset = 0.001\%\ v/v$) and at pH=10. (a) TiO_2 NPS with $d_{eff,agg} = 458\ nm$, (b) Al_2O_3 NPS with $d_{eff,agg} = 221\ nm$, and (c) $TiO_2 + Al_2O_3$ NPS with $d_{eff,agg} = 796\ nm$.

Figure 5.12 shows the particle agglomeration curves for the NPSs, and the average (effective) particle agglomerate size ($d_{eff,agg}$) is shown for the individual and hybrid NPSs using the DLS technique. This figure shows the significant effect of the pH value in comparison to other parameters on the stability of the different types of NPSs.

It can be observed from Figure 5.12, that a low particle agglomeration rate is achieved for all the NPSs types at pH=2. A high agglomeration rate (large particle agglomerate size) is obtained for the individual NPSs at pH=6, while the hybrid NPSs at this pH value (pH=6) show the minimum agglomeration rate. On the other hand, a low rate of particle agglomeration is shown for the individual NPSs at pH=10 in comparison with the hybrid NPSs types. In general, the NPSs at a low pH (acidic) have a slightly lower particle agglomeration rate in comparison with the others at a high pH (basic) considering the effect of the isoelectric point of the particles. The low particle agglomeration rate refers to the inclusion of strong barriers between the particles and compact particle agglomerates (the case of RLCA) that are formed. A compact shape of the particle agglomerate is obtained when the pH value of a NPS is far from the pH_{iso} of the particle (Munday, 2000; Russel et al., 1989). The results show that the individual and hybrid NPSs have almost the same average particle agglomerates sizes at pH=2. The effect of the particle volume fraction on the particle agglomeration rate is clarified where the particle agglomerate size is directly proportional to the particle volume fraction. The comparison between these three Figures 5.12-a, 5.12-b, and 5.12-c shows that the pH value has a significant impact on the particle agglomeration behavior, while the particle volume fraction shows a low effect in comparison to the effect of the pH value. According to the chemical fundamentals of the particulate media, the particle agglomerates size and structure are

the major parameters that indicate the long term stability of the colloidal suspensions.

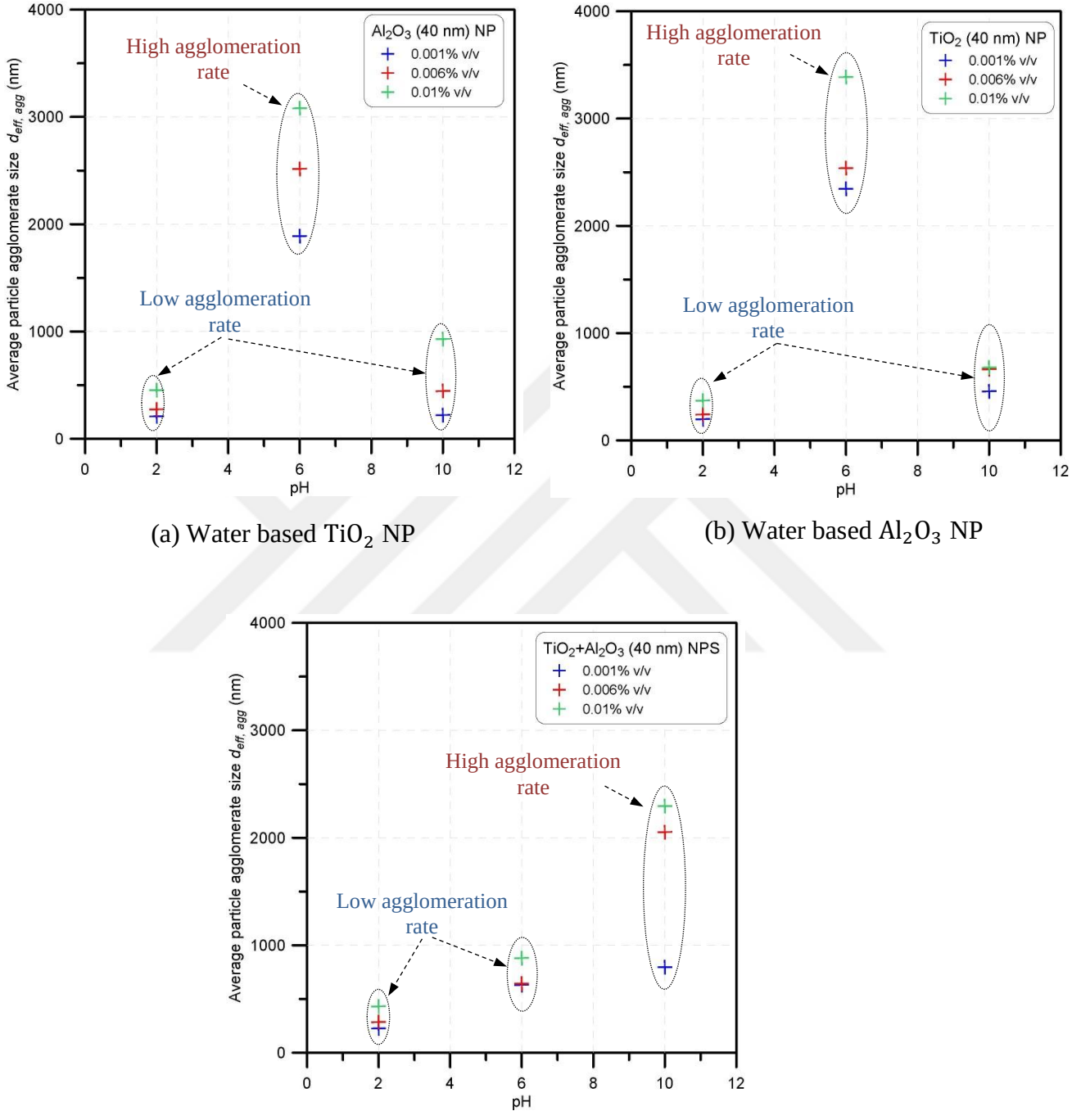

(a) Water based TiO_2 NP

(b) Water based Al_2O_3 NP

(c) Water based $TiO_2 + Al_2O_3$ NPs

Figure 5.12 Particle agglomeration curves for the individual and hybrid NPSs.

Another important parameter for the stability is the sedimentation velocity, which is displayed in Figure 5.13. With the increase in the effective particle agglomerate size, the sedimentation velocity becomes larger as expected under the effect of gravitational force. Also the sedimentation rate of the particles is strongly affected by the structure of the particle agglomerates (DLCA and RLCA). In comparison with other two types of NPSs, the maximum sedimentation rate is obtained with the TiO_2 nanoparticles at pH=6 and $\emptyset = 0.01\%$. Under these conditions, a large effective particle agglomerate size and the case of DLCA occurred relative to the other conditions for the same particle as well as for the other types of NPSs is.

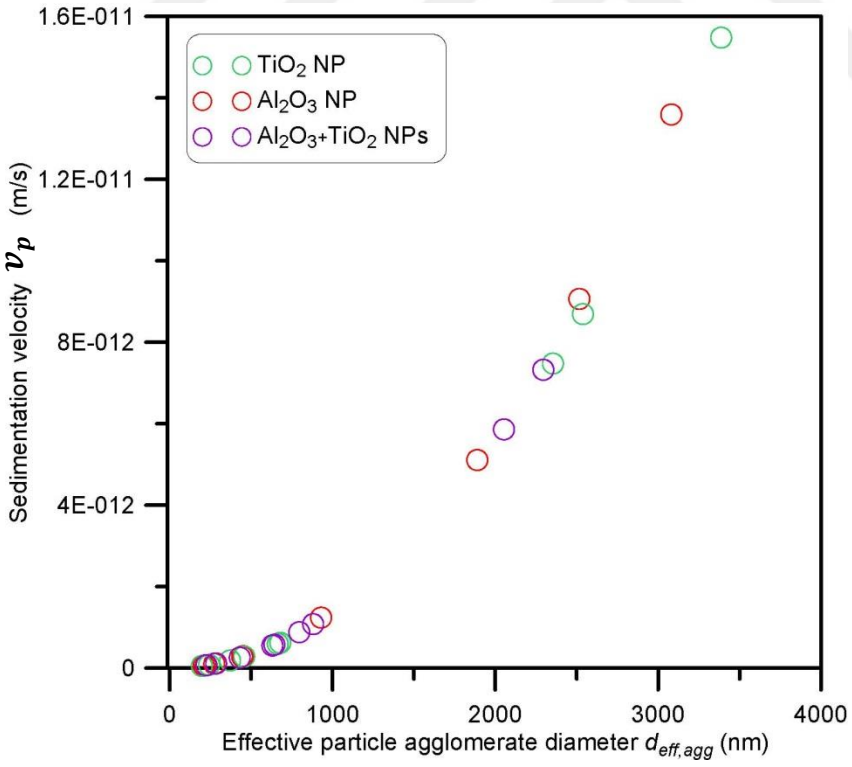

Figure 5.13 Sedimentation velocity curve of nanoparticle agglomerates for the NPSs. Each point inside the figure represents a NPS at particular conditions (pH and particle volume fraction) as shown in Figure 5.12.

Figure 5.14 demonstrates the effect of the particle agglomeration on the surface to surface particles distance ($h_{sur,p}$). The relationship is shown between the $\log h_{sur,p}$ and $\emptyset$ for the different pH values. The average (effective) particle agglomerate size for each type of NPS is specified at each point in this figure. According to Woodcock's equation (Equation 5.5), $h_{sur,p}$ is a function of $\emptyset$ and particle size. Increasing the particle size leads to increases in the $h_{sur,p}$. Therefore, the individual NPSs at pH=6 show high $h_{sur,p}$ as a result of the large particle agglomerate size. While the hybrid NPSs at pH=10 show the higher value of the $h_{sur,p}$.

In Figure 5.14, all the experimental results from the particle agglomeration (heterogeneous NPSs) are also compared with the theoretical calculations (homogeneous NPSs) with the particle size ($d_p = 40$ nm) regardless of the particle agglomeration. These comparisons show the influence of increasing the particle size on $h_{sur,p}$ under the effect of the pH. Homogeneous NPSs with a small particle size have a low clearance between the suspended particles. The distance between the particles has a significant impact on the radiative transfer (dependent or independent scattering, as discussed in Chapter Five). The effect of the dependent scattering becomes more important in the NPSs as the particles become close to each other. That is to say that, by decreasing the distance between the particle surfaces under the effect of the small particle size and/or increasing the particle number causes these NPSs to fall into the Rayleigh regime, where multiple and dependent scattering happen. The effect of the pH value on the $h_{sur,p}$, is one of the most important observations. For a particular NPS in the same conditions, different particle agglomeration behavior can be obtained by changing the pH value with respect to the isoelectric point of the nanoparticles.

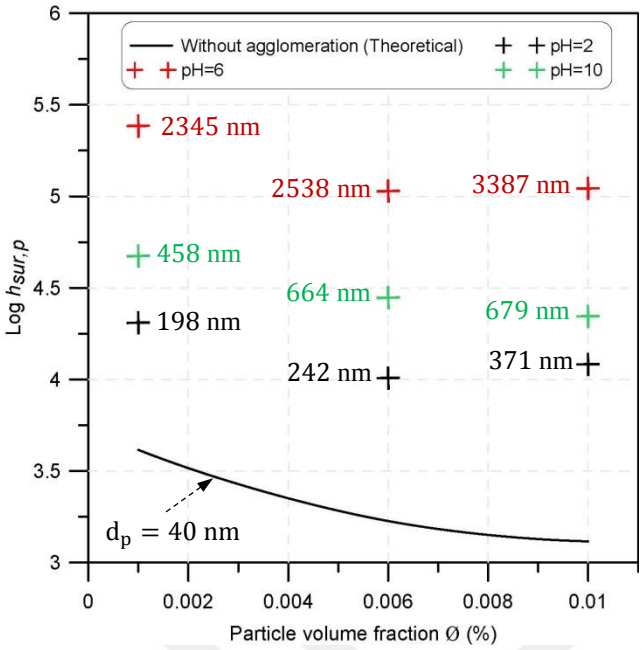

(a) Water based TiO_2 NP

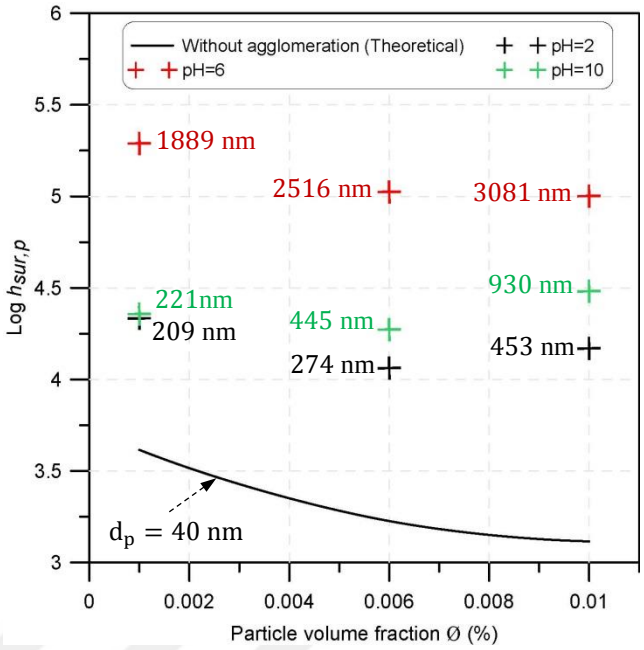

(b) Water based Al_2O_3 NP

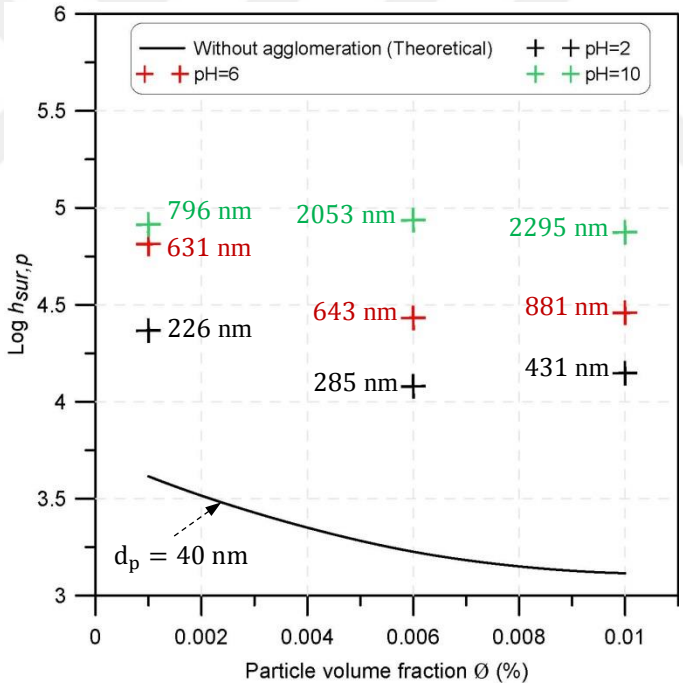

(c) Water based $TiO_2 + Al_2O_3$ NPs

Figure 5.14 Log surface to surface particle distance for the NPSs versus particle volume fraction at different pH, each symbol in the figure represents a NPS type and average (effective) particle agglomerates sizes are shown in the curve for each NPS.

CHAPTER VI

LIGHT SCATTERING AND RADIATIVE TRANSFER IN NANOPARTICLE SUSPENSIONS

6.1 Introduction

The field of radiative transfer in micro/nanoscale particles in dispersions and understanding the optical and radiative properties in the particulate (participating) media are very important in many applications and research fields; it also exists in our daily life. Through the analysis of the optical and thermal behavior of the particulate medium, it is clear that the NPSs have been introduced as a working medium to improve the efficiency of different systems such as solar thermal power plants where the efficiency of the direct absorption solar collectors (DASC) improves because of the unique optical properties and thermal performance of the NPSs (Li et al., 2011).

The radiation propagation's exact solution in the dispersed media must be determined from the first principles consisting of solving the Maxwell equations for the electromagnetic field. However, such an approach is suitable only for a small number of particles because of the difficulties of including large systems in the calculations. A frequently used alternative approach consists of considering the dispersed system as a continuous one and to treat the radiative issue within the framework of the radiative transfer theory, which consists of solving the radiative transfer equation (RTE). Although it was originally established from the energy balance of corpuscles in an elementary volume, the RTE is derived from the equations of a multiple scattering of waves. The RTE has, as main parameters, propagation constants called "radiative properties" (Howell et al., 2015).

6.2 Dependent and independent scattering phenomena

Studying the scattering of electromagnetic radiation by NPSs and their agglomerates is quite important, and understanding this interaction provides a clear idea of the radiative transfer of energy in complex systems. The different size and structure of particle agglomerates exhibit different thermal, radiative, physical, rheological, and chemical properties. Radiation scattering is strongly affected by particle agglomeration, where different scattering behaviors can be obtained from the different size and structure of the particle agglomerates (Howell et al., 2015; Modest, 2013). The characteristics of the particles dramatically affect the radiative properties of the NPSs; these characteristics include the particle size and shape, the number of particles, the particle size distribution, and the refractive index. In addition, the relationship between all these parameters with the incident wavelength has significant implications in the radiative properties of the NPSs (Doicu et al., 2006; Mishchenko et al., 2002).

If the radiation scattering by one particle is not affected by the presence of the surrounding particles, the interaction between the particles is neglected. In other words, the hypothesis of the independent scattering indicates that there is no systematic relationship between the scattered radiations by different particles. Such assumption can be proposed if the particles are far from each other at a sufficient distance in respect to the wavelength. In a particulate media, the particle number, size, and size distribution should be examined to explore the dependent and independent scattering. The number of particles and size affect the distance between the particles and its relationship with the incident wavelength has the significant effect in dependent and independent scattering (Otanicar et al., 2009; Prasher and Phelan, 2005; Swamy et al., 2009). Dependent scattering is introduced into the radiative properties

by two mechanisms. The first is the near field (the near-field inter-particle) effect due to the multiple scattering at the internal fields of the particles, which changes both the extinction and scattering properties of the system. The second effect comes from the far field which is manifested by a change in the scattering properties only. The dependent scattering has significant impacts on the radiative transfer in particulate suspensions (Agrawal and Mengüç, 1991; Aslan et al., 2006; Ivezić and Mengüç, 1996). In compact NPSs (particles are closely and neatly packed together; dense), the dependent scattering should be considered and examined. While for loose NPSs (particles are separated with considerable clearance; non-dense), the independent scattering can be suggested.

The effects of dependent scattering become more important as the particle concentration increases, at which point the clearance between the particles decreases, and they become close to each other. For independent scattering, the conditions of $\phi < 0.6\%$ or $h_{sur,p}/\lambda > 0.5$ are required, where, λ is the wavelength (Howell et al., 2015; Modest, 2013). The boundaries of the dependent and independent scattering regimes (DISRs) were first demarcated by Tien et. al. (Tien and Drolen, 1987). A wide range of particulate media at different particle volume fractions and size parameters was covered by these boundaries. Then, different investigations were carried out on the boundaries of the DISRs for different media in various conditions, where the effects of the different parameters were included (Howell et al., 2015). The condition ($h_{sur,p}/\lambda$) separates between the boundaries of the DISRs, and radiative scattering occurs in the independent scattering regime when the $h_{sur,p}/\lambda$ value is larger than 0.5. However, when the value of $h_{sur,p}/\lambda$ is below than 0.5, the NPSs fall into the Rayleigh regime. This is when dependent scattering needs be considered. In other words, for an independent scattering case, the distance between the particle to particle

surfaces should be large enough in comparison with the incident wavelength to overcome the effect of the scattering from the other particles.

The stability of the NPSs is a very important parameter. As the particles agglomerate, or as they settle down, their interaction with radiation can be more complicated and cannot be predicted. One of the objectives of this research is to investigate the effects of different parameters (pH, d_p, particle shape, $h_{sur,p}$, and $\emptyset$) on how the particles scatter radiation, and to determine if the dependent or independent scattering regimes can be used to determine the radiative properties of the NPSs. Indeed, for a particular particulate media, different boundaries can be specified by adjusting the pH at different values, where various particle agglomeration behaviors are obtained. Including the effect of the pH and the isoelectric point of particles in the boundaries of the DISRs serve as important indications in the scattering (dependent and independent), and can be utilized in a wide range of practical applications. Most of the studies on the radiative properties of the NPSs are completed without taking the effects of the dependent/independent scattering into consideration (Dietz, 2004; Muhammad et al., 2016). Because of this, a detailed discussion of the dependent and independent scattering concept is required.

6.3 Photo-thermal energy conversion in nanoparticle suspensions

Nanoparticle suspensions are implemented for use in solar harvesting systems, where the concentrated sunlight is directly absorbed by a NPS. One of the most important renewable energy sources is solar radiation; solar energy is a reliable solution. These days the utilization of sustainable energy is one of the most important challenges that society is facing. The earth and atmosphere absorb approximately equal to 4×10^{24} J/year of solar energy; where, the solar energy captured by the

earth in one hour is much more than the total energy consumed by the whole world in one year (Morton, 2006; Xu, 2001).

Nanoparticle suspensions have a high potential to be used in the direct solar absorber to improve their performances. The particle agglomeration and stability of the NPSs have significant impacts on the thermal radiation (thermal and radiative) behavior of NPSs (Egerton, 2014; IveziĆ et al., 1997). The selection of suitable base-fluids and the nanoparticles is the first and the foremost step in designing volumetric absorption-based solar thermal systems. Particularly, when particles are in suspension, the solid-fluid and solid–solid heat transfer modes increases and the overall thermal performance can be enhanced. Several investigations have shown that an innovative method of improving the thermal behavior of the base fluid is to suspend small solid particles in a nano-size range within it. The main characteristic that delineates the NPSs based direct absorption volumetric systems from their surface absorption counterparts is that here the working fluid actively (directly) interacts with the solar irradiation and thus increases the overall heat transfer of the system (Milanese et al., 2016; Taylor et al., 2011). An energy harvesting system is shown in Figure 6.1, and the concentrated sunlight is directly absorbed by a NPS. This method can then be used as the heat source for various thermal processes including heat engines.

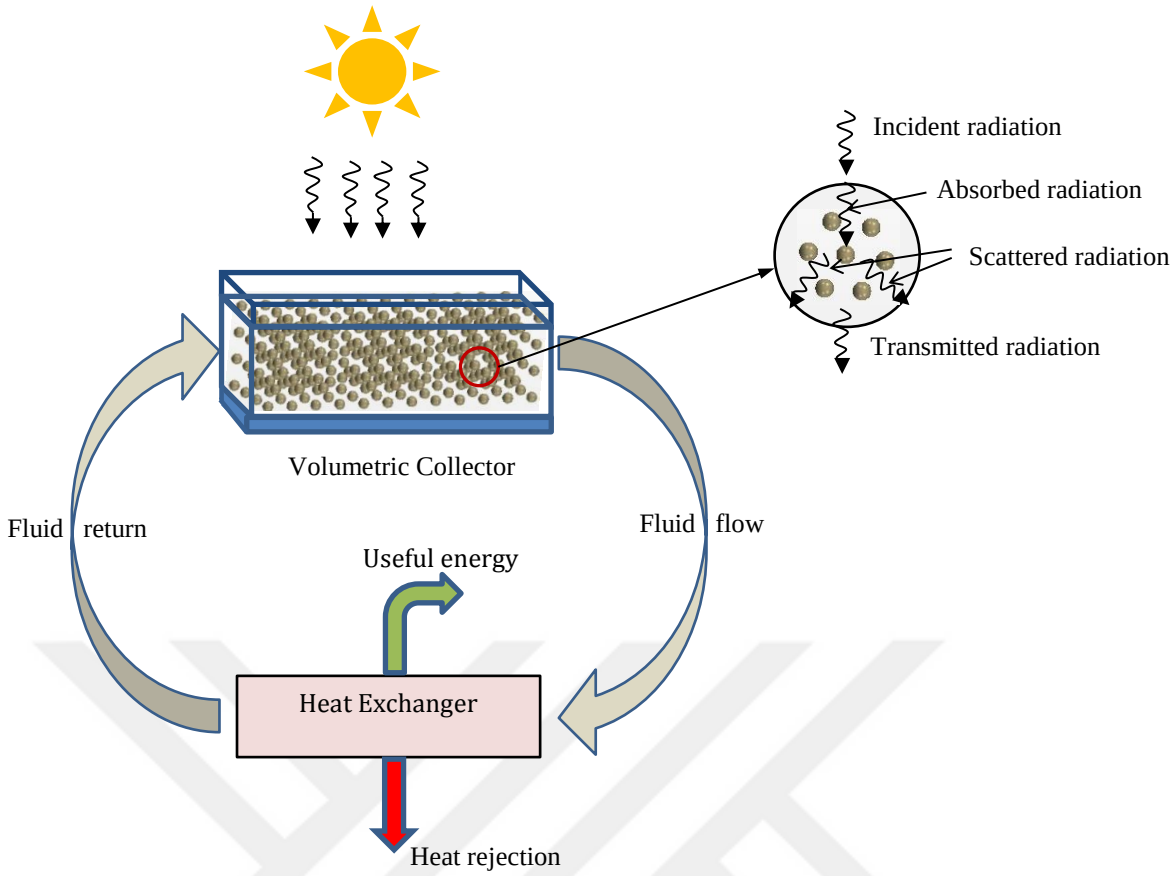

Figure 6.1 Energy harvesting system includes volumetric (direct-absorption) solar thermal collector.

The intensity of incident radiation can be augmented and attenuated as it propagates along a path, which is a fundamental principle of radiative heat transfer. Photo-thermal energy conversion is an efficient technique for thermal radiation transfer, where incident radiation energy is converted into thermal energy by a volume of a particulate media (participating media). To enhance the efficiency and to reduce the size of photo-thermal energy conversion systems, nanoparticles are used. The particulate media absorb and enhance the efficiency of the thermal transfer between the nanoparticles and base fluid when compared to a surface absorber, where the radiative transfer equation (RTE) governs this process. The RTE covers the energy balance of incident radiation intensity I_λ in the s direction. The change in radiation

intensity is found by summing the contributions from the emission and absorption, and the scattering into and away from a unit vector into a specific direction. The RTE equation is expressed in regard to the radiation intensity for a specific wavelength, as (Howell et al., 2015):

$$\frac{dI_\lambda}{ds} = -\beta_{et,\lambda} I_\lambda + \kappa_{am,\lambda} I_{b,\lambda} + \frac{\sigma_{sm,\lambda}}{4\pi} \int_{4\pi} I_\lambda(\Omega) d\Omega + \kappa_{ap,\lambda} I_{pb,\lambda}$$

$$+ \frac{\sigma_{sp,\lambda}}{4\pi} \int_{4\pi} I_\lambda(\Omega) d\Omega \qquad (6.1)$$

where I_λ is the radiative intensity at the wavelength, s is the distance in the solid angle (Ω), $\beta_{et,\lambda}$ is the total extinction coefficient of a NPS at the wavelength, $\kappa_{am,\lambda}$ and $\kappa_{ap,\lambda}$ are the absorption coefficients of the medium and the nanoparticles at wavelength respectively, $\sigma_{sm,\lambda}$ and $\sigma_{sp,\lambda}$ are the scattering coefficients of the medium and the nanoparticles at wavelength respectively, $I_{b,\lambda}$ is the black body intensity at the wavelength, and $I_{pb,\lambda}$ is the particle black body intensity at the wavelength and current particle temperature.

The expression for the radiation spectra emitted by the media is for a perfect black body stated as (Howell et al., 2015; Modest, 2013):

$$I_{b,\lambda}(\lambda, T) = \frac{2\, C_1}{\lambda^5 \left[exp\left(\frac{C_2}{\lambda T}\right) - 1 \right]} \qquad (6.2)$$

where $C_1 = 0.595522 \times 10^{-16}\ (W.m^2/s)$, $C_2 = 0.01439\ (m.K)$, T is the temperature of a NPS.

The boundary condition applied to the RTE for each wavelength λ is:

$$I_\lambda(s) = \varepsilon_{w,\lambda} I_{b,\lambda} + \frac{\rho^d_{w,\lambda}}{\pi} \int_{(n.\acute{s}<0)} I_\lambda(\acute{s}) |\boldsymbol{n}.\acute{s}|\, d\Omega + \rho^s_{w,\lambda} I_\lambda(s^s) + \tau_{w,\lambda} I_\lambda(s) \qquad (6.3)$$

where $\varepsilon_{w,\lambda}$ is the diffuse emissivity, $\rho^d_{w,\lambda}$ is the diffuse reflectivity, $\rho^s_{w,\lambda}$ is the specular

reflectivity, $\tau_{w,\lambda}$ is the transmissivity, $\boldsymbol{n}$ is the unit surface vector directed outwards from the boundary, $\acute{s}$ is the unit vector along the distance coordinate leaving the boundary, and s^s is the unit vector from the incoming ray considered for the specular reflection.

The incoming ray direction, s^s, is expressed as:

$$s^s = s - 2(s.\boldsymbol{n})\boldsymbol{n} \qquad (6.4)$$

In order to determine the volumetric heat flux inside a participating medium, the spectral intensity must be integrated over the wavelength spectrum and over the solid angle (Howell et al., 2015; Modest, 2013):

$$q_{r,\lambda} = \int_0^\infty \int_{4\pi} I_\lambda(s) s \, d\Omega \, d\lambda \qquad (6.5)$$

Inside the medium, on the other hand, it should be determined as to how much net radiative energy is deposited into (or withdrawn from) each volume element. The radiation solution is coupled into the fluid dynamic solution through the radiative heat flux divergence. This term exchanges energy between a NPS and the radiant energy field. In other words, the volumetric heating is a result of the absorbed solar radiation and a volumetric heat loss because of the thermal re-radiation (emission) from the NPS at high temperatures. Then, the spectral radiative heat flux is computed as (Howell et al., 2015):

$$\nabla . q_{r,\lambda} = \kappa_{at,\lambda} \left(4\pi I_{b,\lambda} - \int_{4\pi} I_\lambda \, d\Omega \right) \qquad (6.6)$$

Equation 6.6 is a spectral relationship, i.e., it gives the heat flux per unit wavelength at a certain wavelength. The divergence of the complete heat flux is required in order to include the radiation source term in the energy equation. For this purpose, Equation 6.6 is integrated over the whole spectrum. The resulting volumetric

radiative source term is:

$$\nabla . q_{r,source} = \nabla . \int_0^{\infty} q_{r,\lambda} d\lambda = \int_0^{\lambda} \kappa_{at,\lambda} \left(4\pi I_{b\lambda} - \int_{4\pi} I_{\lambda} \, d\Omega \right) d\lambda \qquad (6.7)$$

Equation 6.7 implies that the net loss of the radiative energy by a control volume including a NPS is equal to the emitted radiation minus the absorbed energy; in the energy equation a positive value is equal to the negative of the divergence of the radiative heat flux.

A tool to transform the equation of transfer into a set of simultaneous partial differential equations is the discrete ordinate method (DOM). The DOM is dependent on a discrete representation of the directional variation of the radiative intensity. The numerical solution is performed here by using the DOM, where the field equations for the radiation intensity are solved. The solution is obtained for a 3D cubic geometry. The DOM requires the specification of a solid angle number (ordinates), for which a sphere surrounding a particular point is discretized as shown in Figure 6.2.

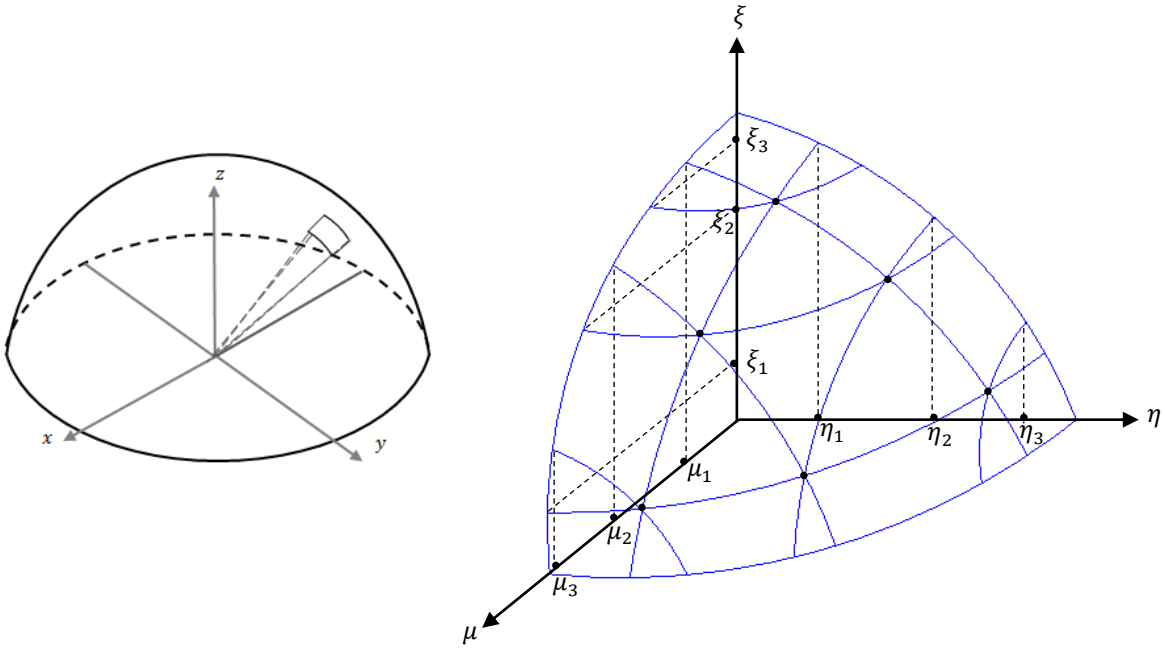

Figure 6.2 Solid angle displayed as part of a hemisphere and discretization.

From Equation 6.1, the ordinate equation is (Howell et al., 2015; Modest, 2013):

$$s_i \nabla I_{i,\Delta\lambda} = -\beta_{et,\Delta\lambda} I_{i,\Delta\lambda} + \kappa_{am,\Delta\lambda} I_{b,\Delta\lambda} + \frac{\sigma_{sm,\Delta\lambda}}{4\pi} \sum_{j=1}^{n} w_j I_{j,\Delta\lambda} + \bar{k}_{ap,\Delta\lambda} I_{pb,\Delta\lambda}$$

$$+ \frac{\bar{\sigma}_{sp,\Delta\lambda}}{4\pi} \sum^{n} w_j I_{j,\Delta\lambda} \qquad (6.8)$$

where $\Delta\lambda$ represents a wavelength band from λ_m to λ_n, w_j represents quadrature weights, and these are dependent on the selected ordinates, n is the number of ordinates, $\bar{k}_{ap,\Delta\lambda}$ is the equivalent particle absorption coefficient, and $\bar{\sigma}_{sp,\Delta\lambda}$ is the equivalent particle scattering coefficient (Howell et al., 2015; Modest, 2013).

The black body emission is:

$$I_{b,\Delta\lambda} = \int_0^{\lambda_n} I_{b,\lambda} d\lambda - \int_0^{\lambda_m} I_{b,\lambda} d\lambda \qquad (6.9)$$

The transport equation is discretized using the same discretization and solved independently for each ordinate direction. The discretized boundary condition is given in the form:

$$I_{i\Delta\lambda,w} = \varepsilon_{w,\Delta\lambda} I_{b,\Delta\lambda} + \frac{\rho^d_{w,\lambda}}{\pi_{eff}} \int_{(n.\acute{s}<0)} I_{j,\Delta\lambda} \left| n.\acute{s}_j \right|_w + f \rho^s_{w,\Delta\lambda} I_{\Delta\lambda}(s^s)$$

$$+ \tau_{w,\Delta\lambda} I_{\Delta\lambda} \qquad (6.10)$$

where f is the correction factor which is used for adjusting the direction of the spectral reflection with the discrete ordinate direction, and π_{eff} represents the half moment for the ordinate set and it is defined as:

$$\pi_{eff} = \sum_{n.\acute{s}>0} w_j (n.\acute{s}_j)_w \qquad (6.11)$$

The discretized form of the radiation energy source is defined as:

$$\nabla . q_{r,source} = \sum_{\lambda} \kappa_{at,\Delta\lambda} \left(4\pi I_{b,\Delta\lambda} - \sum_{j=1}^{n} w_j I_{j,\Delta\lambda} \right) \qquad (6.12)$$

The thermal flux efficiency of a NPS collector is obtained from the ratio of the volumetric energy source (heat flux) in a control volume to the total incident radiation as:

$$\eta_{ther} = \frac{\nabla . q_{r.source} . H}{q_{inc}} \qquad (6.13)$$

In the solar thermal systems, solar thermal collectors are the most important part. They are categorized according to their design and working temperature as shown in Figure 6.3. The flat plate collector is the most common type of solar thermal collector. In this type, the energy is absorbed by the surface, and then it transfers in a heat form to a working fluid. The efficiency of the flat plate collectors is limited not only by the absorptivity of the surface, but also by how effectively the energy is transferred to the working fluid. To improve the efficiency of the collectors, a method was proposed where the solar energy is directly absorbed by the fluid volume, this situation is known as the volumetric or direct absorption solar collector DASC, and has an important role in photo-thermal energy conversion.

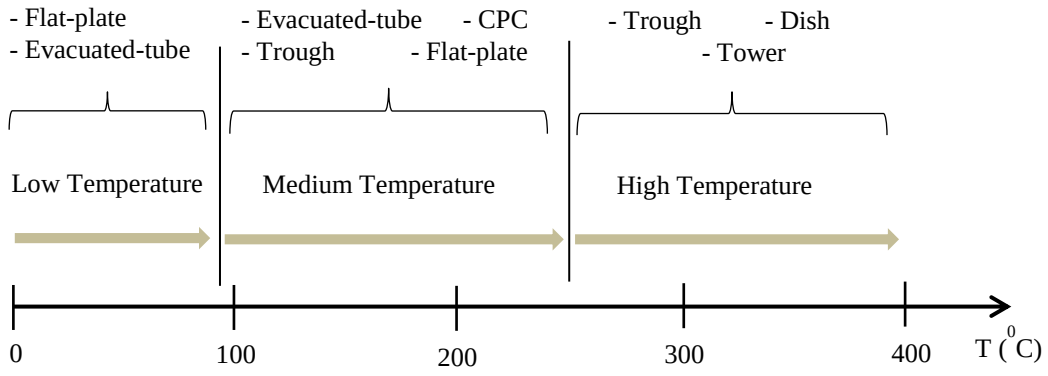

Figure 6.3 Types of solar thermal collectors based on operation temperature ranges.

collector system with the dimension ($1 \times 1 \times 1$ cm^3), where the NPSs are capable of completely attenuating solar radiation within an optical depth of 1 cm (Milanese et al., 2016). As shown in Figure 6.4, this collector contains NPSs with a differing particle agglomerate size. The upper surface has a black body emission ($\varepsilon = 1$) and the radiative heat flux ($q = 1000\, W/m^2$), which represents the approximate incident solar energy on the collector surface at solar noon on a bright summer day in the northern hemisphere (Gorji and Ranjbar, 2017). All the other surfaces are assumed adiabatic, and the bottom surface is considered as a perfect reflector ($\rho = 1$). The above specified conditions of the collector represent a direct absorption solar thermal collector, which is used for photo-thermal energy conversion. The aim is to examine the impact of the particle agglomeration (change in the effective particle size) on the thermal radiative transfer. Examined under the same conditions, is the different particle agglomerate size attained from the experimental part.

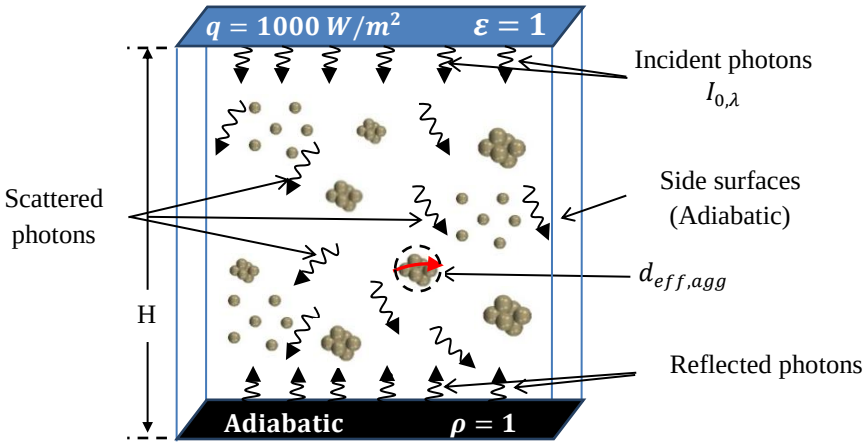

Figure 6.4 Schematic of the DASC collector system including a NPS with different particle agglomerates.

6.4 Results and discussion

The results of the radiative transfer in the NPSs are explained in this chapter, and the results are classified in many sections. The optical properties (refractive and absorption indices) of the nanoparticles and the medium are shown in Table 6.1. The radiative properties of the individual (TiO_2 and Al_2O_3) and hybrid ($TiO_2 + Al_2O_3$) NPSs are obtained experimentally in the UV/visible wavelength range using the UV/Vis spectroscopy technique. The dependent and independent scattering phenomena in the NPSs are explored under different conditions; the boundaries of the dependent and independent scattering are demarcated. The optical and radiative properties of the two NPS types (TiO_2 and Al_2O_3) based on the Lorenz-Mie theory are observed to explain the effects of the different particle size on the optical and radiative properties. The radiative properties of the compact particle agglomerates are obtained theoretically in different wavelength ranges. The main aim is to examine the impact of the distribution of the particle size on the radiative properties of a certain NPS and to make a comparison with the theoretical results and the experimental ones. The final part is to explain the effects of the particle agglomerate size on the radiative transfer in the NPSs where size of the particle agglomerate shows a significant impact on the volumetric radiative heat flux and thermal flux efficiency.

Table 6.1 The optical properties of the nanoparticles and the medium (Said et al., 2015).

Wavelength (nm)	Real (n) and complex (k) parts of refractive indices					
	TiO_2 NP		Al_2O_3 NP		Water	
	n	k	n	k	n	k
200	4.0782	-	1.9127	-	1.4242	1.10E-07
250	3.4454	-	1.8337	-	1.3776	3.35E-08
300	3.129	-	1.8148	-	1.3592	1.60E-08
350	2.9708	-	1.7971	-	1.3495	6.50E-09
400	2.8917	-	1.7861	-	1.3436	1.86E-09
450	2.8126	-	1.7793	-	1.3396	1.02E-09
500	2.7114	-	1.7746	-	1.337	1.89E-09
550	2.6479	-	1.771	-	1.3347	3.79E-09
600	2.6049	-	1.768	-	1.329	1.24E-08
650	2.5742	-	1.7655	-	1.3314	1.87E-08
700	2.5512	-	1.7634	-	1.3301	3.39E-08
750	2.5336	-	1.7615	-	1.3291	1.64E-07
800	2.5197	-	1.7598	-	1.3281	1.37E-07
850	2.5086	-	1.7584	-	1.3272	2.80E-07
900	2.4995	-	1.7571	-	1.3264	4.56E-07
950	2.492	-	1.7559	-	1.3256	2.21E-06
1000	2.4854	-	1.7545	-	1.3249	3.20E-06
1050	2.4803	-	1.7539	-	1.3241	1.40E-06
1100	2.4757	-	1.7531	-	1.3234	1.67E-06
1150	2.4717	-	1.753	-	1.3226	8.65E-06
1200	2.4683	-	1.7521	-	1.3218	1.20E-05
1250	2.4653	-	1.7513	-	1.3233	4.19E-05
1300	2.4626	-	1.7504	-	1.3225	7.39E-05
1350	2.4603	-	1.7496	-	1.3217	1.05E-04
1400	2.4582	-	1.7487	-	1.321	1.38E-04
1450	2.4564	-	1.7479	-	1.32	1.24E-04
1500	2.4547	-	1.747	-	1.319	1.11E-04

6.4.1 Optical and radiative properties of TiO_2 and Al_2O_3 NPs

The effects of the different particle size of TiO_2 and Al_2O_3 NPs in the optical and radiative properties at a specified wavelength are explained in Figure 6.5. This

figure shows the scattering and absorption efficiencies obtained from the Lorenz-Mie theory (LMT). These NPs have different optical properties (refractive indices), and they have different radiative properties at different wavelengths. The calculation is made for the particle refractive index in the wavelength of 400 nm, and the zero absorption efficiency is taken into consideration because the particles have no absorption index at this wavelength. This is displayed in the imaginary part of the complex refractive index. Consequently, the extinction and scattering efficiencies curves are exactly the same. This figure is representative of the optical efficiencies in regard to the size parameter (x). The extinction efficiency approaches to 2 as the size parameter increases because of the increase in the particle size (Howell et al., 2015). The extinction efficiency corresponding to this value is known as the extinction paradox, which refers to the asymptotic limit of extinction efficiency as the particle size becomes much larger than the incident wavelength. This condition means that a large particle can remove exactly twice the amount of the incident radiation that it is possible intercept. For this particle, the reflection from the particle surface becomes very important because of the relationship between the particle size and wavelength and its effect on the radiative efficiencies.

The particle size is one of the most important parameters when incident radiation interacts with the particulate media. Other parameters also affect the radiative heat transfer phenomena including the refractive indices of the particle and medium as well as the wavelength of the incident radiation. Highly dependent on these parameters is scattering. Accordingly, three particle sizes vary from a large (macroscopic) size to a size close to the wavelength, and finally to a considered smaller size which is relative to the wavelength of the incident radiation. When the particle size is closer to the wavelength, the scattering is because of diffraction. In

general, the scattering is the strongest when there is a large difference between the refractive indices of the particle and the medium and when the particle size and wavelength are close to each other (Bohren and Huffman, 2008).

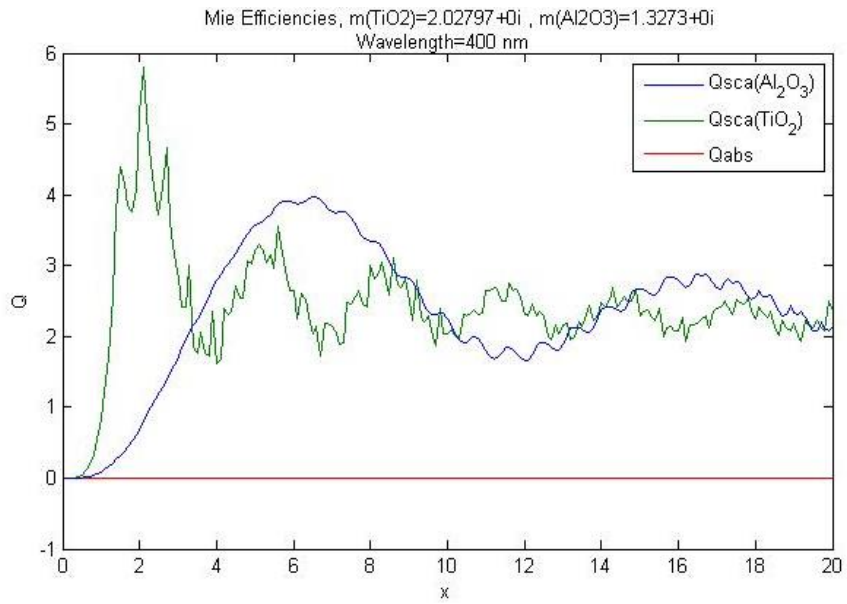

Figure 6.5 Absorption and scattering efficiencies curve for TiO_2 and Al_2O_3 nanoparticles at $\lambda = 400$ nm based on the Lorenz-Mie theory.

6.4.2 Radiative properties of the individual and hybrid NPSs (experiments)

The radiative properties of the individual and hybrid NPSs are experimentally investigated in the UV/visible wavelength range. Since electromagnetic radiation has higher energy in this range, enhancing the radiative properties within this specification is desired for the photo-thermal energy conversion applications (He et al., 2013; Zhang et al., 2014). Figures 6.6 and 6.7 show the scattering and extinction (the particle scattering and medium absorption) coefficients of the NPSs, which were obtained experimentally from the UV/Visible spectroscopy test at room temperature. The effects of the different parameters on the radiative properties can be observed in these figures where the effects of the pH value, particle type, particle agglomeration, particle

size distribution, and particle concentration are shown. Figures 6.6-a and 6.7-a represent the radiative properties of the water-based TiO_2 NPSs. Figures 6.6-b and 6.7-b show the radiative properties of the water-based Al_2O_3 NPSs. Figures 6.6-c and 6.7-c represent the radiative properties of the water-based $TiO_2 + Al_2O_3$ (hybrid) NPSs.

According to these results, the scattering and extinction coefficients reach their maximum at the ultraviolet radiation range (200-400 nm) but they decrease in the visible range (400-800 nm). Generally, these coefficients are inversely proportional to the wavelength, and there is a considerable effect of particle volume fraction on all the types of NPSs. What has a significant impact on the radiative properties is the particle size. The strength of the scattering depends on various factors which are the refractive indices of a particle and surrounding medium, particle size, and structure, and also the wavelength of the incident radiation. When the particle size is similar to the wavelength, the scattering behavior is dominated by diffraction. For a small particle size, with a diameter smaller than the wavelength, a strong scattering performance is attained at a shorter wavelength. On the other hand, for the large particle ($x \gg 1$) it removes twice the amount of radiation that is intercepted by the equivalent cross section area. Of these radiations passing within the equivalent cross section area, some will be refracted and others reflected at the particle surface (Howell et al., 2015).

The effect of the dissimilar particles agglomeration on the scattering and extinction coefficient of the NPSs is one of the most important observations. These particles produce composite particle agglomerates which include various optical properties to that of the existence of the individual particle. Thus, all the aspects of the particle agglomeration; including size and composition are considered in the investigation in addition to the other parameters. The oscillation in these figures for the water based TiO_2 and $TiO_2 + Al_2O_3$ NPSs in the ultraviolet wavelength range can

be explained as the following: The oscillation produced from the interfaces of the refracted and transmitted radiation, and another effect being the multiple reflections from the surface of the particle agglomerates, and the reflected radiation intensity rises by increasing the difference in the refractive indices of a particle and medium (Bohren and Huffman, 2008; Hulst and van de Hulst, 1957; Mishchenko, 2014). In addition, the high refractive index of a particle leads to increasing the oscillation, where the TiO_2 particle has a refractive index three times that of the Al_2O_3 particle within this wavelength range. This affects the scattering efficiency, where different behavior can be observed from these two types of particles. It is observed that the oscillation decreases slightly in the hybrid NPSs in comparison with the individual (water based TiO_2) type. From Figure 6.6, one can deduce how the scattered radiation must depend on the shape, and size, as well as its optical properties.

From Figures 6.6 and 6.7, it can be observed that hybrid NPSs show considerable radiative properties in comparison with the two individual types in addition to their better stability behavior at specified pH values, which allows them to be used in different applications. One of the most important parameters for the solar thermal collectors is radiation attenuation. A particulate suspension with high radiation attenuation is desired for solar thermal utilization in terms of light-induced energy conversion. This is the principle of the direct absorption solar collectors, at which the solar radiation incident interacts directly with the working media.

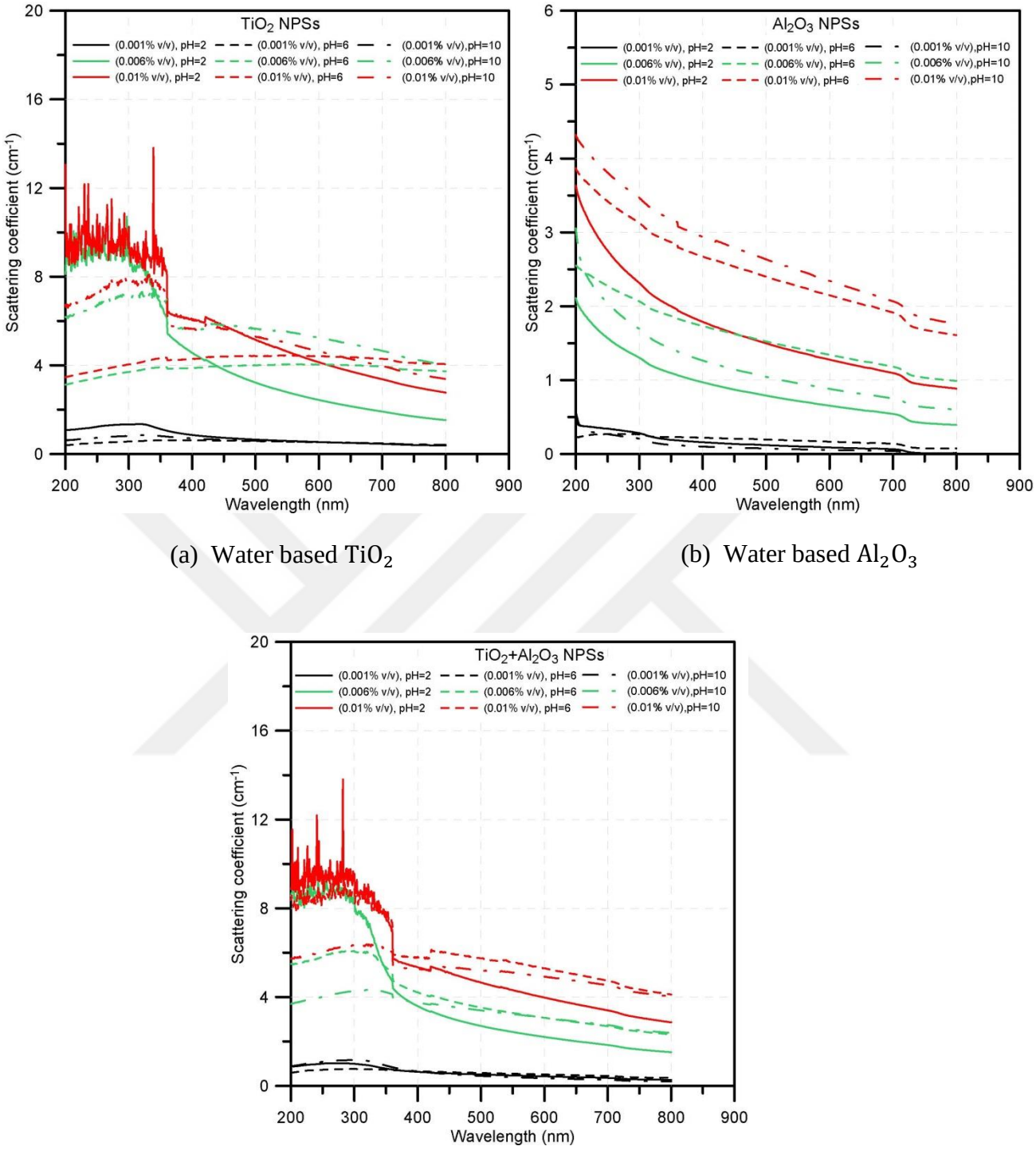

(a) Water based TiO_2

(b) Water based Al_2O_3

(c) Water based $TiO_2 + Al_2O_3$

Figure 6.6 Scattering coefficient of the NPSs based on UV-Visible spectroscopy test.

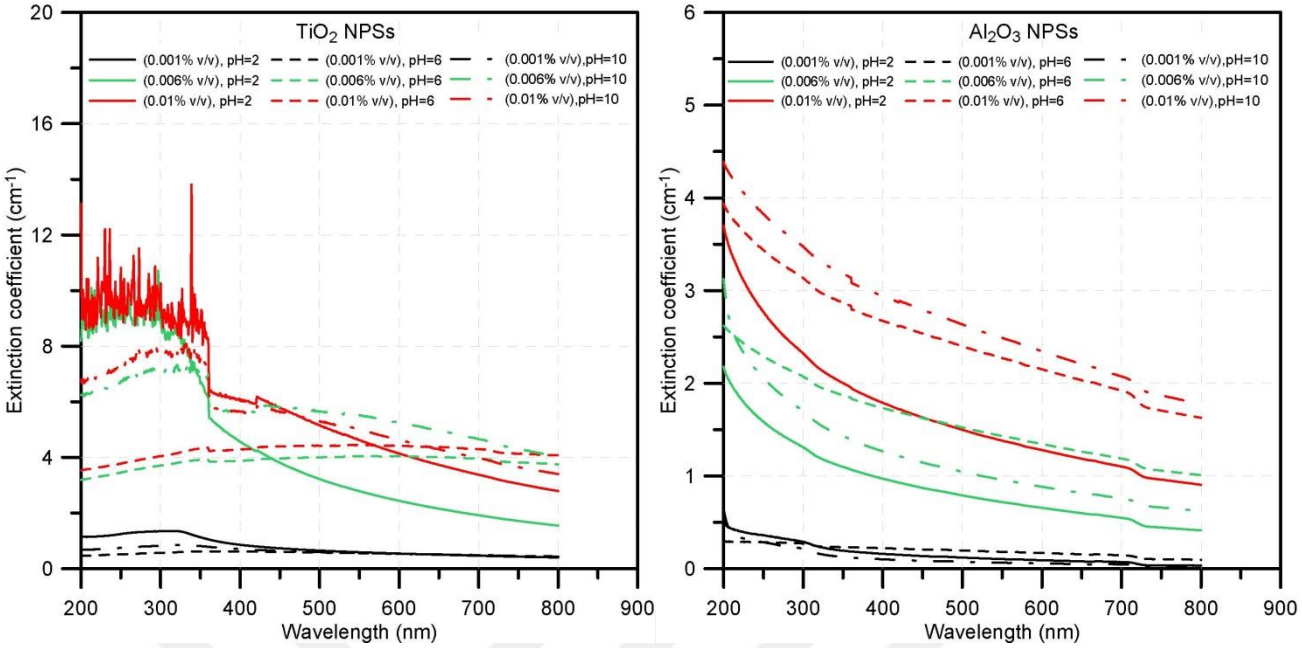

(a) Water based TiO_2

(b) Water based Al_2O_3

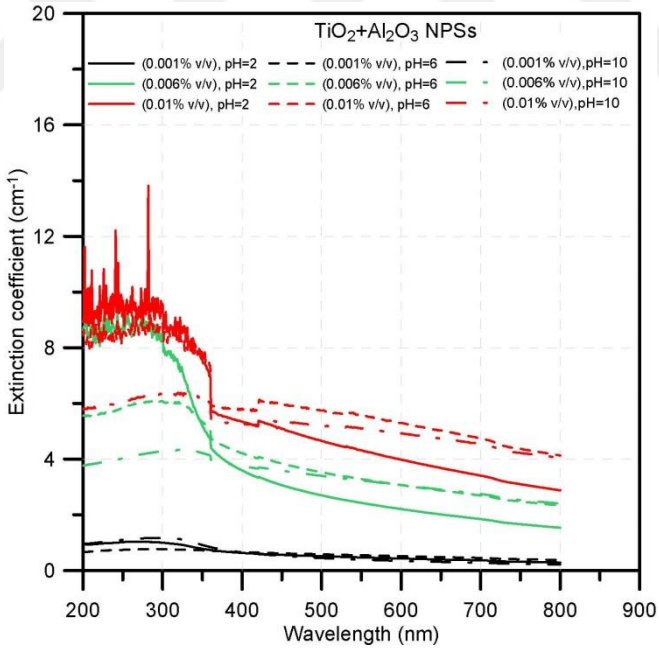

(c) Water based $TiO_2 + Al_2O_3$

Figure 6.7 Extinction (absorption and scattering) coefficient of the NPSs based on UV-Visible spectroscopy test.

The absorption effect of the medium (water) is very low in comparison with the effect of the scattering in the extinction coefficient. Water is an effective media in the near infrared wavelength range, while, scattering is dominant in the ultraviolet–visible wavelength ranges. Therefore, the scattering and extinction figures look identical. Figure 6.8 shows the absorption coefficient of the pure base fluid (water), which is a very poor absorber medium in the range of the ultraviolet-visible light spectrum. Water can be regarded as a transparent medium in the wavelength range of 250–900 nm. However, when the wavelength moves to the near-infrared region, then water becomes a very effective absorber. The nanoparticles that are added introduce the ability to improve the extinction coefficient in the ultraviolet-visible wavelength ranges. This can be seen in Figure 6.8.

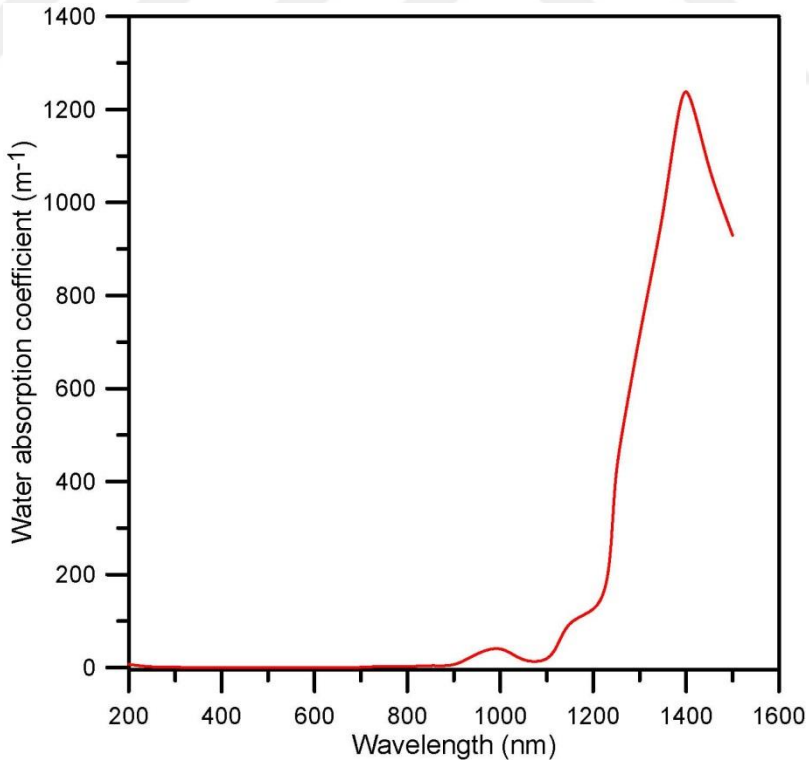

Figure 6.8 Absorption coefficient of water (Taylor et al., 2011).

The ratio of the scattering coefficient to the extinction coefficient, i.e. the single scattering albedo is calculated to demonstrate the effect of scattering coefficient and its contribution in the extinction coefficient. Figure 6.9 shows the single scattering albedo of the individual and hybrid NPSs. Water based TiO_2 NPSs (individual) and water based $TiO_2 + Al_2O_3$ NPSs (hybrid) show high values of single scattering albedo because these NPSs have a high scattering coefficient as seen in Figures 6.9-a and 6.9-c. Water based Al_2O_3 NPSs have slightly low values of a single scattering albedo in comparison with other two types of the NPSs; while water based Al_2O_3 NPSs with low particle volume fraction ($\emptyset = 0.001\% \; and \; 0.006 \; v/v$) have significant low values of single scattering albedo at wavelength longer than 700 nm as seen in Figures 6.9-b. In general, for all the NPSs types, the single scattering albedo decreases with the particle volume fraction.

The scattering is significant and has an important effect on the extinction coefficient at a shorter wavelength, but the nanoparticle has an important role in the radiative properties at the ultraviolet-visible wavelength ranges. The effects of the different parameters on the single scattering albedo are explained in Figure 6.9.

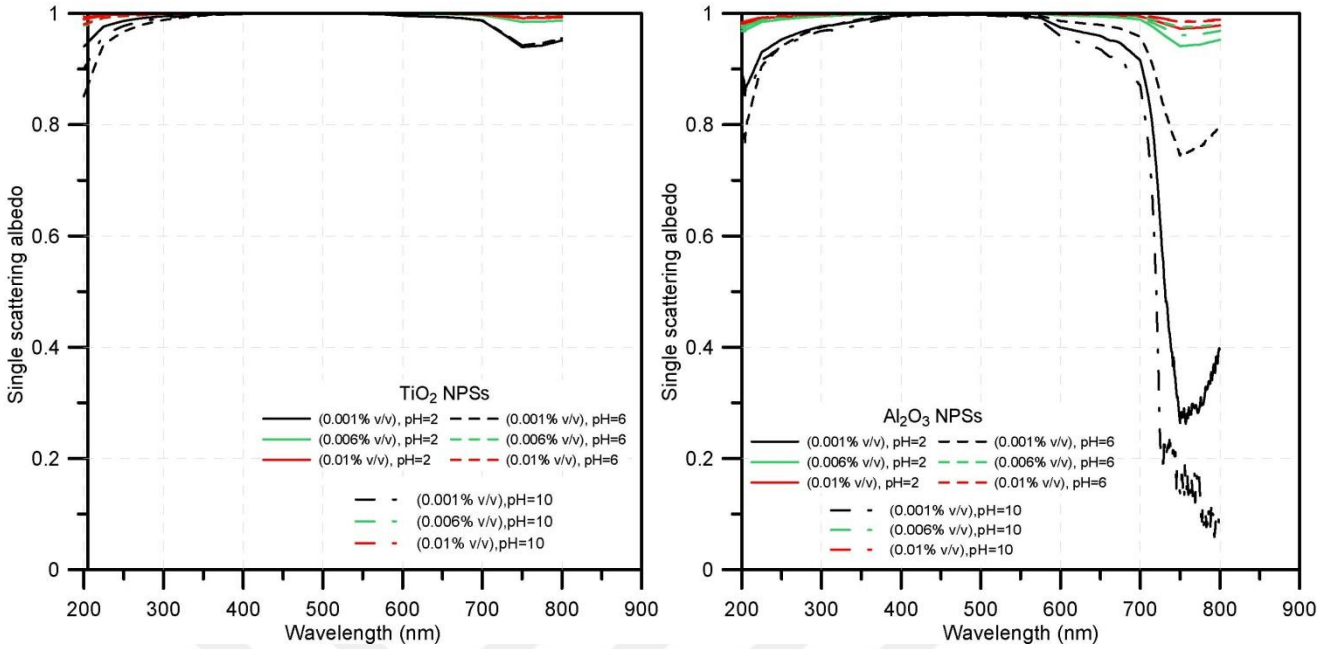

(a) Water based TiO_2

(b) Water based Al_2O_3

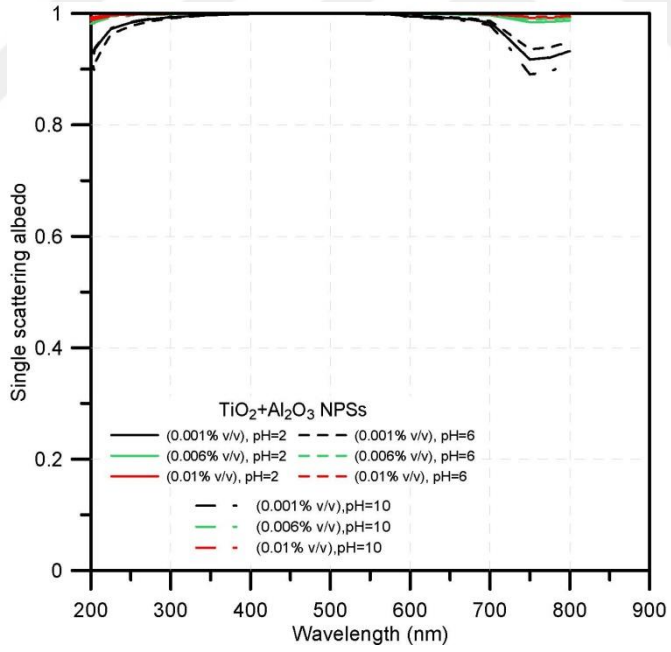

(c) Water based $TiO_2 + Al_2O_3$

Figure 6.9 Single scattering albedo curves of the NPSs based on UV-Visible spectroscopy test.

Figure 6.10 shows the extinction coefficients of the NPSs at the specified values of the pH, and all the results are obtained at the wavelength value ($\lambda = 400\,nm$). The results explain how the particle agglomeration affects the extinction coefficient of both the hybrid and individual NPSs at the same wavelength. In fact, the NPSs show a different particle size distribution under a different condition where the particle agglomerates size and structure are different. In addition, an extra influence from the composite particle agglomerates appears on the radiative properties of the hybrid NPSs where each type of nanoparticle shows different optical properties. Therefore, different radiative properties (extinction coefficient) can be observed, which can be utilized in specific applications where desired radiative properties are needed. Water based $TiO_2 + Al_2O_3$ NPSs (hybrid) and water based TiO_2 NPSs (individual) exhibit high extinction coefficients in comparison with the water based Al_2O_3 NPSs. The effect of the particle volume fraction on the extinction coefficient can be observed, and different extinction coefficients are obtained for the different particle size and structure of the NPSs under the effect of the pH value.

The manipulation of the radiative properties of any material no matter whether it is rigid or a particulate medium in the same conditions is very important and is desired in different applications. In this research, different radiative properties are obtained by changing the pH value of the NPSs in the same conditions (the particle size and shape, and $\emptyset$) and in the same medium. In addition, different radiative properties are obtained from the synthesis hybrid system that includes dissimilar particle agglomerates. As observed from the results, the scattering coefficient has a great impact in the extinction coefficient. Therefore, the relationship between the pH and particle scattering behavior can be observed clearly.

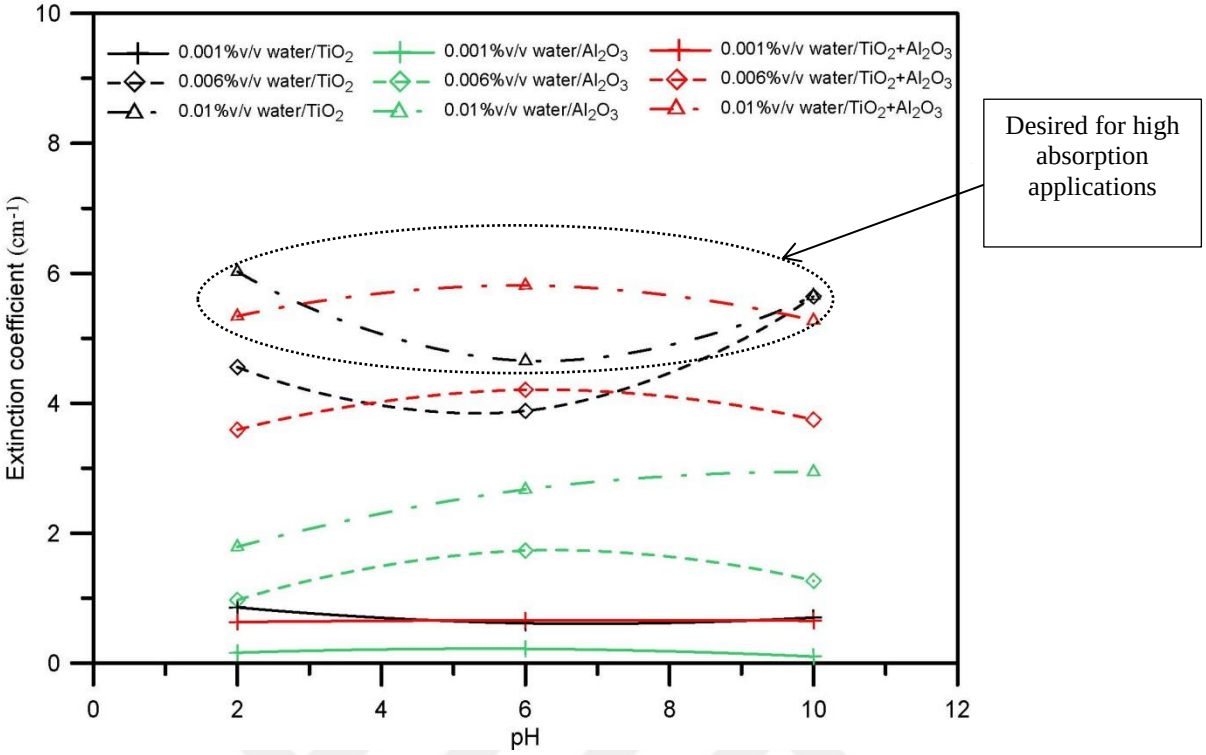

Figure 6.10 pH versus extinction coefficient for the NPSs at wavelength ($\lambda = 400$ nm).

6.4.3 Dependent and independent scattering

The effects of the different parameters (pH, ∅, and particle type and size) on the boundaries of the dependent and independent scattering regimes (DISRs) are discussed in this section. All of these parameters are in relation to the incident wavelength in the NPSs. One can specify the relationship between $h_{\mathrm{sur,p}}$ and the wavelength (λ), and the boundaries of DISRs can be demarcated. Figure 6.11 shows the DISRs for the NPSs in the UV-Vis-NIR wavelength ranges to explain the effects of different parameters of the NPSs in the DISRs at these wavelength ranges.

It can be observed from the results in Figure 6.11-a and 6.11-b (Water based TiO_2 and Water based Al_2O_3 NPSs) that the NPSs at pH=6 show $h_{sur,p}/\lambda \gg 0.5$ ($h_{sur,p}$ is much higher than the wavelength) because these NPSs at pH=6 have a high

particle agglomerates size, which leads to the increase in the clearance between the particles. Different behavior is observed in the hybrid (Water based $TiO_2 + Al_2O_3$) NPSs as shown in Figure 6.11-c, where the NPSs at pH=10 show $h_{sur,p}/\lambda$ values lower than the values from the NPSs at pH=2, and slightly lower than the values of $h_{sur,p}/\lambda$ from the NPSs at pH=6.

In general, increasing the particle volume fraction leads to approach the boundary of the dependent scattering regime for the NPSs. $h_{sur,p}/\lambda$ approaches the boundary of the dependent scattering regime specifically at longer wavelengths as a result of the low particle agglomerate size in comparison with the wavelength of the incident radiation.

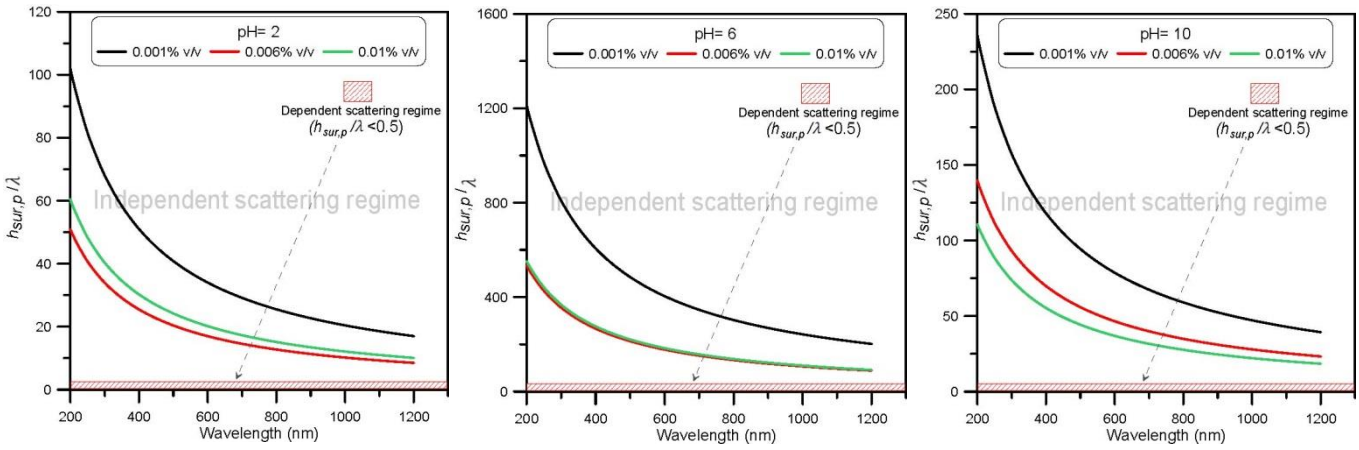

(a) Water based TiO_2

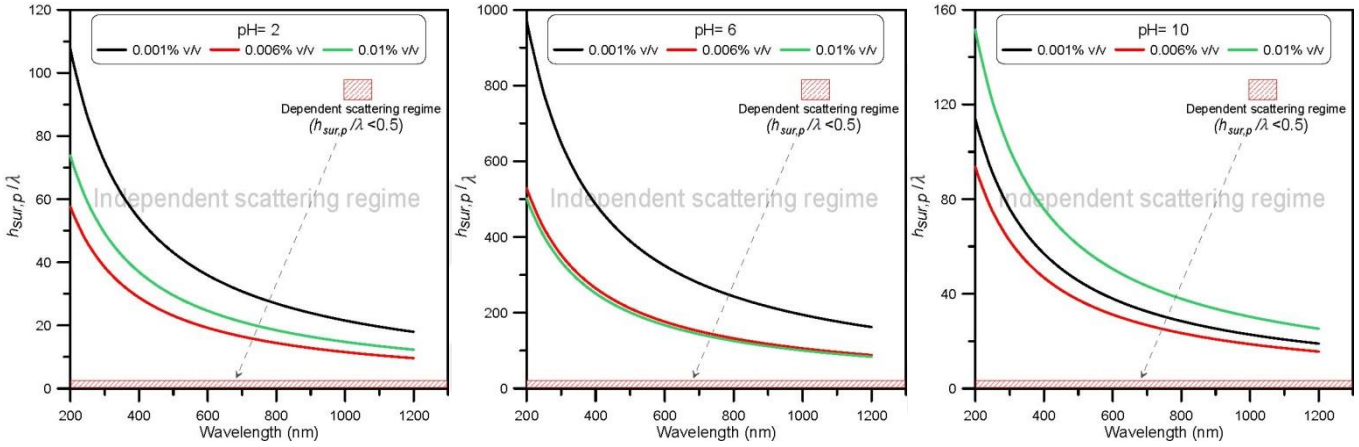

(b) Water based Al_2O_3

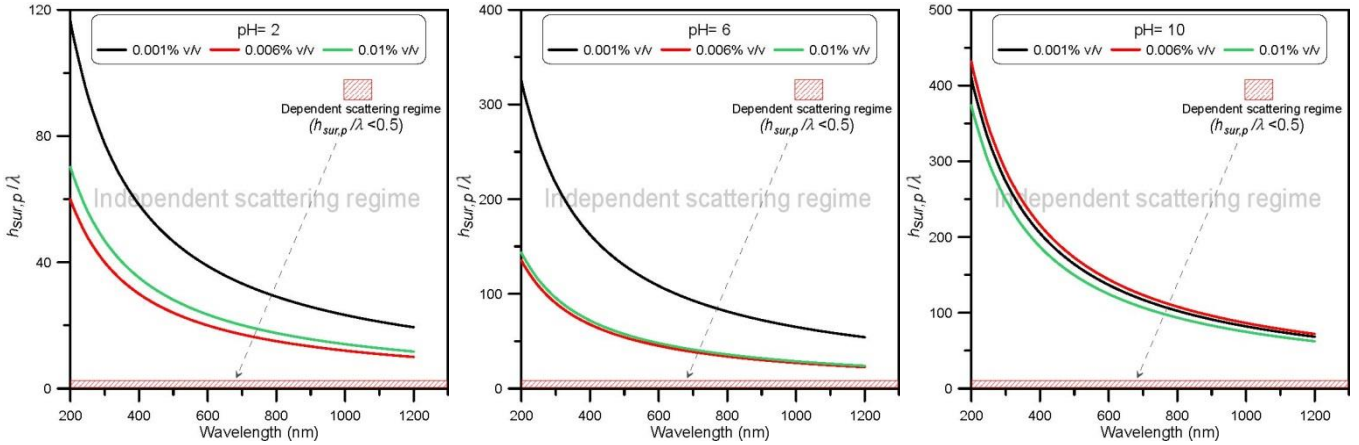

(c) Water based $TiO_2 + Al_2O_3$

Figure 6.11 Dependent and independent scattering regimes for individual NPSs at different conditions (pH and ∅). (a) Water based TiO_2 NPSs, (b) Water based Al_2O_3, and (c) Water based $TiO_2 + Al_2O_3$ NPSs.

Figure 6.12 is to show the effect of the nanoparticles and their agglomerates under the effect of the pH on the dependent and independent scattering regimes. The effects of the experimental results are by means of the particle agglomeration under the effect of the pH with different particle volume fractions and the theoretical calculations regardless of the particle agglomeration ($d_p = 40\,nm$) in the UV-Vis-NIR wavelength ranges.

In Figure 6.12, the pH value shows a considerable effect on the demarcation of the dependent and independent scattering regimes (DISRs) for all the NPSs types (Water based TiO_2 , Water based Al_2O_3, and Water based $TiO_2 + Al_2O_3$) in the same conditions, the change of the pH value affects the results. The modification of the DISRs for the same NPSs by altering the pH value has significant indications, and opens the door to new questions. One of the most important questions one can ask: 'For a particular NPS under specified conditions, how does different pH values make the medium more sparse (independent scattering regime) or more compact (dependent scattering regime)?' The answer to this question is explained using Figure 6.12, where three values of the pH for a specified NPS in the same conditions show different locations near the boundaries of the DISRs. The general condition of the DISRs is represented by the relationship between the wavelength and the distance between the particle to particle surfaces. The NPSs approach the dependent scattering regime that is specifically for the NPSs containing a small size of the nanoparticles and their agglomerates in comparison to the incident wavelength when the wavelength becomes longer and there is an increase in the particle volume fraction,.

Since the figure of the boundaries of the dependent and independent scattering regimes was demarcated by Tien and his work group (Tien and Drolen, 1987), an extensive investigation has been carried out in this area to specify the dependent and

independent scattering boundaries for different colloidal suspensions (Aslan et al., 2006; Lee, 1994; Otanicar et al., 2009). In this research, the effects of the particle agglomeration with different parameters ($pH, h_{sur,p}, \phi,$ and d_p), as well as different particle types in the suspension (individual and hybrid systems) are demarcated on the boundaries of dependent and independent scattering regimes as shown in Figure 6.12. As shown in this figure, the researchers suggested the conditions of the independent scattering as $\phi < 0.6\%$ or $h_{sus,p}/\lambda > 0.5$, where $h_{sus,p} = f(\phi \; and \; d_p)$. However, it is still not clear how a particulate suspension with ultra-fine particles at a low volume fraction behaves and how DISRs are defined. In other words, for a particular particulate suspension, it may not be possible to suggest the independent scattering at low particle volume fractions for all the particle sizes. To explore these concepts, the effects of all the parameters (pH, $h_{sur,p}$, $\emptyset$, and d_p) that affect the DISRs with their relationship to the incident wavelength should be considered.

It is noteworthy to mention that NPSs approach the boundaries of the dependent scattering regime at a specified wavelength range. This happens either when the particle size becomes smaller and/or when the number of the particles become larger, where the clearance between particles ($h_{sur,p}$) drops under the impact of the particle size and the amount of particles. Due to the small size of the particles compared with the wavelength, the Rayleigh regime is considered and dependent scattering should be examined. For that, we demarcate a new boundary (read line) to explain the effect of particle size at a particular particle concentration for NPSs. This line has been drawn using the results obtained for homogenous TiO_2 and Al_2O_3 NPSs with particle size ~10 nm, NPSs under these conditions ($\emptyset$, and particle size) fall in the dependent scattering regime; specifically in the NIR wavelength range because the particle size is much smaller than the wavelength of the incident radiation. Beyond any

doubt, increasing the particle size results in increasing the clearance between particle to particle surfaces, which mean that the effect of the dependent scattering disappears at the same wavelength. In the case of the NPSs with the large particle agglomerates, the independent scattering condition becomes $h_{sur,p}/\lambda \gg 0.5$. In contrast, in the NPSs without the particle agglomeration regime, the linear relationship between the particle size parameter and wavelength can be observed because the particle agglomeration is omitted, and the particles are assumed to have a fixed size ($40\ nm$).

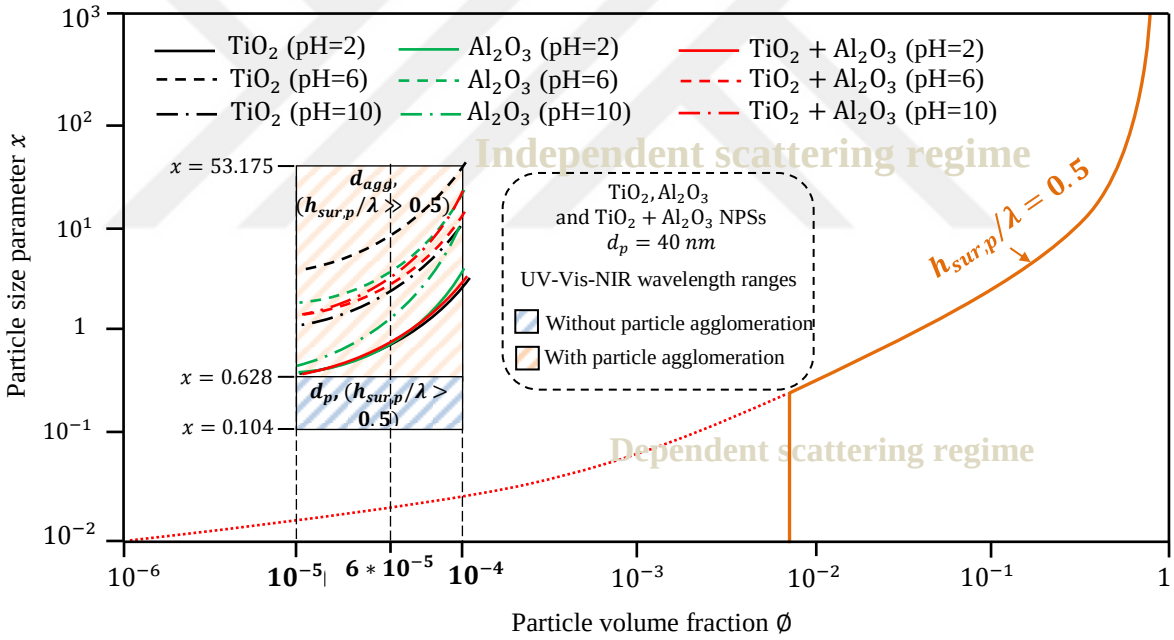

Figure 6.12 The boundaries of independent and dependent scattering regimes for NPSs at different ∅ and pH values (regarding to particle agglomeration) and the theoretical results (regardless to particle agglomeration) are included.

6.4.4 Scattering and physical cross sectional area under the pH effect

Figure 6.13 shows the effect of the pH and particle agglomeration on the scattering cross sectional area (C_{sca}) and the physical cross sectional area of the TiO_2 nanoparticle. The C_{sca} depends on the incident wavelength, the particle size, and the refractive indices for both the particles and the medium. It represents the relative area over which the radiative scattering by the particles occurs, which can also refer to the scattering footprint. The scattering intensity can change from the particle to another under the effects of the differences between the refractive indices of the particles and the medium, and the size of the particle (the particle agglomeration under the effect of the pH value). In this figure, the results correspond to the wavelength of 600 nm to have a representative value for applications related to solar thermal collectors. These results are also valid for the reflection of visible light by coatings, as the human eye is most sensitive to green light at about 550 nm wavelength.

The effects of the pH value on the TiO_2 NPSs specify three regimes as shown in Figure 6.13. Region A represents the TiO_2 NPSs at pH=2, where a small particle agglomerates size is generated. Region B represents the TiO_2 NPSs at pH=10, where the NPSs under this condition have a particle agglomerates size slightly larger than those from the TiO_2 NPSs at pH=2. While region C represents the TiO_2 NPSs at pH=6, and under this condition the NPSs include a large particle agglomerates size. In these three regimes, the comparison between the C_{sca} and the physical cross sectional area shows that in the A and B regions the C_{sca} and the physical cross sectional area are approximately identical to each another; while in the C region, the C_{sca} is larger than the physical cross sectional area, and the particles in this condition can scatter a large amount of the incident light than it is incident on it.

In Figure 6.13, it can be observed that the pH value has a significant effect on both the C_{sca} and the physical cross sectional area and their relationship with the incident radiation. The pH value for a particular particulate suspension under specified conditions can be adjusted to obtain a desired scattering behavior, which can be utilized in different applications.

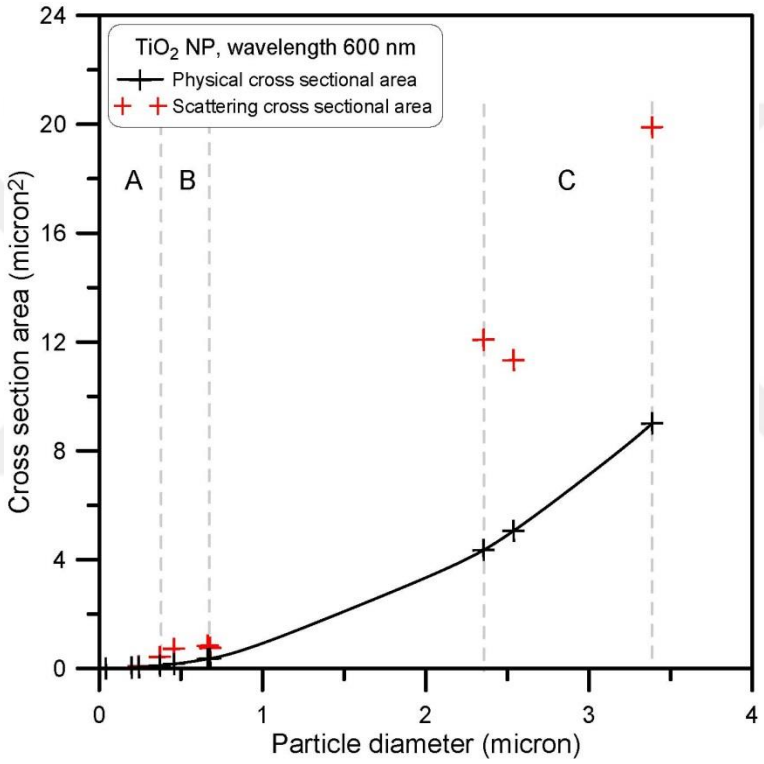

Figure 6.13 The scattering cross sectional area and physical area of different TiO_2 particle agglomerates with different particle volume fractions, three regions are specified: (A) NPSs at pH=2, (B) NPSs at pH=10, and (C) NPSs at pH=6.

6.4.5 Radiative properties of of TiO_2 and Al_2O_3 NPSs (theoretical)

The radiative properties of the compact particle agglomerates which are obtained at pH=2 and 10 for TiO_2 and Al_2O_3 NPSs are calculated using the Lorenz-

Mie theory (LMT). The obtained results in the theoretical part (LMT results) are compared with the experimental results (UV-Vis spectroscopy technique), and to quantify the effect of the particle size distribution on the radiative properties for the NPSs under different conditions using the LMT. Figures 6.14 and 6.15 show the radiative efficiencies (scattering and absorption) under different conditions (the pH and particle volume fraction). The radiative efficiencies obtained from the LMT depend on the particle size and refractive indices of both the particle and the medium, and the pH and particle volume fraction affect the particle size.

The radiative efficiencies for Al_2O_3 nanoparticle at pH= 2 and 10 are shown in Figure 6.14. In addition, the scattering efficiency drop with the decreasing particle volume fraction (i.e. decreasing particle agglomerate size) and it is inversely proportional to the wavelength. Different scattering behavior can be observed at different pH values resulting in a different particle agglomeration rate. The scattering efficiency approaches zero at wavelengths longer than 800 nm at the two pH values in general, apart from in the results at pH=10 and $\emptyset = 0.01\%$ as this is where a large particle agglomerate size ($d_{agg} \approx 980$ nm) is attained.

The radiative efficiencies for the TiO_2 nanoparticles are displayed in Figure 6.15. In a situation such as this, the scattering efficiencies shows a fluctuating behavior, and this grows with the particle agglomerate size as can be seen for the NPSs at pH=10. Such fluctuations occur when there is a large difference in the refractive indices between the particle and the medium and for mono-size particles. TiO_2 particles have a refractive index that is three times bigger than that of the Al_2O_3 particles for the ultraviolet-visible wavelength range. Moreover, the effect of the fluctuation grows with the particle size with the impact of the multiple reflections from the particle surface. The TiO_2 nanoparticles at pH=2 have large values of

scattering efficiency for wavelengths that are up to 800 nm at particle volume fractions of 0.001 and 0.006%. While nanoparticles at pH=10 have large values of scattering efficiency over the whole wavelength ranges. The two nanoparticle types (Al_2O_3 and TiO_2) have zero absorption efficiency at the specified wavelength range (200-1500 nm) as shown in Figures 6.14 and 6.15.

Particle scattering may enhance the absorption in the medium as the incident radiation travels along a large distance in the media. The incident radiation undergoes two different phenomena (attenuation and augmentation). Radiation attenuation stems from the effects of the radiation absorption and out-scattering (the deviation of incident radiation from the incident direction). The radiation augmentation originates from the effects of the re-radiation (emission) and in-scattering (the scattering from other directions in the direction of incident radiation). In order to allow the incident solar energy to move along a large distance in the medium, the perfect medium for a solar absorber application (photo-thermal energy conversion) should be stable and transparent to the incident radiation. The volumetric interaction between the incident radiation and the working medium is the basis of the volumetric (direct absorption) solar collectors. In the photo-thermal energy conversion, the relationship between the particle size and the incident radiation has also a significant effect on the thermal radiation transfer.

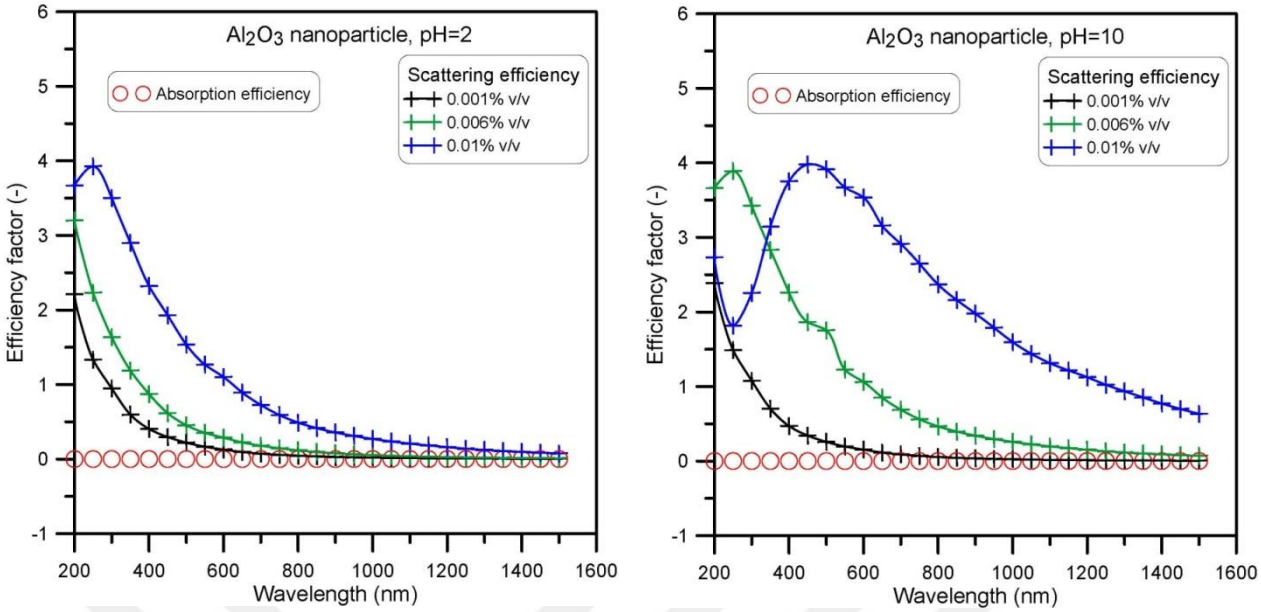

Figure 6.14 Radiative efficiencies of Al_2O_3 nanoparticle calculated from the Lorenz-Mie theory.

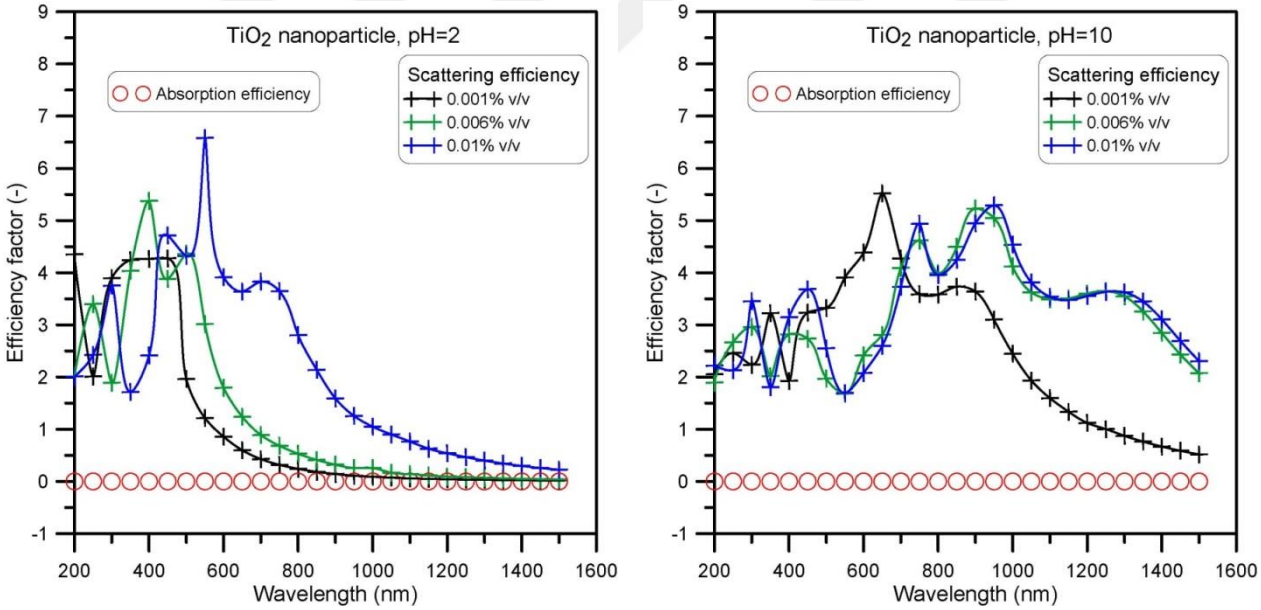

Figure 6.15 Radiative efficiencies of TiO_2 nanoparticle calculated from the Lorenz-Mie theory.

Figure 6.16 shows the scattering coefficient of water-Al_2O_3 and TiO_2 nanoparticles-based NPSs. The different scattering behavior described in Figures 6.14 and 6.15 leads to an impact on the scattering coefficient for the NPSs. Generally, TiO_2 nanoparticles-based NPSs have higher scattering coefficients in comparison to those of Al_2O_3 nanoparticles-based NPSs. The different behavior of the scattering coefficients under the effect of the particle size and size distribution over the wavelength can be noticed. The scattering coefficient for the long-wavelength range ($\lambda > 800$ nm), is raised by the pH and particle agglomeration; especially for NPSs at pH=10 where large particle agglomerates are carried out. It is noteworthy to state that the wavelength range of (200 – 1500) nm is considered because thermal radiation has a tendency to occur for this range. Scattering by suspended particles in a participating media is significant in radiative heat transfer applications, and is an important tool to explain radiation attenuation and energy conversion.

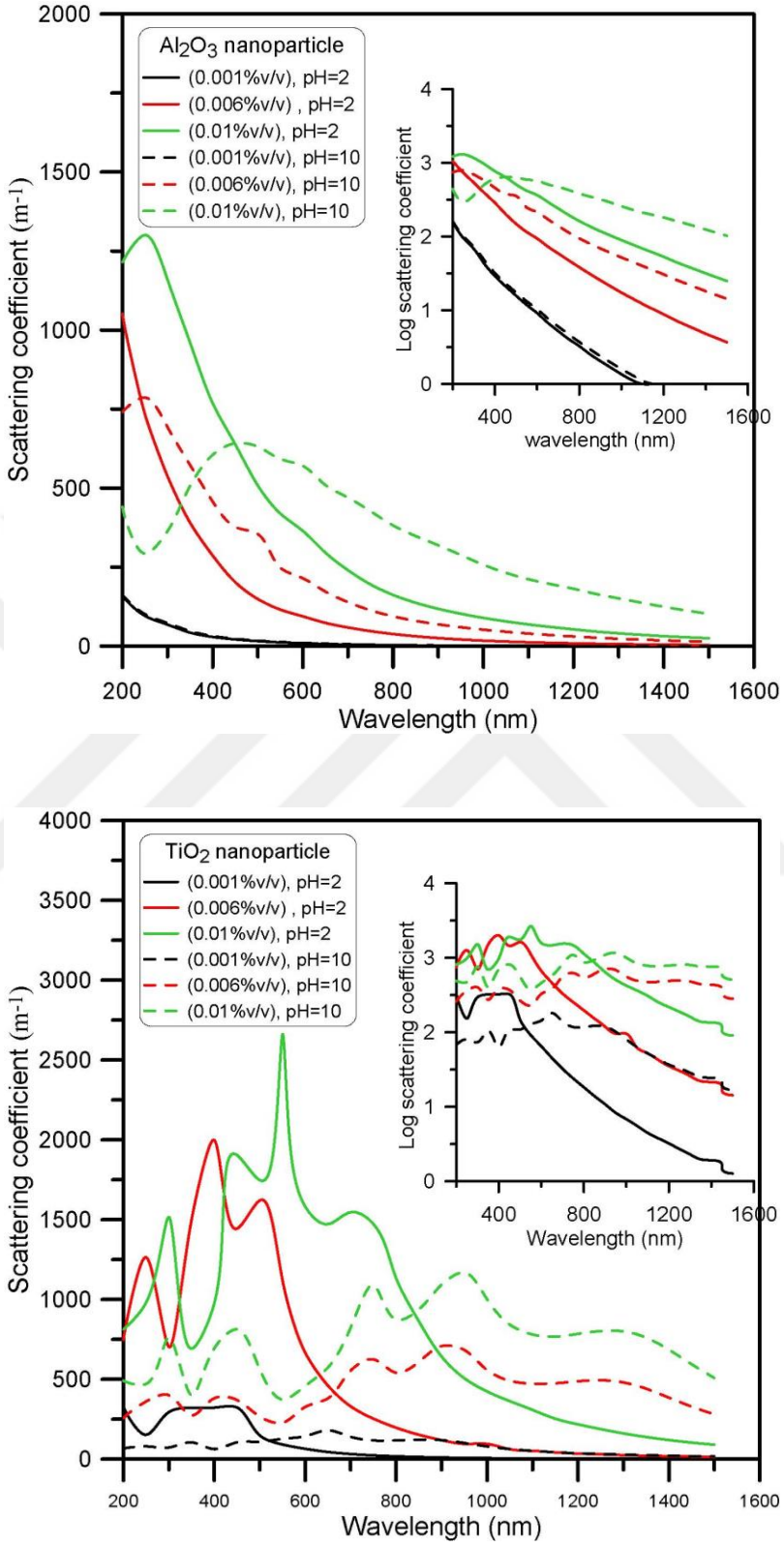

Figure 6.16 Scattering coefficient profiles of water-Al_2O_3 and TiO_2 nanoparticles-based the NPSs.

The extinction coefficient profiles of the NPSs are shown in Figure 6.17. These profiles are almost identical to the scattering coefficient profiles for the wavelengths up to 1000 nm because the extinction coefficient includes the effect of both the scattering coefficient of the particles and the absorption coefficient of the fluid. When compared to the scattering coefficient for the ultraviolet-visible wavelength range, the absorption coefficient of the base fluid is very low; however, for the wavelengths greater than 1200 nm, the impact of the absorption coefficient becomes significant.

From the extinction coefficient curves, it can be observed that the scattering coefficient is dominant in the attenuation of light except in the wavelength range for which the scattering coefficient is a low value or is close to the absorption coefficient, implying that both scattering and absorption effects are present. An improvement in the radiative properties in the UV/Vis wavelength range is displayed in the two NPSs types. This has an important effect on the solar thermal utilization, where radiation with short wavelengths carries high energy and a big amount of the incident solar radiation is exhausted within this wavelength (UV/Vis wavelength) because of the effect of the low absorptance of the base fluids (Phelan et al., 2013; Tyagi et al., 2009).

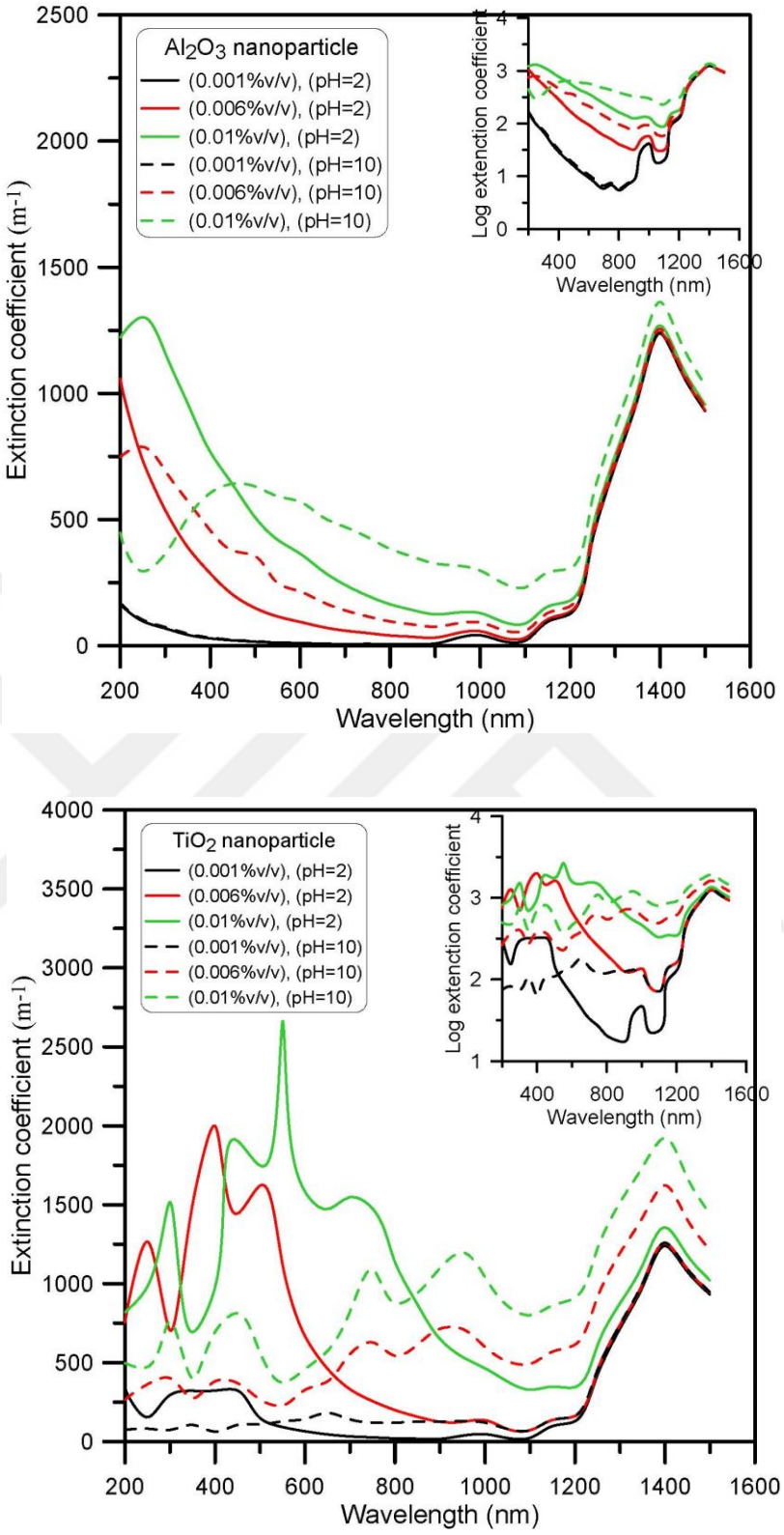

Figure 6.17 Extinction coefficient profiles of water-Al_2O_3 and TiO_2 nanoparticles-based NPSs.

6.4.6 Effect of the particle size distribution on the radiative properties NPSs

Particle size distribution (PSD) is a very important parameter of NPSs; different particle size distributions are obtained for TiO_2 NPSs at different pH values. The radiative properties of NPSs are significantly affected by PSD. The effect of the PSD on the scattering coefficient of TiO_2 NPSs including the compact particle agglomerates is shown in Figures 6.18 and 6.19, and the Lorenz-Mie theory (LMT) is used for this purpose. As we discussed, the compact particle agglomerates based on the pH value are obtained for TiO_2 NPSs at pH=2 and 10. Figure 6.18 shows the effect of the PSD on the scattering coefficient for TiO_2 NPSs at pH=2, and Figure 6.19 shows such effect for TiO_2 NPSs at pH=10. The PSD shows a different particle agglomerate size (d_{agg}) and average (effective) particle agglomerate size ($d_{eff,agg}$) for each type of TiO_2 NPSs. The effects of the d_{agg} and $d_{eff,agg}$ on the scattering coefficient are shown in Figures 6.18 and 6.19.

In Figure 6.18, more efficient scattering in the wavelength up to 800 nm under the effect of particle agglomerate size is observed, where TiO_2 NPSs at pH=2 showing small particle agglomerates play an important role on the scattering behavior in the UV-Vis wavelength range. In Figure 6.19, the results show that the efficient scattering is obtained in the UV-Vis-NIR wavelength range; specifically for TiO_2 NPSs with 0.006% and 0.01% v/v (Figures. 6.19-b and 6.19-c). TiO_2 NPSs at pH=10 show compact particle agglomerates size larger than those for TiO_2 NPSs at pH=2; therefore, the efficient scattering behavior is extended to the NIR wavelength range.

The comparison between the scattering behavior obtained from the Lorenz-Mie and the experimental results (UV-Vis spectroscopy test) shows good agreement between them. Where the comparison is made between the scattering coefficient of the average (effective) particle agglomerate in Figures 6.18 and 6.19 with the results

shown in Figure 6.6.

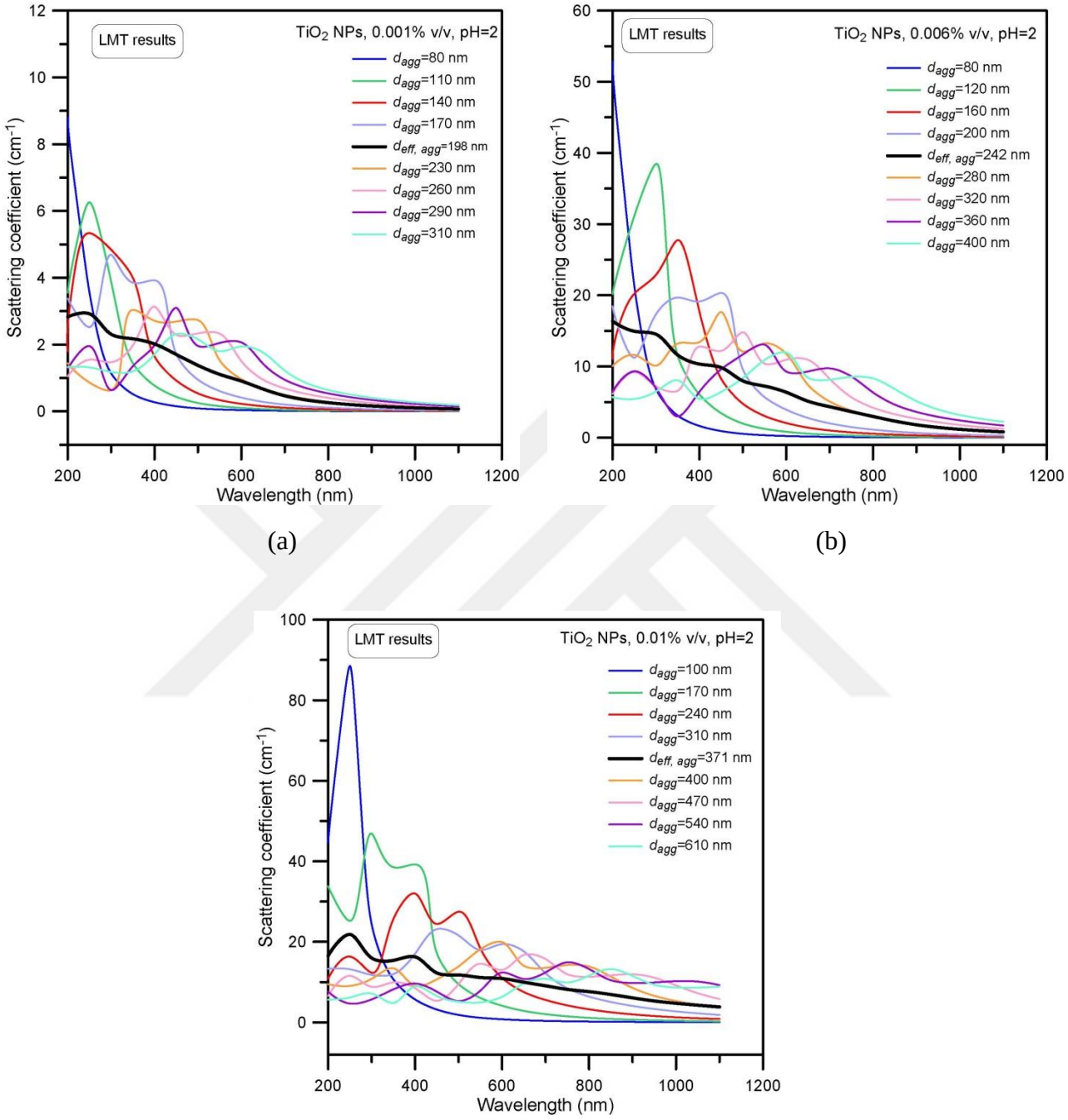

Figure 6.18 Impact of particle size distribution on the scattering coefficient of TiO_2 NPSs at pH=2 based on the Lorenz-Mie theory: (a) NPS with 0.001% v/v, (b) NPS with 0.006% v/v, and (c) NPS with 0.01% v/v.

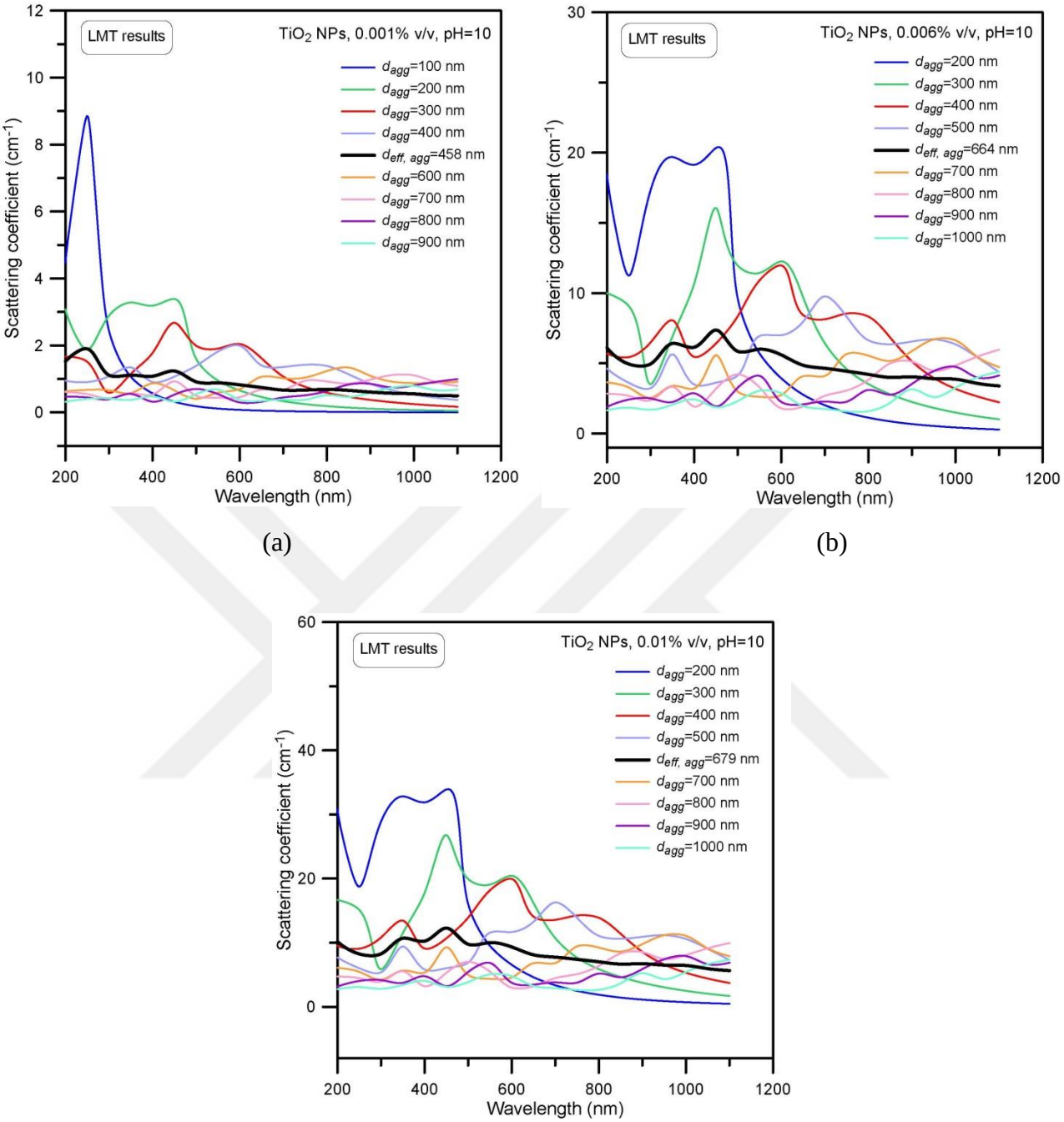

Figure 6.19 Impact of particle size distribution on the scattering coefficient of TiO_2 NPSs at pH=10 based on the Lorenz-Mie theory: (a) NPS with 0.001% v/v, (b) NPS with 0.006% v/v, and (c) NPS with 0.01% v/v.

6.4.7 Radiative energy transfer

In this section, the investigation on the effect of electrostatic stabilization and nanoparticle agglomeration on the thermal radiation transfer in NPSs is carried out, which carries significant implications on the renewable energy applications and the performance and efficiency of thermal systems. For this purpose, the volumetric radiative heat flux (radiative energy source) in the NPSs with different particle agglomerates is investigated.

The radiative energy source contours in a control volume of the NPSs for particular wavelengths are shown in Figures 6.20 and 6.21. The radiative energy source includes the effects of both radiative energy absorption and emission by a volume of NPS. For each NPS, the results are obtained for wavelengths of 200, 800, and 1500 nm. Inside this control volume, the radiative energy source shows different regimes of optical depth. That both absorption and scattering coefficients affect the radiative energy source is observed. The scattering redirects the incident radiation, where the redirected radiation can have more chance to be absorbed by the particles and/or the medium.

It can be observed that the absorption coefficient of a nanosuspension has an impact on the radiative energy source. Scattering redirects the incident radiation, since redirected or deviated radiation can be absorbed by particles and/or the medium. Al_2O_3 nanoparticles-based nanosuspensions have a radiative energy source slightly larger than that of TiO_2 nanoparticles-based nanosuspensions, since the extinction coefficient of these suspensions are larger than that of Al_2O_3 nanoparticles-based nanosuspensions in the same medium, which implies that the radiative energy absorption of TiO_2 nanoparticles-based nanosuspensions is higher and leads to a decrease in the radiative energy source (flux).

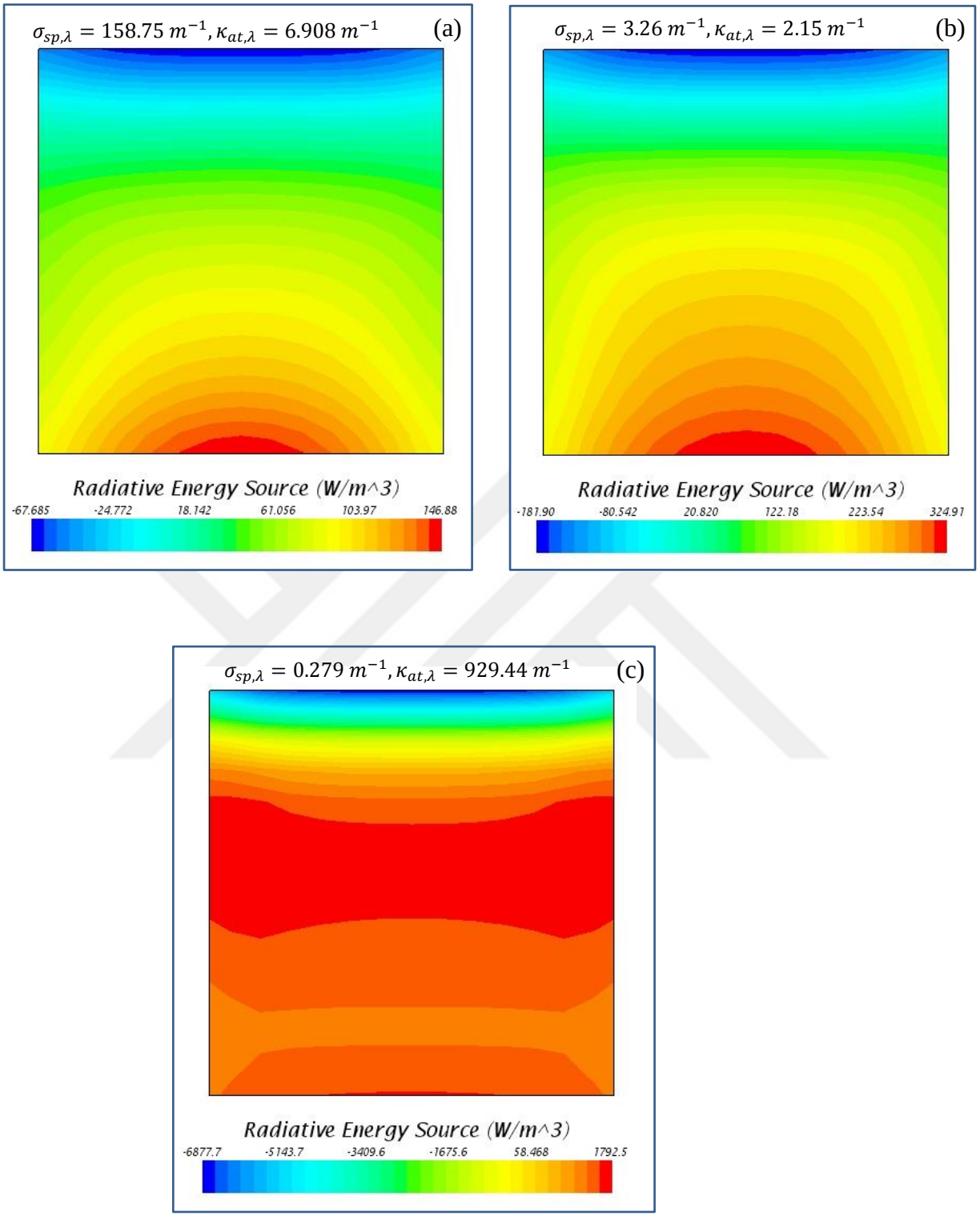

Figure 6.20 The volumetric radiative energy source in water-Al_2O_3 nanoparticles-based NPSs (pH=2 and $\emptyset = 0.001\%$). a) $\lambda = 200\ nm$, b) $\lambda = 800\ nm$ and c) $\lambda = 1500\ nm$.

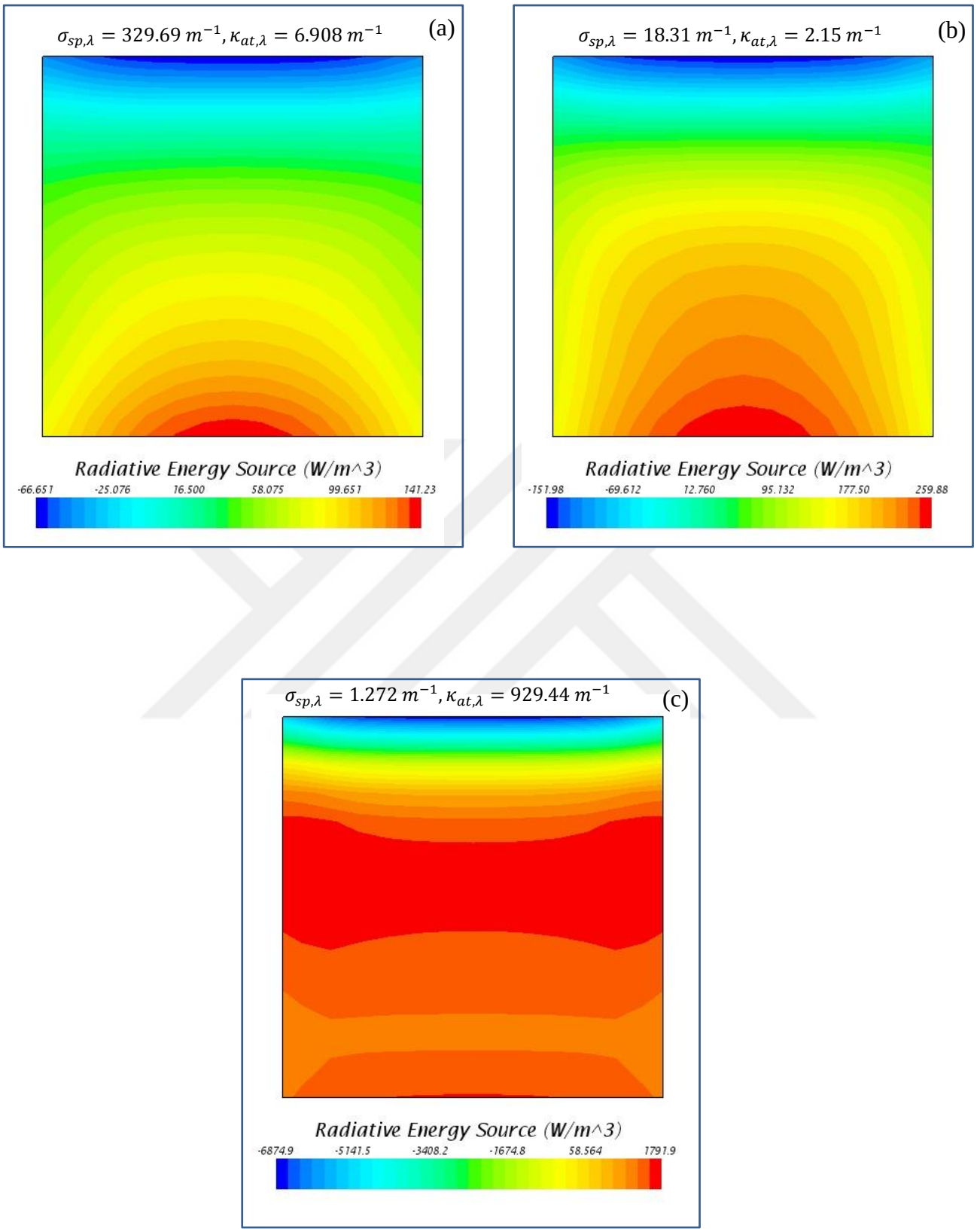

Figure 6.21 The volumetric radiative energy source in water-TiO_2 nanoparticles-based NPSs (pH=2 and $\emptyset = 0.001\%$). a) $\lambda = 200\ nm$, b) $\lambda = 800\ nm$ and c) $\lambda = 1500\ nm$.

Figures 6.22 and 6.23 show the volumetric radiative energy source profiles for both Al_2O_3 and TiO_2 nanoparticles-based NPSs. When compared with those at pH=2 under the effect of the radiative properties of the different particle agglomerate size, the volumetric radiative energy source shows low values for the two NPSs types at pH=10. In general, Al_2O_3 nanoparticles-based NPSs have a higher radiative energy source compared to TiO_2 nanoparticles-based NPSs due to the effect of incident radiation attenuation. A low radiative energy source is acquired at low wavelengths (up to 800 nm) for the NPSs, where the absorption coefficient is low in regard to his wavelength range also. For wavelengths longer than 800 nm, the radiative energy source has higher magnitudes due to the effect of the more dominant absorption coefficient. The particle agglomerate size increase with a rise in pH has a negative impact on the radiative energy source (radiative heat flux) in the NPSs. All the results in these figures are compared with the volumetric radiative energy source of pure water, and they all display a drop in the volumetric radiative energy source under the effects of both the nanoparticles and their agglomerates.

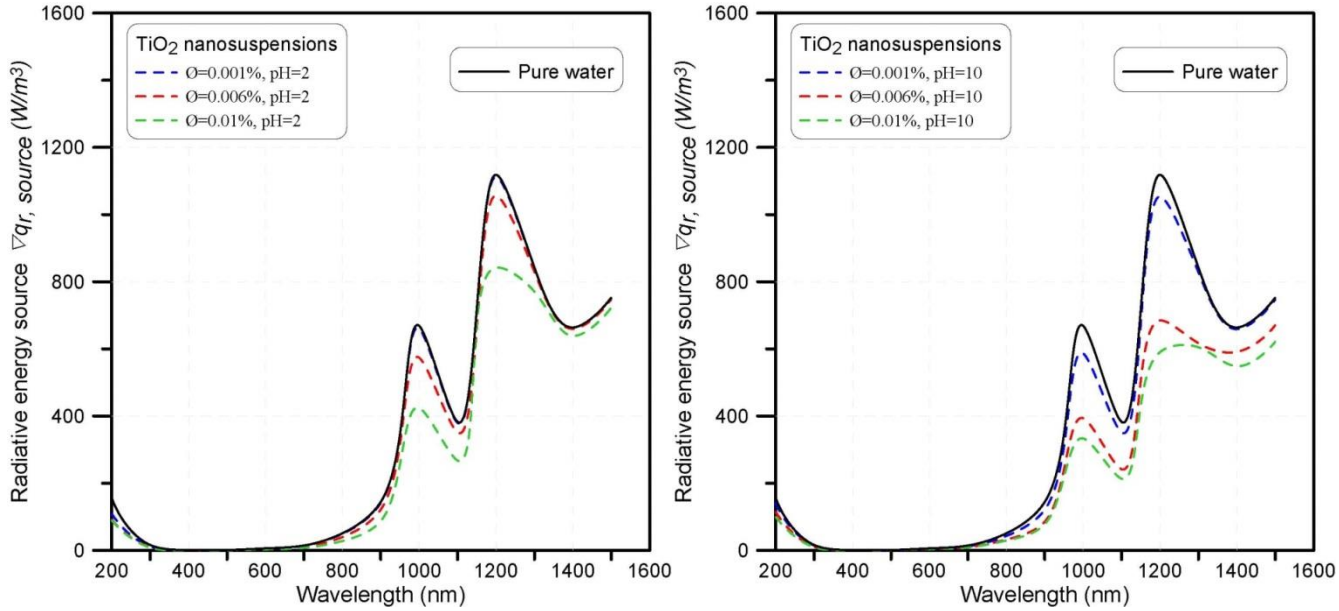

Figure 6.22 The volumetric radiative energy source in TiO_2 nanoparticles-based NPSs for different wavelengths.

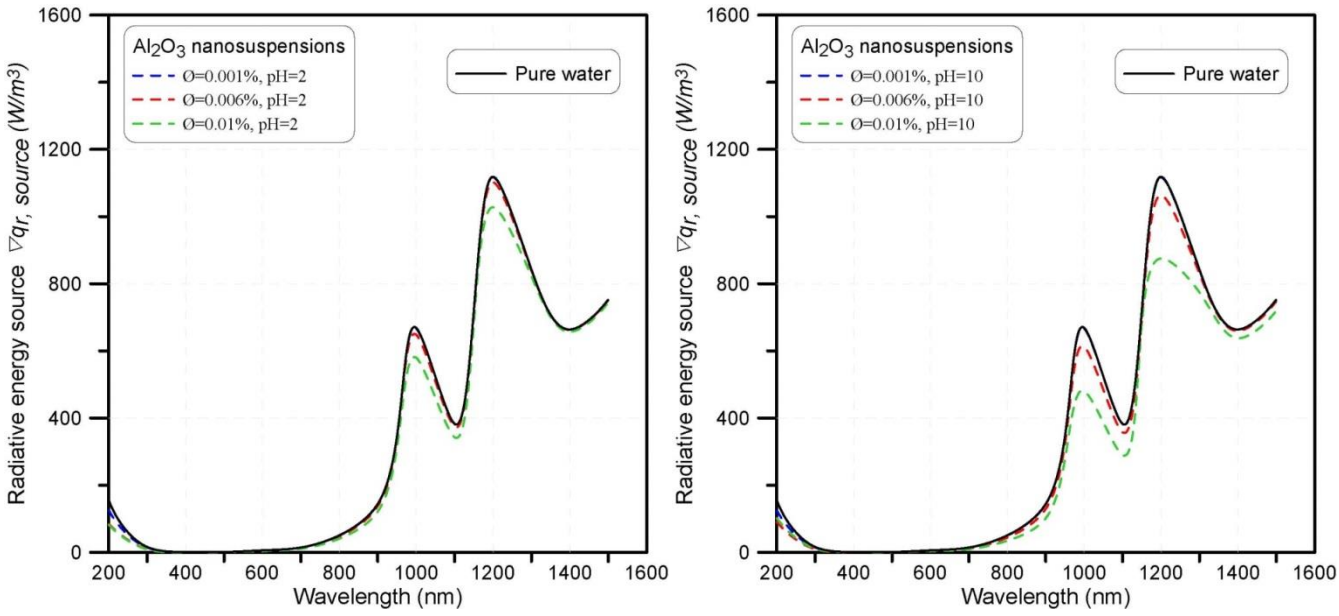

Figure 6.23 The volumetric radiative energy source in Al_2O_3 nanoparticles-based NPSs for different wavelengths.

The rise in volumetric radiative energy source suggests that the emission (re-radiation) of the radiative energy rise and/or the radiative absorption drops, and vice versa. In fact, the enhancement of the scattering coefficient by the particle agglomeration has a significant impact on these parameters (radiative energy absorption and emission), while the total extinction coefficient (radiation attenuation) of the NPSs is also adjusted.

Figure 6.24 shows the radiative energy source under different conditions (pH and ϕ) over the wavelength range (200-1500 nm). A rise in the particle volume fraction causes a drop in the radiative energy source, where increasing the particle volume fraction (particle number) leads to an improvement in the radiative properties (radiation attenuation) and increased radiation absorption in the NPSs. For the NPSs at pH=10 the radiative energy source is lower when compared to those at pH=2. Al_2O_3 nanoparticles-based NPSs have a higher radiative energy source in comparison to TiO_2 nanoparticles-based NPSs for the same volume fraction, where the TiO_2 nanoparticles-

based NPSs have a large extinction coefficient compared with the Al_2O_3 nanoparticles-based NPSs under the same conditions.

Figure 6.25 shows the thermal flux efficiency profiles, which present the ratio between the radiative energy source by a control volume of NPSs in an optical depth to the total incident radiation on the control volume. Al_2O_3 nanoparticles-based NPSs have a higher thermal flux efficiency compared with the TiO_2 nanoparticles-based NPSs, which implies that the radiative loss is high in Al_2O_3 nanoparticles-based NPSs under the same conditions as can be seen. Thermal flux efficiency is inversely proportional with the particle volume fraction, where the increasing particle concentration leads to an increase in the extinction coefficient and enhances the absorption of the NPSs. Figures 6.24 and 6.25 display how important the NPSs are under differing conditions in the thermal radiation flux performance, and this has significant implications for both the working medium and collector design, and play an important part in the photo- thermal energy conversion.

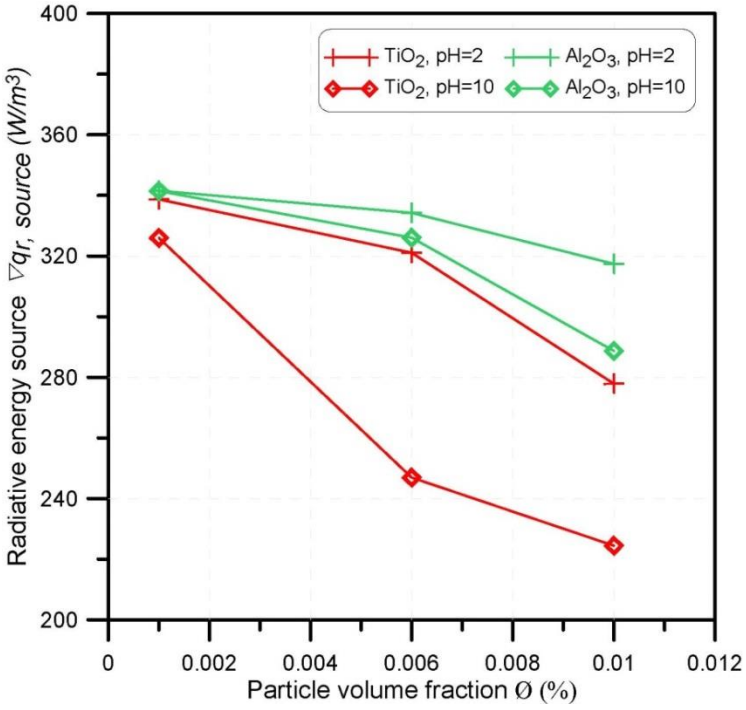

Figure 6.24 The volumetric radiative energy source in water-Al_2O_3 and TiO_2 nanoparticles-based NPSs over the whole wavelength range.

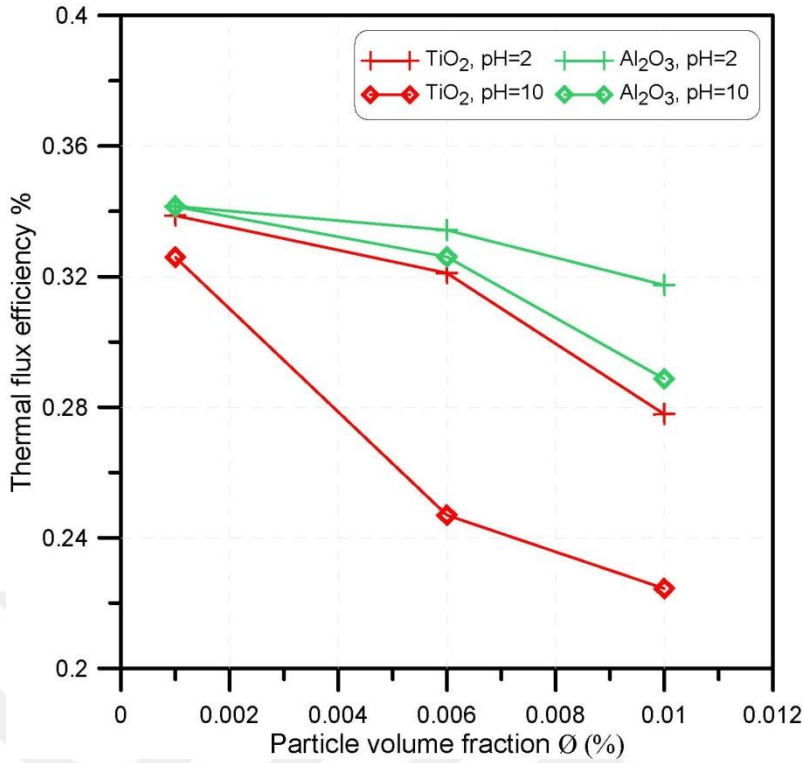

Figure 6.25 Thermal flux efficiency of a control volume of water-$Al_2O_3$and TiO_2 nanoparticles-based NPSs.

The results obtained in this study reveal the importance of NPSs' electrostatic stabilization and particle characteristics on radiative heat transfer, with the consideration of radiative properties and radiative energy transfer. The electrostatic stabilization of NPSs is vital in heat transfer applications, which is proven in this study with its effects on radiative transfer. Particle agglomeration enhances radiative properties of particulate suspensions to a certain limit, where the relationship between the wavelength of incident radiation and particle size is quite important in addition to the particle stability condition. For that reason, different radiative properties are observed for different particle agglomerate size and structure based on the PSD and for different nanoparticle types in different wavelength ranges.

CHAPTER VII

CONCLUDING REMARKS AND FUTURE STUDIES

7.1 Summary

Nanoparticle suspensions (NPSs) have been used in different engineering applications, including in concentrating solar power systems for effective harvesting of solar energy. Yet, particle agglomeration causes major problems and adversely affects the sustainable and long term use of use NPSs in these systems. As discussed in this dissertation, one way of avoiding this problem is possible by electrostatic stabilization (pH adjustment) of nanoparticle suspensions, which yields long term stable particulate suspensions. This method is preferable over steric stabilization (surfactants), which have many drawbacks in thermal applications. Stability of nanoparticle suspensions affects particle agglomeration which is a common phenomenon due to attractive forces between the suspended particles such as Van der Walls force. This can yield to unwanted effects due to the increase of the attractive force between the nanoparticles and it results in particles settlement. The structure of agglomerates depends on different parameters which are related to the particles composition and the boundary conditions

The interaction of electromagnetic waves with particulate suspensions is of critical importance, as this interaction dictates how much solar energy is absorbed and can be converted to thermal energy. The absorption and scattering of light by particles depends on particle size, structure and the dielectric constants of particles. Using Lorenz-Mie theory (for spherical particles), discrete dipole approximations (DDA) (for

agglomerates), or T-Matrix methods (for irregular-shaped particles), absorption, scattering and extinction coefficients of particulate matter can be determined (Howell et al., 2015; Mishchenko et al., 2002). If the particles are stable (low agglomeration rate), the optical and radiative properties of NPSs can be more predictable. Then, for particle applications, a more controlled path can be followed, which improved the system performance and the cost. The radiative properties of the NPSs may change with the nanoparticles properties, and these properties are affected by individual particles and the clouds of particles. Indeed, manipulating with radiative properties for a particular media is quite important when specific radiative properties are needed. In addition, the characterization of the radiative properties of the particles and their agglomerates plays a critical role in determining the radiative transfer of the surfaces in terms of the particle surface deposition and coating applications.

This dissertation is focused on understanding the effect of electrostatic stabilization on particle agglomerations, and in return on their impact on the radiation transfer in different types of NPSs. Different parameters such as particle type, the pH value, particle size and size distribution, and particle volume fraction are considered. The spectral radiative properties of the NPSs are obtained for different NPSs under different conditions, where the effect of the electrostatic stabilization has a great effect on the radiative properties for the individual and hybrid NPSs.

Although independent scattering assumption is valid in most radiation heat transfer applications, dependent scattering must be taken into account for densely packed systems that include ultrafine particles and agglomerates. It is thus important to quantify and demarcate the effect of the pH value of a particular nanoparticle suspension in the dependent/independent scattering regimes. Adjusting the pH value far from the pH_{iso} of a particle may produces ultrafine particles and/or small size

agglomerates, the dependent scattering may occur at this value of pH. The particle agglomerate size and surface to surface particle distances with respect to the wavelength are the two most important parameters in dependent and independent scattering regimes (DISRs).

The present study shows for the first time the effects of pH value on the agglomeration behavior of particles agglomeration (composite agglomerate) and on the stability and radiative properties of NPSs. Ability to control particle agglomeration rate with different radiative properties opens the door for different applications. This can be important for both the particle agglomerates in suspension or for particle deposition and surfaces coating with heterogeneous particles. Then, the desired radiative properties of different surfaces can be generated to meet specific applications. In that sense this research has significant impact on many industrial and engineering applications including solar thermal systems and thermal surfaces (cooling or heating). Radiation attenuation can increase with the particle size; particularly when the particle size approaches the wavelength of incident radiation. Large particle agglomerates affect the stability of nanosuspensions, suggesting that large agglomerates should be avoided as much as possible. Radiation absorption can be enhanced by the nanoparticles in NPSs, which influences the thermal flux efficiency of thermal radiation systems.

7.2 Future studies

The outcomes addressed in this study can be further expanded to cover several other investigations, which may be critical applications of particulate media and particulate deposits. Although the observations and findings from this dissertation are useful in understanding the effects and contributions of the pH value on the radiation-

particle interaction, many questions have arisen requiring some additional directions to be recommended to continue this research in future studies.

First of all, the particle agglomeration process is quite complicated. In addition, the effect of the temperature on suspended particles agglomeration should be investigated extensively, specifically for thermal applications. A combined effect of temperatures and different pH values on the properties of NPSs should be explored.

Yet, the effect of the pH value on the particle agglomeration processes (DLCA and RLCA) is clarified in this research experimentally, where the different structures of particle agglomerate can be produced. However, a numerical model is required to explain the particle agglomeration process and the heterogeneity of particulate systems under the effect of the pH value as well as other parameters. In this model, the different types of nanoparticles in the same media with different pH values can be included to obtain the behavior of the agglomeration.

It is also important to note that the heterogeneous particulate deposits have a significant impact on the radiative properties of surfaces. It is necessary to establish a clear and simple methodology to describe the effects of the optical and structural characteristics of particulate deposits and substrates. The results in this dissertation can be extended for the investigation of the effects of the particle agglomerate deposits on the radiative transfer of coatings. The particulate deposits affect the radiative transfer and the radiative properties of surfaces with two distinct mechanisms. Randomly stacked particles inside the deposits have different scattering and absorbing effects than the original particles due to the pacing effects. Consequently, the reflection on the substrate and the upper interface of particulate deposits become more complicated, altering the radiative properties of surfaces.

APPENDIX A

CHARACTERIZATION OF THE NANOPARTICLE SUSPENSIONS

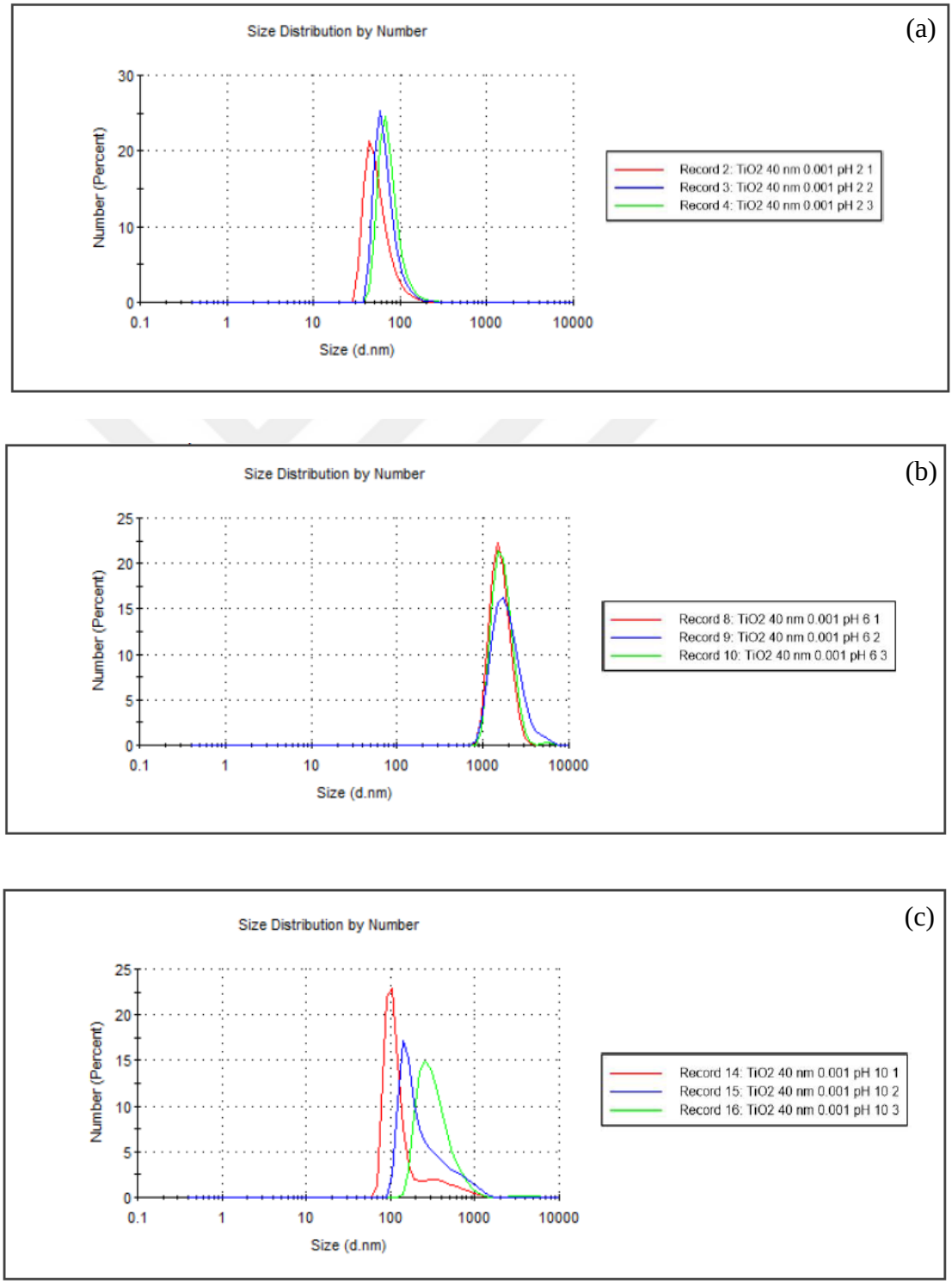

Figure A.1 Particle size distribution by particle number for TiO_2 NPSs with ($\emptyset = 0.001\%\ v/v$). (a) At pH=2 and with $d_{eff,agg} = 198\ nm$, (b) At pH=6 and with $d_{eff,agg} = 2345\ nm$, and (c) At pH=10 and with $d_{eff,agg} = 458\ nm$.

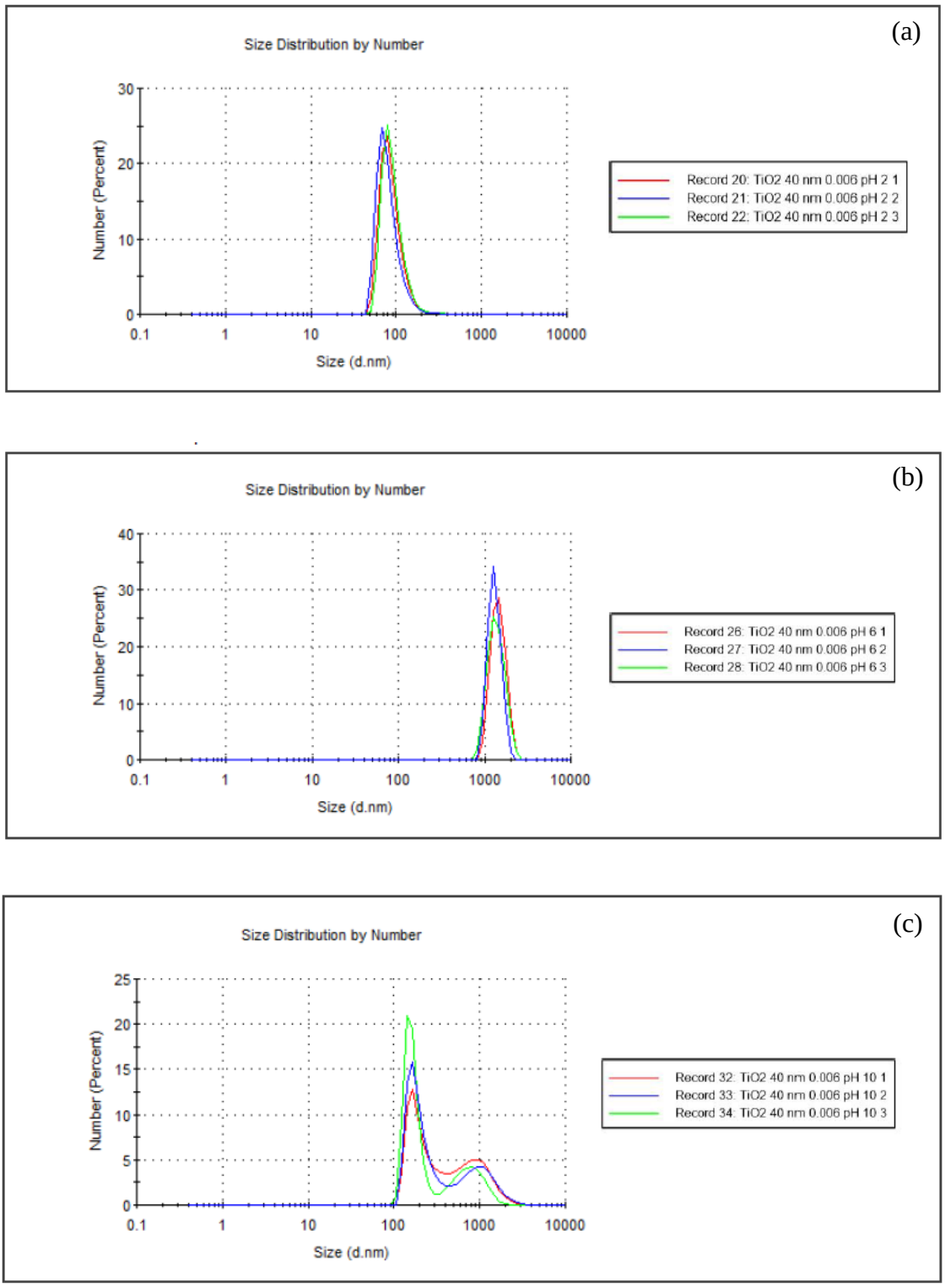

Figure A.2 Particle size distribution by particle number for TiO_2 NPSs with ($\emptyset = 0.006\% \, v/v$). (a) At pH=2 and with $d_{eff,agg} = 242 \, nm$, (b) At pH=6 and with $d_{eff,agg} = 2538 \, nm$, and (c) At pH=10 and with $d_{eff,agg} = 664 \, nm$.

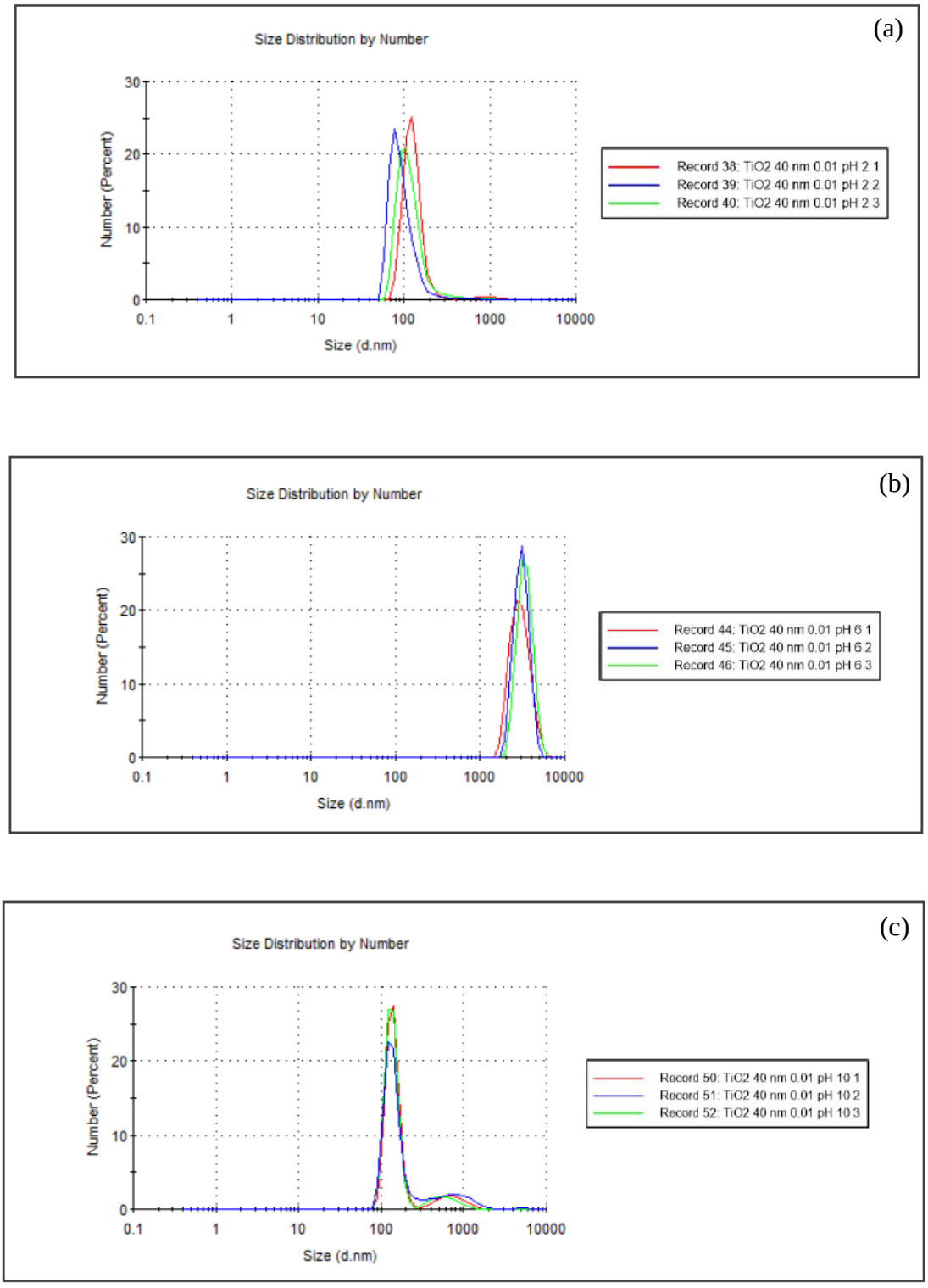

Figure A.3 Particle size distribution by particle number for TiO_2 NPSs with ($\emptyset = 0.01\% \, v/v$). (a) At pH=2 and with $d_{eff,agg} = 371 \, nm$, (b) At pH=6 and with $d_{eff,agg} = 697 \, nm$, and (c) At pH=10 and with $d_{eff,agg} = 3387 \, nm$.

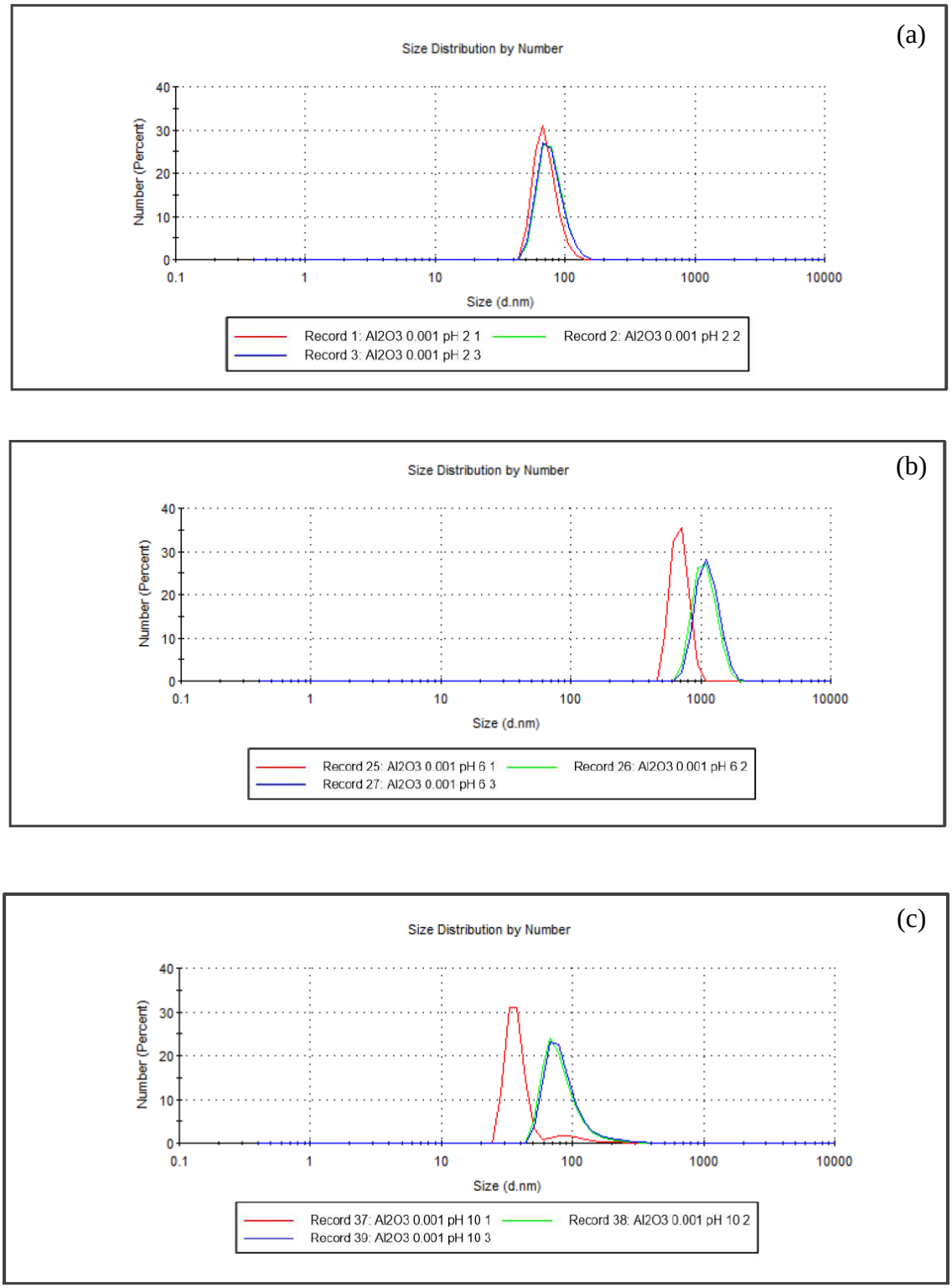

Figure A.4 Particle size distribution by particle number for Al_2O_3 NPSs with ($\emptyset = 0.001\%\ v/v$). (a) At pH=2 and with $d_{eff,agg} = 209\ nm$, (b) At pH=6 and with $d_{eff,agg} = 1889\ nm$, and (c) At pH=10 and with $d_{eff,agg} = 221\ nm$.

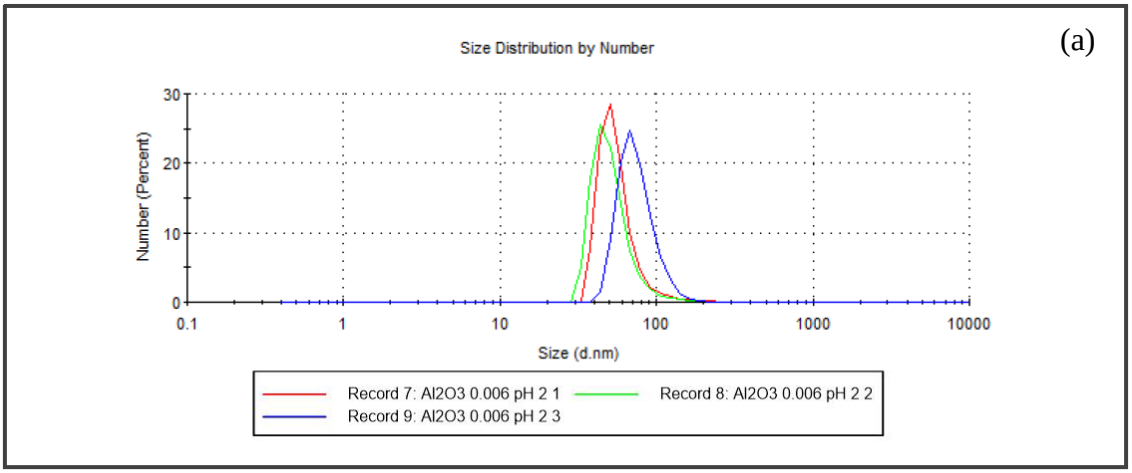

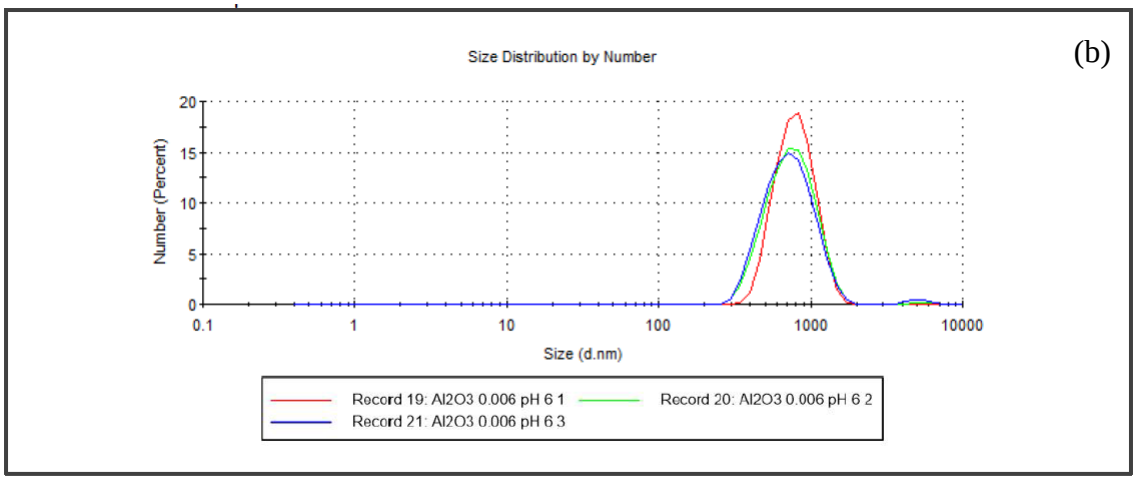

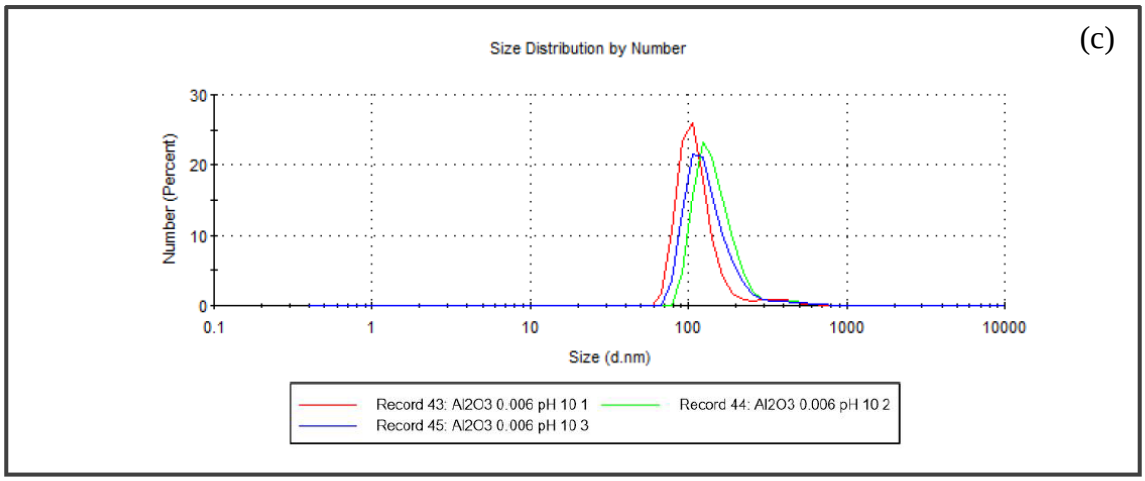

Figure A.5 Particle size distribution by particle number for Al_2O_3 NPSs with ($\emptyset = 0.006\%\ v/v$). (a) At pH=2 and with $d_{eff,agg} = 274\ nm$, (b) At pH=6 and with $d_{eff,agg} = 445\ nm$, and (c) At pH=10 and with $d_{eff,agg} = 2516\ nm$.

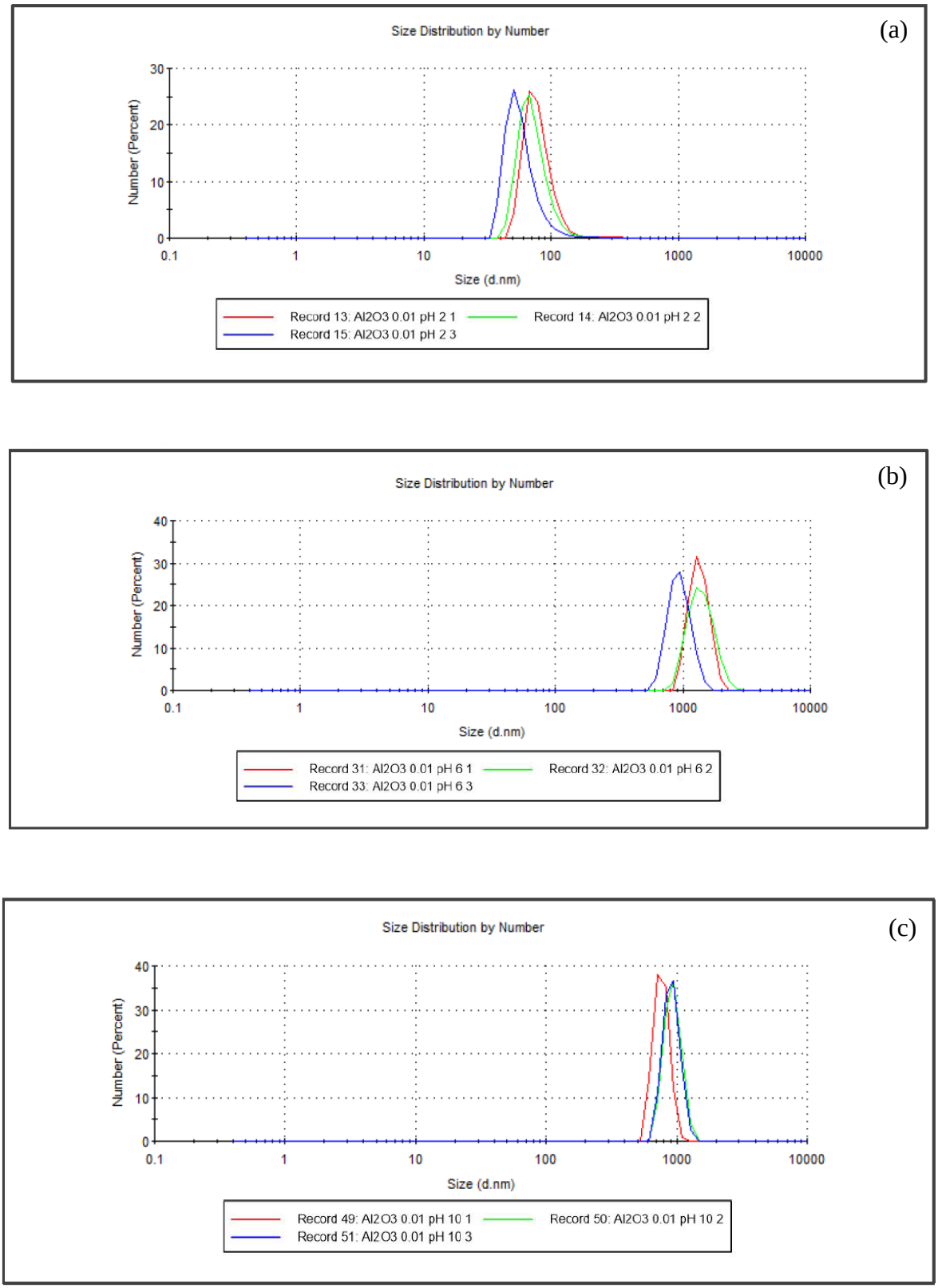

Figure A.6 Particle size distribution by particle number for Al_2O_3 NPSs with ($\emptyset = 0.01\%\ v/v$). (a) At pH=2 and with $d_{eff,agg} = 453\ nm$, (b) At pH=6 and with $d_{eff,agg} = 3081\ nm$, and (c) At pH=10 and with $d_{eff,agg} = 930\ nm$.

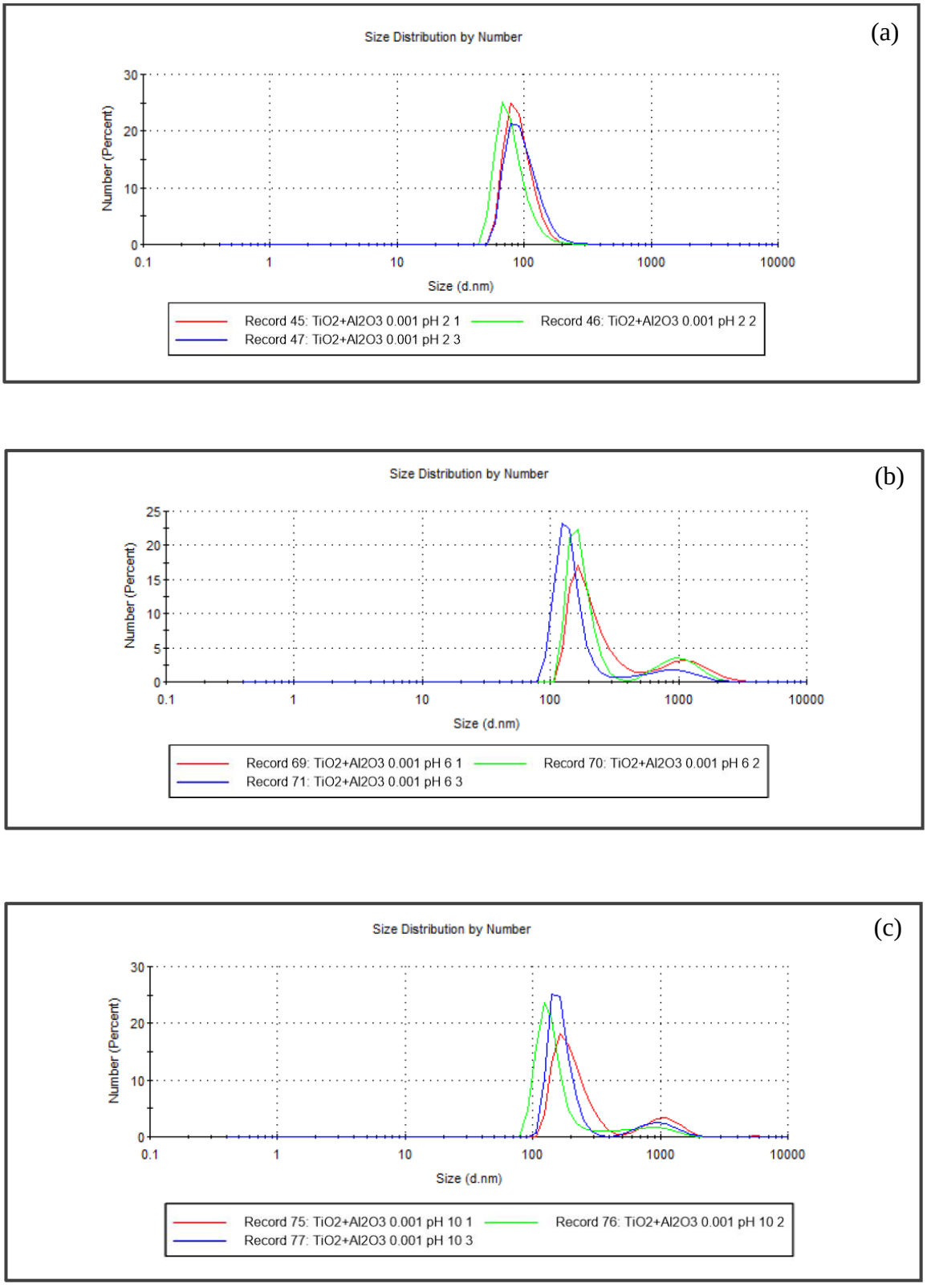

Figure A.7 Particle size distribution by particle number for $TiO_2 + Al_2O_3$ NPSs with ($\emptyset = 0.006\%\ v/v$). (a) At pH=2 and with $d_{eff,agg} = 285\ nm$, (b) At pH=6 and with $d_{eff,agg} = 643\ nm$, and (c) At pH=10 and with $d_{eff,agg} = 2053\ nm$.

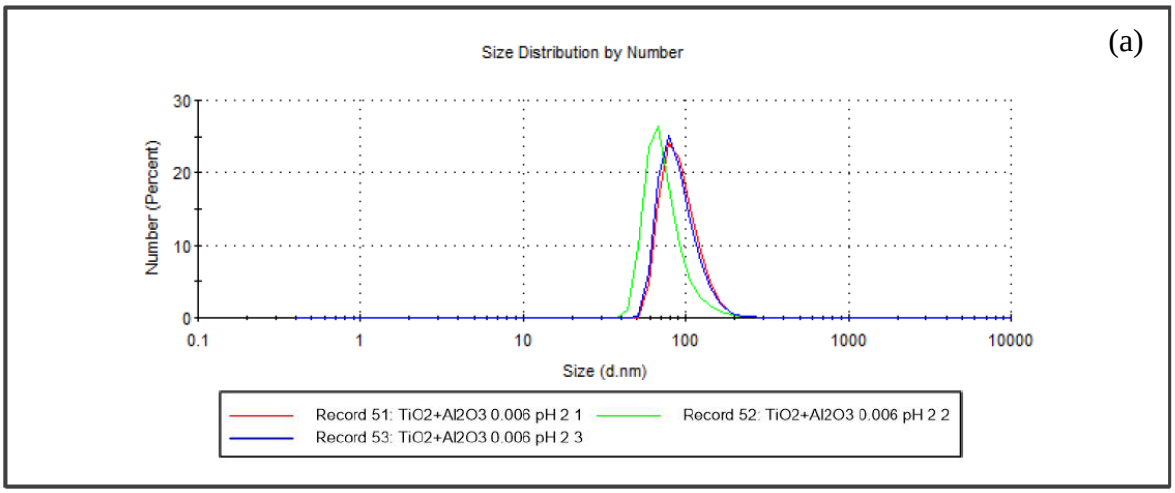

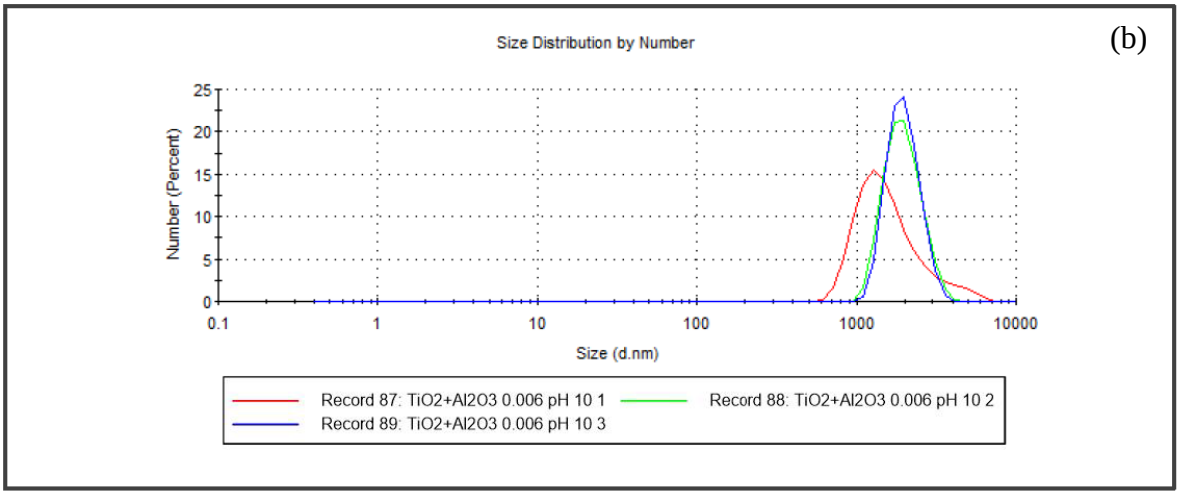

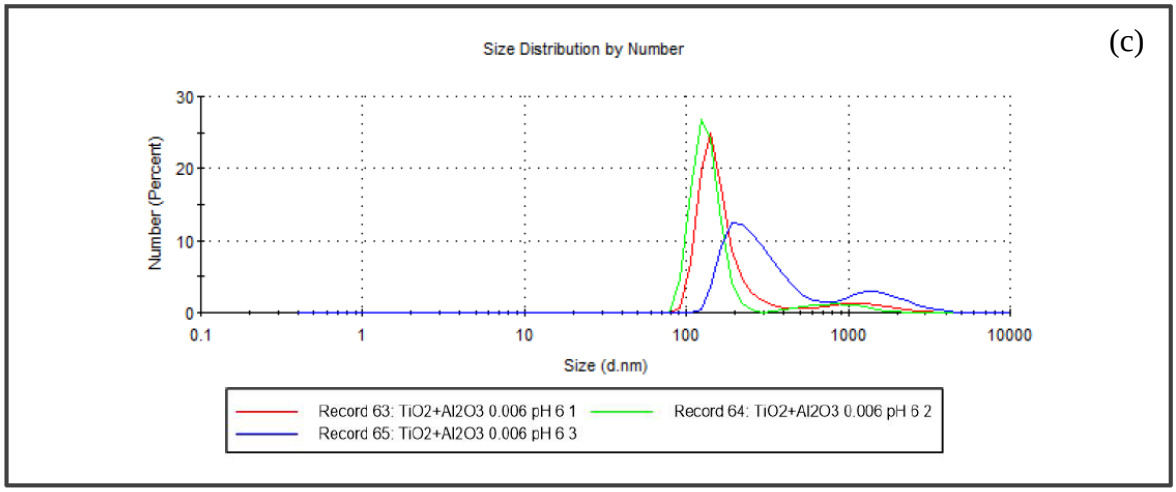

Figure A.8 Particle size distribution by particle number for $TiO_2 + Al_2O_3$ NPSs with ($\emptyset = 0.006\%\ v/v$). (a) At pH=2 and with $d_{eff,agg} = 285\ nm$, (b) At pH=6 and with $d_{eff,agg} = 643\ nm$, and (c) At pH=10 and with $d_{eff,agg} = 2053\ nm$.

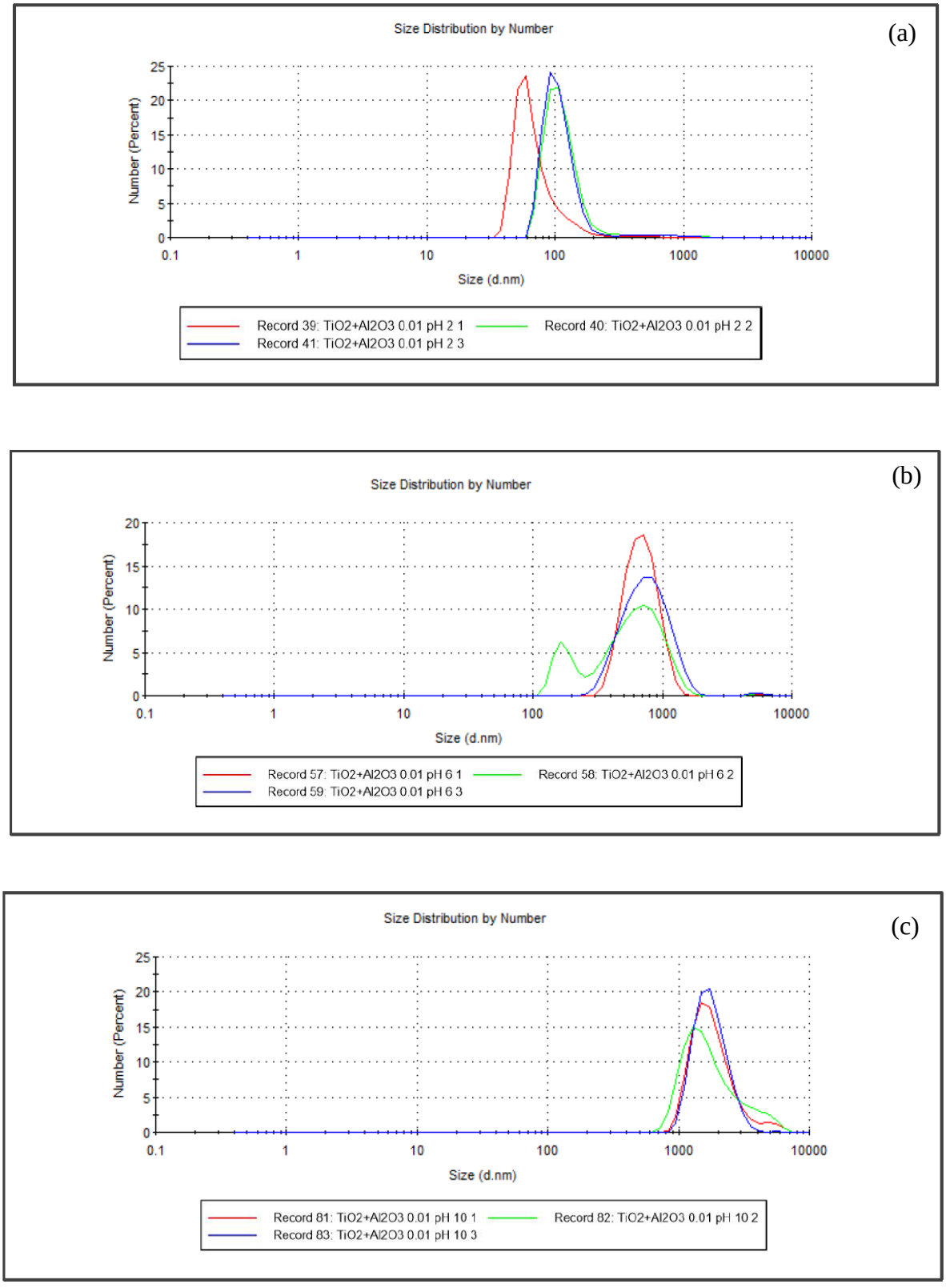

Figure A.9 Particle size distribution by particle number for $TiO_2 + Al_2O_3$ NPSs with ($\emptyset = 0.01\%\ v/v$). (a) At pH=2 and with $d_{eff,agg} = 431\ nm$, (b) At pH=6 and with $d_{eff,agg} = 881\ nm$, and (c) At pH=10 and with $d_{eff,agg} = 2295\ nm$.

LIST OF REFERENCES

Abedini, E., Zarei, T., Afrand, M., and Wongwises, S. (2017). Experimental study of transition flow from single phase to two phase flow boiling in nanofluids. Journal of Molecular Liquids, 231, 11-19.

Afrand, M., Abedini, E., and Teimouri, H. (2017). Experimental investigation and simulation of flow boiling of nanofluids in different flow directions. Physica E: Low-dimensional Systems and Nanostructures, 87, 248-253.

Agrawal, B. M., and Mengüç, M. P. (1991). Forward and inverse analysis of single and multiple scattering of collimated radiation in an axisymmetric system. International Journal of Heat and Mass Transfer, 34(3), 633-647.

Allahyar, H., Hormozi, F., and ZareNezhad, B. (2016). Experimental investigation on the thermal performance of a coiled heat exchanger using a new hybrid nanofluid. Experimental Thermal and Fluid Science, 76, 324-329.

Almohammed, N., and Breuer, M. (2016). Modeling and simulation of agglomeration in turbulent particle-laden flows: A comparison between energy-based and momentum-based agglomeration models. Powder Technology, 294, 373-402.

Anushree, C., and Philip, J. (2016). Assessment of long term stability of aqueous nanofluids using different experimental techniques. Journal of Molecular Liquids, 222, 350-358.

Aslan, M., Yamada, J., Meng-uacute, M., and -atilde. (2003). Characterization of individual cotton fibers via light-scattering experiments. Journal of thermophysics and heat transfer, 17(4), 442-449.

Aslan, M. M., Mengüç, M. P., Manickavasagam, S., and Saltiel, C. (2006). Size and shape prediction of colloidal metal oxide MgBaFeO particles from light scattering measurements. Journal of Nanoparticle Research, 8(6), 981-994.

Babu, J. R., Kumar, K. K., and Rao, S. S. (2017). State-of-art review on hybrid nanofluids. Renewable and Sustainable Energy Reviews, 77, 551-565.

Bae, H., Lee, M., Kim, W., and Rhee, C. (2003). Dispersion properties of TiO2 nano-powder synthesized by homogeneous precipitation process at low temperatures. Colloids and Surfaces A: Physicochemical and Engineering Aspects, 220(1-3), 169-177.

Becker, L., Bunch, T. E., and Allamandola, L. J. (1999). Higher fullerenes in the Allende meteorite. Nature, 400(6741), 227.

Behi, M., and Mirmohammadi, S. A. (2012). Investigation on thermal conductivity, viscosity and stability of nanofluids. Royal Institute of Technology (KTH) School of Industrial Engineering and Management, Stockholm, Sweden.

Berne, B. J., and Pecora, R. (2000). Dynamic light scattering: with applications to chemistry, biology, and physics: Courier Corporation.

Bianco, V., Vafai, K., Manca, O., and Nardini, S. (2015). Heat transfer enhancement with nanofluids: CRC press.

Binnig, G., Rohrer, H., Gerber, C., and Weibel, E. (1982). Surface studies by scanning

tunneling microscopy. Physical review letters, 49(1), 57.

Bohren, C. F., and Huffman, D. R. (2008). Absorption and scattering of light by small particles: John Wiley & Sons.

Boisvert, J.-P., Persello, J., Castaing, J.-C., and Cabane, B. (2001). Dispersion of alumina-coated TiO2 particles by adsorption of sodium polyacrylate. Colloids and Surfaces A: Physicochemical and Engineering Aspects, 178(1-3), 187-198.

Brewster, M., and Tien, C. (1982). Radiative transfer in packed fluidized beds: dependent versus independent scattering. Journal of Heat Transfer, 104(4), 573-579.

Bushell, G., Yan, Y., Woodfield, D., Raper, J., and Amal, R. (2002). On techniques for the measurement of the mass fractal dimension of aggregates. Advances in Colloid and Interface Science, 95(1), 1-50.

Chen, L., Xie, H., Li, Y., and Yu, W. (2008). Nanofluids containing carbon nanotubes treated by mechanochemical reaction. Thermochimica Acta, 477(1-2), 21-24.

Chen, W., Zou, C., Li, X., and Li, L. (2017). Experimental investigation of SiC nanofluids for solar distillation system: stability, optical properties and thermal conductivity with saline water-based fluid. International Journal of Heat and Mass Transfer, 107, 264-270.

Cheng, P., Gu, M., and Jin, Y. (2005). Recent progress in titania photocatalyst operating under visible light. Progress in Chemistry, 17(1), 8-14.

Choi, C., Yoo, H., and Oh, J. (2008). Preparation and heat transfer properties of nanoparticle-in-transformer oil dispersions as advanced energy-efficient coolants. Current Applied Physics, 8(6), 710-712.

Choi, S., Zhang, Z., and Keblinski, P. (2004). Nanofluids, Encyclopedia of Nanoscience and Nanotechnology (HS Nalwa, Editor), Vol. 5. p.(757-773): American Scientific Publisher.

Choi, S. U. (2009). Nanofluids: from vision to reality through research. Journal of Heat Transfer, 131(3), 033106.

Choi, S. U., and Eastman, J. A. (1995). Enhancing thermal conductivity of fluids with nanoparticles. Retrieved from

Colangelo, G., Favale, E., De Risi, A., and Laforgia, D. (2013). A new solution for reduced sedimentation flat panel solar thermal collector using nanofluids. Applied Energy, 111, 80-93.

Cosgrove, T. (2010). Colloid science: principles, methods and applications: John Wiley & Sons.

Council, W. E. (2013). World energy resources. London: World Energy Council.

Das, P. K., Mallik, A. K., Ganguly, R., and Santra, A. K. (2016). Synthesis and characterization of TiO2–water nanofluids with different surfactants. International Communications in Heat and Mass Transfer, 75, 341-348.

Das, S. K., Choi, S. U., and Patel, H. E. (2006). Heat transfer in nanofluids—a review. Heat transfer engineering, 27(10), 3-19.

Das, S. K., Choi, S. U., Yu, W., and Pradeep, T. (2007). Nanofluids: science and technology: John Wiley & Sons.

Daungthongsuk, W., and Wongwises, S. (2007). A critical review of convective heat transfer of nanofluids. Renewable and Sustainable Energy Reviews, 11(5), 797-817.

Dehkordi, R. A., Esfe, M. H., and Afrand, M. (2017). Effects of functionalized single walled carbon nanotubes on thermal performance of antifreeze: an experimental study on thermal conductivity. Applied Thermal Engineering, 120, 358-366.

Derjaguin, B. (1941). Theory of the stability of strongly charged lyophobic sols and the adhesion of strongly charged particles in solutions of electrolytes. Acta Physicochim. USSR, 14, 633-662.

Devendiran, D. K., and Amirtham, V. A. (2016). A review on preparation, characterization, properties and applications of nanofluids. Renewable and Sustainable Energy Reviews, 60, 21-40.

DeVoe, H. (1964). Optical properties of molecular aggregates. I. Classical model of electronic absorption and refraction. The Journal of chemical physics, 41(2), 393-400.

Dhand, C., Dwivedi, N., Loh, X. J., Ying, A. N. J., Verma, N. K., Beuerman, R. W., . . . Ramakrishna, S. (2015). Methods and strategies for the synthesis of diverse nanoparticles and their applications: a comprehensive overview. Rsc Advances, 5(127), 105003-105037.

Dhont, J. K. (1996). An introduction to dynamics of colloids (Vol. 2): Elsevier.

Diebold, M. P. (2014). Application of Light Scattering to Coatings: A User's Guide: Springer.

Dietz, P. (2003). The effect of fine-particle-size extenders and entrapped air on TiO2 in emulsion paints. Paint Coat. Ind, 9, 28-37.

Dietz, P. (2004). The effect of TiO 2 dispersion and entrapped air on the opacity of alkyd and acrylic emulsion paints. Surface Coatings International Part A: Coatings Journal, 87, 18-24.

Doicu, A., Wriedt, T., and Eremin, Y. A. (2006). Light scattering by systems of particles: null-field method with discrete sources: theory and programs (Vol. 124): Springer.

Drexler, K. E., Peterson, C., and Pergamit, G. (1991). Unbounding the future: the nanotechnology revolution. New York: William Morrow and Company. Google Scholar.

Drolen, B., and Tien, C. (1987). Independent and dependent scattering in packed-sphere systems. Journal of thermophysics and heat transfer, 1(1), 63-68.

Du, M., and Tang, G. (2015). Optical property of nanofluids with particle agglomeration. solar energy, 122, 864-872.

Duan, H., and Xuan, Y. (2014). Enhanced optical absorption of the plasmonic nanoshell suspension based on the solar photocatalytic hydrogen production system. Applied Energy, 114, 22-29.

Duffie, J. A., and Beckman, W. A. (2013). Solar engineering of thermal processes: John Wiley & Sons.

Egerton, T. A. (2014). UV-absorption—the primary process in photocatalysis and some practical consequences. Molecules, 19(11), 18192-18214.

Esfe, M. H., Afrand, M., Gharehkhani, S., Rostamian, H., Toghraie, D., and Dahari, M. (2016). An experimental study on viscosity of alumina-engine oil: effects of temperature and nanoparticles concentration. International Communications in Heat and Mass Transfer, 76, 202-208.

Esfe, M. H., Akbari, M., Karimipour, A., Afrand, M., Mahian, O., and Wongwises, S. (2015). Mixed-convection flow and heat transfer in an inclined cavity equipped to a hot obstacle using nanofluids considering temperature-dependent properties. International Journal of Heat and Mass Transfer, 85, 656-666.

Eshgarf, H., and Afrand, M. (2016). An experimental study on rheological behavior of non-Newtonian hybrid nano-coolant for application in cooling and heating systems. Experimental Thermal and Fluid Science, 76, 221-227.

Faraday, M. (1857). Experimental relations of gold (and other metals) to light./9A24A 51 243 35E831 AC3 8 185 3 30 2D 2 147. 145v181.

Fazio, S., Guzman, J., Colomer, M., Salomoni, A., and Moreno, R. (2008). Colloidal stability of nanosized titania aqueous suspensions. Journal of the European Ceramic Society, 28(11), 2171-2176.

Fedele, L., Colla, L., Bobbo, S., Barison, S., and Agresti, F. (2011). Experimental stability analysis of different water-based nanofluids. Nanoscale research letters, 6(1), 300.

Feynman, R. P. (1959). There's plenty of room at the bottom. Miniaturization, 282-296.

Ghadimi, A., and Metselaar, I. H. (2013). The influence of surfactant and ultrasonic processing on improvement of stability, thermal conductivity and viscosity of titania nanofluid. Experimental Thermal and Fluid Science, 51, 1-9.

Gibbs, J. W. (1879). On the equilibrium of heterogeneous substances.

Gleiter, H. (1981). Materials with ultra-fine grain sizes. Paper presented at the 2nd Riso Int. Symp/Metall. and Mat. Sci.

Goodarzi, M., Kherbeet, A. S., Afrand, M., Sadeghinezhad, E., Mehrali, M., Zahedi, P., . . . Dahari, M. (2016). Investigation of heat transfer performance and friction factor of a counter-flow double-pipe heat exchanger using nitrogen-doped, graphene-based nanofluids. International Communications in Heat and Mass Transfer, 76, 16-23.

Gorji, T. B., and Ranjbar, A. (2017). A review on optical properties and application of nanofluids in direct absorption solar collectors (DASCs). Renewable and Sustainable Energy Reviews, 72, 10-32.

Gorji, T. B., Ranjbar, A., and Mirzababaei, S. (2015). Optical properties of carboxyl functionalized carbon nanotube aqueous nanofluids as direct solar thermal energy absorbers. solar energy, 119, 332-342.

Govindan, R., Manickavasagam, S., and Menguc, M. P. (1995). On measuring the mueller matrix elements of soot agglomerates. Paper presented at the ICHMT DIGITAL LIBRARY ONLINE.

Green, M. A. (1982). Solar cells: operating principles, technology, and system applications.

Gu, Y., Zhao, X., Liu, Y., and Lv, Y. (2014). Preparation and tribological properties of dual-coated TiO 2 nanoparticles as water-based lubricant additives. Journal of Nanomaterials, 2014, 2.

Gupta, H., Agrawal, G., and Mathur, J. (2012). An overview of Nanofluids: A new media towards green environment. International Journal of environmental sciences, 3(1), 433-440.

Gupta, H. K., Agrawal, G. D., and Mathur, J. (2015). Investigations for effect of Al2O3–H2O nanofluid flow rate on the efficiency of direct absorption solar collector. Case Studies in Thermal Engineering, 5, 70-78.

Haddad, Z., Abid, C., Oztop, H. F., and Mataoui, A. (2014). A review on how the researchers prepare their nanofluids. International Journal of Thermal Sciences, 76, 168-189.

Hassellöv, M., Readman, J. W., Ranville, J. F., and Tiede, K. (2008). Nanoparticle analysis and characterization methodologies in environmental risk assessment of engineered nanoparticles. Ecotoxicology, 17(5), 344-361.

He, Q., Wang, S., Zeng, S., and Zheng, Z. (2013). Experimental investigation on photothermal properties of nanofluids for direct absorption solar thermal energy systems. Energy conversion and management, 73, 150-157.

He, Y., Jin, Y., Chen, H., Ding, Y., Cang, D., and Lu, H. (2007). Heat transfer and flow behaviour of aqueous suspensions of TiO2 nanoparticles (nanofluids) flowing upward through a vertical pipe. International Journal of Heat and Mass Transfer, 50(11-12), 2272-2281.

Hewakuruppu, Y. L., Taylor, R. A., Tyagi, H., Khullar, V., Otanicar, T., Coulombe, S., and Hordy, N. (2015). Limits of selectivity of direct volumetric solar absorption. solar energy, 114, 206-216.

Hoffman, C., and Driggers, R. (2016). Encyclopedia of Optical and Photonic Engineering, (Online): Crc Press.

Hordy, N., Rabilloud, D., Meunier, J.-L., and Coulombe, S. (2014). High temperature and long-term stability of carbon nanotube nanofluids for direct absorption solar thermal collectors. solar energy, 105, 82-90.

Hossain, M. S., Saidur, R., Sabri, M. F. M., Said, Z., and Hassani, S. (2015). Spotlight on available optical properties and models of nanofluids: A review. Renewable and Sustainable Energy Reviews, 43, 750-762.

Hottel, H., Sarofim, A., Dalzell, W., and Vasalos, I. (1971). Optical properties of coatings. Effect of pigment concentration. AIAA Journal, 9(10), 1895-1898.

Howell, J. R., Menguc, M. P., and Siegel, R. (2015). Thermal radiation heat transfer.

Hulst, H. C., and van de Hulst, H. C. (1957). Light scattering by small particles: Courier Corporation.

Hunter, R. J. (2001). Foundations of colloid science: Oxford university press.

Hwang, Y., Lee, J.-K., Lee, J.-K., Jeong, Y.-M., Cheong, S.-i., Ahn, Y.-C., and Kim, S. H. (2008). Production and dispersion stability of nanoparticles in nanofluids. Powder Technology, 186(2), 145-153.

Ivezić, Z., and Mengüç, M. P. (1996). An investigation of dependent/independent scattering regimes using a discrete dipole approximation. International Journal of Heat and Mass Transfer, 39(4), 811-822.

IveziĆ, Ž., Mengüç, M. P., and Knauer, T. G. (1997). A procedure to determine the onset of soot agglomeration from multi-wavelength experiments. Journal of Quantitative Spectroscopy and Radiative Transfer, 57(6), 859-865.

Jamil, M., Sidik, N. C., and Yazid, M. M. (2016). Thermal performance of thermosyphon evacuated tube solar collector using TiO2/water nanofluid. J. Adv. Res. Fluid Mech. Therm. Sci., 20(1), 12-29.

Jing, D., and Song, D. (2017). Optical properties of nanofluids considering particle size distribution: Experimental and theoretical investigations. Renewable and Sustainable Energy Reviews, 78, 452-465.

Jyothirmayee Aravind, S., and Ramaprabhu, S. (2012). Graphene wrapped multiwalled carbon nanotubes dispersed nanofluids for heat transfer applications. Journal of Applied Physics, 112(12), 124304.

Kameya, Y., and Hanamura, K. (2011). Enhancement of solar radiation absorption using nanoparticle suspension. solar energy, 85(2), 299-307.

Kandasamy, R., Muhaimin, I., and Rosmila, A. (2014). The performance evaluation of unsteady MHD non-Darcy nanofluid flow over a porous wedge due to renewable (solar) energy. Renewable Energy, 64, 1-9.

Karami, M., Akhavan-Behabadi, M., Dehkordi, M. R., and Delfani, S. (2016). Thermo-optical properties of copper oxide nanofluids for direct absorption of solar radiation. Solar Energy Materials and Solar Cells, 144, 136-142.

Karimzadehkhouei, M., Ghorbani, M., Sezen, M., Şendur, K., Pınar Mengüç, M., Leblebici, Y., and Koşar, A. (2016). Increasing the stability of nanofluids with cavitating flows in micro orifices. Applied Physics Letters, 109(10), 104101.

Karimzadehkhouei, M., Shojaeian, M., Şendur, K., Mengüç, M. P., and Koşar, A. (2017). The effect of nanoparticle type and nanoparticle mass fraction on heat transfer enhancement in pool boiling. International Journal of Heat and Mass Transfer, 109, 157-166.

Kaszuba, M., McKnight, D., Connah, M. T., McNeil-Watson, F. K., and Nobbmann, U. (2008). Measuring sub nanometre sizes using dynamic light scattering. Journal of Nanoparticle Research, 10(5), 823-829.

Kawanami, T., and Sakurai, K. (2007). Cooling performance of room-temperature magnetic refrigerator with active magnetic regenerator (Numerical analysis on cooling performance). Trans. JSME (B), 73(735), 2323-2330.

Keblinski, P., and Cahill, D. G. (2005). Comment on "Model for Heat Conduction in Nanofluids". Physical review letters, 95(20), 209401.

Keblinski, P., Eastman, J. A., and Cahill, D. G. (2005). Nanofluids for thermal transport. Materials today, 8(6), 36-44.

Kestell, A. E., and DeLorey, G. T. (2009). Nanoparticles: Properties, Classification, Characterization, and Fabrication: Nova Science Publishers, Incorporated.

Khullar, V. (2016). Heat transfer analysis and optical characterization of nanoparticle dispersion-based solar thermal systems.

Khullar, V., Tyagi, H., Hordy, N., Otanicar, T. P., Hewakuruppu, Y., Modi, P., and Taylor, R. A. (2014). Harvesting solar thermal energy through nanofluid-based volumetric

absorption systems. International Journal of Heat and Mass Transfer, 77, 377-384.

Kim, H., Ham, J., Park, C., and Cho, H. (2016). Theoretical investigation of the efficiency of a U-tube solar collector using various nanofluids. Energy, 94, 497-507.

Klusek, C., Manickavasagam, S., and Mengüç, M. P. (2003). Compendium of scattering matrix element profiles for soot agglomerates. Journal of Quantitative Spectroscopy and Radiative Transfer, 79, 839-859.

Koichi, N. (1991). New design concept of structural ceramics-ceramics nanocomposites. Journal of Ceramic Society of Japan, 99(3), 974-982.

Konakanchi, H., Vajjha, R. S., Chukwu, G. A., and Das, D. K. (2015). Measurements of pH of three nanofluids and development of new correlations. Heat transfer engineering, 36(1), 81-90.

Kozan, M., and Mengüç, M. P. (2008). Exploration of fractal nature of WO3 nanowire aggregates. Journal of Quantitative Spectroscopy and Radiative Transfer, 109(2), 327-336.

Kozan, M., Thangala, J., Bogale, R., Mengüç, M. P., and Sunkara, M. K. (2008). In-situ characterization of dispersion stability of WO3 nanoparticles and nanowires. Journal of Nanoparticle Research, 10(4), 599-612.

Kumbhakar, P., Ray, S. S., and Stepanov, A. L. (2014). Optical properties of nanoparticles and nanocomposites. Journal of Nanomaterials, 2014.

Lane, N. (2001). The grand challenges of nanotechnology. Journal of Nanoparticle Research, 3(2-3), 95-103.

Lattuada, M., Sandkühler, P., Wu, H., Sefcik, J., and Morbidelli, M. (2003). Aggregation kinetics of polymer colloids in reaction limited regime: experiments and simulations. Advances in Colloid and Interface Science, 103(1), 33-56.

Lax, M. (1952). Multiple scattering of waves. II. The effective field in dense systems. Physical Review, 85(4), 621.

Lee, S.-C. (1994). Dependent vs independent scattering in fibrous composites containing parallel fibers. Journal of thermophysics and heat transfer, 8(4), 641-646.

Lee, S.-H., and Jang, S. P. (2013). Extinction coefficient of aqueous nanofluids containing multi-walled carbon nanotubes. International Journal of Heat and Mass Transfer, 67, 930-935.

Lee, S., Choi, S.-S., Li, S., and, and Eastman, J. (1999). Measuring thermal conductivity of fluids containing oxide nanoparticles. Journal of Heat Transfer, 121(2), 280-289.

Lee, S. H., Cho, E., Jeon, S. H., and Youn, J. R. (2007). Rheological and electrical properties of polypropylene composites containing functionalized multi-walled carbon nanotubes and compatibilizers. Carbon, 45(14), 2810-2822.

Li, X., Zhu, D., and Wang, X. (2007). Evaluation on dispersion behavior of the aqueous copper nano-suspensions. Journal of colloid and interface science, 310(2), 456-463.

Li, X., Zhu, D., Wang, X., Wang, N., Gao, J., and Li, H. (2008). Thermal conductivity enhancement dependent pH and chemical surfactant for Cu-H2O nanofluids. Thermochimica Acta, 469(1-2), 98-103.

Li, Y., Xie, H. Q., Yu, W., and Li, J. (2011). Investigation on heat transfer performances of

nanofluids in solar collector. Paper presented at the Materials Science Forum.

Liu, M.-S., Lin, M. C.-C., Huang, I.-T., and Wang, C.-C. (2005). Enhancement of thermal conductivity with carbon nanotube for nanofluids. International Communications in Heat and Mass Transfer, 32(9), 1202-1210.

Luo, Z., Wang, C., Wei, W., Xiao, G., and Ni, M. (2014). Performance improvement of a nanofluid solar collector based on direct absorption collection (DAC) concepts. International Journal of Heat and Mass Transfer, 75, 262-271.

Lv, W., Phelan, P. E., Swaminathan, R., Otanicar, T. P., and Taylor, R. A. (2013). Multifunctional core-shell nanoparticle suspensions for efficient absorption. Journal of Solar Energy Engineering, 135(2), 021004.

Lv, Y.-z., Li, C., Sun, Q., Huang, M., Li, C.-r., and Qi, B. (2016). Effect of dispersion method on stability and dielectric strength of transformer oil-based TiO 2 nanofluids. Nanoscale research letters, 11(1), 515.

Madhesh, D., and Kalaiselvam, S. (2014). Energy efficient hybrid nanofluids for tubular cooling applications. Paper presented at the Applied Mechanics and Materials.

Mahian, O., Kianifar, A., Heris, S. Z., Wen, D., Sahin, A. Z., and Wongwises, S. (2017). Nanofluids effects on the evaporation rate in a solar still equipped with a heat exchanger. Nano Energy, 36, 134-155.

Mahl, D., Diendorf, J., Meyer-Zaika, W., and Epple, M. (2011). Possibilities and limitations of different analytical methods for the size determination of a bimodal dispersion of metallic nanoparticles. Colloids and Surfaces A: Physicochemical and Engineering Aspects, 377(1-3), 386-392.

Manickavasagam, S., and Mengüç, M. (1997). Scattering matrix elements of fractal-like soot agglomerates. Applied optics, 36(6), 1337-1351.

Manickavasagam, S., and Mengüç, M. P. (1998). Scattering-matrix elements of coated infinite-length cylinders. Applied optics, 37(12), 2473-2482.

Matsui, I. (2005). Nanoparticles for electronic device applications: a brief review. Journal of chemical engineering of Japan, 38(8), 535-546.

Mengüç, M., and Manickavasagam, S. (1998). Characterization of size and structure of agglomerates and inhomogeneous particles via polarized light. International Journal of Engineering Science, 36(12-14), 1569-1593.

Mengüç, M. P. (2003). Characterization of fine particles via elliptically-polarized light scattering. Purdue Heat Transfer Celebration, West Lafayette, IN.

Mewis, J., and Wagner, N. J. (2012). Colloidal suspension rheology: Cambridge University Press.

Michaelides, E. E. (2013). Transport properties of nanofluids. A critical review. Journal of Non-Equilibrium Thermodynamics, 38(1), 1-79.

Michaelides, E. E. S. (2013). Heat and mass transfer in particulate suspensions: Springer Science & Business Media.

Michaelides, E. E. S. (2014). Nanofluidics: thermodynamic and transport properties: Springer.

Mie, G. (1908). Beiträge zur Optik trüber Medien, speziell kolloidaler Metallösungen.

Annalen der physik, 330(3), 377-445.

Milanese, M., Colangelo, G., Cretì, A., Lomascolo, M., Iacobazzi, F., and De Risi, A. (2016). Optical absorption measurements of oxide nanoparticles for application as nanofluid in direct absorption solar power systems–Part II: ZnO, CeO2, Fe2O3 nanoparticles behavior. Solar Energy Materials and Solar Cells, 147, 321-326.

Minardi, J. E., and Chuang, H. N. (1975). Performance of a "black" liquid flat-plate solar collector. solar energy, 17(3), 179-183.

Minkowycz, W., Sparrow, E. M., and Abraham, J. P. (2016). Nanoparticle heat transfer and fluid flow: CRC press.

Mishchenko, M. I. (2014). Electromagnetic scattering by particles and particle groups: an introduction: Cambridge University Press.

Mishchenko, M. I., Hovenier, J. W., and Travis, L. D. (1999). Light scattering by nonspherical particles: theory, measurements, and applications: Academic press.

Mishchenko, M. I., Travis, L. D., and Lacis, A. A. (2002). Scattering, absorption, and emission of light by small particles: Cambridge university press.

Modest, M. F. (2013). Radiative heat transfer: Academic press.

Moghadassi, A., Ghomi, E., and Parvizian, F. (2015). A numerical study of water based Al2O3 and Al2O3–Cu hybrid nanofluid effect on forced convective heat transfer. International Journal of Thermal Sciences, 92, 50-57.

Morton, O. (2006). Solar energy: A new day dawning?: Silicon Valley sunrise: Nature Publishing Group.

Mu, L., Zhu, Q., and Si, L. (2009). Radiative properties of nanofluids and performance of a direct solar absorber using nanofluids. Paper presented at the ASME 2009 Second International Conference on Micro/Nanoscale Heat and Mass Transfer.

Muhammad, M. J., Muhammad, I. A., Sidik, N. A. C., Yazid, M. N. A. W. M., Mamat, R., and Najafi, G. (2016). The use of nanofluids for enhancing the thermal performance of stationary solar collectors: a review. Renewable and Sustainable Energy Reviews, 63, 226-236.

Munday, D. (2000). Surfaces, Interfaces and Colloids—Principles and Applications, by D. Myers, Wiley-VCH, New York, 1999, xx+ 501 pp., ISBN 0-471-33060-4;£ 61.50: Elsevier.

Murdock, R. C., Braydich-Stolle, L., Schrand, A. M., Schlager, J. J., and Hussain, S. M. (2008). Characterization of nanomaterial dispersion in solution prior to in vitro exposure using dynamic light scattering technique. Toxicological sciences, 101(2), 239-253.

Muthusamy, Y., Kadirgama, K., Rahman, M., Ramasamy, D., and Sharma, K. (2016). Wear analysis when machining AISI 304 with ethylene glycol/TiO 2 nanoparticle-based coolant. The International Journal of Advanced Manufacturing Technology, 82(1-4), 327-340.

Nagarajan, R., and Hatton, T. A. (2008). Nanoparticles: synthesis, stabilization, passivation, and functionalization: ACS Publications.

Nogi, K., Hosokawa, M., Naito, M., and Yokoyama, T. (2012). Nanoparticle technology

handbook: Elsevier.

Ortega, M. A., Rodriguez, L., Castillo, J., Fernández, A., and Echevarria, L. (2008). Thermo-optical Properties of Nanofluids. Paper presented at the AIP Conference Proceedings.

Otanicar, T., Hoyt, J., Fahar, M., Jiang, X., and Taylor, R. A. (2013). Experimental and numerical study on the optical properties and agglomeration of nanoparticle suspensions. Journal of Nanoparticle Research, 15(11), 2039.

Otanicar, T., Taylor, R. A., Phelan, P. E., and Prasher, R. (2009). Impact of size and scattering mode on the optimal solar absorbing nanofluid. Paper presented at the ASME 2009 3rd International Conference on Energy Sustainability collocated with the Heat Transfer and InterPACK09 Conferences.

Otanicar, T. P., Phelan, P. E., Prasher, R. S., Rosengarten, G., and Taylor, R. A. (2010). Nanofluid-based direct absorption solar collector. Journal of renewable and sustainable energy, 2(3), 033102.

Pang, C., Lee, J. W., and Kang, Y. T. (2015). Review on combined heat and mass transfer characteristics in nanofluids. International Journal of Thermal Sciences, 87, 49-67.

Phelan, P., Otanicar, T., Taylor, R., and Tyagi, H. (2013). Trends and opportunities in direct-absorption solar thermal collectors. Journal of Thermal Science and Engineering Applications, 5(2), 021003.

Powers, K. W., Brown, S. C., Krishna, V. B., Wasdo, S. C., Moudgil, B. M., and Roberts, S. M. (2006). Research strategies for safety evaluation of nanomaterials. Part VI. Characterization of nanoscale particles for toxicological evaluation. Toxicological sciences, 90(2), 296-303.

Prasher, R., Phelan, P. E., and Bhattacharya, P. (2006). Effect of aggregation kinetics on the thermal conductivity of nanoscale colloidal solutions (nanofluid). Nano letters, 6(7), 1529-1534.

Prasher, R. S., and Phelan, P. E. (2005). Modeling of radiative and optical behavior of nanofluids based on multiple and dependent scattering theories. Paper presented at the ASME 2005 International Mechanical Engineering Congress and Exposition.

Purcell, E. M., and Pennypacker, C. R. (1973). Scattering and absorption of light by nonspherical dielectric grains. The Astrophysical Journal, 186, 705-714.

Raja, M., Vijayan, R., Dineshkumar, P., and Venkatesan, M. (2016). Review on nanofluids characterization, heat transfer characteristics and applications. Renewable and Sustainable Energy Reviews, 64, 163-173.

Rajagopalan, R., and Hiemenz, P. C. (1997). Principles of colloid and surface chemistry. Marcel Dekker, New-York, 3e édition, ISBN 0, 8247(9397), 8.

Randrianalisoa, J., and Baillis, D. (2010). Radiative transfer in dispersed media: comparison between homogeneous phase and multiphase approaches. Journal of Heat Transfer, 132(2), 023405.

Rao, N., Gahane, L., and Ranganayakulu, S. (2014). Synthesis, applications and challenges of nanofluids–review. IOSR Journal of Applied Physics, 21-28.

Rayleigh, J. W. S. B. (1870). On the Light from the Sky: Its Polarization and Colour.

Roco, M. (1999). Towards a US national nanotechnology initiative. Journal of Nanoparticle Research, 1(4), 435-438.

Rodgers, P. (2010). Nanoscience and technology: a collection of reviews from Nature journals: Macmillan Publishers Limited.

Russel, W. B., Saville, D. A., and Schowalter, W. R. (1989). Colloidal dispersions: Cambridge university press.

s Vicsek, T. (1992). Fractal growth phenomena: World scientific.

Safaei-Naeini, Y., Aminzare, M., Golestani-Fard, F., Khorasanizadeh, F., and Salahi, E. (2012). Suspension stability of titania nanoparticles studied by UV-VIS spectroscopy method. Iranian Journal of Materials Science and Engineering, 9(1), 62-68.

Said, Z., Saidur, R., and Rahim, N. (2014). Optical properties of metal oxides based nanofluids. International Communications in Heat and Mass Transfer, 59, 46-54.

Said, Z., Saidur, R., and Rahim, N. (2015). Corrigendum to "Optical properties of metal oxides based nanofluids"[Int Commun Heat Mass 59 (2014) 46–54]. International Communications in Heat and Mass Transfer(62), 58-59.

Said, Z., Sajid, M., Alim, M., Saidur, R., and Rahim, N. (2013). Experimental investigation of the thermophysical properties of AL2O3-nanofluid and its effect on a flat plate solar collector. International Communications in Heat and Mass Transfer, 48, 99-107.

Sajid, M., Said, Z., Saidur, R., Adikan, F., Sabri, M., and Rahim, N. (2014). A time variant investigation on optical properties of water based Al2O3 nanofluid. International Communications in Heat and Mass Transfer, 50, 108-116.

Saltiel, C., Chen, Q., Manickavasagam, S., Schadler, L., Siegel, R., and Menguc, M. (2004). Identification of the dispersion behavior of surface treated nanoscale powders. Journal of Nanoparticle Research, 6(1), 35-46.

Saltiel, C., Manickavasagam, S., Mengüc, M. P., and Andrews, R. (2005). Light-scattering and dispersion behavior of multiwalled carbon nanotubes. JOSA A, 22(8), 1546-1554.

Sarkar, J. (2011). A critical review on convective heat transfer correlations of nanofluids. Renewable and Sustainable Energy Reviews, 15(6), 3271-3277.

Sarkar, J., Ghosh, P., and Adil, A. (2015). A review on hybrid nanofluids: recent research, development and applications. Renewable and Sustainable Energy Reviews, 43, 164-177.

Schmid, G. (2005). Nanoparticles: Wiley VCH.

Schwarzkopf, J. D., Sommerfeld, M., Crowe, C. T., and Tsuji, Y. (2011). Multiphase flows with droplets and particles: CRC press.

Seinfeld, J. H., and Pandis, S. N. (2016). Atmospheric chemistry and physics: from air pollution to climate change: John Wiley & Sons.

Sen, S., Govindarajan, V., Pelliccione, C. J., Wang, J., Miller, D. J., and Timofeeva, E. V. (2015). Surface modification approach to TiO2 nanofluids with high particle concentration, low viscosity, and electrochemical activity. ACS applied materials &

interfaces, 7(37), 20538-20547.

Sepyani, K., Afrand, M., and Esfe, M. H. (2017). An experimental evaluation of the effect of ZnO nanoparticles on the rheological behavior of engine oil. Journal of Molecular Liquids, 236, 198-204.

Shamshirband, S., Malvandi, A., Karimipour, A., Goodarzi, M., Afrand, M., Petković, D., . . . Mahmoodian, N. (2015). Performance investigation of micro-and nano-sized particle erosion in a 90 elbow using an ANFIS model. Powder Technology, 284, 336-343.

Shan, F., Tang, F., Cao, L., and Fang, G. (2014). Comparative simulation analyses on dynamic performances of photovoltaic–thermal solar collectors with different configurations. Energy conversion and management, 87, 778-786.

Sheldon, K. F. (2000). Smoke, Dust, and Haze: Fundamentals of Aerosol Dynamics: Oxford Univ. Press, New York.

Shih, W.-H., Hirata, Y., and Carty, W. M. (2012). Colloidal ceramic processing of nano-, micro-, and macro-particulate systems (Vol. 152): John Wiley & Sons.

Simakov, S. A., and Tsur, Y. (2007). Surface stabilization of nano-sized titanium dioxide: improving the colloidal stability and the sintering morphology. Journal of Nanoparticle Research, 9(3), 403-417.

Singham, S. B., and Bohren, C. F. (1988). Light scattering by an arbitrary particle: the scattering-order formulation of the coupled-dipole method. JOSA A, 5(11), 1867-1872.

Sinz, C., Woei, H., Khalis, M., and Abbas, S. (2016). Numerical study on turbulent force convective heat transfer of hybrid nanofluid, Ag/HEG in a circular channel with constant heat flux. J. Adv. Res. Fluid Mech. Therm. Sci., 24(1), 1-11.

Soltanimehr, M., and Afrand, M. (2016). Thermal conductivity enhancement of COOH-functionalized MWCNTs/ethylene glycol–water nanofluid for application in heating and cooling systems. Applied Thermal Engineering, 105, 716-723.

Song, D., Hatami, M., Wang, Y., Jing, D., and Yang, Y. (2016). Prediction of hydrodynamic and optical properties of TiO2/water suspension considering particle size distribution. International Journal of Heat and Mass Transfer, 92, 864-876.

Sundar, L. S., Sharma, K., Singh, M. K., and Sousa, A. (2017). Hybrid nanofluids preparation, thermal properties, heat transfer and friction factor–a review. Renewable and Sustainable Energy Reviews, 68, 185-198.

Swamy, J., Crofcheck, C., and Mengüç, M. (2009). Time dependent scattering properties of slow decaying liquid foams. Colloids and Surfaces A: Physicochemical and Engineering Aspects, 338(1-3), 80-86.

Şeşen, M., Tekşen, Y., Şahin, B., Şendur, K., Pınar Mengüç, M., and Koşar, A. (2013). Boiling heat transfer enhancement of magnetically actuated nanofluids. Applied Physics Letters, 102(16), 163107.

Şeşen, M., Tekşen, Y., Şendur, K., Pınar Mengüç, M., Öztürk, H., Yağcı Acar, H., and Koşar, A. (2012). Heat transfer enhancement with actuation of magnetic nanoparticles suspended in a base fluid. Journal of Applied Physics, 112(6), 064320.

Taborda, E. A., Franco, C. A., Lopera, S. H., Alvarado, V., and Cortés, F. B. (2016). Effect of nanoparticles/nanofluids on the rheology of heavy crude oil and its mobility on porous media at reservoir conditions. Fuel, 184, 222-232.

Tadros, T. F. (2012). Dispersion of powders in liquids and stabilization of suspensions: John Wiley & Sons.

Takabi, B., and Shokouhmand, H. (2015). Effects of Al 2 O 3–Cu/water hybrid nanofluid on heat transfer and flow characteristics in turbulent regime. International Journal of Modern Physics C, 26(04), 1550047.

Taylor, R., Coulombe, S., Otanicar, T., Phelan, P., Gunawan, A., Lv, W., . . . Tyagi, H. (2013). Small particles, big impacts: a review of the diverse applications of nanofluids. Journal of Applied Physics, 113(1), 1.

Taylor, R. A., Phelan, P. E., Otanicar, T. P., Adrian, R., and Prasher, R. (2011). Nanofluid optical property characterization: towards efficient direct absorption solar collectors. Nanoscale research letters, 6(1), 225.

Tien, C.-L., and Drolen, B. (1987). Thermal radiation in part1culate media with dependent and independent scattering. Annual Review of Heat Transfer, 1(1).

Toghraie, D., Chaharsoghi, V. A., and Afrand, M. (2016). Measurement of thermal conductivity of ZnO–TiO2/EG hybrid nanofluid. Journal of Thermal Analysis and Calorimetry, 125(1), 527-535.

Trisaksri, V., and Wongwises, S. (2007). Critical review of heat transfer characteristics of nanofluids. Renewable and Sustainable Energy Reviews, 11(3), 512-523.

Turcu, R., Nan, A., Craciunescu, I., Karsten, S., Pana, O., Bratu, I., . . . Eberbeck, D. (2007). Functionalized nanostructures with magnetic core and pyrrole copolymers shell. Journal of nanostructured polymers and nanocomposites, 3(2), 55.

Tyagi, H., Phelan, P., and Prasher, R. (2009). Predicted efficiency of a low-temperature nanofluid-based direct absorption solar collector. Journal of Solar Energy Engineering, 131(4), 041004.

Vakili, M., Mohebbi, A., and Hashemipour, H. (2013). Experimental study on convective heat transfer of TiO2 nanofluids. Heat and Mass Transfer, 49(8), 1159-1165.

van Dyk, A. C., and Heyns, A. M. (1998). Dispersion stability and photo-activity of rutile (TiO2) powders. Journal of colloid and interface science, 206(2), 381-391.

Veeraragavan, A., Lenert, A., Yilbas, B., Al-Dini, S., and Wang, E. N. (2012). Analytical model for the design of volumetric solar flow receivers. International Journal of Heat and Mass Transfer, 55(4), 556-564.

Verwey, E. (1947). Theory of the stability of lyophobic colloids. The Journal of Physical Chemistry, 51(3), 631-636.

Viskanta, R., and Menguc, M. (1989). Radiative transfer in dispersed media. Applied Mechanics Reviews, 42(9), 241-259.

Vollath, D. (2013). Nanoparticles-Nanocomposites Â–Nanomaterials: An Introduction for Beginners: John Wiley & Sons.

Wamkam, C. T., Opoku, M. K., Hong, H., and Smith, P. (2011). Effects of p H on heat transfer nanofluids containing ZrO 2 and TiO 2 nanoparticles. Journal of Applied

Physics, 109(2), 024305.

Wang, B.-X., Zhou, L.-P., and Peng, X.-F. (2003). A fractal model for predicting the effective thermal conductivity of liquid with suspension of nanoparticles. International Journal of Heat and Mass Transfer, 46(14), 2665-2672.

Wang, X.-Q., and Mujumdar, A. S. (2007). Heat transfer characteristics of nanofluids: a review. International Journal of Thermal Sciences, 46(1), 1-19.

Wang, X.-Q., and Mujumdar, A. S. (2008). A review on nanofluids-part I: theoretical and numerical investigations. Brazilian Journal of Chemical Engineering, 25(4), 613-630.

Waterman, P. (1965). Matrix formulation of electromagnetic scattering. Proceedings of the IEEE, 53(8), 805-812.

Wee, A. T. (2009). Selected topics in nanoscience and nanotechnology: World Scientific.

Wei, W., Fedorov, A. G., Luo, Z., and Ni, M. (2012). Radiative properties of dense nanofluids. Applied optics, 51(25), 6159-6171.

Wen, D., Lin, G., Vafaei, S., and Zhang, K. (2009). Review of nanofluids for heat transfer applications. Particuology, 7(2), 141-150.

Widegren, J., and Bergström, L. (2002). Electrostatic stabilization of ultrafine titania in ethanol. Journal of the American Ceramic Society, 85(3), 523-528.

Williams, D. N., Ehrman, S. H., and Holoman, T. R. P. (2006). Evaluation of the microbial growth response to inorganic nanoparticles. Journal of nanobiotechnology, 4(1), 3.

Witten Jr, T., and Sander, L. M. (1981). Diffusion-limited aggregation, a kinetic critical phenomenon. Physical review letters, 47(19), 1400.

Wong, K. V., and De Leon, O. (2010). Applications of nanofluids: current and future. Advances in Mechanical Engineering, 2, 519659.

Woodcock, L. V. (1987). Schools of Chemical Engineering University of Bradford Bradford, BD7 1DP England. Paper presented at the Molecular Dynamics and Relaxation Phenomena in Glasses: Proceedings of a Workshop Held at the Zentrum Für Interdisziplinäre Forschung Universität Bielefeld, Bielefeld, FRG, November 11-13, 1985.

Wu, Y., Yang, W., Wang, C., Hu, J., and Fu, S. (2005). Chitosan nanoparticles as a novel delivery system for ammonium glycyrrhizinate. International journal of pharmaceutics, 295(1-2), 235-245.

Xia, X., and Xia, J. (2010). Evaluation of potential for developing renewable sources of energy to facilitate development in developing countries. Paper presented at the Power and Energy Engineering Conference (APPEEC), 2010 Asia-Pacific.

Xian-Ju, W., Hai, L., Xin-Fang, L., Zhou-Fei, W., and Fang, L. (2011). Stability of TiO2 and Al2O3 nanofluids. Chinese Physics Letters, 28(8), 086601.

Xiao, B., Chen, H., Xiao, S., and Cai, J. (2017). Research on relative permeability of nanofibers with capillary pressure effect by means of Fractal-Monte Carlo technique. Journal of Nanoscience and Nanotechnology, 17(9), 6811-6817.

Xiao, B., Yang, Y., and Chen, L. (2013). Developing a novel form of thermal conductivity of nanofluids with Brownian motion effect by means of fractal geometry. Powder

Technology, 239, 409-414.

Xie, H., Fujii, M., and Zhang, X. (2005). Effect of interfacial nanolayer on the effective thermal conductivity of nanoparticle-fluid mixture. International Journal of Heat and Mass Transfer, 48(14), 2926-2932.

Xu, R. (2001). Particle characterization: light scattering methods (Vol. 13): Springer Science & Business Media.

Xuan, Y., Duan, H., and Li, Q. (2014). Enhancement of solar energy absorption using a plasmonic nanofluid based on TiO 2/Ag composite nanoparticles. Rsc Advances, 4(31), 16206-16213.

Xuan, Y., and Li, Q. (2000). Heat transfer enhancement of nanofluids. International Journal of heat and fluid flow, 21(1), 58-64.

Yang, L., Chen, X., Xu, M., and Du, K. (2016). Roles of surfactants and particle shape in the enhanced thermal conductivity of TiO2 nanofluids. AIP Advances, 6(9), 095104.

Yang, L., and Du, K. (2017). A comprehensive review on heat transfer characteristics of TiO2 nanofluids. International Journal of Heat and Mass Transfer, 108, 11-31.

Yang, L., and Hu, Y. (2017). Toward TiO 2 Nanofluids—Part 1: Preparation and Properties. Nanoscale research letters, 12(1), 417.

Yousefi, T., Shojaeizadeh, E., Veysi, F., and Zinadini, S. (2012). An experimental investigation on the effect of pH variation of MWCNT–H2O nanofluid on the efficiency of a flat-plate solar collector. solar energy, 86(2), 771-779.

Yu, W., France, D. M., Routbort, J. L., and Choi, S. U. (2008). Review and comparison of nanofluid thermal conductivity and heat transfer enhancements. Heat transfer engineering, 29(5), 432-460.

Yu, W., and Xie, H. (2012). A review on nanofluids: preparation, stability mechanisms, and applications. Journal of Nanomaterials, 2012, 1.

Yurkin, M. A., Maltsev, V. P., and Hoekstra, A. G. (2007). The discrete dipole approximation for simulation of light scattering by particles much larger than the wavelength. Journal of Quantitative Spectroscopy and Radiative Transfer, 106(1-3), 546-557.

Zhang, H., Chen, H.-J., Du, X., and Wen, D. (2014). Photothermal conversion characteristics of gold nanoparticle dispersions. solar energy, 100, 141-147.

Zhang, Y. F., Han, K., Xu, B. L., and Chang, Z. R. (2012). Experimental Study on Heat Transfer Performance of the Solar Collector with an Inserted Heat Pipe Using Magnetic Nano-Fluids as the Working Fluid. Paper presented at the Applied Mechanics and Materials.

Zhang, Z., He, W., Zheng, J., Wang, G., and Ji, J. (2016). Rice husk ash-derived silica nanofluids: synthesis and stability study. Nanoscale research letters, 11(1), 502.

Zhu, D., Li, X., Wang, N., Wang, X., Gao, J., and Li, H. (2009). Dispersion behavior and thermal conductivity characteristics of Al2O3–H2O nanofluids. Current Applied Physics, 9(1), 131-139.

Zhu, H., Zhang, C., Tang, Y., Wang, J., Ren, B., and Yin, Y. (2007). Preparation and

thermal conductivity of suspensions of graphite nanoparticles. Carbon, 45(1), 226-228.

Zhu, Q., Cui, Y., Mu, L., and Tang, L. (2013). Characterization of thermal radiative properties of nanofluids for selective absorption of solar radiation. International Journal of Thermophysics, 34(12), 2307-2321.

Zubko, E., Shkuratov, Y., and Videen, G. (2015). Effect of morphology on light scattering by agglomerates. Journal of Quantitative Spectroscopy and Radiative Transfer, 150, 42-54.

VITA

Layth Wadhah Ismael Al-Gebory was born on October 30, 1977, in Baghdad, Iraq. He received his B.Sc. degree in mechanical engineering in July 2000 at the University of Technology, Bagdad, Iraq. He got his M.Sc. degree in the mechanical engineering in the University of Technology in August 2005 under the supervision of Prof. Dr. Jaffar M. Hassan and Asst. Prof. Dr. Laith K. Abbas. In February 2013, he enrolled at Özyeğin University in Istanbul, Turkey. He attended English Preparatory School at Özyeğin University. In February 2014, he has started his Ph.D. under the supervision of Prof. Dr. M. Pinar Mengüç at Özyeğin University.

This dissertation research concentrated on the radiative transfer in nanoparticle suspensions. More specific, different issues in the interaction of radiation with nanoparticles and their agglomerates were explained with their applications. He graduated from Özyeğin University with a doctorate degree in mechanical engineering with radiative transfer in nanoparticle suspensions in August 2018.

Journal papers

1. Al-Gebory, L., Mengüç, M. P., Koşar, A., and Şendur, K. (2018). Effect of electrostatic stabilization on thermal radiation transfer in nanosuspensions: Photo-thermal energy conversion applications. Renewable Energy, 119, 625-640.

2. Al-Gebory, L., and Mengüç, M. P. (2018). The effect of pH value on particle agglomeration and radiative transfer in nanoparticle suspensions. Journal of Quantitative Spectroscopy and Radiative Transfer, doi: 10.1016/j.jqsrt.2018.07.020.

3. Al-Gebory, L., and Mengüç, M. P. (2018). Review of Nanoparticle Suspensions for Optical and Radiative Properties Effects of Particle Stability, Agglomeration, and Sedimentation. (in progress).

4. Al-Gebory, L. and Mengüç, M. P. (2018). Effects of particle agglomerate deposits on

the optical and radiative properties of heterogeneous coatings. (In progress).

Conference papers and presentation

1. Al-Gebory, L, and Mengüç, M. P. (2016). Spectral transmittance of nanoparticulate media for solar thermal collectors: effects of the particle size and size distribution. Solar Conference and Exhibtion (SOLARTR 2016), Istanbul, Turkey.

2. Al-Gebory, L, and Mengüç, M. P. (2016). An investigation on the effects of particle agglomeration on the thermal behavior of nanosuspensions. Internetional Energy Technologies Conference IV (ENTECH 16), Istanbul, Turkey.

3. Al-Gebory, L, and Mengüç, M. P. (2017). The effect of pH value on particle agglomeration and the radiative properties of nanoparticle suspensions. The 16th Electromagnetic and Light Scattering Conference ELS-XVI, Maryland, USA.

4. Al-Gebory, L, and Mengüç, M. P. (2017). The effect of Al_2O_3 particle agglomeration on the spectral radiative properties of nanoparticle suspensions. International Conference on Energy and Thermal Engineering, Istanbul, Turkey.

5. Al-Gebory, L, Karagoz, A., and Mengüç, M. P. (2017). Investigation of thermophysical properties and thermal performance of nanosuspensions considering the effect of particle size growth", 13th Nanoscience and Nanotechnology Conference, Antalya,Turkey.

6. Al-Gebory, L, and Mengüç, M. P. (2018). Effects of particle agglomerate deposits on the radiative response of heterogeneous coatings. The 17th Electromagnetic and Light Scattering Conference ELS-XVII, Texas, USA.